



Cape Peninsula
University of Technology

**EFFECT OF SHARP CRESTED ORIFICE SHAPE AND NEWTONIAN AND NON-
NEWTONIAN FLUID PROPERTIES ON DISCHARGE FROM A TANK**

by

Morakane Charlotte Khahledi

Dissertation submitted in fulfilment of the requirements for the degree

Doctor of Engineering: Civil Engineering

in the Faculty of Engineering and Built Environment

at the Cape Peninsula University of Technology

Supervisor: Prof R Haldenwang
Co-supervisors: Prof R Chhabra and Prof V Fester

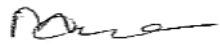
Bellville/Cape Town
May 2020

CPUT copyright information

This dissertation may not be published either in part (in scholarly, scientific or technical journals), or as a whole (as a monograph), unless permission has been obtained from the University.

DECLARATION

I, Morakane Charlotte Khahledi, declare that the contents of this dissertation represent my own unaided work, and that the dissertation has not previously been submitted for academic examination towards any qualification. Furthermore, it represents my own opinions and not necessarily those of the Cape Peninsula University of Technology.



Signed**20-May-2020**

Date

ABSTRACT

The flow rate measurement of Newtonian liquids through orifices of various shapes from tanks and pipes has been extensively studied, but not for non-Newtonian liquids. Non-Newtonian liquids have complex rheological properties that make it difficult to determine the discharge through orifices, from tanks. The only literature available was the flow rate measurement of Power law liquids through circular orifices, from a tank. Therefore, the aim of this work was to determine the flow rate of Newtonian and non-Newtonian liquids using circular, square and triangular sharp crested orifices out of a tank, as a function of liquids flow properties. The sharp-crested circular, square and triangular orifices with 8 mm, 12 mm, 16 mm, and 20 mm hydraulic diameters were fitted at the bottom of a square cross-sectioned tank to measure the flow rate of the liquids. A rectangular tank was suspended from a weighbridge with a load cell to capture the flow rate data. A high-speed camera was used to capture the videos for water test calibration purposes. A concentric cylinder viscometer was used to obtain the rheological parameters of the test liquids. The liquids tested included: Newtonian, Power law, Bingham and Herschel–Bulkley model systems.

The discharge coefficient (C_d) and Reynolds number (Re) were calculated from the experimental results. The calibration average C_d value for all the orifices was 0.62, which is close to the oft-quoted value of 0.61 for Newtonian liquids and equal to the average C_d value found from a similar study. The C_d - Re relationship indicated that the orifice shape did not have an effect on the flow rate measurement of Newtonian and non-Newtonian liquids from a tank. It was found that for each model test liquid, there is a unique flow curve in the laminar region. The Newtonian, Power-Law, Herschel–Bulkley and Bingham liquids started at Re 11, 53, 232 and 330 respectively, for all orifice shapes. This was due to the varying rheological behavior of the liquids. In the turbulent region, all data coincided with Newtonian C_d values, with an average value of 0.64, not far off from the average C_d value of 0.67 found in previous studies. The range of Reynolds numbers tested in this study was between Re =11 and Re =63000. The idea of an effective shear rate for flow through the orifice was used to develop a new Reynolds number for different liquids, to consolidate the C_d - Re relationship to the Newtonian liquid curve in the laminar flow regime. The effective shear rate of $0.3v/d_h$ was developed to consolidate the Power-law liquids C_d - Re relationship to Newtonian liquid curve.

To collapse the Bingham and Herschel-Bulkley liquids on the Newtonian liquid data for the C_d - Re relationship in the laminar and transitional flow, the Bingham number was used to account

for yield stress. The Herschel–Bulkley liquids were adjusted by alpha to change the Reynolds number to Newtonian liquids Re. A single composite model was used to predict the relationship between C_d and Re and the discharge equation was determined for all liquid-orifice combinations used in this work. The discharge equation is only applicable for $8 \text{ mm} < d < 20 \text{ mm}$, $0 < L/d < 0.125$ and $11 < Re_2 < 63000$. The predicted model can be used in engineering designs and processes.

ACKNOWLEDGEMENTS

I wish to thank:

- The Department of Higher Education and Training (Republic of South Africa) for giving me the opportunity to be part of the New Generation of Academics Programme (nGap);
- My supervisors, Professors Haldenwang, Chhabra and Fester, for believing in me, and for their time, wisdom and patience;
- Mr Sutherland, for assisting with instrumentation design and fabrication of the experimental set-up, data capturing spread sheets, numerical derivations and technical support;
- Mr Nazeem George for conducting the rheology and particle size distribution tests and advice on analysing their data.
- Mr du Toit for technical support;
- Miss Mohajane for technical and emotional support;
- Mr Xashimba for technical assistance;
- Mr Makhala and Mrs Huevel for administrative support;
- Ms Kamalie, Mrs Manyumwa, Mr Mambwe and Dr Bukenya for support;
- Dr Tshilumbu for advice on analysing the rheology data.
- My family – Mr Tshediso Khahledi, Miss Bohlale Khahledi and Mr Motlatsi Khahledi – for their support and understanding;
- My parents and my late grandmother for their encouragement and support;
- My siblings for their support;
- Mr Lefu Thamae's family for believing in me; and
- Mrs Limpopo Makhula for her support.

DEDICATION

To my family – for being my pillar of strength

“For I know the plans I have for you’ declares the lord, ‘plans to prosper you and not to harm you, plans to give you hope and a future” (Jeremiah 29:11).

Table of Contents

DECLARATION.....	2
ABSTRACT	3
ACKNOWLEDGEMENTS	5
Symbols	12
Greek letters	14
	15
 Terms and concepts	
CHAPTER ONE: INTRODUCTION	16
1.1 Introduction	16
1.2 Statement of research problem	17
1.3 Research question.....	17
1.4 Aims and objectives.....	17
1.5 Scope of the work.....	18
1.6 Delineation.....	18
1.7 Significance of the research	18
1.8 Outcomes, results and contributions of the research.....	18
1.9 Organisation of dissertation	19
CHAPTER TWO: LITERATURE REVIEW.....	20
2.1 Introduction.....	20
2.2 Rheology of liquids	20
2.3 Rheometer	21
2.4 Newtonian liquids.....	21
2.5 Non-Newtonian liquids.....	22
2.5.1 Time-independent liquids	22
2.5.2 Shear-thinning or pseudoplastic.....	23
2.5.3 Viscoplastic liquid	24
2.5.4 Viscosity	24
2.6 Dimensionless parameters	25
2.6.1 Bingham number	25
2.6.2 Reynolds number	26
2.6.3 Slatter and Lazarus (1993) Reynolds numbers	27
2.6.4 Slatter (1997) Reynolds numbers	27
2.6.5 Metzner and Reed (1955) Reynolds numbers	29
2.6.6 Euler number.....	31
2.7 Orifices.....	32
2.7.1 Orifice discharge coefficient	32
2.7.2 Orifice discharge equation	33
2.7.3 Effect of orifice shape.....	35
2.7.3.1 Tank flow	35
2.7.3.2 Pipe flow	37
2.7.3.3 Nozzle/sprays flow	39
2.7.3.4 Gas flow	40
2.7.4 Liquid flow through orifices from tanks.....	41
2.7.4.1 Swamee and Swamee (2010)	41
2.7.4.2 Marcinkowski and Dziubiński (2004) and Dziubiński and Marcinkowski (2006)	44
2.7.4.3 Liu <i>et al.</i> (2001)	47
2.7.4.4 Della Valle <i>et al.</i> (2000)	48
2.7.4.5 Kiljański (1993).....	49
2.7.4.6 Combined tank flow results	50
2.7.5 Liquid flow through orifices in pipes	51
2.8 Other similar research	54
2.9 Data analysis	54
2.10 Conclusion.....	55
CHAPTER THREE: RESEARCH METHODS.....	59
3.1 Introduction	59
3.2 Equipment.....	59
3.2.1 Rheometer.....	59
3.2.2 Tank and orifices	59

3.2.3	Load cells	62
3.2.4	Data logger.....	63
3.2.5	Camera.....	64
3.2.6	Test liquids	65
3.2.7	Material composition	65
3.3	Experimental procedures.....	70
3.3.1	DAQ system and load cell calibration	71
3.3.2	Orifice calibration and flow rate tests for all the liquids.....	74
3.4	Liquid preparation	75
3.5	Rheology tests	78
3.6	Data analysis	80
3.6.1	Orifice calibration and liquid flow rate measurement	80
3.6.2	Rheology	87
3.6.3	Reynolds number and C_d relationship.....	89
3.6.4	Effect of orifice size and shape	90
3.7	Experimental errors	90
3.7.1	Unsteady-flow dynamics	90
3.7.2	Relative and absolute errors	90
3.7.3	Combined errors	94
3.8	Conclusion	100
CHAPTER FOUR: RESULTS AND ANALYSIS.....		101
4.1	Introduction	101
4.2	Rheology results	101
4.2.1	Kaolin suspensions	102
4.2.2	Bentonite suspensions	102
4.2.3	CMC solutions	103
4.2.4	Glycerine solutions	105
4.3	Effect of orifice shape (water results)	105
4.4	Flow rate test	108
4.5	Effect of orifice shape (Newtonian and non-Newtonian liquids).....	111
4.6	Metzner and Reed (1955) Reynolds number	112
4.7	Conclusion	113
CHAPTER FIVE: DISCUSSION		115
5.1	Introduction	115
5.2	Calibration results	115
5.3	Effect of orifice shape (water results)	116
5.4	Effect of orifice shape (Newtonian and non-Newtonian liquids).....	121
5.5	Flow behaviour of liquids through orifices	122
5.6	Conclusion	124
CHAPTER SIX: MODEL PREDICTIONS.....		125
6.1	Introduction	125
6.2	Model predictions.....	125
6.3	Conclusion	136
CHAPTER SEVEN: SUMMARY, NEW CONTRIBUTIONS AND RECOMMENDATIONS.....		138
7.1	Introduction	138
7.2	Summary	138
7.3	New contributions	139
7.4	Application in the industry.....	141
7.5	Recommendations.....	141
APPENDICES		151

REFERENCES

REFERENCES 1.....	143
-------------------	-----

LIST OF FIGURES

Figure 2.1 Schematic representation of unidirectional shearing flow	21
Figure 2.2 Types of time-independent flow curves (Chhabra & Richardson, 2008)	23
Figure 2.3 Unsheared plug geometry (Slatter, 1997)	28
Figure 2.4 Different shapes of sharp crested orifices	32
Figure 2.5 Flow from a tank at atmospheric pressure	33
Figure 2.6 C_d vs head (m) for circular and square orifices (Brater <i>et al.</i> , 1996)	36
Figure 2.7 C_d vs. h (mm) for circular, equilateral triangular and square orifices.....	37
Figure 2.8 C_d versus Re_3 for short, square-edged circular, sharp and round apex triangular orifices with an equivalent diameter ratio of $\beta=0.57$ (Ntamba Ntamba, 2011)	39
Figure 2.9 Re versus flow rate (ml/hr) for circular, equilateral triangular and square orifices	41
Figure 2.10 Re - C_d relationship for $L/d = 0$ (Brater <i>et al.</i> , 1996; Swamee & Swamee, 2010)	42
Figure 2.11 Re - C_d relationship for $L/d = 0$ (Dziubiński & Marcinkowski, 2006)	47
Figure 2.12 Re - Eu relationship for Boger fluids (Della Valle <i>et al.</i> , 2000)	49
Figure 2.13 Re - C_d relationship for $L/d = 0$ (Kiljański, 1993).....	50
Figure 2.14 Re - C_d relationship for $L/d = 0$ (Brater <i>et al.</i> , 1996; Swamee & Swamee, 2010; Kiljański, 1993; Dziubiński & Marcinkowski, 2006)	51
Figure 3.1 Rectangular tank supported by a steel frame	60
Figure 3.2 Tank base	61
Figure 3.3 Triangular, square and circular orifice	61
Figure 3.4 Weigh bridge with load cell	63
Figure 3.5 Data acquisition unit (DAQ)	64
Figure 3.6 Tripod and camera setup	65
Figure 3.7 Particle size distribution (microns) for kaolin	67
Figure 3.8 Particle size distribution (microns) for bentonite	68
Figure 3.9 Particle size distribution (microns) for bentonite	69
Figure 3.10 Load cell calibration results – 100 kg	73
Figure 3.11 Load cell calibration results – 250 kg	73
Figure 3.12 Rheograms for bentonite suspensions (Equilibrium flow curves for 6.99%)	79
Figure 3.13 Hysteresis loops of bentonite suspensions at 6%, 8% and 10% concentrations and comparison with the Herschel–Bulkley model (Bekkour <i>et al.</i> , 2005).....	80
Figure 3.14 Example of the head versus time for 8 mm diameter orifice calibration.....	82
Figure 3.15 Flow rate (m^3/s) versus head (m) for circular orifice (8 mm hydraulic diameter)	83
Figure 3.16 Flow rate (m^3/s) versus head (m) for square orifice (8 mm hydraulic diameter)	83
Figure 3.17 Flow rate (m^3/s) versus head (m) for triangular orifice (8 mm hydraulic diameter)	84
Figure 3.18 C_d versus head for circular orifices	85
Figure 3.19 C_d versus head for square orifices.....	85
Figure 3.20 C_d versus head for triangular orifices.....	86
Figure 3.21 Rheogram for 100% glycerine	87
Figure 3.22 Rheogram for 7.55% CMC solution.....	88
Figure 3.23 Rheogram for 20.34% kaolin suspension	88
Figure 3.24 Rheogram for 7.3% bentonite suspension	89
Figure 3.25 Standard deviation versus average voltage (V) for 8 mm hydraulic diameter orifices	92
Figure 3.26 Maximum expected % error in head (m) for circular orifices	96
Figure 3.27 Maximum expected % error in head for square orifices	96
Figure 3.28 Maximum expected % error in head for triangular orifices	97
Figure 3.29 Maximum expected % error of orifice velocity for circular orifices.....	98
Figure 3.30 Maximum expected % error of orifice velocity for square orifices	99
Figure 3.31 Maximum expected % error of orifice velocity for triangular orifices	99
Figure 4.1 Rheograms for kaolin suspensions.....	102
Figure 4.2 Rheograms for bentonite suspensions	103
Figure 4.3 Rheogram for 2.4% CMC solution	104
Figure 4.4 Rheograms for CMC solutions.....	104
Figure 4.5 Rheograms for glycerine solutions	105
Figure 4.6 Water C_d versus head (m) for 8 mm hydraulic diameters orifices	106
Figure 4.7 Water C_d versus head (m) for 12 mm hydraulic diameters orifices	106
Figure 4.8 Water C_d versus head (m) for 16 mm hydraulic diameters orifices	107

Figure 4.9 C_d versus head (m) for 20 mm hydraulic diameters orifices.....	108
Figure 4.10 C_d versus Re_2 for circular orifices	109
Figure 4.11 C_d versus Re_2 for square orifices.....	110
Figure 4.12 C_d versus Re_2 for triangular orifices.....	111
Figure 4.13 C_d - Re_2 relationship for Newtonian and non-Newtonian liquids for circular, square and triangular orifices.....	112
Figure 4.14 C_d versus Re_{MR} and Re_2 relationship for CMC solutions and Newtonian liquids through circular orifice	113
Figure 5.1 water C_d versus generalised Re for circular, square and triangular orifices.....	116
Figure 5.2 water C_d versus head (m) for 8 mm and 10 mm hydraulic diameters	117
Figure 5.3 water C_d versus head (m) for 10 mm, 12 mm and 20 mm hydraulic diameters	118
Figure 5.4 C_d versus head (m) for 16 mm and 20 mm hydraulic diameters	119
Figure 5.5 C_d versus head (m) for 20 mm hydraulic diameters	120
Figure 5.6 C_d vs Re_{MR} for Newtonian and non-Newtonian liquids for L/d of 0	123
Figure 6.1 flow chart describing the steps taken to develop a consolidated C_d - Re_{new} correlation.....	128
Figure 6.2 C_d (actual) and C_d (pred) versus Reynolds numbers for Newtonian liquids.....	130
Figure 6.3 C_d (actual) and C_d (pred) versus Reynolds numbers (Re_{new-PL} , Re_{new-BP} , Re_{new-HB})	133
Figure 6.4 C_d (pred) versus C_d (actual)	133
Figure 6.5 $Q_{(pred)}$ versus $Q_{(actual)}$ for laminar flow.....	134
Figure 6.6 $Q_{(pred)}$ versus $Q_{(actual)}$ for transitional flow.....	135
Figure 6.7 $Q_{(pred)}$ versus $Q_{(actual)}$ for turbulent flow.....	135

LIST OF TABLES

Table 2.1 Summary of previous research on flow of Newtonian and non-Newtonian liquids through orifices from tanks	58
Table 3.1 Orifice dimensions.....	62
Table 3.2 Dimensions of the load cells in mm	63
Table 3.3 Kaolin specification	66
Table 3.4 bentonite specification.....	67
Table 3.5 Glycerine specification	70
Table 3.6 Average C_d values for circular, square and triangular orifices.....	86
Table 3.7 Calibration details for 250 kg and 100 kg load cells	91
Table 3.8 Load cell data points for 250 kg	92
Table 3.9 % average maximum error for orifice velocity.....	98
 Table 4.1 Rheological and physical parameters of the test liquids.....	101
 Table 5.1: Average C_d values for circular, square and triangular orifices.....	121

GLOSSARY

Symbols

Symbol	Meaning (units)
A	Surface area (m^2) (Eq. 2.1)
A_{ann}	Area of the annulus in pipes (m^2) (Eq. 2.18)
A_{plug}	Area of the plug in pipes (m^2) (Eq. 2.19)
A_T	Area of the tank (m^2)
A_o	Area of the orifice (mm^2 and m^2)
Bi	Bingham number
B	Constant in Eq. 2.61
C	Constant in Eq. 2.61
C_d	Coefficient of discharge
C_{dpre}	Predicted coefficient of discharge
C_v	Concentration by volume
D	Pipe diameter (m)
D_{plug}	Diameter of the plug in pipes (m) (Eq. 2.21)
D_{shear}	Diameter over the sheared zone in pipes (m) (Eq. 2.21)
d	Orifice diameter (m)
D_h	Hydraulic diameter (m)
d_h	Orifice hydraulic diameter (m)
Eu	Euler number
F	Constant in Eq. 2.57
F	Force (N) in Eq. 2.1
f	Fanning friction factor (Eqns. 2.22 and 2.65)
g	Acceleration due to gravity (m/s^2)
H	Flow height at intermediate position measured from surface of liquid level in a tank (m)
H_0	Initial liquid head in a tank (m)
H_1	Final liquid head in a tank (m)
h	Liquid height (m) (Eq. 2.44)
k	Liquid consistency index (Pa.s^n)
k'	Apparent liquid consistency index (Pa.s^n)
k_L	factor in Eq. 2.65
L	Orifice thickness (mm) (Eqns. 2.62 and 2.65)
LSE	Log standard error

m	Constant in Eqns. 2.14; 2.15 and 2.16
n	Flow behaviour index
n'	Apparent flow behaviour index
P	Pressure (Pa or N/m ²)
P_{atm}	Atmospheric pressure (Pa or N/m ²)
P_1	Pressure at the surface level of liquid in a tank (Pa or N/m ²)
P_2	Pressure at the orifice exit (Pa or N/m ²)
P_w	Wetted perimeter (m and mm)
Q	Flow rate in pipes (m ³ /s) (Eq. 2.19)
Q_{ann}	Flow rate within the annulus (m ³ /s) (Eq. 2.19)
Q_1	Flow rate in a tank (m ³ /s)
Q_2	Flow rate at the orifice (m ³ /s)
Q_{pre}	Predicted flow rate (m ³ /s)
Q_{plug}	Plug flow rate (m ³ /s) (Eq. 2.19)
R	Vertical shift (Eq. 2.68)
R	Pipe radius (m) (Eq. 2.20)
R^2	Correlation coefficient
R_d	Relative density
Re	Reynolds number (Eq. 2.11)
Re_B	Bingham Reynolds number (Eq. 2.13)
Re_F	Reynolds number (Eq. 2.58)
Re_g	Generalised Reynolds number (Eq. 2.66)
Re_{Gen}	Generalised Reynolds number (Eq. 2.10)
Re_{GenPL}	Generalised Reynolds number for power law liquids (Eq. 2.12)
Re_{GenB}	Generalised Reynolds number Bingham liquids (Eq. 2.14)
Re_{GenHB}	Generalised Reynolds number for Herschel-Bulkely liquids (Eq. 2.16)
Re_H	Haldenwang Reynolds number
Re_{MR}	Metzner and Reed Reynolds number (Eq. 2.26)
Re_3	Slatter Reynolds number (Eq. 2.18)
r_{plug}	Radius at the point of a plug in pipes (Eq. 2.20)
T	Time (s)
u_{plug}	Point velocity of a plug in pipes (m/s) (Eq. 2.19)
v	Velocity (m/s)
v_{ann}	Average velocity of the annulus (m/s) (Eq. 2.18)
v_1	Velocity in the tank (m/s)
v_2	Velocity in at the orifice (m/s)
ν	Kinematic fluid viscosity (m ² /s)

Greek letters

Symbol	Meaning (units)
β	Beta ratio,
ρ	Density (kg/m^3)
ρ_w	Density of water (kg/m^3)
η	Shear viscosity (Pa.s) (Eq. 2.63)
η_E	Extensional viscosity (Pa.s) (Eq. 2.63)
τ	Shear stress (Pa)
τ_w	Shear stress (Pa)
τ_{yx}	Shear stress (Pa) (Eq. 2.1)
τ_y	Yield stress (Pa)
$\tau_{y(B)}$	Bingham yield stress (Pa)
$\dot{\gamma}$	Shear rate (1/s)
μ	Viscosity (Pa.s)
μ'	Apparent viscosity (Pa.s)
μ_B	Bingham viscosity (Pa.s)
μ_{HB}	Herschel-Bulkley viscosity (Pa.s^n)

Terms and concepts

Term	Explanation
Aspect ratio (L/d)	Ratio of orifice length to orifice diameter
Beta ratio	Ratio of orifice diameter to pipe diameter, an equivalent diameter ratio for short square-edged circular, sharp and round apex triangular orifices
Coefficient of discharge	Ratio between the actual discharge and the theoretical flow discharge
Euler number	Ratio of pressure forces to inertial forces
Froude number	Ratio of inertial and gravitational forces
Hydraulic diameter	Four times the ratio of the cross sectional area and wetted perimeter of the orifice
Laminar flow	Viscous forces dominating the flow behaviour and the liquid particles moving in smooth paths
Newtonian liquid	A liquid whose flow curve (shear stress versus shear rate) is linear and passes through the origin (Chhabra & Richardson, 2008)
Non-Newtonian liquid	A liquid whose flow curve (shear stress versus shear rate) is not linear and/or does not pass through the origin
Reynolds Number	The ratio of inertial to viscous forces
Rheology	The science of deformation and flow of materials
Transition	Region between laminar and turbulent flow regimes
Turbulent flow	Region where inertial forces dominate over viscous forces and liquid particles move in irregular paths
Viscosity	The internal resistance of fluids to flow
Weissenberg number	The ratio between elastic and viscous forces in a viscoelastic liquid
Yield stress	Stress at which a material begins to deform like a fluid

CHAPTER ONE: INTRODUCTION

1.1 Introduction

Non-Newtonian liquids have very complex and different flow characteristics from Newtonian liquids. These characteristics depend on particle size distribution, concentration, dynamic viscosity, temperature of the slurry, level of liquid turbulence and size of the conduit (Abulnaga, 2002). Some slurry mixtures consist of very fine solids at high concentration. Examples of such slurries are drilling mud, sewage sludge, soft clays and fine limestone. Most industrial processes consist of the storage and transportation of these liquids from one point to another, involving a flow through orifices. An orifice is a small opening in the wall or at the bottom of a tank and is commonly used for liquid flow control and measurement. Orifices can be classified according to shape.

According to Dziubiński and Marcinkowski (2006), the flow measurement of Newtonian liquids from tanks using orifices has been extensively discussed in literature (Medaugh & Johnson, 1940; Leinhard, 1984; Spencer, 2013; Adam *et al.*, 2016). Flow rate measurement of non-Newtonian liquids in pipes, by means of orifices, has been studied by Ntamba Ntamba (2011), Chowdhury and Fester (2012) and Rituraj and Vacca (2018). As far as can be ascertained, the only work on the measurement of non-Newtonian liquids through orifices out of a tank was reported by Dziubiński and Marcinkowski (2006). The project, however, only studied the discharge measurement of water, ethylene glycol and solutions of starch syrup in water (Newtonian liquids) and Carboxymethylcellulose (CMC) solutions (non-Newtonian liquids) using different diameter orifices, out of tanks. Only circular orifices and liquids without a yield stress were tested. The data for Newtonian and non-Newtonian liquids did not coincide, as was the case in orifices within pipes. Therefore, two correlations were presented for discharge through orifices from tanks: one for Newtonian liquids and one for non-Newtonian liquids. Previous work on the Newtonian and non-Newtonian liquid flow through sudden contractions in pipes (Pienaar, 2004) and non-Newtonian liquids through orifices in pipes (Chowdhury, 2010; Ntamba Ntamba, 2011) indicated that by using a Reynolds number which could account for the rheology of the liquids, the results for both Newtonian and non-Newtonian liquids would collapse onto the same line. The same correlation could then be used to predict the pressure loss or discharge coefficient. Dziubiński and Marcinkowski (2006) did not expand on the reason this approach did not work. Considering they did not provide data, the approach could not be tested to verify that their results would coincide when other Reynolds number approaches are used. Furthermore, the effect of yield stress should also be evaluated. There has not been a study done for the discharge of non-Newtonian liquids through any other orifice

shape other than a circular from a tank. The available research for the flow of non-Newtonian liquids through circular and triangular orifices was using pipes, covering the laminar, transition and turbulent flow conditions (Ntamba Ntamba, 2011). The data presented showed that the orifice shape does not have any effect on pipe flow. King and Wisler (1922) studied the discharge of water through circular, square and triangular orifices and Brater *et al.* (1996) presented results obtained for the flow of water through circular and square orifices from tanks. The data presented covered only the turbulent region. Therefore, the effects of orifice shape for non-Newtonian liquids discharge from a tank should be investigated.

1.2 Statement of research problem

Orifices are commonly used to regulate and measure the discharge of Newtonian liquids, due to their simplicity and ease of mechanical construction (McCabe *et al.*, 1993). However, there has been little research into flow rate measurement of non-Newtonian liquids using orifices, especially the flow from storage tanks. Storage tanks susceptible to atmosphere are often used on site to store different liquids. Pressure can build up in closed tanks when, for example, volatile liquids are stored. Overfilling, as well as overly rapid filling or emptying can result in additional pressure fluctuations. Leaks, pinholes or general corrosion can also affect tank levels and corresponding flow rates. The flow of non-Newtonian liquids through sharp crested orifices out of a tank, including factors which improve the efficiency of flow regulation and the accuracy of flow rate measurements, are currently not well understood.

1.3 Research question

Can a C_d -Re relationship be developed for Newtonian and non-Newtonian discharge through different orifice shapes from a tank by incorporating an effective shear rate?

1.4 Aims and objectives

The aim of this work is to determine the flow rate of Newtonian and non-Newtonian liquids using different shapes (circular, square and equilateral triangle) of sharp crested orifices out of a tank, as a function of the liquid flow properties and Reynolds number.

The objectives of the study were as follows:

- To determine the flow rates for various types and concentrations of Newtonian and non-Newtonian liquids through circular, triangular and square orifices;

- To measure the rheological properties of test liquids to evaluate the viscosity model parameters; and
- To establish a correlation between C_d values and Reynolds number for Newtonian and non-Newtonian liquids for all the orifices and develop the discharge model.

1.5 Scope of the work

The circular, triangular and square orifices were calibrated and the C_d values for each orifice were determined. Different concentrations of glycerine (v/v), CMC solutions (w/w), and bentonite (w/w) and kaolin (w/w) suspensions were prepared. The flow rate and rheology tests were conducted for each liquid concentration. The C_d values for different concentrations of the liquids and each orifice's shape and size was determined. The Reynolds number values for each liquid and orifice was calculated. The C_d -Re relationship was established and a discharge model developed.

1.6 Delineation

This study included flow rate measurements using circular, square and triangular orifices. Only sharp crested orifices were used.

1.7 Significance of the research

The success of this research will expand knowledge upon existing literature on the accuracy of measuring the flow rate of Newtonian and non-Newtonian liquids out of tanks by means of orifices. The industries which will benefit from this research include mining, chemical, food processing, wastewater treatment and medical-related applications.

1.8 Outcomes, results and contributions of the research

A new flow rate model for liquids (Newtonian and non-Newtonian) flowing through circular, square and equilateral triangular orifices out of a tank were established from this research. The results add to the existing database of the similar scant work by Dziubiński and Marcinkowski (2006). For the first time, this work presents a relationship for the prediction of C_d for flow out of a tank through different shapes of orifices. It also includes both Newtonian

and non-Newtonian liquids over a wide range of Reynolds numbers, covering both laminar and turbulent flow regions.

1.9 Organisation of dissertation

Chapter Two discusses the literature related to the flow rate measurement of Newtonian and non-Newtonian liquids using sharp-crested circular, square and triangular orifices from a tank. The rheology of Newtonian and non-Newtonian liquids is explained. It includes the effect of orifice shape on the flow of liquids in various experimental set up such as tanks, pipes, nozzles and gas flow. The study of the flow rate measurement of Newtonian and non-Newtonian liquids from tanks and pipes is discussed. The relationship between the non-dimensional numbers and the flows of non-Newtonian liquids in open channels, pipes and through weirs has been discussed.

Chapter Three describes in detail the equipment and research methodology used to complete this study. This includes the experimental procedure followed for the calibration of the equipment and the experimental procedure for the new flow rate measurement tests with Newtonian and non-Newtonian test liquids.

Chapter Four presents the rheological characterisation of test liquids, calibration and flow rate measurement results. The results are analysed and discussed in detail, along with the estimated uncertainties of the results.

Chapter Five discusses the calibration results of the orifices, the effect of orifice shape, the relationship between the C_d and Reynolds numbers, and a critical comparison with seminal results from the referenced literature.

Chapter Six explains the procedure for developing the prediction model for this study. The effective viscosity was obtained, and new definitions of Reynolds numbers proposed before using the single composite equation to develop the model for flow rate measurement of Newtonian and non-Newtonian liquids using circular, square and triangular orifices from the tank.

Chapter Seven draws together the conclusions and recommendations of this research, describing how the research question has been answered as well as research outcomes achieved. Recommendations for future studies are made.

CHAPTER TWO: LITERATURE REVIEW

2.1 Introduction

Liquids are classified as Newtonian and non-Newtonian. For Newtonian liquids, shear stress and shear rate have a linear relationship, passing through the origin, and the gradient of the linear graph being the coefficient of viscosity. Non-Newtonian liquids behave differently from Newtonian liquids. The relation between shear stress and shear rate varies for each type of non-Newtonian liquids, and additionally, some may exhibit yield stress. Therefore, a constant viscosity cannot be defined. These complex properties make it complicated to predict the non-Newtonian liquids' performance during storage, handling, transportation, processing and other applications, (Triantafillopoulos, 1988). An orifice used for gravitational tank drainage can be a challenge, especially under the laminar flow conditions (Joye *et al.*, 2003). Shah *et al.* (2012) stated that orifices are common hydraulic devices used to measure the flow rate of liquids, gases or slurries. A limited study has been conducted on the flow rate measurement of non-Newtonian liquids out of tanks using orifices (Dziubiński & Marcinkowski, 2006), therefore the discharge of liquids through orifices in pipes, nozzles and gas flow has been included in this study for comparison purpose. This study concentrates on the discharge of fluids through sharp-crested orifices with an L/d ratio of almost zero. The following topics are reviewed:

- rheology of liquids;
- orifices; and
- flow of Newtonian and non-Newtonian fluids through orifices

2.2 Rheology of liquids

Rheology is the science of deformation and flow of matter (Bingham, 1916). Newtonian liquids show a linear relationship between shear stress and shear rate. Non-Newtonian liquids do not have a linear relationship, nor do they obey Newton's law of viscosity in other aspects (Metzner & Reed, 1955; Malkin & Isayev, 2006; Chhabra & Richardson, 2008). Non-Newtonian liquids are grouped into three categories: time-independent, time-dependent and viscoelastic. In this work, the liquids tested were characterised by three rheological models, namely, the Bingham plastic, pseudoplastic and yield-pseudoplastic models (Malkin & Isayev, 2006).

2.3 Rheometer

A rheometer is used to measure the rheology of liquids, to predict their steady shear behaviour during handling, transportation, processing and application. The consistency curves of the liquids are produced by plotting the observed torque against revolutions per minute. The liquid characterisation is based on determining the absolute viscosity and displaying shear stress as a function of shear rate (Triantafillopoulos, 1998). There are various types of rheometers, including rotational and tube. Rotational rheometers use various shearing geometries such as concentric cylinders, wide gap rotational, cone-and-plate and parallel plate.

Metzner and Reed (1955) stated that it is generally satisfactory to use rotational viscometers to evaluate liquid consistency index (k) and flow behaviour index (n) values. However, it is ideal to carry out the viscometric test over the shear rate range, which will be encountered in the application at hand (Chhabra & Richardson, 2008).

2.4 Newtonian liquids

A Newtonian liquid is identified by having a linear relationship between the applied shear stress and shear rate under laminar and incompressible conditions (Myles 2003; Chhabra & Richardson, 2008; Kobo, 2009; Sochi, 2009). The liquid shear, due to the application of force F , is at a steady state condition over the distance between two parallel plates (Fig. 2.1). The force F is balanced by an equal and opposite internal, frictional force in the liquid.

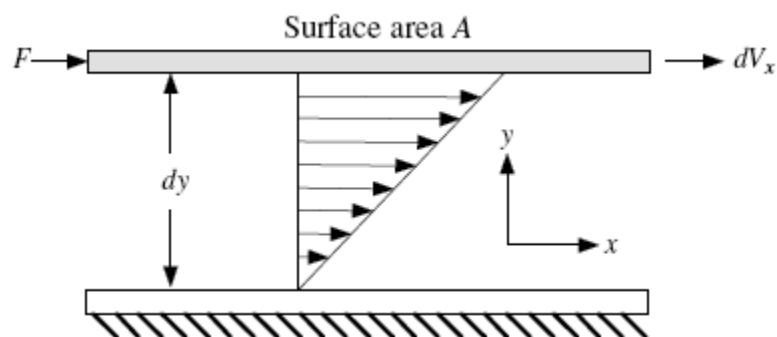


**Figure 2.1 Schematic representation of unidirectional shearing flow
(Chhabra & Richardson, 2008)**

Therefore, the shear stress is expressed as directly proportional to the shear rate, having a constant viscosity. This linear relationship is expressed in Eq. 2.1 (Chhabra & Richardson, 2008).

$$\frac{F}{A} = \tau_{yx} = \mu \left(-\frac{dv_x}{dy} \right) = \mu \dot{\gamma}_{yx} \quad (2.1)$$

2.5 Non-Newtonian liquids

Non-Newtonian liquids are identified by their nonlinearity or initial yield-stress when articulated in terms of the relationship between shear stress and strain rate (Metzner & Reed, 1955; Malkin & Isayev, 2006; Chhabra & Richardson, 2008; Sochi, 2009). They are classified into three groups: time-independent, time-dependent and visco-elastic liquids (Rashaida, 2005; Chhabra & Richardson, 2008; Sochi, 2009).

2.5.1 Time-independent liquids

Time-independent liquids are defined by the dependence of shear rate on shear stress, at a given point. The viscosity of time-independent liquids appears to be Newtonian at low shear rates, but it varies with increasing shear rates (Skelland, 1967; Sochi, 2009). If the viscosity decreases, the liquid is defined as pseudoplastic or shear-thinning, and shear-thickening if the viscosity increases with the increasing shear rate (Sochi, 2009). If the liquid requires an initial stress before flowing, it is called a yield-stress or viscoplastic liquid. Figure 2.2 presents the flow curves for different types of time-independent liquids.

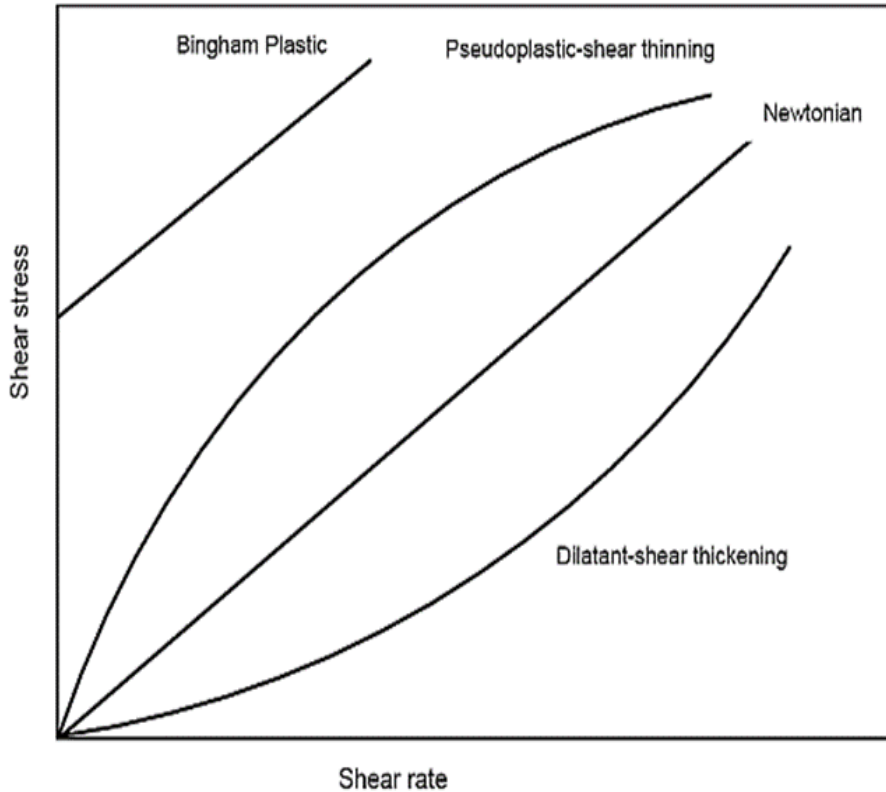


Figure 2.2 Types of time-independent flow curves (Chhabra & Richardson, 2008)

2.5.2 Shear-thinning or pseudoplastic

The relationship between shear stress and shear rate for shear-thinning liquids is easily described by a double logarithmic scale plot and is estimated by a straight line on a shear stress-shear rate plot (power law model). The model is expressed by Eq. 2.2 (Chhabra & Richardson, 2008; Sochi, 2009):

$$\tau = k \left(-\frac{dv}{dy} \right)^n \quad (2.2)$$

When $n < 1$, the liquid is pseudoplastic (shear-thinning); when $n > 1$, the liquid is known as dilatant (shear-thickening); and when $n = 1$, the liquid is Newtonian and $k = \mu$.

2.5.3 Viscoplastic liquid

Viscoplastic liquids behave like solids below a certain critical shear stress. For these liquids to flow, they must be subjected to an initial stress to initiate shearing. Once the yield-stress value is exceeded, the material flows like a liquid. Bingham plastic and yield-pseudoplastic liquids are classified as viscoplastic liquids.

Once the Bingham plastic liquids start to flow, they exhibit a linear relationship between shear stress and shear rate (Rashaida, 2005). The Bingham plastic model is expressed in Eq. 2.3.

$$\tau = \tau_{y(B)} + k \left(-\frac{dv}{dy} \right) \quad (2.3)$$

The Herschel–Bulkley model (Herschel & Bulkley, 1926) is normally used for the yield-pseudoplastic behaviour and is formulated as:

$$\tau = \tau_y + k \left(-\frac{dv}{dy} \right)^n \quad (2.4)$$

2.5.4 Viscosity

Viscosity is described as the internal friction of a liquid that opposes any change in its motion. Viscosity is defined as the ratio of shear stress to shear rate, in steady-state flow. The apparent viscosity for non-Newtonian liquids is expressed by Eq. 2.5 (Kestin, 1988; Bird *et al.*, 2002).

$$\mu = \frac{\tau}{\frac{dv}{dy}} \quad (2.5)$$

The apparent viscosity for power law liquids decreases with the increasing shear rate. It is expressed by Chhabra and Richardson (2008) as shown in Eq. 2.6:

$$\mu = k(\dot{\gamma})^{n-1} \quad (2.6)$$

The k value can be viewed as an apparent viscosity at the shear rate of unity in Pa.sⁿ.

The apparent viscosity for viscoplastic liquids decreases with increasing shear rate. Bingham plastic liquids are denoted by a constant plastic viscosity (Chhabra & Richardson, 2008). The apparent viscosity for Bingham plastic liquids is given in Eq. 2.7:

$$\mu'_B = k + \left(\frac{\tau_y}{\dot{\gamma}} \right) \quad (2.7)$$

For yield-pseudoplastic liquids, apparent viscosity is expressed in Eq. 2.8 as:

$$\mu' = k\dot{\gamma}^{n-1} + \left(\frac{\tau_y}{\dot{\gamma}} \right) \quad (2.8)$$

Chhabra and Richardson (2008) stated that it is still a challenge to obtain appropriate rheological data for sudden changes in geometry, such as orifice plates, especially for non-Newtonian liquids.

2.6 Dimensionless parameters

Dimensionless numbers are typically used to outline information about the physics of problems in liquids mechanics. They are incorporated in the number of experiments, to understand the role of different parameters. The dimensionless numbers that tend to infinity or zero help determine the limiting cases. Newtonian liquids are clearly a reference to non-Newtonian liquids. Dimensionless numbers, such as the Bingham number, is zero in the case of Newtonian liquids and so they express the viscoplastic characteristics of non-Newtonian liquids (Thompson & Soares, 2016).

2.6.1 Bingham number

The Bingham number is the ratio of the yield-stress to viscous stress. It can be defined by Eq. 2.9 (Thompson & Soares, 2016; Csizmadia & Till, 2018):

$$Bi = \frac{\tau_{y(B)} D}{\mu'_B v} \quad (2.9)$$

2.6.2 Reynolds number

The Reynolds number (Re) is a ratio of the inertial forces to viscous forces. The generalised Reynolds number is illustrated in Eq. 2.10 and can be applied to any rheological model (Csizmadia & Till, 2018).

$$Re_{Gen} = \frac{8\rho v^2}{\tau_w} \quad (2.10)$$

The pipe Reynolds number for Newtonian liquids is expressed as:

$$Re = \frac{\rho v D}{\mu} \quad (2.11)$$

For non-Newtonian liquids, there are different definitions of Re derived from the generalised Reynolds number, as presented in Eqns. 2.12, 2.13, 2.14 and 2.16 (Csizmadia & Till, 2018).

Power law liquid:

$$Re_{GenPL} = \frac{\rho v^{2-n} D^n}{8^{n-1} k \left(\frac{3n+1}{4n} \right)^n} \quad (2.12)$$

Bingham plastic liquid:

For Bingham liquid flows, the appropriate Reynolds number definition depends only on the Bingham viscosity as given in Eq. 2.13.

$$Re_B = \frac{\rho v D}{\mu'_B} \quad (2.13)$$

or

$$Re_{GenB} = \frac{\rho v D}{\frac{\tau_y}{8} \left(\frac{D}{v} \right) + \mu_B \left(\frac{3m+1}{4m} \right)} \quad (2.14)$$

Where

$$m = \frac{\mu_B \left(\frac{8v}{D} \right)}{\tau_y + \mu_B \left(\frac{8v}{D} \right)} \quad (2.15)$$

Herschel-Bulkley liquid:

$$Re_{GenHB} = \frac{\rho v^{2-n} D^n}{\frac{\tau_y (D)}{8}^n + 8^{n-1} \mu_{HB} \left(\frac{3m+1}{4m} \right)^n} \quad (2.16)$$

2.6.3 Slatter and Lazarus (1993) Reynolds numbers

Slatter and Lazarus (1993) defined the Herschel-Bulkley liquids Reynolds number by incorporating yield-stress into the Clapp Reynolds number as given in Eq. 2.17.

$$Re_2 = \frac{8\rho v^2}{\tau_y + k \left(\frac{8v}{D} \right)^n} \quad (2.17)$$

2.6.4 Slatter (1997) Reynolds numbers

Slatter (1997) developed Re_3 given in Eq. 2.18, derived from the definition of Slatter and Lazarus (1994) Re for pipe flow by rejecting the plug-flow region as non-liquid behaviour and considering only the sheared liquid in the annulus. Figure 2.3 illustrates the geometry of the pipe flow and plug. The Slatter (1997) Reynolds number was used to illustrate the flow of non-Newtonian liquids through orifices installed in pipes (Chowdhury, 2010; Ntamba Ntamba, 2011).

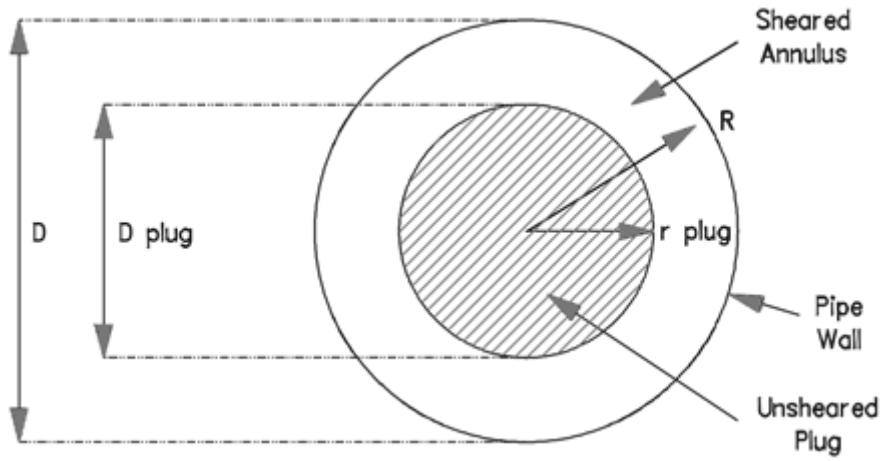


Figure 2.3 Unsheared plug geometry (Slatter, 1997)

$$Re_3 = \frac{8V_{\text{ann}}^2 \rho}{\tau_y + k \left(\frac{g V_{\text{ann}}}{D_{\text{shear}}} \right)^n} \quad (2.18)$$

Where

$$V_{\text{ann}} = \frac{Q_{\text{ann}}}{A_{\text{ann}}} \text{ where } Q_{\text{ann}} = Q - Q_{\text{plug}} \text{ and } Q_{\text{plug}} = u_{\text{plug}} A_{\text{plug}} \quad (2.19)$$

A_{ann} is given in Eq. 2.20

$$A_{\text{ann}} = \pi(R^2 - r_{\text{plug}}^2) \text{ and } r_{\text{plug}} = \frac{\tau_y}{\tau_0} R \quad (2.20)$$

And

$$D_{\text{shear}} = D - D_{\text{plug}} \text{ where } D_{\text{plug}} = 2r_{\text{plug}} \quad (2.21)$$

2.6.5 Metzner and Reed (1955) Reynolds numbers

Metzner and Reed (1955) developed a generalised Reynolds number for the time-independent non-Newtonian liquids, for laminar flow in circular pipes. They substituted wall shear stress in terms of the Fanning friction factor (f) Eq. 2.22:

$$f = \frac{2\tau_w}{\rho v^2} \quad (2.22)$$

They used an expression for true shear rate at the wall ($\dot{\gamma}_w$), from the nominal shear rate ($8v/D$) developed by Rabinowitsch-Mooney to determine the slope (n') of the log-log plot of wall shear stress vs. ($8v/D$) for time-independent, non-Newtonian liquids. Therefore, the wall shear stress is expressed as:

$$\tau_w = k' \left(\frac{8v}{D} \right)^{n'} \quad (2.23)$$

Substituting Eq. 2.23 in Eq. 2.22:

$$f = \frac{2}{\rho v^2} k' \left(\frac{8v}{D} \right)^{n'} \quad (2.24)$$

The Reynolds number was defined so that it is related to f in the same way as it is for Newtonian liquids in the laminar flow region.

$$f = \frac{16}{Re_{MR}} \quad (2.25)$$

And

$$Re_{MR} = \frac{\rho v^{2-n} D^{n'}}{8^{n'-1} k'} = \frac{8 \rho v^2}{k' \left(\frac{8v}{D} \right)^{n'}} \quad (2.26)$$

For power law liquids, n' and k' are constants (Chhabra & Richardson, 2008; Benslimane *et al.*, 2016).

$$n = n' \quad (2.27)$$

$$k' = k \left(\frac{3n+1}{4n} \right)^n \quad (2.28)$$

For Bingham plastic liquids n and k are given in Eqns. 2.29 and 2.30.

$$n' = \frac{1 - \frac{4}{3}\phi + \frac{\phi^4}{3}}{1 - \phi^4} \quad (2.29)$$

$$k' = \tau_w \left[\frac{\mu_B}{\tau_w \left(1 - \frac{4}{3}\phi + \frac{\phi^4}{3} \right)} \right]^{n'} \quad (2.30)$$

Where

$$\phi = \frac{\tau_y}{\tau_w} \quad (2.31)$$

Desouky and Al-Awad (1998) expressed n' and k' for yield-pseudoplastic liquids (Herschel-Bulkley model), as shown in Eq. 2.32:

$$\frac{1}{n'} = \frac{1}{n} + \frac{\lambda_1}{\lambda_2}, \quad (2.32)$$

Where

$$k' = \frac{\tau_w}{\lambda_3^{n'}}, \quad (2.33)$$

And

$$\lambda_1 = \phi(1 - \phi)^{n_3 - 1} + (1 - \phi)^{n_2 - 1} [2\phi^2 - 2\phi(1 - \phi)/n_2] + (1 - \phi)^{n_1 - 1} [\phi^3 - 2\phi^2(1 - \phi)/n_1] \quad (2.34)$$

$$\lambda_2 = (1 - \phi)^{n_3}/n_3 + 2\phi(1 - \phi)^{n_2}/n_2 + \phi^2 (1 - \phi)^{n_1}/n_1 \quad (2.35)$$

$$\lambda_3 = \left[4(\tau_w/k)^{1/n'} \lambda_2 \right]^{n'} \quad (2.36)$$

$$n_1 = (1 + n)/n \quad (2.37)$$

$$n_2 = (1 + 2n)/n \quad (2.38)$$

$$n_3 = (1 + 3n)/n \quad (2.39)$$

Poole and Ridley (2007) concluded that at a high Reynolds numbers in pipe flow, Re_{MR} collapses the constant development length of power-law liquids curves onto the Newtonian curve. However, at lower Re_{MR} , the constant development length is a function of n . Fester *et al.* (2008) established the relationship between the pressure loss coefficient in sudden pipe contractions and different definitions of Reynolds number, including (Re_{Gen} , Re_{MR} and Re_3) for Newtonian liquids and Non-Newtonian liquids, mainly for Power law and yield-pseudoplastic liquids. The Reynolds numbers that best accounted for the rheological properties of the liquids collapsed the pressure loss coefficient data of non-Newtonian liquids curve to the Newtonian liquids curve in the laminar, transition and turbulent regions. The gravitational flow of Newtonian and non-Newtonian liquids (power law) from tanks, studied by Dziubiński and Marcinkowski (2006), shows that the use of Re_{MR} fails to collapse the non-Newtonian liquids curve to Newtonian liquids curve.

2.6.6 Euler number

Euler number is the ratio of pressure force to inertial force. Eq. 2.40 is used to calculate the Euler number (Della Valle *et al.*, 2000)

$$Eu = \frac{\Delta p}{\left(\frac{1}{2}\right)\rho v^2} \quad (2.40)$$

2.7 Orifices

Orifices are commonly used to control the discharge rate from pipes, channels, reservoirs and tanks (Tullis *et al.*, 2008). They come in different types, shapes and sizes. Figure 2.4 shows different shapes of sharp-crested orifices. Orifices can be installed on the side of the tank to distribute flow to parallel processes such as flocculation basins, sedimentation tanks and aeration basins in water and wastewater treatment plants (Ramamurthy *et al.*, 1986). Sometimes, orifices are used for bubble formation in industrial processes. The bubble formation sets the initial conditions for chemical reactions from a dispersed gaseous phase to liquid phase, heat and mass transfer and hydrodynamics (Dietrich *et al.*, 2013).

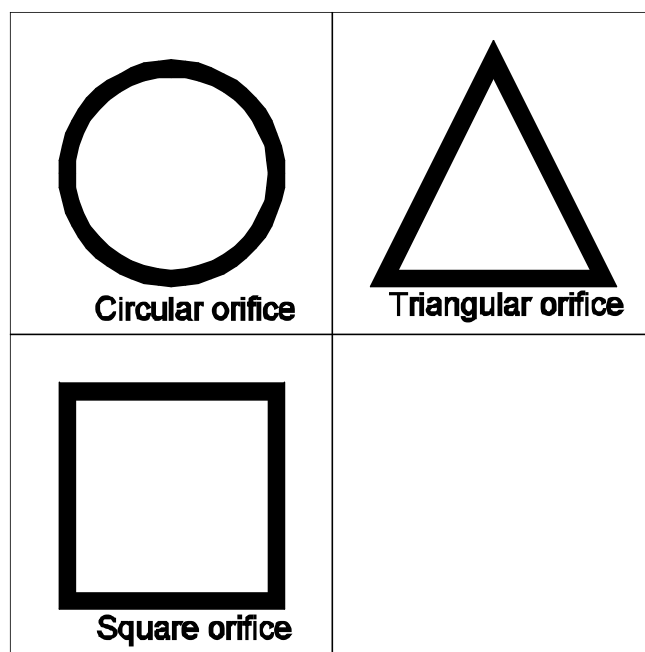


Figure 2.4 Different shapes of sharp crested orifices
(van Melick & Geurts, 2013; Dandwate *et al.*, 2016)

2.7.1 Orifice discharge coefficient

Orifice discharge coefficient (C_d), a ratio between theoretical and actual flow, is a function of orifice geometry, liquid properties and flow conditions. The physical quantities that affect the discharge include tank width, orifice diameter, length and entrance shape. If the orifice is much smaller than the tank, the width of the tank is not a significant parameter (Tuğçe, 2010). However, Joye *et al.* (2003) illustrated that for the laminar flow through an orifice, the C_d is a strong function of the Reynolds number. For turbulent flow, $C_d = 0.61$ is commonly used as a

coefficient for sharp crested orifices. Spencer (2013) indicated that a range of 0.60 to 0.64 is suggested by Bos (1989), depending on the orifice diameter.

2.7.2 Orifice discharge equation

Determining an orifice flow rate relation typically starts with the application of the Bernoulli in Eq. 2.41 (Prohaska, 2008; Hicks & Slaton, 2014).

Figure 2.5 illustrates a schematic diagram of flow from a tank at atmospheric pressure through an orifice fitted at the bottom.

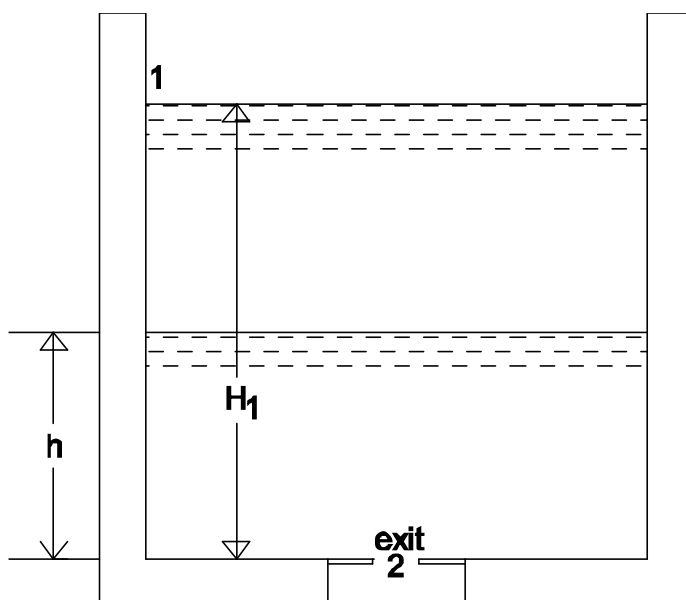


Figure 2.5 Flow from a tank at atmospheric pressure

Consider liquid flow moving from position 1, some distance from the orifice to position 2, at the orifice exit in Fig. 2.5.

$$\frac{v_1^2}{2g} + \frac{P_1}{\rho g} + H_1 = \frac{v_2^2}{2g} + \frac{P_2}{\rho g} \quad (2.41)$$

The two points are at atmospheric pressure and therefore can be derived from Eq. 2.41:

$$P_1 = P_2 = P_{atm}, \quad (2.42)$$

and

$$v_1 \ll v_2 \quad (2.43)$$

Therefore

$$v_2^2 = 2gH_1 \quad (2.44)$$

For continuous flow, the velocity is not constant from the initial height (H_1) to any height (h) between position 1 and 2.

Therefore, $H_1 \geq h$ and the theoretical velocity at the outlet is

$$v_2 = \sqrt{2gh} \quad (2.45)$$

The actual velocity is given by Eq. 2.46

$$v_{2\text{act.}} = C_d \sqrt{2gh} \quad (2.46)$$

The continuity equation yields

$$Q_1 = Q_2, \quad (2.47)$$

Therefore, for an incompressible liquid,

$$A_T v_1 = A_0 v_2 \quad (2.48)$$

Substituting Eqns. 2.45 and 2.47 into Eq. 2.46, Q_1 becomes:

$$Q_1 = C_d A_0 \sqrt{2gh} \quad (2.49)$$

2.7.3 Effect of orifice shape

Orifices are used in the following applications: flow from a tank, pipe, and nozzle/spray as well as for airflow. For reference, and comparative purposes, it is important to include the study of fluid discharge using different shaped orifices under these applications. Liquids are transported through pipes and stored in tanks. Orifices are used to regulate and measure the flow rate of the liquids into pipes. They are inserted in tanks and in spraying systems to discharge fluids (Swamee & Swamee, 2010; Ntamba Ntamba, 2011; Novák & Koza, 2013). The C_d versus head relationship has been used to illustrate the effect of orifice shape for water especially for orifices with different sizes. For non-Newtonian and viscous Newtonian liquids C_d versus Reynolds number curves have been used to compare the orifice shapes because their discharge depends on orifice geometry and rheological characteristics.

2.7.3.1 Tank flow

Brater *et al.* (1996) presented Smith's (1886) water experiment data for circular and square orifices with equal hydraulic diameters (Fig. 2.6). From Fig. 2.6, the C_d values of square orifices are higher than the C_d values of circular orifices for diameters larger than 5 mm. However, the experimental results of Smith (1886) and Prohaska (2008) showed that the smaller the orifice diameter, the higher the coefficient of discharge and the lower the Re values; and as the size of the orifice increases, the coefficient of discharge decreases and Re values increase. Prohaska (2008) showed that there is a significant increase in the C_d values for head values below one meter because the driving force is reducing as the liquid get discharged.

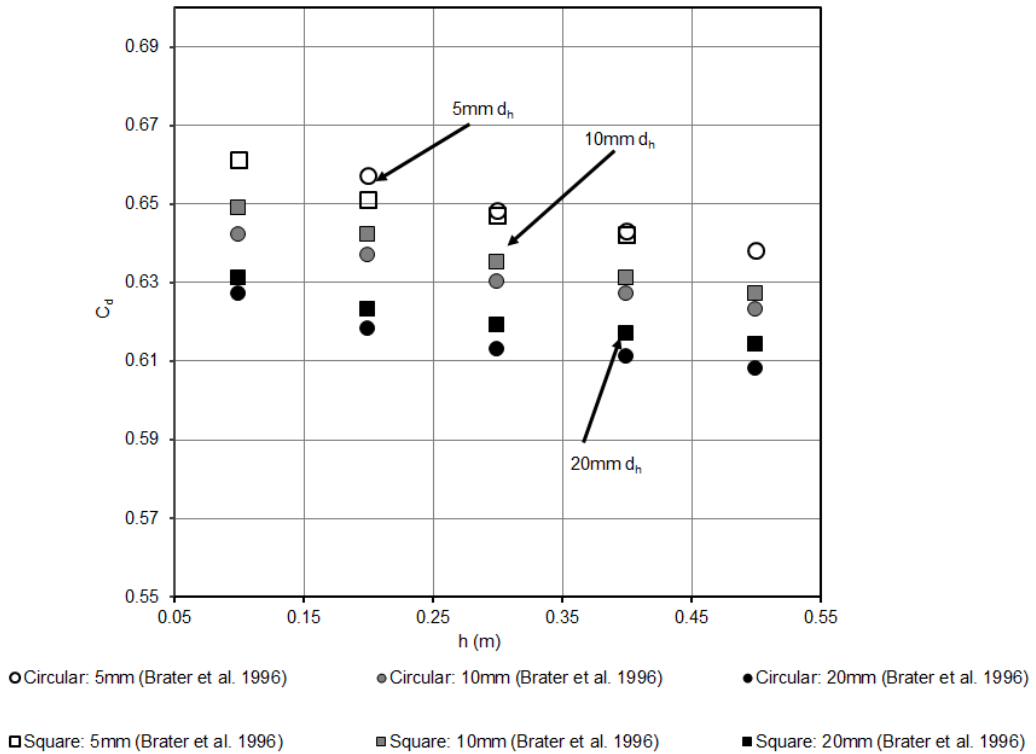
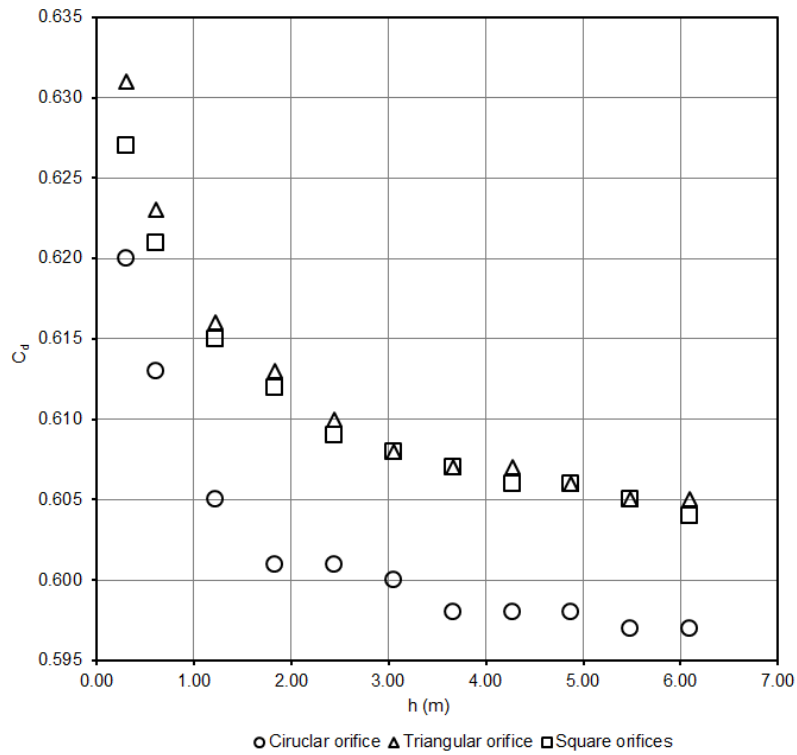


Figure 2.6 C_d vs head (m) for circular and square orifices (Brater et al., 1996)

In the early 1900s, hydraulics books, such as those written by Bovey (1901) and King and Wisler (1922), presented results of the flow of water from a tank through different shaped orifices. Circular, triangular and square orifices were used. The area of the equilateral triangular orifice was $3.23 \times 10^{-3} \text{ m}^2$ and $4.03 \times 10^{-5} \text{ m}^2$ for the circular and square orifices. Figure 2.7 exhibits the relationship between the C_d values and head of the orifice flows. The average C_d value for a circular orifice was 0.60 and the average C_d values for square and triangular orifices were 0.61. This is due to the restricted back flow and reduced forward flow caused by the angles of the non-circular orifices. The square and triangular orifices average C_d values were within $\pm 2\%$ of the average circular orifice C_d value.



**Figure 2.7 C_d vs. h (mm) for circular, equilateral triangular and square orifices
(King & Wisler, 1922)**

2.7.3.2 Pipe flow

Dandwate *et al.* (2016), studying the effect of orifice shape through a pipe, found the C_d value of 0.68 for a 15 mm diameter orifice and 0.695 for the 20 mm equilateral triangular orifice and the difference between these orifices C_d values is within $\pm 2\%$. Van Melick and Geurts (2013) conducted direct numerical simulation (DNS) on circular, square, triangular, star and Koch-2 shaped orifices in laminar and turbulent pipe flow. In evaluating a pressure drop at $Re=1$ (laminar flow) and $Re=4300$ (turbulent flow), they determined that the pressure drop in the laminar region increased with the increasing complexity of the orifice perimeter, and it was higher for fractal-shape orifices as compared to the circular orifices. The perimeter of the larger fraction of the fractal-shape orifices is closer to the pipe wall and that resulted in stronger decelerating viscous forces and higher velocities near the center of the orifice. Therefore, the larger velocity gradients increased the pressure drop for laminar flow.

For turbulent flow, the circular orifices showed a higher pressure drop than fractal-shaped orifices, and this is in agreement with the findings of Abou El-Azm Aly (2010) and Elsaey *et al.* (2014). Elsaey *et al.* (2014), who carried out numerical simulations using a CFD package for flow measurement of water through circular and fractal-shaped orifices, included an equilateral triangular shape. The flow through fractal-shaped orifices experienced constrained back flow behind the sharp protruding corners and that caused the forward flow to reduce. The circular orifice had a continuous back and forward flow which lead to the higher pressure drop.

The velocity of the liquid, after flowing through the equilateral triangular orifice, recovered faster as compared to the circular orifice due to the flow restriction and decrease with complexity of fractal generation. Abou El-Azm Aly (2010) experimentally studied the pressure drop of water for circular, an equilateral triangle and fractal-shaped orifices installed in turbulent pipe flows. The circular and triangular orifices had an equal area. Triangular orifices are considered to be geometrically similar to circular orifices and not classified as a fractal-shape. Thus, there was no difference between the pressure drop for circular and triangular orifices (Abou El-Azm Aly, 2010; van Melick & Geurts, 2013; Elsaey *et al.* 2014).

Ntamba Ntamba (2011) carried out discharge experiments in pipes using short square-edged orifice plates for water (Newtonian liquid), CMC solutions, and kaolin and bentonite suspensions (non-Newtonian liquids). They used circular orifices with 0.2, 0.3, 0.57 and 0.7 diameter ratios and the triangular shaped orifice with a diameter ratio of 0.57 with sharp apex and round apex. The data analysis for his study was based on a coefficient of discharge and Reynolds number relationship. For diameter ratios of 0.57 for circular and triangular orifices, the transition zone ranged from $Re = 400$ to $Re = 1000$, and the turbulent region occurred at $Re > 1000$. The average C_d values for circular and triangular with sharp apex and round apex orifices were found to be 0.63, 0.65 and 0.64 respectively. The orifice shapes did not have a

significant effect on the discharge measurement of non-Newtonian liquids in pipe flow, as shown in Fig. 2.8, especially at high Reynolds numbers.

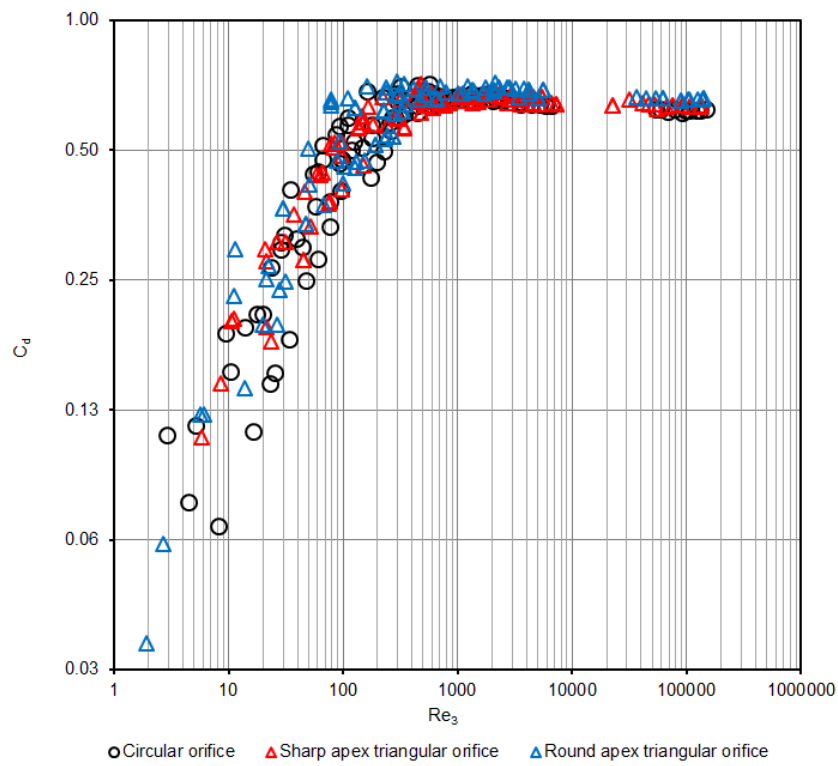


Figure 2.8 C_d versus Re_3 for short, square-edged circular, sharp and round apex triangular orifices with an equivalent diameter ratio of $\beta=0.57$ (Ntamba Ntamba, 2011)

2.7.3.3 Nozzle/sprays flow

Rajesh *et al.* (2016) studied the characteristics of interfacial oscillations of water, water-glycerol mixture and aviation kerosene discharging from a tank under pressure by means of a compressed air supply and air pressure regulator through non-circular orifices. The elliptical, triangular, and square shapes of equivalent diameters in the range 4.82-4.97 mm, with an equal area were used to conduct the tests. They analysed the wavelength of the flow for all the liquids and orifices. The square orifice had the shortest wavelength compared to the triangular orifice. The liquid jet of aviation kerosene underwent a larger increase in wavelength along the axis of the jet, as compared to the jets of water and water-glycerol. This might be due to the different viscous properties of the liquids.

Wang and Fang (2015) studied the liquid jet breakup for non-circular orifices at low pressures through a nozzle. The hydraulic diameters of circular, square and triangular orifices were, 0.308, 0.288 and 0.256 mm, respectively. They concluded that circular orifices produce stable flows contrasting square and triangular orifices. Square and triangular jets are more prone to wind effect and very unstable at high pressure conditions (Wang & Fang, 2015). The non-circular jet can, however, be used as an efficient technique for passive flow control to improve sprays in practical applications such as nozzle design on the spray droplets (Gutmark & Grinstein, 1999; McGuinness *et al.*, 2005). Wang and Fang (2015) stated that the circular orifices have the largest Reynolds numbers followed by square, triangular and rectangular orifices. The difference in the Reynolds number is due to the difference in the hydraulic diameters. The circular and square orifice's Reynolds numbers are similar at low pressure but differ as the pressures increases. At high pressure the introduction of sharp corners in the square nozzle lead to the significant increase of the fine-scale turbulence.

2.7.3.4 Gas flow

Novák and Koza (2013), measuring the discharge of gases through circular, square and triangular orifices from a tank, concluded that the discharge coefficient of circular and square orifices with the same flow areas are closely related but differ as the area increases. The discharge coefficients for triangular orifices were much higher than the circular orifices, but the difference in the results decreased with the increasing area of the orifice. Hanafizadeh *et al.* (2018), studying the effect of orifice shapes on the bubble formation mechanism, determined the relationship between Re and flow rate. The Re-flow rate relationship was the same for all the orifice shapes.

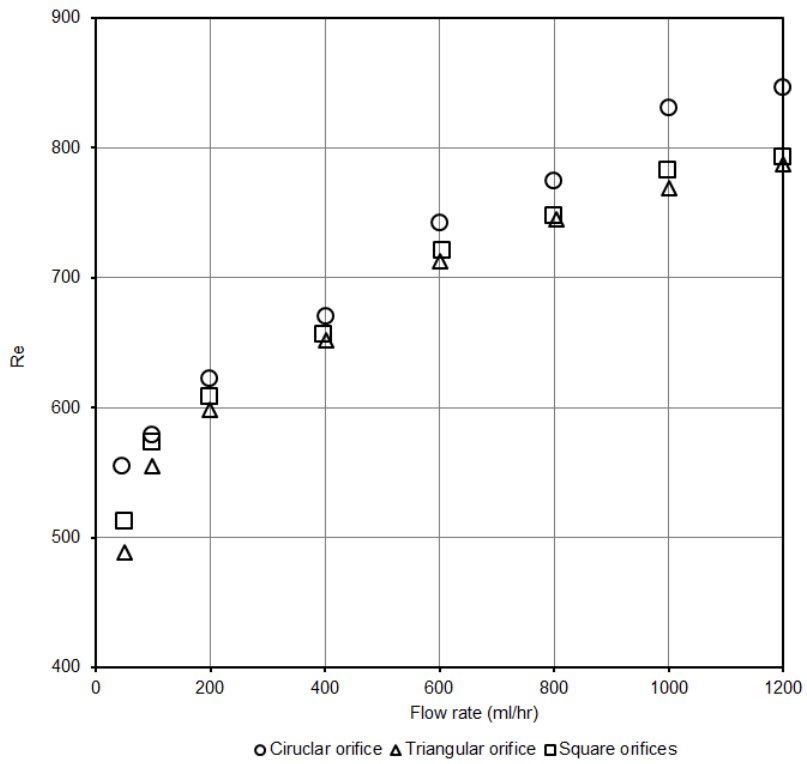


Figure 2.9 Re versus flow rate (ml/hr) for circular, equilateral triangular and square orifices
(Hanafizadeh et al., 2018)

2.7.4 Liquid flow through orifices from tanks

2.7.4.1 Swamee and Swamee (2010)

Swamee and Swamee developed a unified discharge equation for sharp-crested orifice flow that provided a smooth transition between laminar and turbulent flow. They used Lea's (1942) results that were re-analysed and presented by Brater *et al.* (1996), as shown in Fig. 2.10. Lea (1942) measured the discharge of highly viscous Newtonian liquids from a tank using orifices.

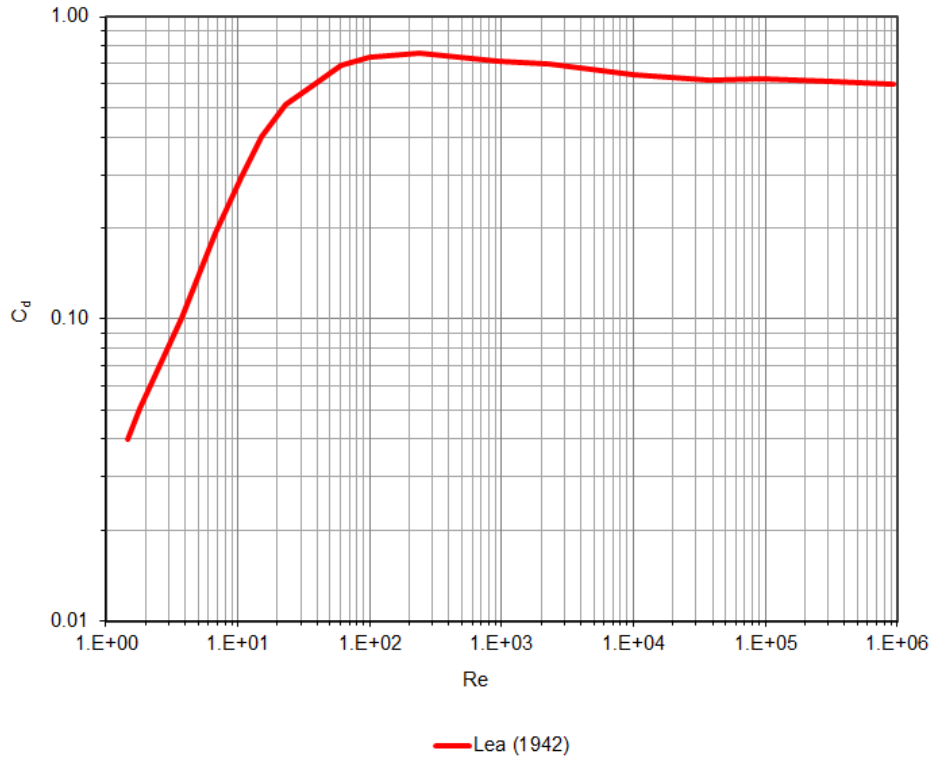


Figure 2.10 Re- C_d relationship for $L/d = 0$ (Brater et al., 1996; Swamee & Swamee, 2010)

Swamee and Swamee (2010) indicated that the discharge coefficient depends on the composite parameter given by (Eq. 2.50).

$$\frac{d(gh)^{1/2}}{\nu} \quad (2.50)$$

For small values of Reynolds numbers, the C_d versus Re relationship is linear on a double logarithmic plot. Therefore, C_d is expressed by Eq. 2.51 as:

$$C_d = \frac{0.0268d\sqrt{gh}}{\nu} \quad (2.51)$$

For higher values of Re, the discharge coefficient is fitted to Eq. 2.52:

$$C_d = 0.611 \left(1 + \frac{4.5v}{d\sqrt{gh}} \right)^{0.882} \quad (2.52)$$

Eqns. 2.51 and 2.52 were combined to produce Eq. 2.53. The equation was fitted to Lea's (1942) data and the error of the fitted predicted C_d values was within $\pm 1\%$.

$$C_d = 0.611 \left[87 \left(\frac{v}{d\sqrt{gh}} \right)^{1.43} + \left(1 + \frac{4.5v}{d\sqrt{gh}} \right)^{-1.26} \right]^{-0.7} \quad (2.53)$$

The orifice discharge was calculated using Eq. 2.54:

$$Q = \frac{\pi}{4} C_d d^2 \sqrt{2gh} \quad (2.54)$$

By combining Eq. 2.53 and 2.54, Q is predicted by Eq. 2.55:

$$Q = 0.679 d^2 \sqrt{gh} \left[87 \left(\frac{v}{d\sqrt{gh}} \right)^{1.43} + \left(1 + \frac{4.5v}{d\sqrt{gh}} \right)^{-1.26} \right]^{-0.7} \quad (2.55)$$

When viscosity is equal to 0 and at a very high Reynolds number, the flow rate reduces to Eq. 2.56.

$$Q = 0.679 d^2 \sqrt{gh} \quad (2.56)$$

When μ is infinity, for highly viscous flow, Eq. 2.55 reduces to Eq 2.57,

$$Q = \frac{0.0298 d^3 g h}{v} \quad (2.57)$$

This means that at high Reynolds numbers, the average C_d value depends on the size and shape of the orifice, at the same time the viscous effects in the laminar flow cannot be eliminated, but this study is proposing a method to account for it. This is in agreement with the study done by Smith's (1886) and Prohaska (2008). The developed discharge equations apply only for Newtonian liquids and do not include non-Newtonian liquids.

2.7.4.2 Marcinkowski and Dziubiński (2004) and Dziubiński and Marcinkowski (2006)

Marcinkowski and Dziubiński (2004) studied the flow of non-Newtonian liquids from different diameter orifices from tanks. They used orifices with diameter ratios of 0, 0.35, 0.5, 0.75, 1 and 3 and diameters 5, 8, 12.5 and 17 mm. They tested various concentrations of CMC solutions and established a relationship between C_d values and Re_{MR} , arguing that the shear rate obtained from the discharge of orifices from tanks is not $8v/d$, as it is for pipe flows. $8v/D$ is the bulk shear rate in pipe flow. In laminar Newtonian pipe flow it is the shear rate at the pipe wall, and thus related to the shear stress at the pipe wall. For non-Newtonian fluids, the true shear rate at the wall is higher, but $8v/d$ remains to be used to determine the shear rate as pseudo shear rate, flow characteristic or bulk shear rate (Slatter, 1994). Marcinkowski and Dziubiński (2004) stated that in sharp crested orifices fitted to a tank, the flow is not fully developed and therefore the rheological properties of the liquid depend on the average shear rate in the orifice which can be shown in Eq. 2.58:

$$\dot{\gamma} = \frac{Fv}{d_h} \quad (2.58)$$

The factor: $F < 8$ for gravitational discharge of liquids through orifices from a tank.

Marcinkowski and Dziubiński (2004) used numerical simulation to obtain the F factor that was used to determine the shear rate. The F factors depended on the length over diameter ratio (L/d) for a fixed shape. The F factors, however, were not stated for each orifice. They concluded that Re_{MR} should be modified to Eq. 2.59:

$$Re_F = \frac{vd\rho}{k\left(\frac{Fv}{d}\right)^{n-1}} \quad (2.59)$$

Dziubiński and Marcinkowski (2006) conducted experiments using a cylindrical glass tank 0.2m in diameter with various test liquids: water, ethylene glycol and water solutions of starch syrup (Newtonian liquid), and CMC solutions (non-Newtonian liquid). The discharge coefficient was calculated using Eq. 2.60:

$$C_d = \frac{2D^2(\sqrt{H_0} - \sqrt{H_1})}{Td^2\sqrt{2g}} \quad (2.60)$$

Where

H_0 and H_1 are the initial and final water heads in a tank respectively. T is the time taken for water to drop from H_0 to H_1 .

The Reynolds number for Newtonian and non-Newtonian liquid discharge from tanks was calculated from the classical Reynolds number equation and Metzner and Reed (1955) Eqns. 2.12 and 2.26, respectively.

The discharge coefficient of Newtonian liquids and CMC solutions were plotted against Reynolds numbers, Re and Re_{MR} respectively. They established that the discharge coefficient for both Newtonian liquids and CMC solutions increased with an increasing Reynolds number for the laminar flow region which became constant in the turbulent flow region. The discharge coefficient value for Newtonian liquids was 0.62 and became constant at $Re > 100$ and for non-Newtonian liquids, the value is 0.67 for $Re_{MR}>100$ because of the different rheological properties of the non-Newtonian liquids.

The experimental points were used to fit the separate discharge coefficient models for Newtonian and non-Newtonian liquids. For $Re<10$, the experimental points were approximated by the curves that are described by the Power-law Eq. 2.61.

$$C_d = BRe^C \quad (2.61)$$

The constants B and C depend on the orifice geometry including L/d and orifice area. Coefficient C , for all Newtonian liquids and orifices, was close to 0.5 and it was substituted in Eq. 2.62 while for non-Newtonian liquids it was approximated to 0.426.

$$C_d = B'\sqrt{Re} \quad (2.62)$$

Coefficient B' depends on the ratio of orifice length to diameter (L/d) only and is approximated by:

$$B' = A_1 + A_2 \left(\frac{L}{d}\right)^{A_3} \quad (2.63)$$

The experimental data was correlated to obtain coefficients A_1 , A_2 , A_3 . Based on the above two Eqns. 2.62 and 2.63, the following correlation equations describe the discharge coefficient for the flow of Newtonian and non-Newtonian liquids, respectively, from tanks through small cylindrical orifices:

$$C_d = \left[0.186 - 0.0756 \frac{L^{0.333}}{d} \right] \sqrt{Re_{Gen}} \quad (2.64)$$

Eq. 2.64 has the following limiting factors:

$0.005 \text{ m} < d < 0.017 \text{ m}$; $0 < L/d < 3$; $0.273 \text{ Pa s} < \mu < 26.2 \text{ Pa s}$; $0.00226 < Re < 10$.

And

$$C_d = \left[0.101 - 0.0164 \left(\frac{L}{d}\right)^{0.48} \right] Re_{MR}^{0.426} \quad (2.65)$$

Eq. 2.65 has the following limitations:

$0.005 \text{ m} < d < 0.017 \text{ m}$; $0 < L/d < 3$; $1.45 \text{ Pa s}^n < k < 15.1 \text{ Pa s}^n$; $0.457 < n < 0.606$; $0.0495 < Re_{MR} < 100$.

Figure 2.11 presents the $Re-C_d$ relationship for $L/d=0$. The C_d values for non-Newtonian liquids are at different Reynolds numbers as compared to Newtonian liquids for the laminar flow region. This indicates that the rheological properties of non-Newtonian liquids have a notable effect during the gravitational discharge of the liquids through orifices. A similar behaviour is observed for all other L/d ratios of the orifices.

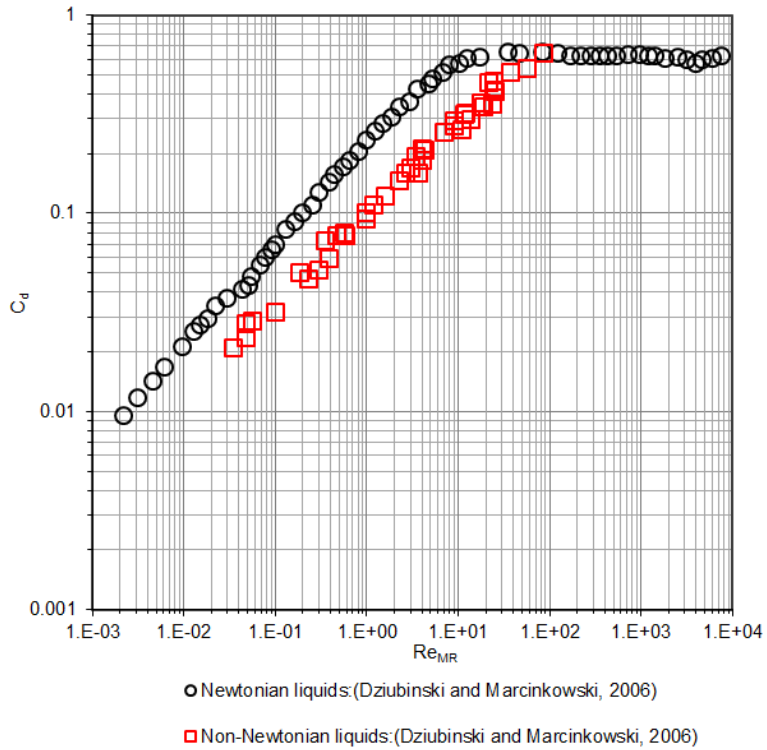


Figure 2.11 Re-C_d relationship for L/d = 0 (Dziubiński & Marcinkowski, 2006)

2.7.4.3 Liu et al. (2001)

Liu et al. (2001) conducted discharge experiments with water and machine oil, using two Plexiglas tanks connected on the side by an orifice. The outlet tubes with valves and differential pressure cells were connected to the tanks. They used a centrifugal pump to circulate the liquid through the loop. In this way, Liu et al. (2001) developed a model for the flow of water and oil through orifices based on the Fanning friction factor (f) for high Reynolds numbers flows through short circular pipes (Eq. 2.66).

$$fRe = 16 + k_L \frac{d}{L} Re \quad (2.66)$$

Where k_L is a function of $8/d$ and Re .

They stated that Eq. 2.66 is in agreement with the free flow through orifices. Liu et al. (2001) established that at high Reynolds numbers, $f Re$ is a linear function of Re and becomes constant at low Reynolds numbers. Thus, at low Re , the C_d value is proportional to the square root of the Reynolds number and becomes constant at high Reynolds numbers.

2.7.4.4 Della Valle et al. (2000)

This study investigated the extensional properties of various Newtonian and non-Newtonian liquids (Boger liquids and kaolin clay suspensions) at very high strain rates, similar to the strain rates encountered in the paper industry using an orifice. The Boger liquids used were diluted solutions of high molecular weight polyacrylamide in corn syrup. Newtonian liquids (mineral oils, corn syrup and water) were used for calibration purposes. A suspension of delaminated kaolin clay mixed with polyethylene glycol and water was also tested. The shear viscosity of the non-Newtonian liquids was measured with a concentric rheometer. The data used was obtained from the experimental set up and numerical data using CFD. An orifice was fitted between two identical cylindrical tanks. The measured pressure drop was used to calculate the Re and Eu numbers. The generalised Re (Eq. 2.12) was used for Newtonian liquids and Eq. 2.67 was used to calculate Re for the rest of the liquids.

$$Re_g = \frac{dvp}{k(F_d^v)^{n-1}} \quad (2.67)$$

The researchers analysed the plots of Eu versus Re. For Newtonian liquids, they found that at low Re, the flow is laminar and the pressure drop increases with the increase in viscosity, whilst the turbulent region indicates the pressure drop to be independent of the viscosity. The laminar region was encountered at Re<30.

The non-Newtonian liquids shear rate calculation from Eq. 2.58 suggested by Marcinkowski and Dziubiński (2004) was used to calculate the F value. The non-Newtonian liquids curves were similar to Newtonian liquids curve, but shifted. The area of the shift depended on the n value.

The Boger fluids data was collapsed to the Newtonian liquids master curve, by application of the effective flow rate where the F value obtained was 2.1

The Boger liquids showed positive, large deviations from Newtonian liquids because of their high extensional viscosity. They concluded that the vertical shift (R) between Newtonian liquids and Boger liquids was due to the ratio between the actual extensional viscosity and the Newtonian extensional viscosity (Trouton ratio) and it was three times greater than the shear viscosity multiplied by R. Figure 2.12 shows the flow curve obtained for Boger fluids and the Newtonian liquids master curve in a solid line.

$$\eta_E = 3\eta R \quad (2.68)$$

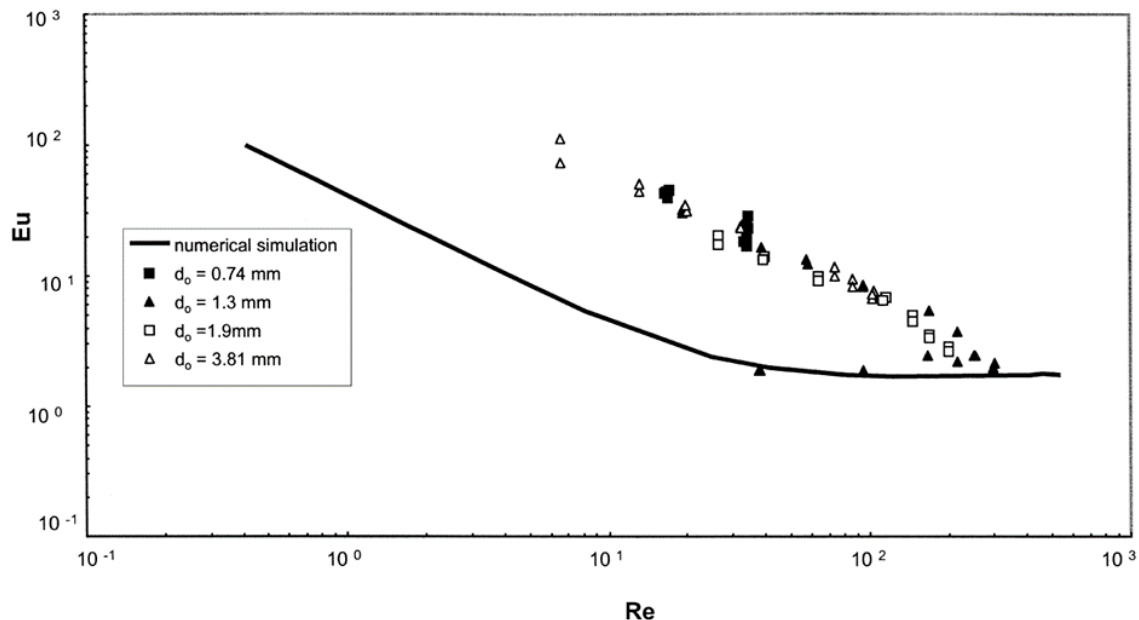


Figure 2.12 Re-Eu relationship for Boger fluids (Della Valle et al., 2000)

A similar trend was observed for the kaolin suspensions. The vertical shift obtained for Boger liquids was used to extract the extensional viscosity of the kaolin suspensions as a function of extension rate. However, the Trouton ratio was much higher than 3 (16, 12 and 10 for the 50, 60 and 65 wt.% suspensions, respectively). They deduced that the behaviour of kaolin suspensions in extensional flow is more complex than that of the Newtonian liquids.

2.7.4.5 Kiljański (1993)

In 1993, Kiljański studied the flow of ethylene glycol, potato syrup and glycerol solutions through five orifices from the bottom of a tank. Three orifices had an aspect ratio of 0.5 and diameters of 2, 3, and 5 mm. The other two had 3 mm diameters and aspect ratios of 1 and 0 (sharp-edged). They measured the discharge volume under constant head for a given time. Eq. 2.41 was used to calculate the discharge coefficient. Re values were calculated using the generalised Re equation (Eq. 2.12).

Figure 2.13 illustrates the C_d -Re relationship from the data for a sharp crested orifice, for L/d of 0.

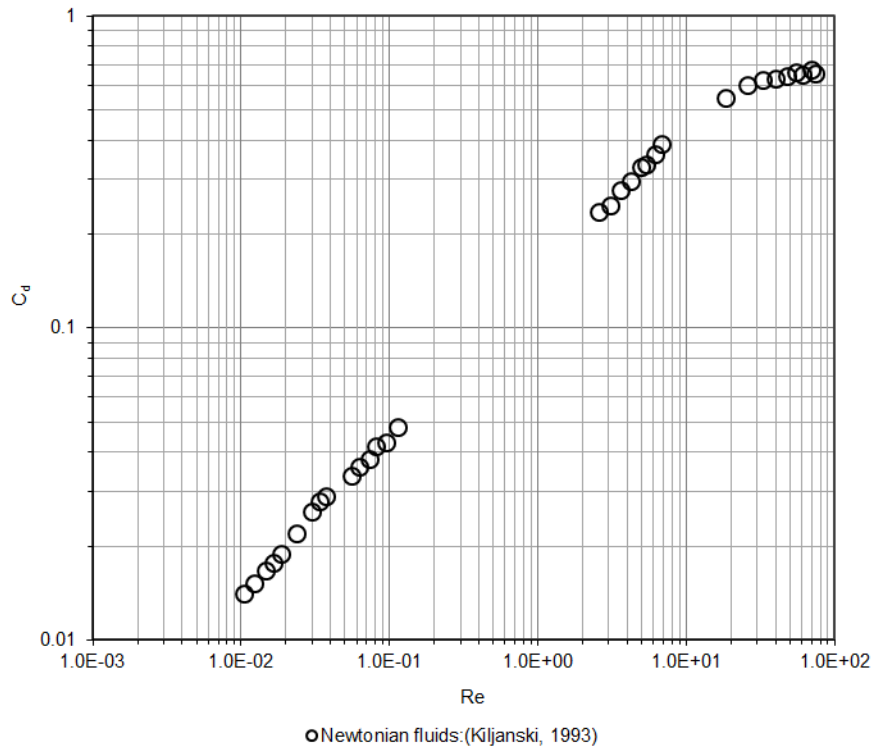


Figure 2.13 Re-C_d relationship for L/d = 0 (Kiljański, 1993)

Kiljański (1993) proposed the C_d-Re relationship by Eq. 2.69:

$$C_d = B\sqrt{Re} \quad (2.69)$$

The constant B was experimentally determined based on the aspect ratio. He established that the value of B increased as the aspect ratio of the orifice increased. The value of B was obtained as 0.142 and substituted in the C_d value equation as given Eq. 2.70. The C_d values increased with increasing Re and the curves converged between Re > 10 and Re = 300, and became constant at Re > 300.

$$C_d = 0.142Re^{0.5036} \quad (2.70)$$

2.7.4.6 Combined tank flow results

Figure 2.14 illustrates the flow rate measurement results obtained by Lea, (1942) as presented by Brater *et al.* (1996), Swamee and Swamee (2010), Kiljański (1993) and Dziubiński and Marcinkowski (2006) for Newtonian and non-Newtonian liquids. The Newtonian liquid's C_d values for Dziubiński and Marcinkowski, (2006) are at lower Reynolds numbers as compared

to that of Kiljanski's (1993) and Lea's (1942) in the laminar flow region. The C_d -Reynolds number relationships for the presented experiments differ because the liquids rheological parameters vary. Therefore, each orifice C_d values should be determined with Newtonian liquids before carrying out the flow rate tests for other liquids (Della Valle *et al.*, 2000). The calibration data can be used for refitting the C_d -Re data and finding new values of the constants.

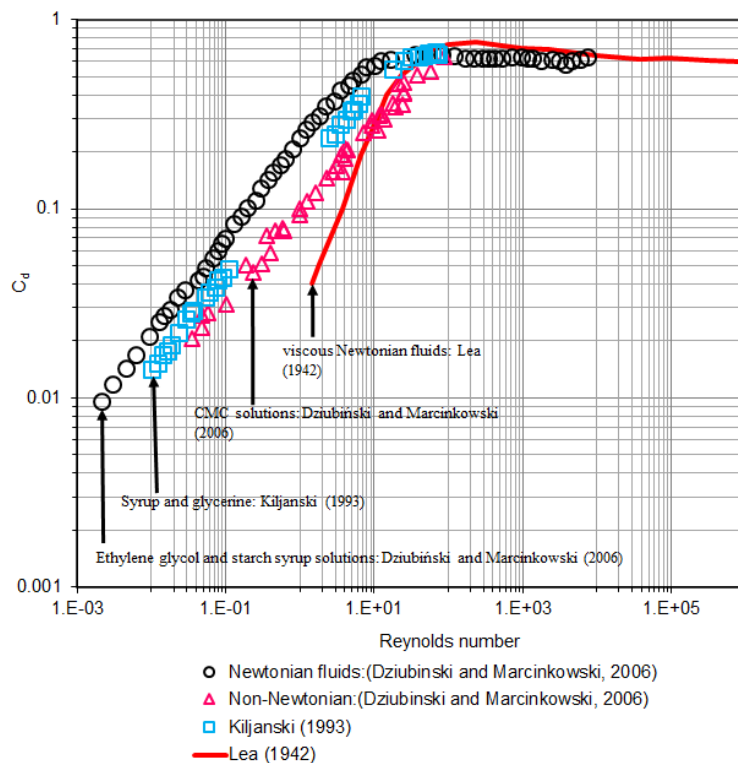


Figure 2.14 Re- C_d relationship for $L/d = 0$ (Brater *et al.*, 1996; Swamee & Swamee, 2010; Kiljański, 1993; Dziubiński & Marcinkowski, 2006)

2.7.5 Liquid flow through orifices in pipes

Johansen (1930) studied the flow characteristics of water, castor oil and mineral oil through sharp-edged orifices with different diameter ratios (β) of 0.090, 0.209, 0.401, 0.595 and 0.794. It was found that for $Re < 10$, C_d values increased linearly, but a further increase in Reynolds number up to 250 resulted in a nonlinear increase in C_d up to its maximum. The C_d values then began to decrease until they reached a steady value of approximately 0.615 as the flow becomes turbulent at $Re > 2000$. It was also observed that the Reynolds number at which transition occurs increased with the diameter ratio. Tuve and Sprenkle (1933) conducted experiments using 45° bevelled orifices. They tested water, light paraffin oil, light motor oil and

heavy motor oil. Based on their results, they recommended that orifice meters should have diameter ratios between 0.2 and 0.5, and that these must be used for flow rates corresponding to $Re > 100$. They compared their results with the works of authors such as Hodgson (1929), Witte (1928) and Johansen (1930), proposing that the slight differences in their results were due to the differences in orifice bevel angle or pipe diameter.

Merrit (1967) established a relationship between the discharge coefficient and the square root of the Reynolds number from pipes and determined that the C_d value is a non-linear function of the Reynolds number. The C_d value was constant at a value of 0.61 for large values of Reynolds number, which is about 10,000 (Joye *et al.*, 2003). The value 0.61 depends on the Reynolds number and the shape and the metal edge defining the orifice hole (Perry *et al.*, 1997). The Merrit (1967) correlation was instrumental in developing an orifice flow model used for calculating energy losses in the laminar and turbulent flow conditions by Borutzky *et al.* (2002).

Alvi *et al.* (1977) and McNeil *et al.* (1999, 2000) established that highly viscous liquids in orifice plates behave different than low viscosity liquids, while Wood and Dickson (1973) concluded that viscosity has little effect on the flow through orifice plates. The study by McNeil and Stuart (2003) confirms the work of Alvi *et al.* (1977) and McNeil *et al.* (1999, 2000) when they investigated the differences in a vertically upward flow in a nozzle and orifice plate. They concluded that an increase in liquid viscosity has a significant effect on nozzle and orifice plate flows.

Steffe and Salas-Valerio (1990) studied the flow of different concentrations of corn starch solutions through orifices. They concluded that the C_d values depended on the orifice diameter, liquid velocity and rheological properties (consistency and Power-law index) of the liquid. At lower velocities, C_d increased with increasing velocity but maintained a constant value at high velocities and decreased as the consistency coefficient increased. They proposed that C_d may be expressed as an exponential function of the generalised Reynolds number.

Pal (1993) studied the flow of emulsions through 16 mm diameter square-edged orifices in pipes. Emulsions behave like non-Newtonian, pseudoplastic liquids at high concentrations. Therefore, the Power law model was used to describe their shear stress-shear rate behaviour. In this instance, the Metzner and Reed (1955) Reynolds number was used: they compared their fit to the results obtained by Stearns *et al.* (1951) and Miller (1983), concluding that the results were similar and follow a single curve for Newtonian and non-Newtonian emulsions.

The inverted emulsions had significantly lower C_d values at low Reynolds numbers and that might be because of the breakup of emulsion droplets.

The automotive industry uses small-diameter, square-edged orifices for the flow of highly viscous oils with varying temperature and pressure. Bohra (2004) addressed the problem of relating flow rate with pressure drop across square-edged orifices, over a wide range of orifice geometries and operating conditions for highly viscous oils. Analysis for this research was based on the Euler number and Reynolds number relationship, to consolidate the results. It was observed that oil behaved like a non-Newtonian liquid at lower temperatures and higher shear rates, causing a decrease in the effective viscosity of the liquid. This decrease in viscosity resulted in an increase in the Reynolds number for a given flow rate, compared to the corresponding Newtonian Re . Similar research, which related the non-dimensional pressure drop to the orifice geometry and Reynolds number, has shown that at low flow rates, C_d is a function of the aspect ratio, the diameter ratio and the orifice Reynolds number. At high Reynolds numbers, however, the C_d value became independent of the Reynolds number and primarily depended on diameter ratio (Lichtarowicz *et al.*, 1965; Grose, 1985; Sahin & Ceyhan, 1996; Mincks, 2002; Bohra, 2004).

Chowdhury (2010) and Chowdhury and Fester (2012) conducted a study to determine pressure loss characteristics of sharp, long, square-edged orifices for laminar to turbulent flow through pipes. The orifices had β (diameter) ratios of 0.36, 0.4, 0.5 and 0.7. The test liquids were water, different concentrations of CMC solutions, kaolin and bentonite suspensions. Their correlation was based on the orifice pressure loss coefficient and Reynolds number, similar to that of Ntamba Ntamba (2011). Further, Chowdhury (2010) and Ntamba Ntamba (2011) also determined the relationship between C_d and Re . The Newtonian and non-Newtonian liquids for both studies coincided in the laminar and turbulent regions for each diameter ratio.

Rituraj and Vacca (2018), carrying out a study on the flow of different shear thinning viscoelastic liquids through sharp-edged orifices in pipes, established a relationship between the Euler number, Reynolds number, diameter ratio and Weissenberg number. They suggested that these dimensionless relationships can be used to relate the pressure drop and flow velocity within the orifice and, therefore, determine the pressure loss for a known flow rate, β ratio and liquid combination.

2.8 Other similar research

Fester *et al.* (2008), studied the energy loss of non-Newtonian liquids in sudden pipe contractions with various test liquids: water, glycerol solutions, lubrication oil, kaolin suspensions and CMC solutions at various concentrations. They presented their data by plotting loss coefficient versus Reynolds number. Newtonian Reynolds number, Metzner-Reed and Slatter Reynolds numbers were used for Newtonian liquids, pseudoplastic liquids and yield-pseudoplastic liquids, respectively. Fester *et al.* (2008) demonstrated an adequate account of the rheological properties of the liquids in the Reynolds number and produced one curve for Newtonian and non-Newtonian liquids.

Haldenwang (2003) studied the flow of water, CMC solutions, kaolin, and bentonite suspensions in open channels, determining the relationship between, Fanning friction factor and the Reynolds number (Re_H) as well as Froude number and Re_H . Khahledi *et al.* (2014) studied the flow rate measurement of non-Newtonian liquids using sharp crested rectangular and 'V' shaped weirs from a tank. Liquids tested were water, CMC solutions, and kaolin and bentonite suspensions. A C_d - Re_H relationship for each weir was established. Haldenwang (2003) and Khahledi *et al.* (2014) included the rheological parameters of non-Newtonian liquids by calculating the values of Re and produced one curve for all non-Newtonian liquids tested.

2.9 Data analysis

Composite curve fitting has been used by various researchers (Garcia *et al.*, 2003; Haldenwang *et al.*, 2012; Khahledi *et al.*, 2014) to predict the range of f - Re and C_d - Re relationships for different multiphase liquids in pipes flowing through weirs. This method is described by Patankar *et al.* (2002). The curve is fitted by a composite power law correlation given in Eq. 2.71.

$$C_d = f_2 + \frac{(f_1 - f_2)}{\left(1 + \left(\frac{Re}{t}\right)^c\right)^d} \quad (2.71)$$

Where f_1 and f_2 are power laws defined as

$$f_1 = a_1 Re^{b_1} \quad (2.72)$$

And

$$f_2 = a_2 Re^{b_2} \quad (2.73)$$

Above, f_1 is obtained from the C_d -Re relationship slope established in the laminar region and a_1 and b_1 could be derived. The parameters: a_2 and b_2 are determined by fitting f_2 in the turbulent region. Equation 2.65 is then applied to all the data points to obtain parameters c, d and t. The composite Power-law predicts the transition flow region to a statistical accuracy, consistent with the experimental data.

2.10 Conclusion

Liquid characteristics differ rheologically from each other. Newtonian liquids have linear relationship between shear stress and shear rate and they are used as a reference material when testing non-Newtonian liquids. Non-Newtonian liquids do not obey Newton's law of viscosity. The focus in this work is on pseudoplastic, Bingham and yield-pseudoplastic liquids. These liquids have dissimilar flow curves. The rheological parameters T_y k and n obtained from these curves are used to determine the dimensionless parameters that are used for characterising the underlying physics of the flow mechanics. The dimensionless parameters used are the Bingham and Reynolds numbers.

Orifices are used in various applications such as storage tanks in chemical, food processing, mining and medical industries. They are used to regulate the flow, distribute flow to parallel process units and discharge the liquids for further processing. It is vital to understand the flow of liquids through the device as the orifice flow coefficient depends on orifice geometry, liquid properties and flow behaviour and conditions. The liquid flow can be laminar or turbulent. In the laminar regime, the C_d value is dependent on Re, but for turbulent flows the C_d value is constant and independent of Re. The standard C_d value in the turbulent region is 0.61 for circular orifices, but Bos (1989) indicated that it can range from 0.60-0.64, depending on the size of the orifice.

The literature reviewed indicates that flow rate measurement studies for Newtonian liquids of low and high viscosity through orifices from tanks have received extensive attention. In the turbulent region, Henry and Bovery (1901), King and Wisler (1922) and Brater *et al.* (1996) have proven that the orifice shape does not influence the flow of Newtonian liquids from tanks. The various shaped orifices are also used for the flow rate measurement of Newtonian liquids in pipes, nozzles and sprays and for gas flow. Ntamba Ntamba (2011) studied the discharge measurement of non-Newtonian liquids (power law, Bingham and yield-pseudoplastic liquids)

using circular and triangular orifices in pipe flow. There was no effect of shape on different non-Newtonian liquids, but there has not been any study done of flow from a tank.

There are limited studies relating to the measurement of the flow rate of non-Newtonian liquids through orifices out of tanks such as that by Dziubiński and Marcinkowski (2006) and Della Valle *et al.* (2000). Dziubiński and Marcinkowski (2006) developed separate models to predict the C_d -Re relationship for Newtonian and non-Newtonian liquids because the data for these liquids do not coincide. Furthermore, they used only power law model liquids to represent non-Newtonian liquids and they conducted tests using circular orifices only. The discharge coefficient and Reynolds number relationship shows different flow trends for Newtonian and non-Newtonian liquids in the laminar region. Della Valle *et al.* (2000) used yield-pseudoplastic (Herschel-Bulkley) liquids. However, the orifice was installed in a tube connecting two tanks. With a focus on the measurement of extensional viscosity, the predicted flow models published in these studies do not have combined models to predict the flow of Newtonian and non-Newtonian liquids through sharp crested orifices out of tanks.

Haldenwang (2003) studied the flow rate measurement of non-Newtonian liquids in open channels and Khahledi *et al.* (2014) conducted experiments for the flow rate measurement of non-Newtonian liquids from a tank using sharp crested weirs. Other similar studies were carried out in pipes (Chowdhury, 2010; Ntamba Ntamba, 2011; Chowdhury & Fester, 2012). The studies for pipe and open channel flows and flow through weirs presented one curve for all the test liquids, but that is not the case for gravitational flow through orifices. Marcinkowski and Dziubiński (2004) and Della Valle *et al.* (2000) explained that the shear rate that is commonly used for pipe flow differs from the one for gravitational discharge through orifices from tanks. This is due to the flow that is not fully developed in orifices from tanks to attain a bulk shear rate similar to the one found in pipe flow. However, the process of determining the effective shear rate for orifices was not clearly outlined. Therefore, it is important to establish the effective shear rate that would assist in aligning the non-Newtonian liquid data with the Newtonian liquid data.

The existing literature lacks experimental data for flow of Newtonian and non-Newtonian liquids through triangular and square shaped orifices from tanks, especially at low Reynolds numbers. The flow of non-Newtonian liquids through circular orifice from tanks used the effective shear rate to predict the C_d vs Reynolds number curves. There is however no predictive model that collapses the non-Newtonian liquids curve to Newtonian liquids curves in the laminar flow. Therefore, an extensive experimental investigation covering wide ranges of orifice shapes and hydraulic diameters and liquid rheological properties is necessary. From

the data a predictive model that can collapse non-Newtonian liquids to Newtonian liquids curve should be determined.

Table 2.1 presents a summary of previous pertinent studies for the flow of Newtonian and non-Newtonian liquids through orifices from tanks.

Table 2.1 Summary of previous research on flow of Newtonian and non-Newtonian liquids through orifices from tanks

Author	Orifice Type	Liquids	Predicted Model
Swamee & Swamee (2010)	Sharp crested circular orifices	Viscous Newtonian liquids	$Q = 0.679d^2\sqrt{gh} \left[87 \left(\frac{\mu}{d\sqrt{gh}} \right)^{1.43} + \left(1 + \frac{4.5\mu}{d\sqrt{gh}} \right)^{-1.26} \right]^{-0.7}$
Dziubiński & Marcinkowski (2006)	Sharp crested circular orifices (5, 8, 12.5 and 17 mm diameters, L/d of 0, 0.35, 0.5, 0.75, 1 and 3)	Newtonian liquids (water, ethylene glycol and water solutions of starch syrup)	$C_d = \left[0.186 - 0.0756 \frac{L}{d}^{0.333} \right] \sqrt{Re}$
Dziubiński & Marcinkowski (2006)	Sharp crested circular orifices (5, 8, 12.5 and 17 mm diameters, L/d of 0, 0.35, 0.5, 0.75, 1 and 3)	Non-Newtonian liquids (CMC solutions)	$C_d = \left[0.101 - 0.0164 \left(\frac{L}{d} \right)^{0.48} \right] Re_{MR}^{0.426}$
Liu <i>et al.</i> (2001)	Circular orifices (1.12 to 4.36 mm diameter, thickness 3.03 mm)	Newtonian liquids (water and machine oil)	$C_d = 16 + 9 \frac{d}{\delta} + B(Re - C)$
Della Valle <i>et al.</i> (2000)	Circular orifices (0.6-3.0 mm diameters)	Newtonian liquids (mineral oils, corn syrup and water, Boger liquids (polyacrylamide in corn syrup))	$Eu = \frac{41.8}{Re}$
Della Valle <i>et al.</i> (2000)	Circular orifices (0.6-3.0 mm diameters)	Non-Newtonian liquids (kaolin clay mixed with polyethylene glycol and water)	-
Kiljanski (1993)	Circular orifices (2, 3, and 5 mm diameters and L/d of 0.5, and 3 mm diameter and L/d of 1 and 0)	Newtonian liquids (ethylene glycol, potato syrup and glycerol solutions)	$C_d = 0.142Re^{0.5036}$

CHAPTER THREE: RESEARCH METHODS

3.1 Introduction

Experimental research methods were used in this work. The experiments were done at the Flow Process and Rheology Centre fluids laboratory at the Cape Peninsula University of Technology. Different concentrations of Newtonian and non-Newtonian liquids were tested. A Paar Physica MCR 300 rheometer was employed to determine the rheological properties of the liquids. The test rig consisted of square tank suspended from a load cell and fitted with orifice plate at the bottom. Four different sizes of sharp crested square, triangular and circular orifices were used. In addition, a high speed video camera was used to record the flow of water out of the tank. The frames were extracted from the video clips and data obtained was used to calculate the volumes and discharge rates. Batch mode was used to feed the tank. The measurements were taken up to approximately 0.1 m above the bottom of the tank to minimise the exit effects. The C_d values and Reynolds numbers were calculated for each liquid and concentration. The information was analysed and further processed to establish a model to predict the flow rate out of the tank for all the liquids and orifice shapes.

3.2 Equipment

3.2.1 Rheometer

A Paar Physica MCR 300 rheometer was used to rheologically characterise the test liquids and was equipped with a coaxial geometry (sand-blasted bob and smooth cup with diameters of 13.33 mm and 14.46 mm respectively). The measuring gap was 1.13 mm and the sampling volume was 19.35 ml.

3.2.2 Tank and orifices

The square tank ($400 \times 400 \times 600$ mm and weighing 42.1 kg) with clear Perspex walls supported by a steel frame was used for the tests (Fig. 3.1). The orifices were fitted to the tank base (Fig. 3.2). Figure 3.3 shows the three shapes of orifices (circular, square and

triangular) used for this study, with dimensions of the orifices illustrated in Table 3.1. Equation 3.1 was used to calculate the orifices d_h . The purposes of having different sizes of the orifices but equal hydraulic diameters (d_h) for each size and all the shapes was to test the effect of orifice shape for flow rate measurement of non-Newtonian liquids from a tank. The orifice was fitted flush with the inside surface of the tank to avoid unstable flow of the liquids.

$$d_h = \frac{4A_0}{P_w} \quad (3.1)$$

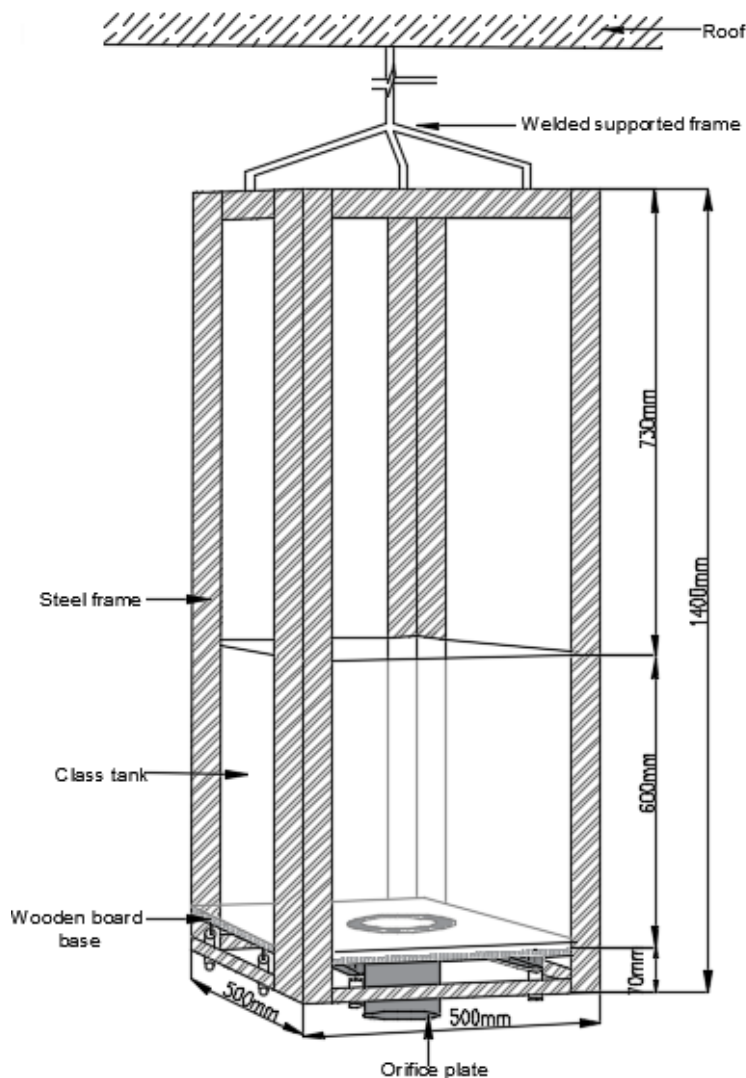


Figure 3.1 Rectangular tank supported by a steel frame

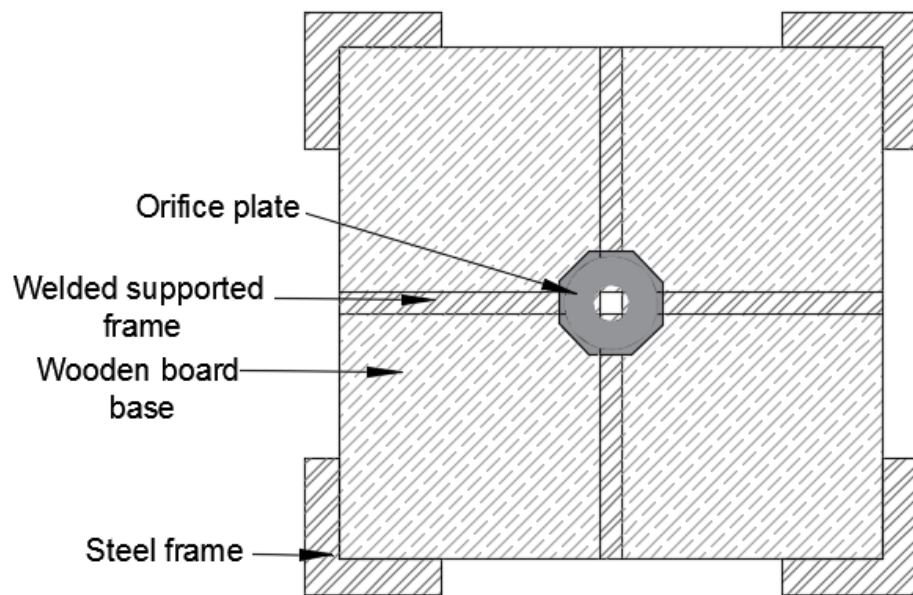


Figure 3.2 Tank base

	d_h (mm)
	8
	12
	16
	20

Figure 3.3 Triangular, square and circular orifice

Table 3.1 Orifice dimensions

Circular				Square				Equilateral triangle			
Diameter (mm)	Area (mm ²)	Wetted perimeter (mm)	d _h (mm)	Side (mm)	Area (mm ²)	Wetted perimeter (mm)	d _h (mm)	Side (mm)	Area (mm ²)	Wetted perimeter (mm)	d _h (mm)
8.0	50.8	25.3	8.0	8.0	64.0	32.0	8.0	13.9	83.1	41.6	8.0
12.0	114	37.8	12.0	12.0	144	48.0	12.0	20.8	187	62.4	12.0
16.0	202	50.4	16.0	16.0	256	64.0	16.0	27.7	333	83.1	16.0
20.0	315	63.0	20.0	20.0	400	80.0	20.0	34.6	520	104	20.0

3.2.3 Load cells

The tank was fitted to a suspended weigh bridge with a load cell (Fig. 3.4) to measure the flow rate of the liquids. The 9363-D3-100KG-20P1-R and 00363-250K-D3-00F models ‘S’ type universal load cells with the capacity of 100 kg and 250 kg were used to measure the mass of the liquids. The load cells were made of alloy steel and manufactured by Vishay Precision Transducers India private Limited. The full scale output of 100 kg and 250 kg load cells were 3.249 mV/V and 3.248 mV/V, respectively. Table 3.2 and Figure 3.5 present the dimensions of the load cell as specified by the supplier. The 100 kg load cell could only carry a liquid mass up to 60 kg. For the liquids such as kaolin and bentonite suspensions with high concentrations, the 60 kg quantity went to the height that did not give enough head before the liquid vortexed. Therefore, a 250 kg load cell was calibrated and used for the flow rate measurements of liquids with higher densities. When a change in weight is applied to the tank, the load is transmitted to the load cell that sends an electrical signal to the PC via a data logger. The data logger continuously samples the voltage with time.

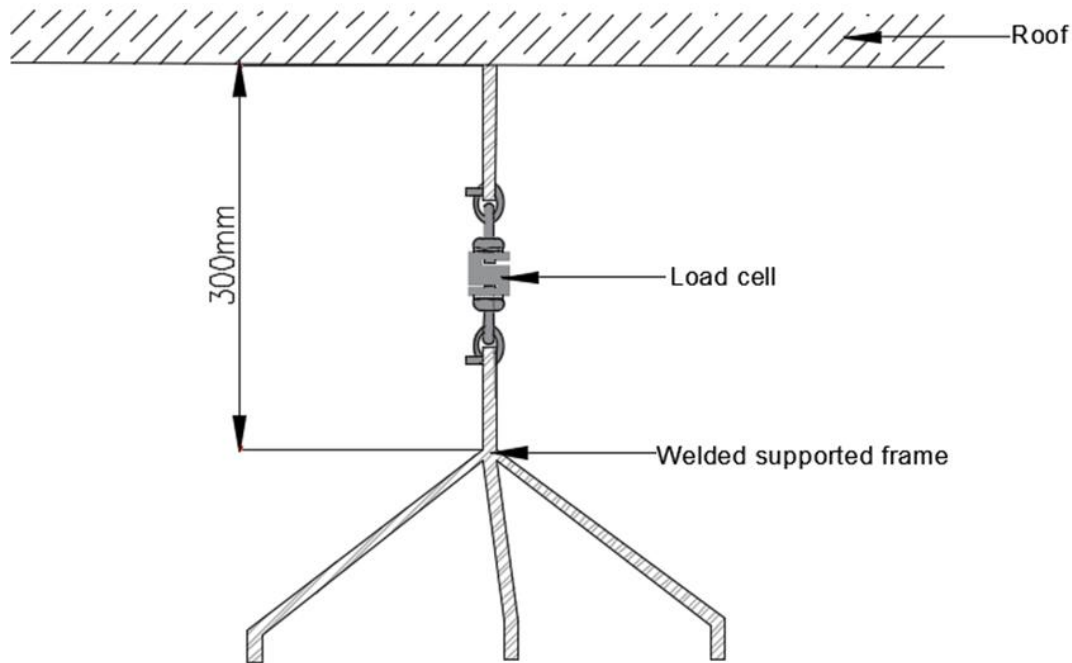


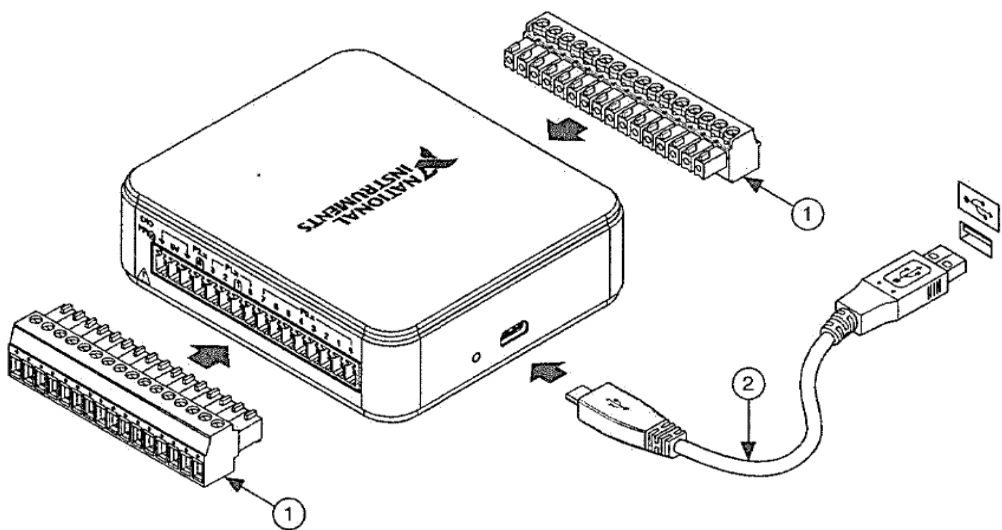
Figure 3.4 Weigh bridge with load cell

Table 3.2 Dimensions of the load cells in mm

Capacity (kg)	50,100	250,500
A	50.8	50.8
B	61.0	61.0
E	M8 x 1.25-6H	M12 x 1.75-6H
F	30.5	30.5
G	8.9	8.9

3.2.4 Data logger

A NI USB-6001/6002/6003 data logger from National Instruments consisted of an amplifier and a data acquisition unit (DAQ). The voltage signal from the load cell was amplified to the DAQ device (fig. 3.5). The DAQ was a full-speed USB device that provided the eight single-ended analogue input (AI) channels, two analogue (AO) channels, 13 digital input/output (DIO) channels and a 32-bit counter. The DAQ device had an input range of $\pm 10V$. Figure 3.6 shows the hardware set up of the device. The micro-b high speed serial bus cable (USB) connected the DAQ device with the laptop. NI-DAQmx driver software was installed to the laptop to configure the virtual and measurement channels. One channel was used for this study. The voltmeter (model and make) was used to calibrate the DAQ and load cell.



1. Screw Terminal Connector Plug 2. Led Indicator 3. Micro-B USB Connector

Figure 3.5 Data acquisition unit (DAQ)

3.2.5 Camera

A video camera was used to capture the flow of water being discharged from the tank. It was set up on a tripod, 1.47 m away from the tank to minimise the possible parallax error (Fig. 3.6). The frame rate of the captured videos was 25 frames per second. The video frames captured were extracted for calculating the flow rate of the water discharged through the orifice. The tape measure was attached to the tank to manually record the height of the water during the tests.

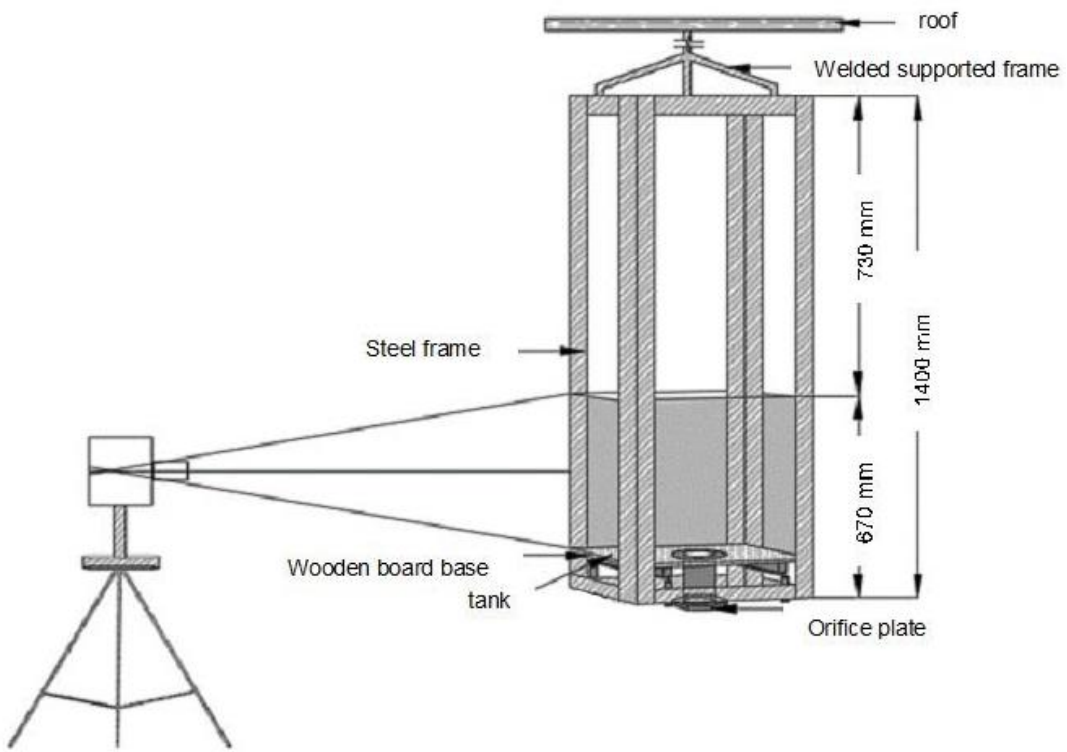


Figure 3.6 Tripod and camera setup

3.2.6 Test liquids

Water was used for calibration purpose. Different concentrations of kaolin (20.34% and 13.14%) and bentonite (7.3%, 6.99% and 3.77%) suspensions, carboxymethyl cellulose (CMC) (7.55%, 6.58%, 5.21%, 2.81% and 2.4%) solutions, and glycerine (100%, 96%, 93% and 65%), were prepared and discharged through an orifice from the bottom of a tank and also rheologically (shear stress-shear rate data) characterised.

3.2.7 Material composition

The particle size distribution tests for kaolin, bentonite and CMC were conducted at the Flow Process and Rheology Centre. The Mastersizer2000 from Malvern Instruments was used for the tests. A small amount of the slurry sample was added to a beaker containing approximately 800 ml of deionised water. Kaolin suspension and CMC solutions were submitted to the laser light scattering. The Bentonite suspension was homogenised by ultrasound application for 5

min before being exposed to the laser light scattering. The particle size distribution curve for one sample was produced from the average of five readings. At least two tests were run for each sample.

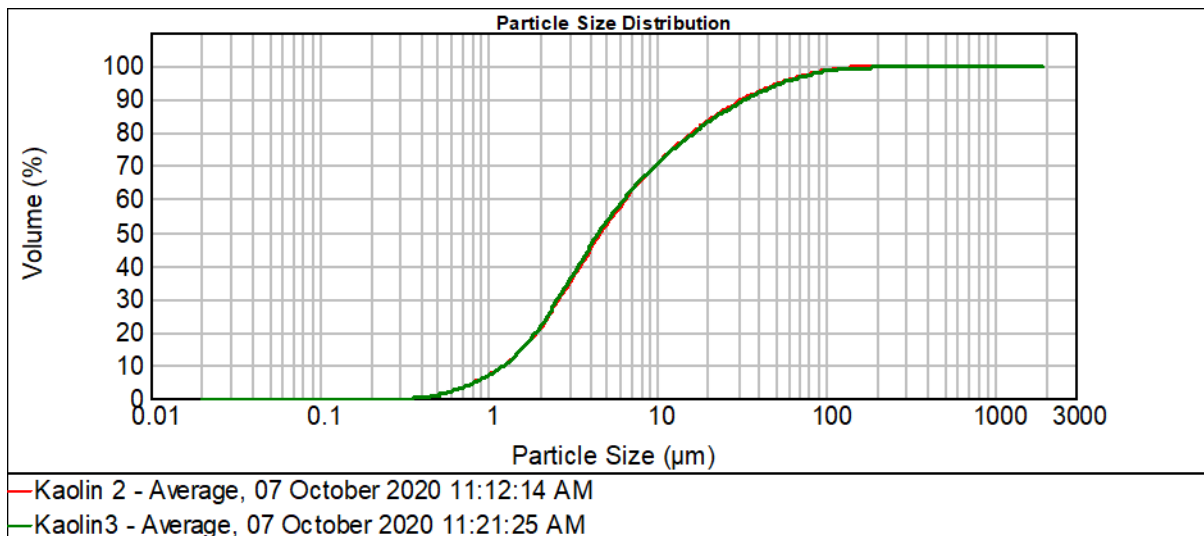
Kaolin

Kaolin was supplied by Serina trading and supplied the typical chemical composition as illustrated in table 3.3. The particle size distribution curve for 13.14% kaolin is given in fig. 3.7.

The volume

Table 3.3 Kaolin specification

kaolin	
Composition	Typical
SiO ₂	46.12%
Al ₂ O ₃	37.86%
Fe ₂ O ₃	0.28%
TiO ₂	0.55%
CaO	0.16%
MgO	0.18%
K ₂ O + Na ₂ O	0.58%
L.O.I.	13.74%
pH	7 - 8



Sample Name	$d (0.1)$	$d (0.5)$	$d (0.9)$
Kaolin 1	1.24	4.68	32.33
Kaolin 2	1.25	4.55	33.52
Average	1.25	4.61	32.92

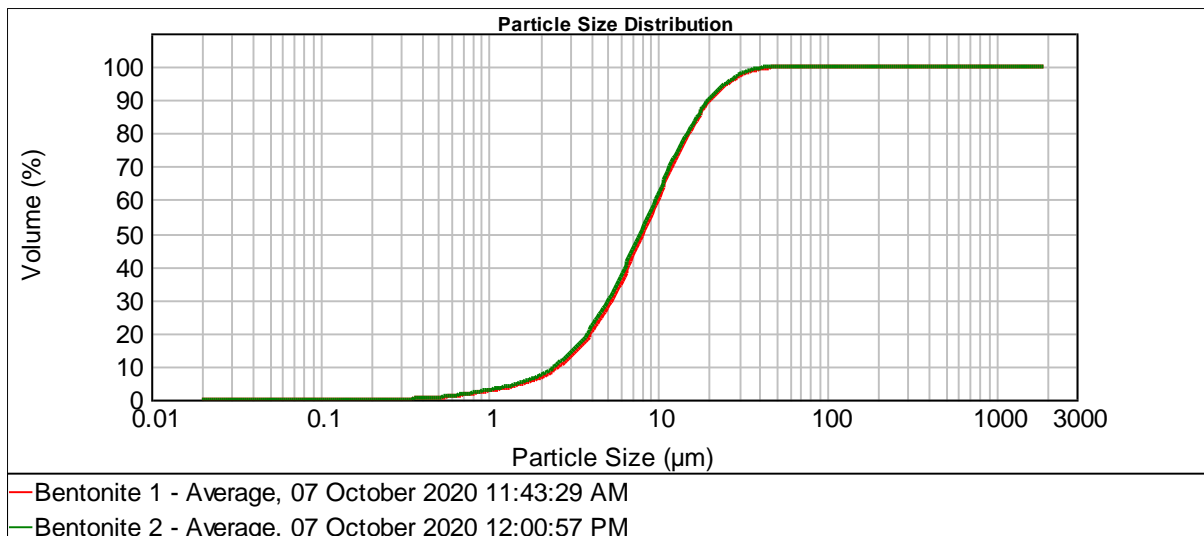
Figure 3.7 Particle size distribution (microns) for kaolin

Bentonite

The bentonite used was from G & W Base & Industrial Minerals (Pty) Ltd. Table 3.4 shows the chemical composition of the used bentonite. The particle size distribution test results for 6.99% bentonite are shown in fig. 3.8.

Table 3.4 bentonite specification

Bentonite (Na)	
Composition	Typical
SiO ₂	61.0%
Al ₂ O ₃	18.9%
CaO	1.37%
Na ₂ O ₃	2.2%
K ₂ O	0.22%
MgO	2.4%
Fe ₂ O ₃	4.38%
TiO ₂	0.45%
L.O.I.	7 - 10
pH	10 – 10.5



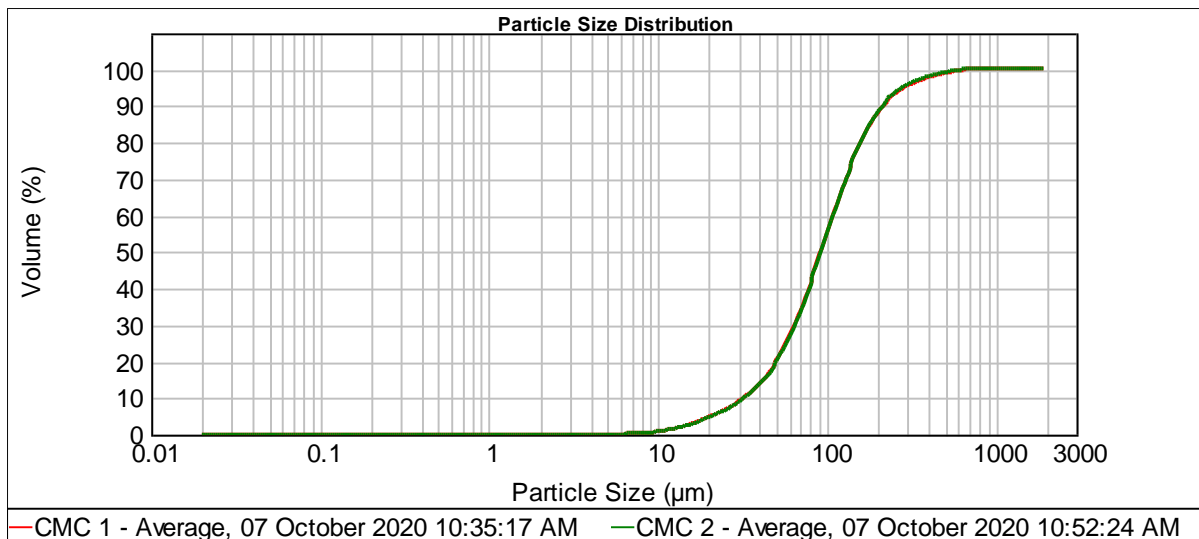
Sample Name	$d (0.1)$	$d (0.5)$	$d (0.9)$
Bentonite 1	2.68	8.33	20.94
Bentonite 2	2.52	8.04	20.51
Average	2.60	8.18	20.73

Figure 3.8 Particle size distribution (microns) for bentonite

CMC

CMC was supplied by Protea Chemicals. It is a white to cream-coloured, odourless powder.

The particle size distribution curve for 6.58% CMC is given in fig. 3.9.



Sample Name	d (0.1)	d (0.5)	d (0.9)
CMC 1	32.83	93.36	217.28
CMC 2	33.22	93.68	215.16
Average	33.03	93.52	216.22

Figure 3.9 Particle size distribution (microns) for bentonite

Glycerine

It is a syrupy liquid, colourless, and very hygroscopic. It was procured from Protea Chemicals.

Table 3.5 shows the specification of the glycerine used.

Table 3.5 Glycerine specification

Analysis	Specification	Result
Glycerol content	98.0% - 101.0%, typical 99.5%	99.86%
Acidity	NMT 0.2ml of 0.1M NaOH	0.05ml
Appearance of solution	Solution is clear and colourless	COMPLIES
Refractive index	1.470-1.475	1.473
Heavy Metals	5ppm max	<5ppm
Chlorides	10ppm max	COMPLIES
Esters	NLT 8.0ml min. of 0.1M HCl	COMPLIES
Halogenated Compounds	Opalescence produced should not be more intense than standard solution	COMPLIES
Sugars	Blue solution with no precipitate – so sugar present	COMPLIES
Sulphated Ash	0.01% max	0.0020%
Impurities A and related substances	Meet requirements (GC)	COMPLIES
Aldehydes	Absorbance @ 522nm not greater standard	PASS
Identification	Meet requirements (IR)	PASS
Water	<2% max, typical 1% max	0.1182%
Relative Density @ 20°	1.261 – 1.264 @20°	1.2619

3.3 Experimental procedures

This section explains the experimental procedures used in this study. The DAQ device and load cells were calibrated by using small predetermined weights and water. The orifices were calibrated and load cells were used to measure the flow rate of the test liquids through the orifices. Before calibration of the load cells and orifices, the tank was emptied and cleaned to ensure that the initial weight is that of the tank and steel frame only. A 60 Hz sampling rate was used during the orifices calibration and discharge measurements for consistency, and only one channel was used to capture the voltage (channel Dev/10). The method for preparing the samples is explained. The rheological parameters of the tested liquids were obtained with a rheometer.

3.3.1 DAQ system and load cell calibration

The procedure below explains how the DAQ system and load cells were calibrated. The voltmeter was used to confirm the voltage captured by the DAQ unit.

Setting the load cell to zero voltage

- Adjust the DAQ to zero voltage by using the voltmeter.
- Fit the tank to the load cell.
- Connect the DAQ to the laptop and open the NI-DAQmx driver software.
- Select channel Dev/10 and sampling rate (frequencies for this procedure varied).
- Start the test and run it for approximately a minute to record the voltage and calculate the average voltage.
- Use a voltmeter to measure the voltage from the DAQ.
- Compare the voltages recorded from the DAQ system and the voltmeter.

Calibration of the load cell

Small weights were used to calibrate the load cell to determine the minimum voltage that the DAQ device can measure. The mass of the objects was measured using a measuring scale before being added to the weight of the tank. Appendix A., Figures A.1 and A.2 show the relationship between voltage and mass measured during calibration with the small weights when the tank was empty and when it contained water, respectively. The DAQ unit can measure the mass within ± 0.002 V.

Calibration from an empty tank (small weights)

- With the tank fitted to the load cell, measure the voltage.
- Add known mass and measure the voltages (Appendix A, Table A.1).
- Remove each object and measure the voltages (Appendix A, Table A.1).
- Plot voltage vs mass (Appendix A, Fig. A.1).

Calibration from 88.02 kg including the tank weight (small weights)

- Fill up the tank with water until the total mass is 88.02 kg, and measure the voltage
- Add small known weights and record the voltages (Appendix A, Table A.2).
- Remove each weight and record the voltages.
- Plot voltage vs mass (Appendix A, Fig. A2).

Effect of different sampling rates

- Measure the voltage of the tank when empty using a DAQ system and a voltmeter.
- Add a known weight and record the voltages at various frequencies (Appendix A, Table A.3).

The different frequencies did not affect the voltage recorded for the same weight. The standard deviation for the recorded readings is 0.0026.

Load cell calibration (water weight)

- Connect the DAQ to the laptop and open the NI-DAQmx software.
- Set the channel to Dev/10 and select 60 Hz sampling rate.
- Seal the bottom of the tank to ensure that there is no leakage.
- Record the tank voltage.
- Weigh the water on a scale to a mass of 10 kg.
- Pour the water inside the tank and record the voltage.
- Increase the weight of the water by 10 kg increments and record the voltages and weight after each increment.
- Increase the weight up to 60 kg and 150 kg for 100 kg and 250 kg load cells, respectively.
- Plot the voltage against weight and obtain the linear equations (Figs. 3.10 and 3.11).

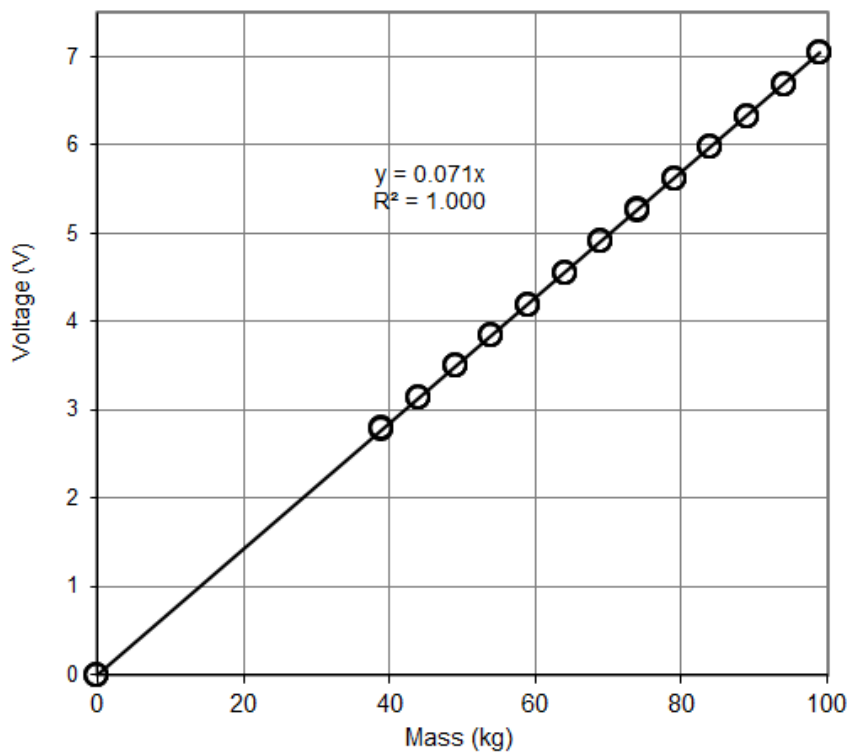


Figure 3.10 Load cell calibration results – 100 kg

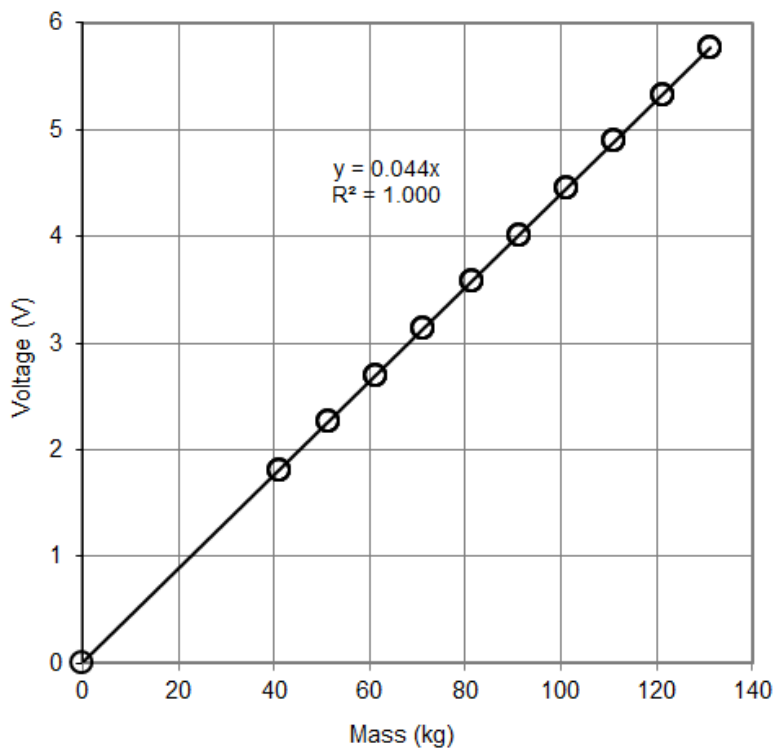


Figure 3.11 Load cell calibration results – 250 kg

3.3.2 Orifice calibration and flow rate tests for all the liquids

The procedure followed for calibration of the orifices is outlined in this section. There were precautions that had to be taken while collecting data, such as to ensure that the orifices flush to the surface of the tank to avoid the experimental error. It was especially important for the 20 mm hydraulic diameter orifice to identify the vortex formation because the liquid flow through the orifices was fast. There was a challenge of appropriately identifying when the vortex forming processes began, especially for the liquids that were not clear. This caused the liquid head to increase substantially and subsequently changing the orifice C_d value. The orifices had to be thoroughly cleaned after use to avoid accumulation of any surface active agents and debris on the orifice edges, due to the sensitivity of the orifice coefficient to the shape of the orifice edge. The flow was not entirely stable immediately after removing the drain plug, and therefore the data during that period could not be used. The batch feeding of the liquids to the tank might have caused the entrapped air in the tank that was difficult to identify due to nature of the liquids. To prevent this, care was taken by slowly filling the tank.

Orifices calibration procedure

- Close the orifice using the universal stopper.
- Fill up the tank with the liquid to the maximum weight that each load cell can handle (58 kg and 150 kg for 100 kg and 250 kg load cells, respectively).
- Record the liquid temperature.
- Open the NI-DAQmx software on the laptop; select the appropriate channel and 60 Hz frequency.
- Fit the camera to the tripod and start the video recording for the water test.
- Remove the plug from the orifice to allow the liquid to flow.
- Start the NI-DAQmx software program on the laptop; record voltage and time.
- Stop capturing data before liquid forms a vortex approximately 0.1 m above orifice.
- Stop the video recording.
- Change the orifice plate and repeat the above procedure.

- Measure and record the temperature of the liquid during and after completing the flow rate test.

Flow rate test for all the liquids

The procedure followed for the flow rate measurement test for all the liquids is explained in this section.

- Close the orifice using the universal stopper.
- Fill the tank with the liquid to the maximum weight that each load cell can handle (58 kg and 150 kg for 100 kg and 250 kg load cells, respectively).
- Record the liquid temperature.
- Open the NI-DAQmx software on the laptop; select the appropriate channel and 60 Hz frequency.
- Remove the plug from the orifice to allow the liquid to flow.
- Start the capturing program on the laptop and record the voltage and time stamp.
- Stop capturing data before the liquid forms a vortex approximately 0.1 m above the orifice.
- Change the orifice plate and repeat the above procedure.
- Measure and record the temperature of the liquid during and after completing the flow rate test.

3.4 Liquid preparation

The materials used in this research were selected to represent a wide range of rheological properties. Water was selected for calibration purposes. Carboxymethyl Cellulose (CMC) was selected for the power-law fluid and is generally regarded as an ideal solution for experimental work (Haldenwang, 2003). Bentonite was selected as the Bingham plastic mineral suspension. The yield pseudoplastic or shear-thinning mineral suspension selected was kaolin clay.

Some of the materials tested were in powder form and needed to be mixed with water to form slurries. The following procedure explains the method for preparing the slurries.

- Calculate the capacity of the tank (0.096 m^3).
- Determine the mass of the total mix
- For kaolin suspension, calculate the amount of powder using Eq. 3.2.

$$w/w = \frac{\text{mass of dry solids}}{\text{mass of total mix}} \times 2.65 \times 100 \quad (3.2)$$

- For bentonite suspension and CMC solution, calculate the amount of powder based on eq. 3.3.

$$w/w = \frac{\text{mass of dry solids}}{\text{mass total mix}} \times 100 \quad (3.3)$$

- Calculate the amount of water by subtracting the calculated mass of powder from the mass of the total mix.
- Measure the quantity of water and pour it into the mixing tank.
- Gradually add powder to the water in the mixing tank and use electric mixer to mix the slurry.
- Mix the slurry and Switch off the mixer.
- Leave the mixture for five days to hydrate thoroughly, and ensure that the liquid is mixed for at least two hours daily with a mixer.
- After five days mix the slurry for at least an hour before carrying out the flow rate test
- After an hour take a sample and carry out relative density test while the slurry is still mixing; determine the percentage of the slurry obtained.
- Manually transfer the liquid to the tank rig, fitted with an orifice
- Discharge the liquid from the tank twice before taking measurements.
- Take samples before and after the flow rate test and record their temperature.
- Carry out the rheology tests.

- Weigh the slurry and calculate the amount of water needed to dilute to the desired concentration.

$$\text{amount of water} = \frac{\text{mass of dry solids}}{\% \text{w/w}} \times 2.65 \times 100 - \text{remaining mass of initial mix} \quad (3.4)$$

$$\text{amount of water} = \frac{\text{mass of dry solids}}{\% \text{w/w}} \times 100 - \text{remaining mass of initial mix} \quad (3.5)$$

- Dilute the slurry and carry out relative density test; determine the percentage of the slurry obtained.
- Discharge the slurry from the tank twice before taking the measurements.
- Carry out the flow rate and rheology tests.
- After completing the test for one material, mix another material and repeat the testing procedure.

Water was used as the Newtonian liquid to calibrate the orifices. Different concentrations of glycerine, carboxymethylcellulose (CMC) solutions and kaolin and bentonite suspensions were prepared and used as test liquids in this study. Glycerine was mixed with water to form a glycerine solution and immediately tested to avoid water absorption. CMC, kaolin and bentonite were in powder form and their required amounts were mixed with water to form CMC solutions, kaolin and bentonite suspensions. The kaolin suspension was allowed three days to hydrate. Bentonite suspensions and CMC solutions were allowed to hydrate for five days. An electric mixer was attached to the mixing tank to stir the liquids. The liquids were mixed in the mixing tank for at least an hour before carrying out the relative density test and they were manually transferred to the testing tank. The slurries were transferred immediately after mixing. Each liquid was allowed to flow through the tank at least twice before the data was collected.

The liquid temperature was recorded before and after the flow rate tests. Samples of the test liquids were stored in a water-tight container before and after the flow rate test to carry out the relative density and rheology tests.

3.5 Rheology tests

The samples for the rheology tests were taken before and after flow test to determine if there was any change in the characteristics of the liquids. The slurry temperature was measured before, during and after flow rate measurement test. The rheology test was carried out two days after flow rate tests and at the same temperature that was obtained during the flow rate measurement test. The shear rate ranges of the test liquids from the orifice were calculated using $8v/d_h$. The shear rate range used for rheology tests varied from 100 s^{-1} to 1000 s^{-1} , to correspond as close as possible with the application shear rate obtained from the flow through the orifices. The liquids were pre-sheared before they could be tested.

A rheometer MCR 300 from Paar Physica was used to conduct the test. The complete assembly of the rheometer consisted of an MCR 300 rheometer, an air compressor, air regulator, the temperature control units with inbuilt heating and cooling systems, a computer data processing unit and US200 software. A concentric standard measuring system comprised of a smooth cylindrical cup and a sandblasted bob. The slip effect was decreased by the rough exterior of the bob and the truncated cone shape reduced the end effects. The sample was shaken before being carefully poured into the measuring cup. The sample and cup were set to the temperature that was recorded during the flow rate test. The sample was left to rest on the edge of the rheometer for at least 15 min prior to the measurements in order to ensure temperature equilibration. At least two flow curves were run before taking the measurements of the flow curves that were used for this study, to ensure the proper pre-shearing and to expel any entrapped air. Each flow curve was run approximately for 10 min. The equilibrium flow curves for which shear stress with the controlled shear rate rheometer and shear rate was recorded as function of time until the equilibrium flow curves were reached.

The example of the equilibrium flow curves is shown in (fig. 3.12). The shearing cycles consisted of successive decreasing shear stress.

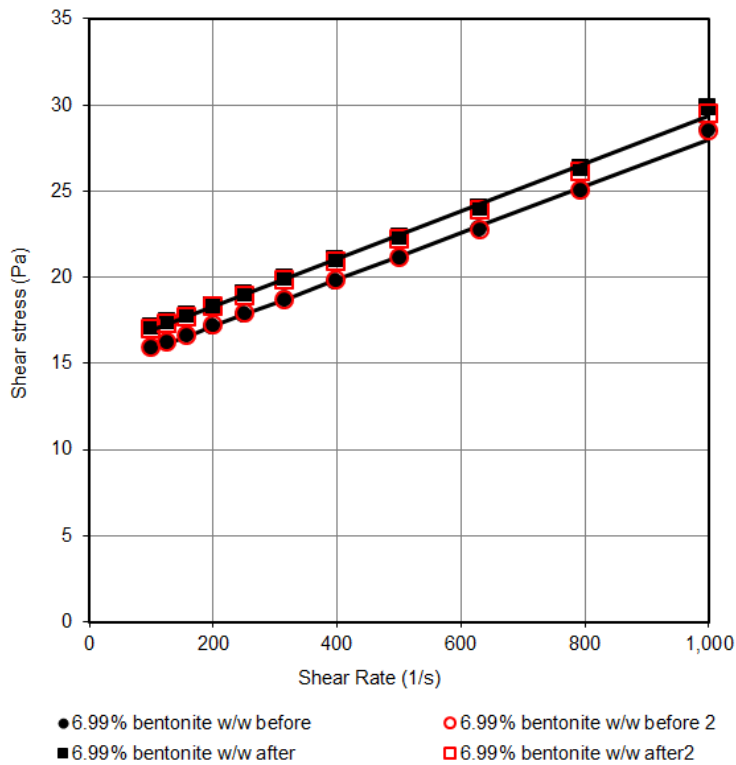


Figure 3.12 Rheograms for bentonite suspensions (Equilibrium flow curves for 6.99%)

Abu-Jdayil (2011) and Bekkour et al. (2005), performed rheological tests for sodium bentonite–water dispersions by increasing shear rate (forward measurement) and then by decreasing the shear rate (backward measurement). The bentonite and kaolin suspensions were left to hydrate for up to 48 hours to reach full hydration and maximum strength. The suspensions used for the current study were allowed to hydrate for five days. The rheology tests were carried out two days after the completion of flow rate tests. Bekkour et al. (2005) carried out the rheology test for 6, 8, and 10% bentonite suspensions. An upward shear stress ramp was done over 60 min, followed by a peak hold for 30 min and downward shear ramp for decreasing flow curve. Fig. 3.13 shows the flow curves obtained by Bekkour et al. (2005). The hysteresis loops present areas that are taken as estimation of degree of thixotropy at the shear rates that are below 100 s^{-1} . For the current study only shear rates that are above 100 s^{-1} were used to obtain the rheological parameters because the range of shear rates in the orifice was between

574 - 3170 s⁻¹. The 6% concentration in fig. 3.13 did not have time dependency effect and an increase of thixotropic properties was found to increase with bentonite concentration, that was found at 8% and 10% concentration. The concentrations used for this study were 7.3%, 6.99% and 3.77%, which were below 8%. The flow curves above 100 s⁻¹ shear rates corresponds to the flow of the suspension, showing the continuous change of the curve slope. Thus, the energy dissipation is viscous and the suspension exhibits a shear-thinning behaviour, which can be captured by the Herschel–Bulkley model (Bekkour et al. 2005).

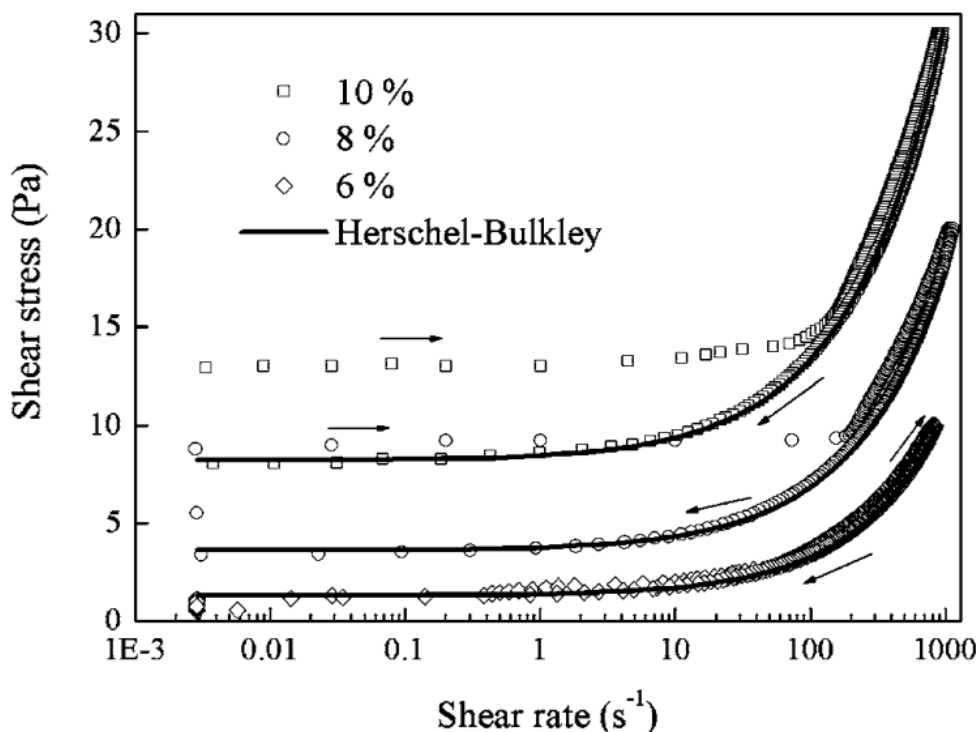


Figure 3.13 Hysteresis loops of bentonite suspensions at 6%, 8% and 10% concentrations and comparison with the Herschel–Bulkley model (Bekkour et al., 2005).

3.6 Data analysis

The processing of the data obtained from rheometer and flow rate tests is explained in sections 3.6.1 to 3.6.5.

3.6.1 Orifice calibration and liquid flow rate measurement

The voltage and time stamp at different heads were captured. Using the calibration constants in Eqns. 3.6 and 3.7 obtained from voltage calibration the mass of the liquid in a tank was calculated.

For 100 kg load cell

$$m = \frac{V}{0.0711} \quad (3.6)$$

For 250 kg load cell

$$m = \frac{V}{0.044} \quad (3.7)$$

The mass was converted to the height by using Eq. 3.8.

$$H = \frac{m}{\rho \times A_T} \quad (3.8)$$

Before capturing the video footage, the camera was set on Pal video format with the frame rate set to 25 frames per second. All the frames were extracted and the frame where there was a change in height of the liquid for every 0.01 m was extracted. The number of frames between each height increment were counted and divided by 25 to obtain the time taken to discharge the liquid from one height to another. The resultant cumulative time and height were calculated. The calibration results are provided in Appendix B, C and D for circular, square and triangular orifices, respectively.

The height of the liquid drained in meters was plotted against time in seconds. A second-order polynomial was fitted to the curve and the derivative of the trend line equation gave the expression of dh/dt as shown in Fig 3.14. The derivative of dh/dt was used to calculate the flow rate at any time using Eq. 3.9.

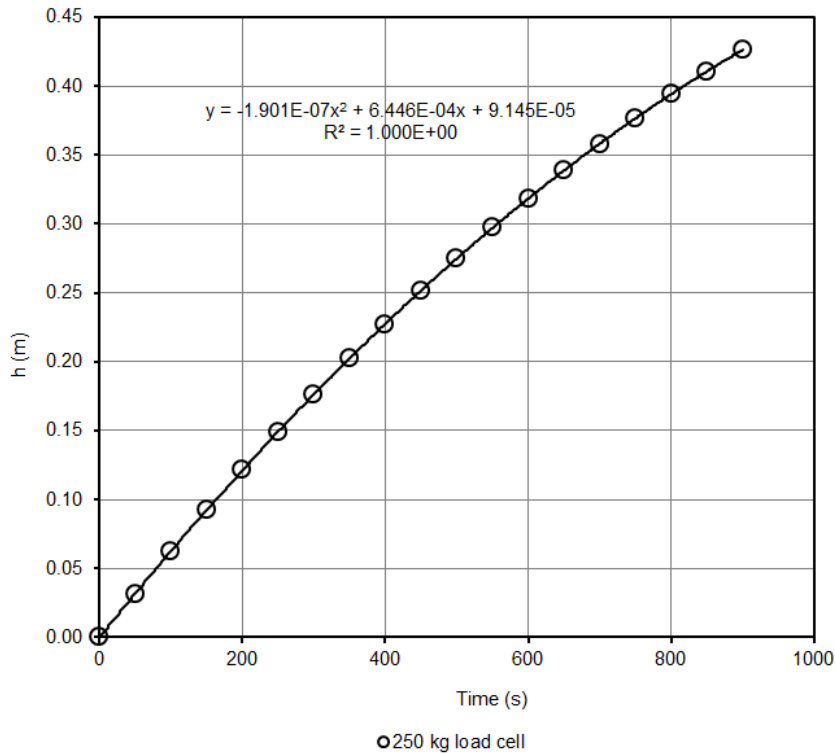


Figure 3.14 Example of the head versus time for 8 mm diameter orifice calibration

$$Q = \frac{dh}{dt} \times A_T \quad (3.9)$$

Figures 3.15, 3.16 and 3.17 show the flow rate against head for 100 kg, 250 kg load cells and camera for circular, square and triangular orifices respectively (8 mm hydraulic diameter). The flow rate versus the head for 12 mm, 16 mm and 20 mm circular, square and triangular orifices are presented in Appendix E. The flow rate obtained from the camera, 250 kg and 100 kg load cell do not differ.

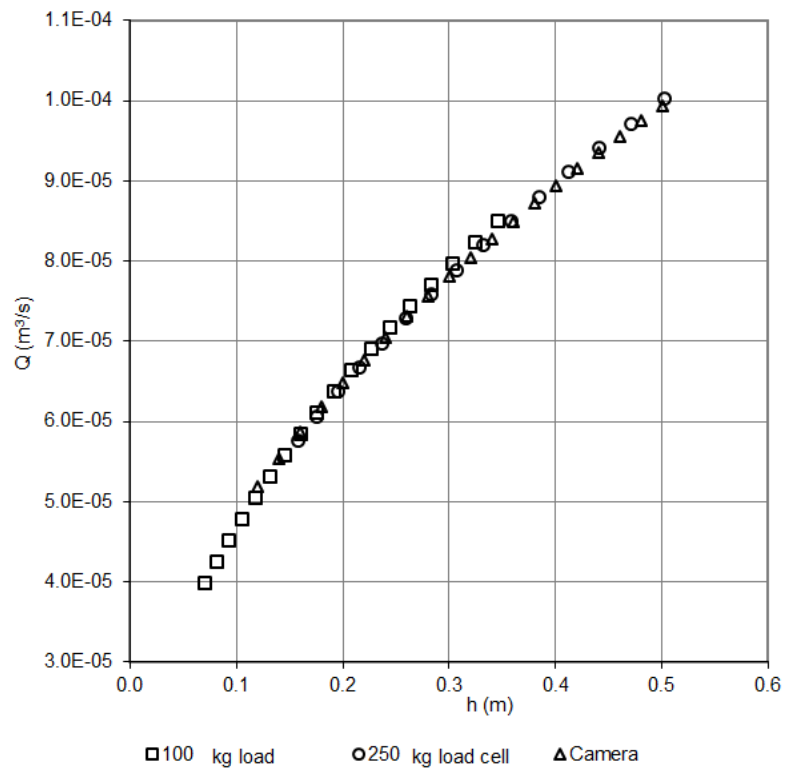


Figure 3.15 Flow rate (m^3/s) versus head (m) for circular orifice (8 mm hydraulic diameter)

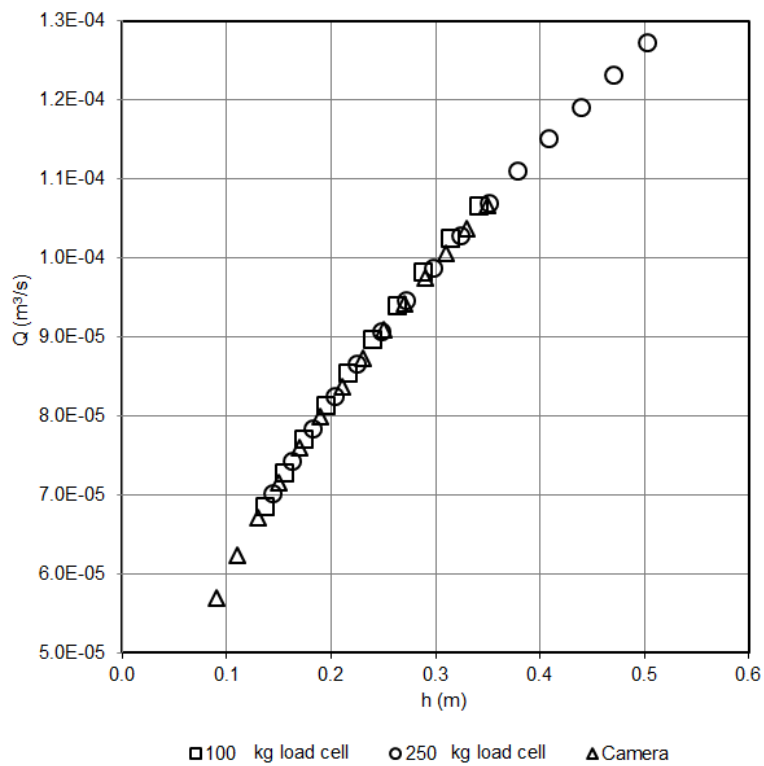


Figure 3.16 Flow rate (m^3/s) versus head (m) for square orifice (8 mm hydraulic diameter)

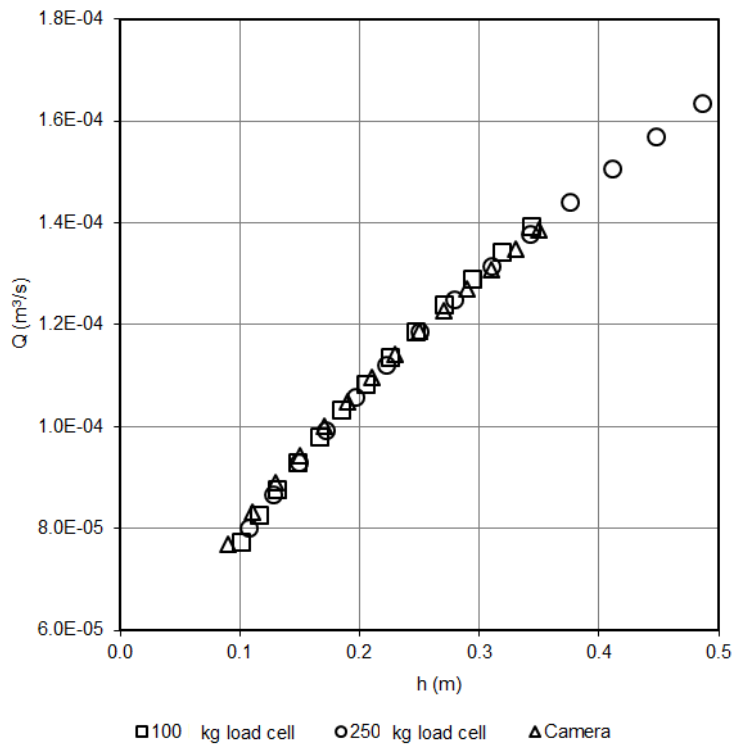


Figure 3.17 Flow rate (m^3/s) versus head (m) for triangular orifice (8 mm hydraulic diameter)

The C_d values were calculated using Eq. 2.44 and the C_d values versus head for circular, square and triangular orifices are presented in Figs. 3.18, 3.19 and 3.20, respectively. They are within $\pm 4\%$ when compared to the standard C_d value of 0.61 for circular curve orifices except for the 8 mm hydraulic diameter data for all the orifice shapes. The average C_d value for each orifice is presented in Table 3.6.

$$Q_1 = C_d A_0 \sqrt{2gh} \quad (2.74)$$

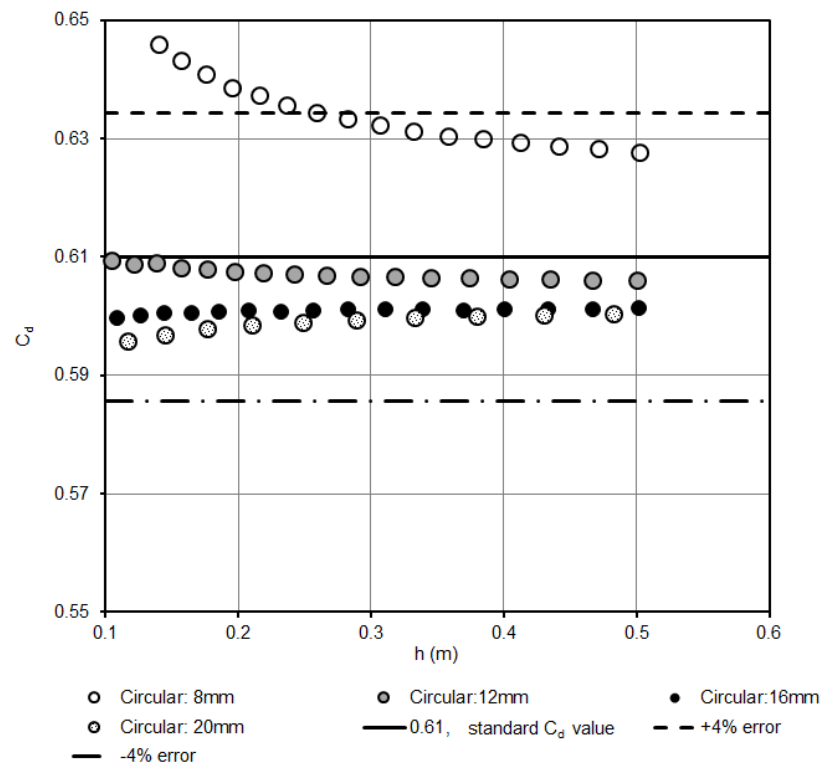


Figure 3.18 C_d versus head for circular orifices

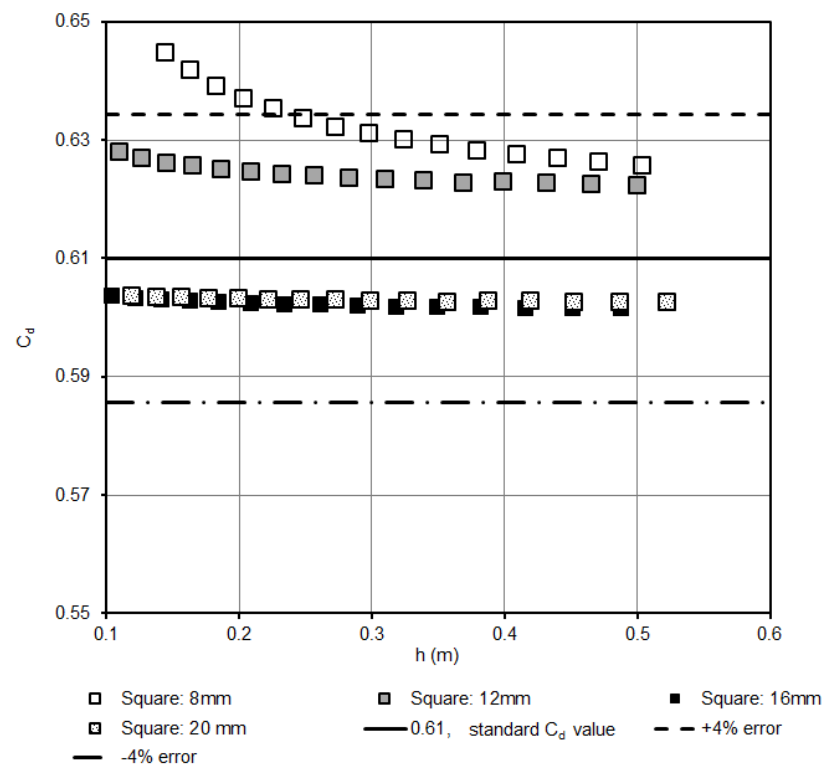


Figure 3.19 C_d versus head for square orifices

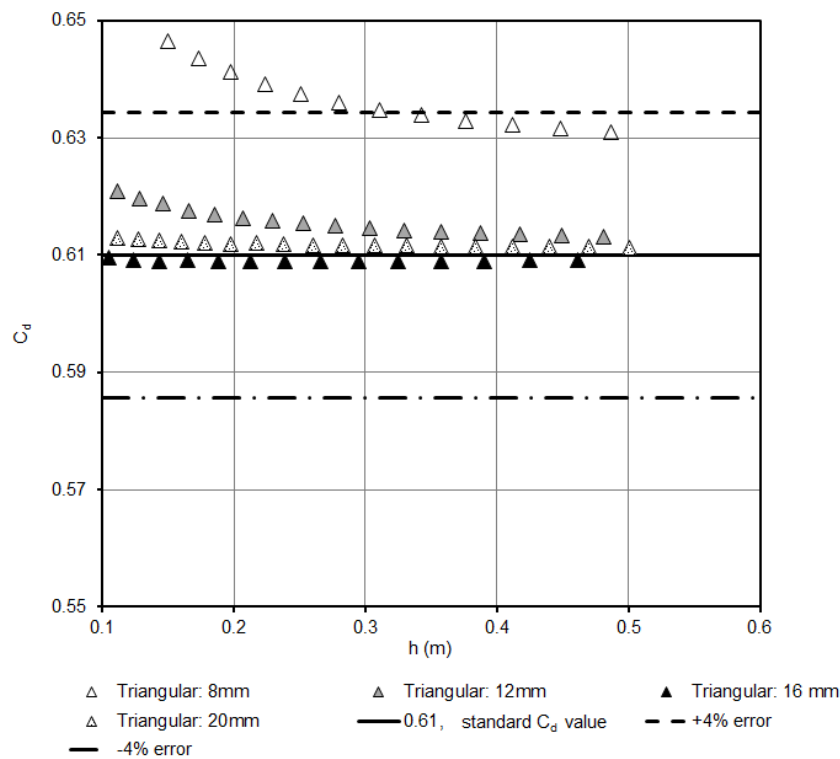


Figure 3.20 C_d versus head for triangular orifices

Table 3.6 Average C_d values for circular, square and triangular orifices

Orifice shape	Hydraulic diameter size (mm)	Average C_d value
Circular	8	0.63
	12	0.61
	16	0.60
	20	0.60
Square	8	0.64
	12	0.63
	16	0.60
	20	0.60
Triangular	8	0.64
	12	0.62
	16	0.61
	20	0.61

3.6.2 Rheology

The shear stresses and shear rates were obtained from the rheometer. Newtonian (Eq. 2.1), power law (Eq. 2.2) and Herschel-Bulkley (Eq. 2.3) models were used to characterise glycerine, CMC solutions and kaolin and bentonite suspensions respectively. Figures 3.21, 3.22, 3.23 and 3.24 show the shear diagrams for 100% glycerine, 7.55% CMC solution, 20.24% kaolin and 7.3% bentonite suspensions respectively. The rheograms for all concentrations of glycerine and CMC solutions; kaolin and bentonite suspensions are shown in Chapter Four.

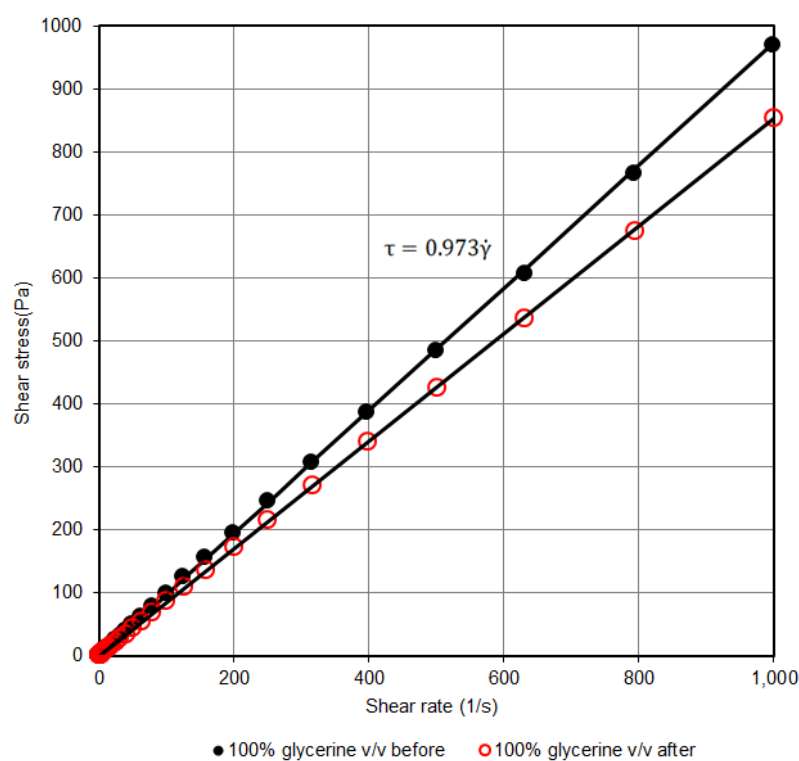


Figure 3.21 Rheogram for 100% glycerine

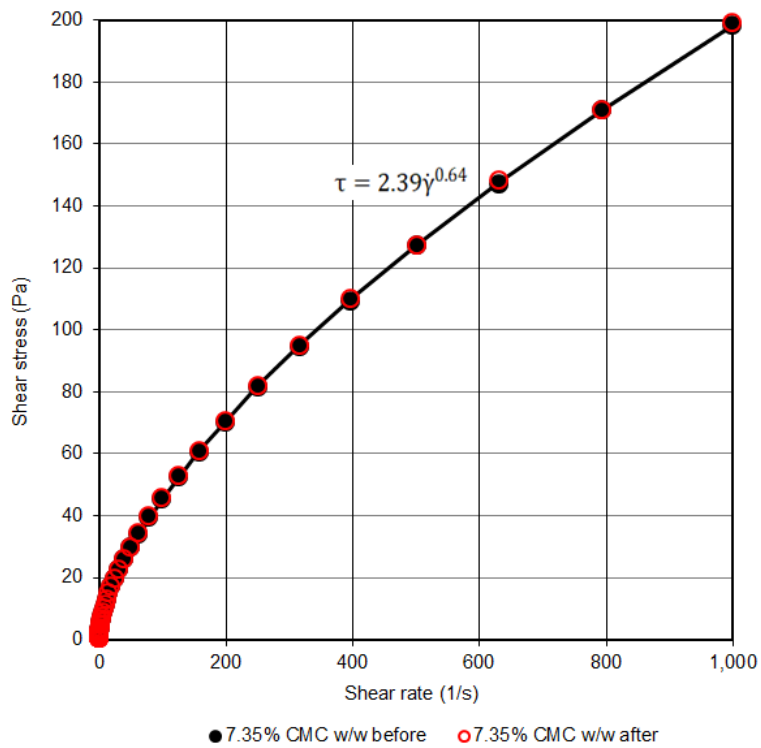


Figure 3.22 Rheogram for 7.55% CMC solution

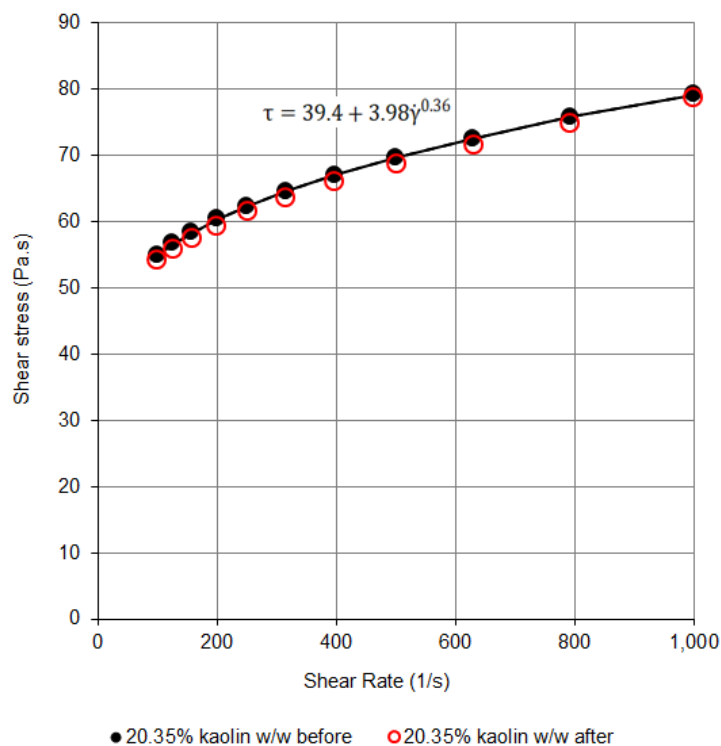


Figure 3.23 Rheogram for 20.34% kaolin suspension

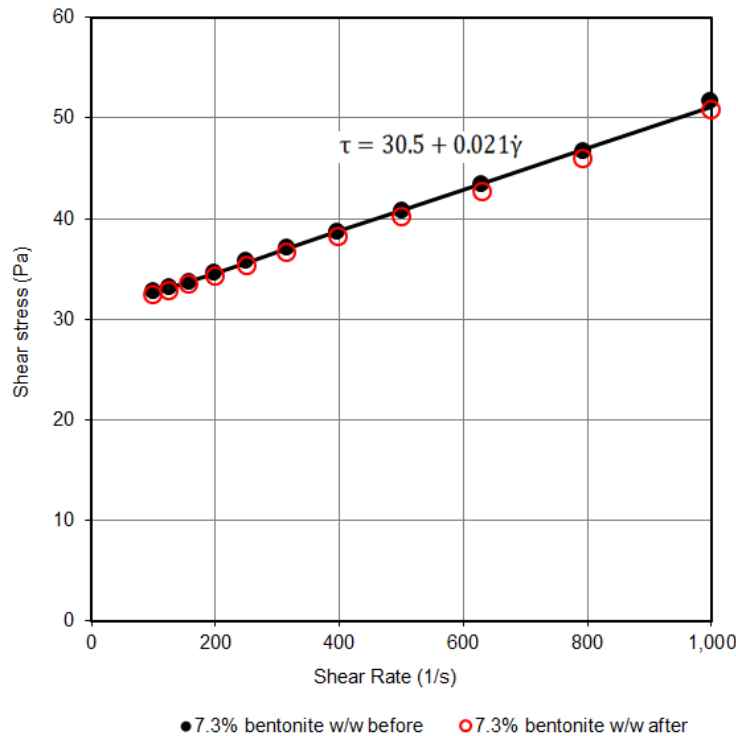


Figure 3.24 Rheogram for 7.3% bentonite suspension

3.6.3 Reynolds number and C_d relationship

A generalised Reynolds number was used to calculate Re for Newtonian liquids (Eq. 2.12). Re_2 in Eq. 2.17 was used to calculate Reynolds numbers for non-Newtonian liquids. The C_d values were plotted against the Reynolds numbers to determined C_d -Re relationship.

$$Re = \frac{\rho v D}{\mu} \quad (2.12)$$

$$Re_2 = \frac{8\rho v^2}{\tau_y + k \left(\frac{8v}{D} \right)^n} \quad (2.17)$$

Re_{MR} (Eq. 2.26) was used to calculate Reynolds numbers for CMC solutions and only used to compare this study's results with the results from the literature.

$$Re_{MR} = \frac{\rho v^{2-n} D^{n'}}{8^{n'-1} k'} = \frac{8\rho v^2}{k' \left(\frac{8v}{D} \right)^{n'}} \quad (2.26)$$

3.6.4 Effect of orifice size and shape

The water C_d values for each hydraulic radius for all the shapes were plotted against the same Reynolds number to establish the effect of shape. The C_d values for all the orifice sizes and shapes and for all the liquids were plotted against Re_2 to determine the effect of shape for both Newtonian and non-Newtonian liquids. The Reynolds numbers for high concentrations of glycerine, CMC solution; kaolin and bentonite suspensions had a unique relationship. Therefore, it was necessary to find a factor that would combine the different $Re-C_d$ relationships.

3.7 Experimental errors

During experimental measurements, there are uncertainties that can and do happen. It is very important to take measurements with great care to reduce the possibility of errors. The main sources of experimental errors can be caused by limited accuracy of the measuring apparatus, limitations and simplifications of the experimental procedure and uncontrolled changes to the environment (Young, 1992; Taylor, 1982; Bevington, 1969).

3.7.1 Unsteady-flow dynamics

The data logger was recording the change in voltage as the liquids are being discharged. The weight of the liquids did not change due to unsteady-flow dynamics and therefore there was no impact on the C_d coefficient. This was confirmed by swinging the tank and recording the voltage using the data logger and comparing it with the voltage recorded without purposely swinging the tank. There was no difference between the two readings. For data that was captured using the camera the frames that were captured when the flow had slightly stabilised, were used to calculate the C_d values.

3.7.2 Relative and absolute errors

The relative error is normally supplied by the manufacturer or it can be expressed as given in Eq. 3.10 or 3.11.

$$\text{Relative error} = \left(\frac{\text{Experimental value} - \text{Accepted value}}{\text{Accepted value}} \times 100 \right) \quad (3.10)$$

or

$$\text{Relative error} = \left(\frac{\text{Experimental value} - \text{theoretical value}}{\text{theoretical value}} \times 100 \right) \quad (3.11)$$

The accuracy of the load cells has been specified by the manufacturer and the calibration details for 100 kg and 250 kg load cells are given in Table 3.7.

Table 3.7 Calibration details for 250 kg and 100 kg load cells

	250 kg	100 kg
Zero balance	$\pm 1\% \text{ FS}$	$\pm 1\% \text{ FS}$
Hysteresis	$\pm 0.02\% \text{ FS}$	$\pm 0.02\% \text{ FS}$
Non-Repeatability	$\pm 0.01\% \text{ FS}$	$\pm 0.01\% \text{ FS}$
Non Linearity	$\pm 0.03\% \text{ FS}$	$\pm 0.02\% \text{ FS}$
Combined Error	$\pm 0.03\% \text{ FS}$	$\pm 0.02\% \text{ FS}$

Orifices

The calibration and flow rate data captured were the voltages and the time stamp. The sampling rate was 60 Hz. That means the data was recorded every 0.01667 sec. Table 3.8 illustrates the data points captured for each orifice during calibration. The data was categorised into blocks that comprised of a specified number of data points. The average of a set of voltage data points in each block was used for further calculation of the mass used. For each block, the standard deviation for voltage was calculated. The range of the standard deviation for all the orifices is between 0.01 and 0.03 as shown in Fig. 3.25 for the 8 mm hydraulic diameter orifices and in Appendix F for the 12 mm, 16 mm and 20 mm hydraulic diameters. The standard deviation for each set of data points (block) differed because of the continuous flow.

Table 3.8 Load cell data points for 250 kg

Orifice shape	Hydraulic diameter (mm)	Data points
Circular orifices	8	56179
	12	26309
	16	14929
	20	11199
Square orifices	8	43659
	12	20279
	16	11969
	20	7499
Triangular orifices	8	33289
	12	14918
	16	8709
	20	5669

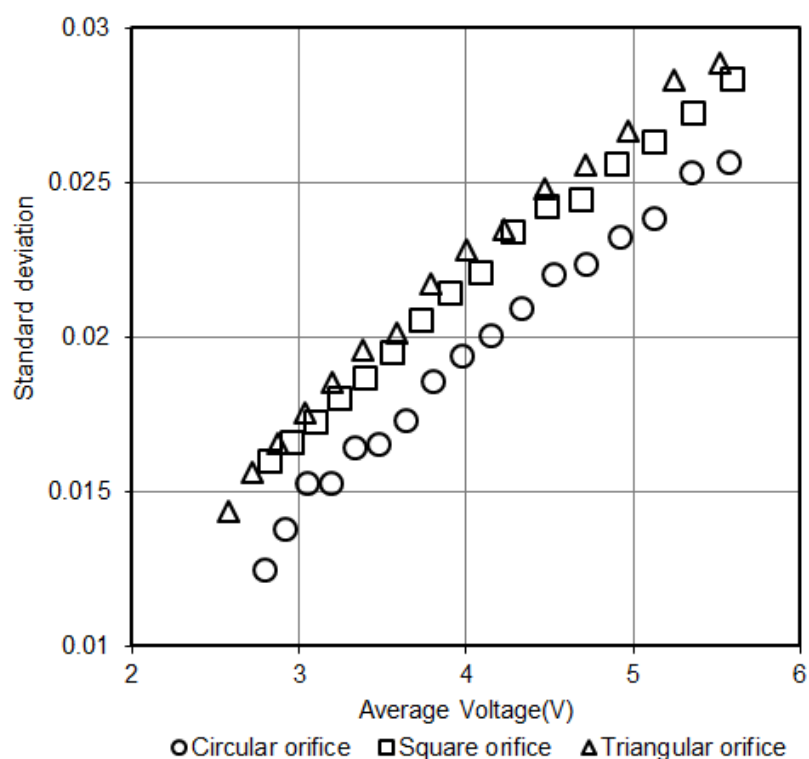


Figure 3.25 Standard deviation versus average voltage (V) for 8 mm hydraulic diameter orifices

Tape measure and camera

The measuring tape was accurate to ± 0.0005 m. The head used was obtained from the frames extracted and each height was taken after a water level drop of 0.01 m. The reflex angle was calculated to determine the parallax error. Therefore, each height recorded was within $\pm 0.39^\circ$.

$$\tan^{-1} = \left[\frac{\text{height difference}}{\text{distance from camera to tank}} \right] = \left[\frac{0.01}{1.47} \right] = 0.39^\circ \quad (3.12)$$

Relative density measurements

The relative density measurements were taken three times for each slurry. The largest error in the measurements taken was found to be 0.4%. The equipment and procedure for relative density measurements test is explained.

The apparatus used are a water bottle with tap water; three volumetric flasks (250 ml); and top pan balance that was accurate to ± 0.001 g. The accuracy of the top pan balance is important because the accurate density measurement highly depend upon accurate weight values. The relative density measurements were taken three times for each slurry. The largest error in the measurements taken was found to be 0.4%.

The following procedure was followed:

- Ensure that the volumetric flasks are clearly labelled (1, 2 and 3), empty and dry.
- Weigh each flask (M_1 , mass of bottle).
- Record the liquid sample and water temperatures.
- Partially fill the empty flasks with the test material and weigh them (M_2 , Mass of bottle and sample).
- Fill each flask with water and ensure that the material clinging to the walls of the flask is carried down with the water poured, to the graduated mark.
- Weigh all three flasks containing sample and water (M_3 , Mass of bottle; sample and water).
- Empty the flasks and clean them thoroughly.
- Fill each flask with water to the graduated mark and weigh the flasks (M_4 , Mass of bottle and water).

- Calculate the relative density of the liquids sample using equation 3.13

$$RD = \left[\frac{M_2 - M_1}{(M_3 - M_2) - (M_4 - M_1)} \times K \right] \quad (3.13)$$

K is a constant for water temperature correction

From Equation 3.13:

$$\rho = RD \times \rho_w \quad (3.14)$$

Liquid temperature

The error in the measurement of the temperature was $\pm 0.2^\circ C$.

3.7.3 Combined errors

A combined error is an error that comes from a variable that has been computed from other variables with their subsequent errors. The procedure that quantifies the combined error has been explained by Brinkworth (1968): it uses the root mean square approach, where the highest expected error ΔX is given in Eq. 3.15, for X as a function of N.

$$\left(\frac{\Delta X}{X}\right)^2 = \sum \left(\frac{\partial X}{\partial N}\right)^2 \left(\frac{N}{X}\right)^2 \left(\frac{\Delta N}{N}\right)^2 \quad (3.15)$$

The correlation coefficient (R^2) and log standard error (LSE) were calculated to compare the performance of the different Reynolds numbers correlations in predicting the C_d values and flow rate (Haldenwang, 2012; Lazarus & Neilson, 1978). From R^2 and LSE the C_d and discharge accuracies were established.

$$R^2 = \frac{\sum(f_{pred} - ave f_{exp})^2}{\sum(f_{exp} - f_{pred})^2 + \sum(f_{pred} - ave f_{exp})^2} \quad (3.16)$$

$$LSE = \frac{\sqrt{\sum(\log(f_{exp}) - \log(f_{pred}))^2}}{N-1} \quad (3.17)$$

The maximum expected error analysis presented in this section are for the shear stress, flow height and orifice velocity.

Rheology

The main sources of error in the concentric cylinder type measuring system comes from the end-effects, wall slip, inertia, secondary flows, viscous heating effects and misalignment of the geometry (Chhabra & Richardson, 2008).

The mean relative squared error was used to determine the accuracy, and compare the performance of the rheological models used.

$$E = \frac{1}{N} \sqrt{\sum_{n=1}^N \left(\frac{\tau_{exp} - \tau_{calc}}{\tau_{exp}} \right)^2} \quad (3.18)$$

Where τ_{exp} is the experimental shear stress and τ_{calc} is the calculated shear stress. The smaller the value of the error obtained the more accurate is the model.

Liquid height

The height was calculated from Eq. 3.19.

$$h = \frac{m}{\rho \times A_T} \quad (3.19)$$

Therefore, the highest expected error was computed from Eq. 3.20.

$$\left(\frac{\Delta h}{h} \right)^2 = \left(\frac{\Delta m}{m} \right)^2 \quad (3.20)$$

The results obtained are shown graphically in Figs 3.26, 3.27 and 3.28 for circular, square and triangular orifices, respectively.

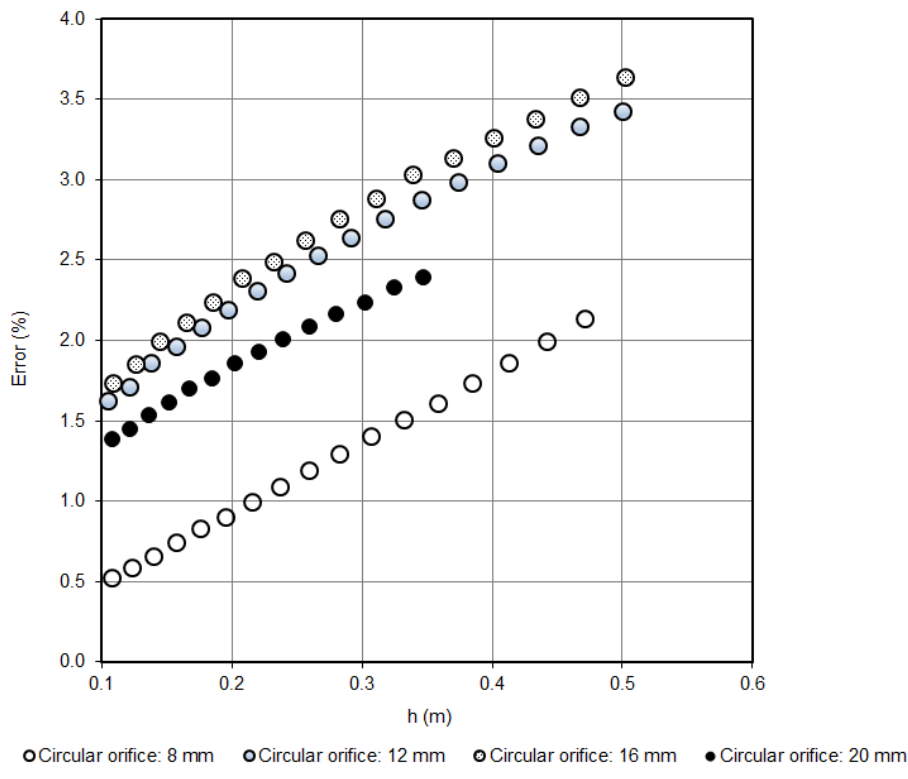


Figure 3.26 Maximum expected % error in head (m) for circular orifices

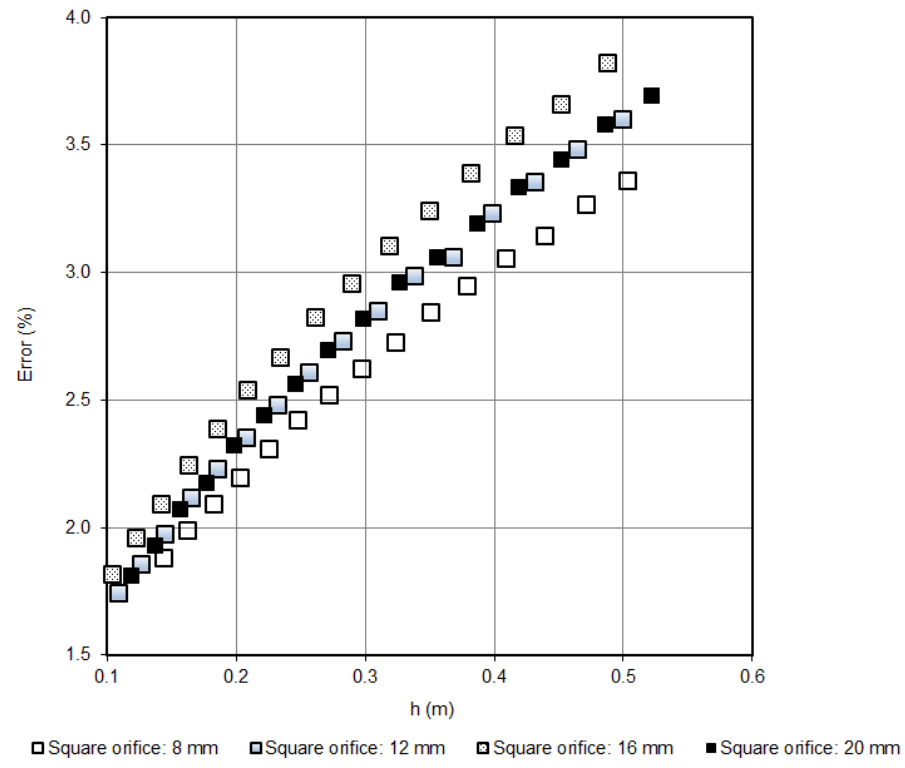
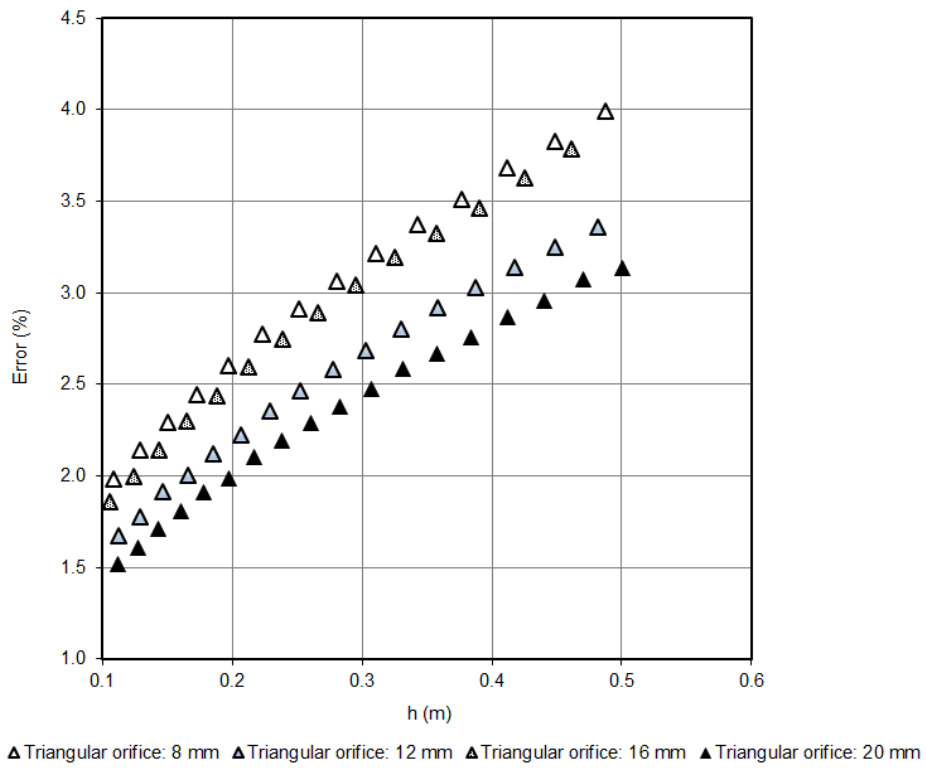


Figure 3.27 Maximum expected % error in head for square orifices



▲ Triangular orifice: 8 mm ▲ Triangular orifice: 12 mm ▲ Triangular orifice: 16 mm ▲ Triangular orifice: 20 mm

Figure 3.28 Maximum expected % error in head for triangular orifices

Orifice velocity

The equation for orifice velocity is given in Eq. 2.40. Therefore, the highest expected error for orifice velocity is:

$$v_2 = \sqrt{2gh} \quad (2.7540)$$

$$\left(\frac{\Delta v}{v}\right)^2 = \left(\frac{\Delta h}{2h}\right)^2 \quad (3.21)$$

The maximum percentage error for orifice velocity is given in Table 3.9 and shown in Figs 3.29, 3.30 and 3.31 for circular, square and triangular orifices respectively.

Table 3.9 % average maximum error for orifice velocity

Orifice shape	Hydraulic diameter (mm)	% Average Maximum error for orifice velocity
Circular orifices	8	10
	12	11
	16	11
	20	9
Square orifices	8	11
	12	11
	16	12
	20	11
Triangular orifices	8	13
	12	11
	16	12
	20	10

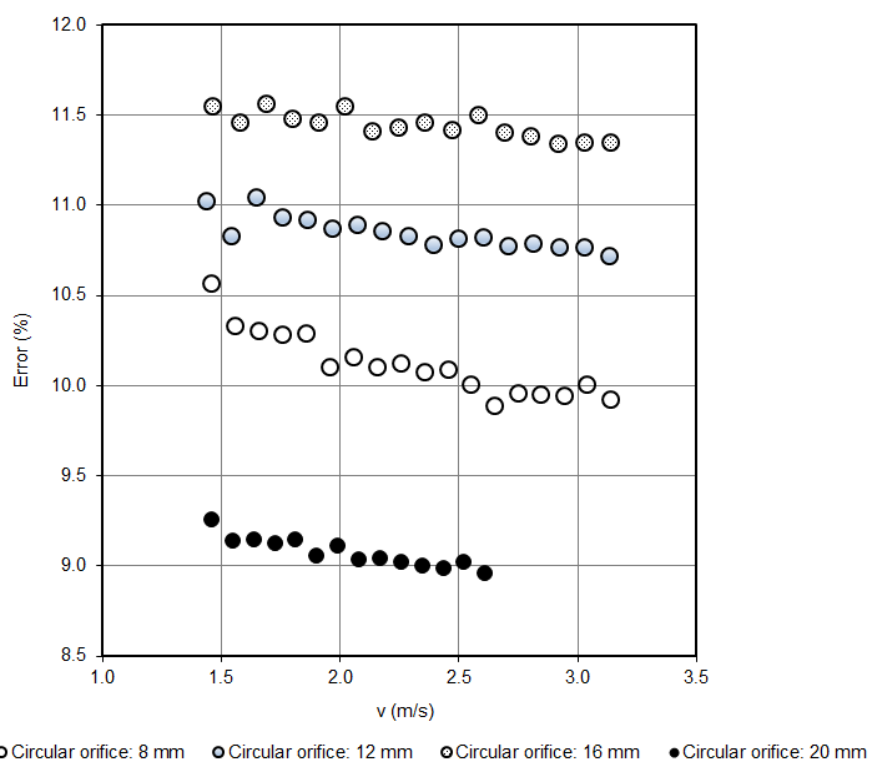


Figure 3.29 Maximum expected % error of orifice velocity for circular orifices

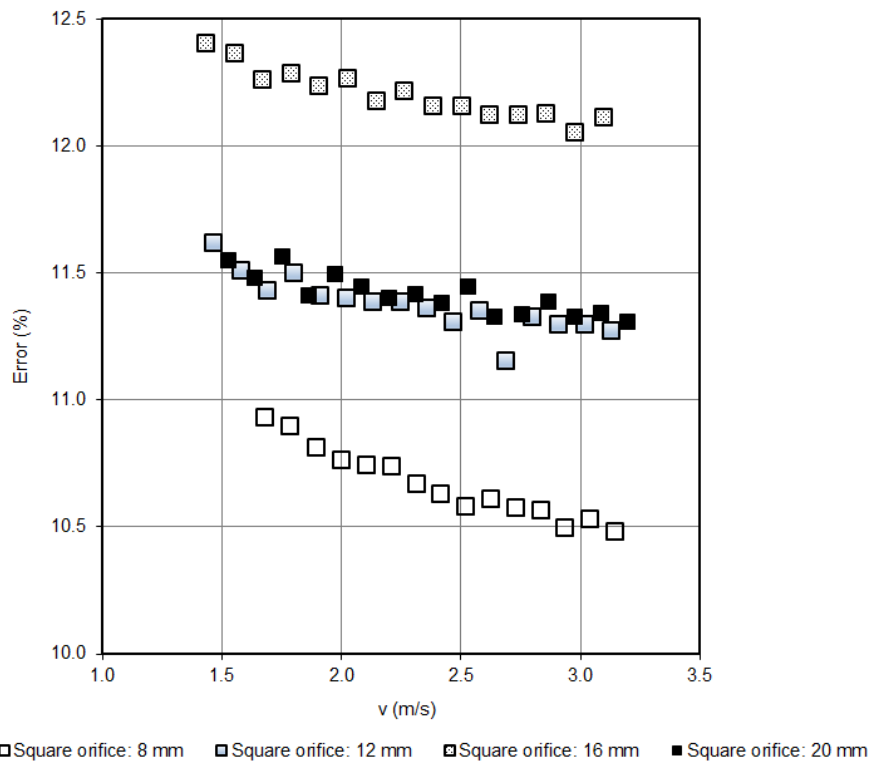


Figure 3.30 Maximum expected % error of orifice velocity for square orifices

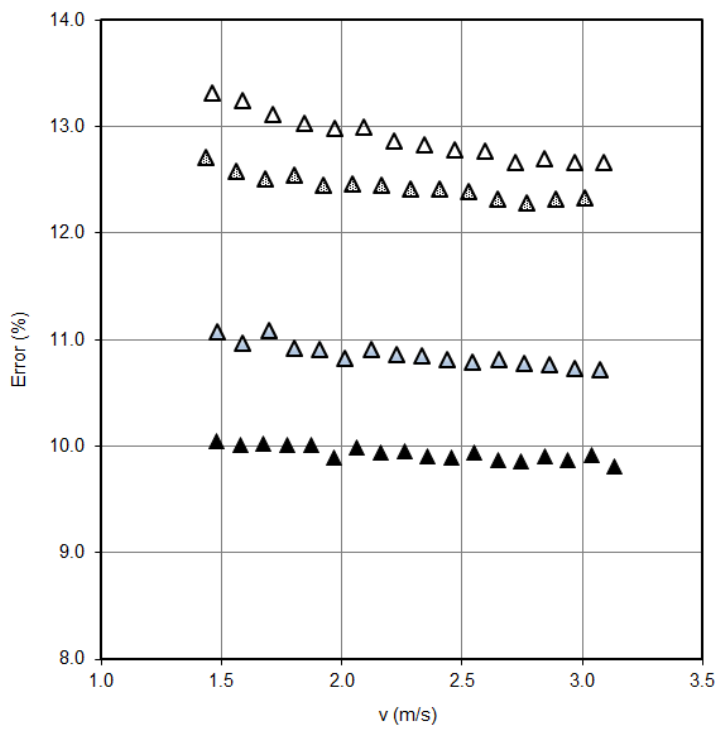


Figure 3.31 Maximum expected % error of orifice velocity for triangular orifices

3.8 Conclusion

The facility and equipment used to carry out the experiments for this study have been discussed. The square tank fitted with orifice plate at the bottom was used to carry out the flow rate measurements. The tank was suspended from a load cell. The triangular, square and circular shapes orifices were used. Moreover, the calibration of the DAQ system and load cell has been discussed. For calibration purposes, a high-speed camera recorded the discharge of water out of the tank, with the frames extracted from the captured video to calculate the flow rate. An MCR 300 Paar Physica rheometer was used to determine the rheological properties of the liquids. The liquids tested were water for calibration purposes, different concentrations of glycerine, CMC solution, kaolin and bentonite suspensions. The method followed to prepare the liquids and carry out the flow rate and rheology tests were discussed.

The processing of data obtained has been explained, including a discussion of orifice calibration data, liquid flow rate measurements data, rheology data and establishing $Re-C_d$ relationship. The orifice calibration C_d values for circular, square and triangular orifices are within $\pm 4\%$ error as compared to the standard used average C_d value of 0.61 for circular orifice. Error calculations based on R^2 and LSE were conducted, and the C_d and discharge accuracies were established.

CHAPTER FOUR: RESULTS AND ANALYSIS

4.1 Introduction

In this chapter, results are presented and analysed. Water was used for calibration purposes. Different percentage volume concentrations of glycerine and kaolin suspensions and percentage mass concentrations of CMC solutions and bentonite suspensions were tested. The rheology and flow rate measurement results obtained are analysed including the effect of orifice shape and rheological properties.

4.2 Rheology results

The rheological and physical parameters of the test liquids are given in Table 4.1. The shear rate calculated from the flow rate measurement through the orifices ranged between $\pm 200 \text{ s}^{-1}$ and $\pm 2600 \text{ s}^{-1}$. The shear rates that could be obtained by the rheometer ranged between 100 s^{-1} to 1000 s^{-1} and this covers the application shear rate of the flow through the orifices reasonably well. Shear rates under 100 s^{-1} were not within the shear rate ranges that were measured through orifices and beyond 1000 s^{-1} the results were developing secondary flow cells (Taylor) because of centrifugal force induced by rotating bob. However, these values are based on the assumption of $8v/d_h$ which would have to be revisited after analysing the experimental results obtained here.

Table 4.1 Rheological and physical parameters of the test liquids

Fluid	Conc.	Density	k	n	T _y	μ	$\frac{8v}{d_h}$ from the orifice	Temp °C
	%	kg/m ³	Pa.s ⁿ		Pa	Pa.s	s ⁻¹	
Kaolin w/w	20.3	1336	3.98	0.36	39.4	-	541-2318	16
	13.1	1217	0.067	0.72	8.9	-	821-2294	18
CMC w/w	7.55	1043	2.39	0.64	-	-	416-2276	18
	6.58	1037	0.882	0.70	-	-	527-2382	18
	5.21	1029	0.206	0.79	-	-	563-2518	18
	2.81	1016	0.017	0.97	-	-	508-2487	18
	2.40	1014	0.006	1.00	-	-	605-2606	25
Bentonite w/w	7.3	1046	0.021	1.00	30.5	-	691-3170	21
	6.99	1044	0.014	1.00	15.7	-	653-2606	17
	3.77	1023	0.006	1.00	1.13	-	574-2571	18
Glycerine v/v	100	1258	-	-	-	0.973	212-1870	18
	96	1248	-	-	-	0.304	467-1786	19
	93	1242	-	-	-	0.129	435-1756	17
	65	1179	-	-	-	0.019	515-2406	18

4.2.1 Kaolin suspensions

Kaolin suspensions, 20.35% and 13.14%, were prepared and tested separately, with their rheograms given in Fig. 4.1.

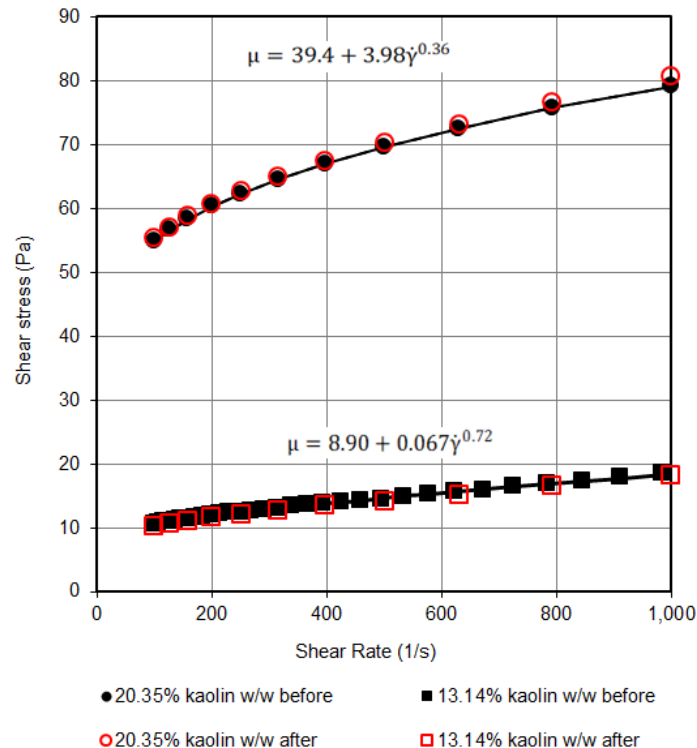


Figure 4.1 Rheograms for kaolin suspensions

4.2.2 Bentonite suspensions

The shear diagrams for 7.3%, 6.99% and 3.77% bentonite suspensions presented in Fig. 4.2 show Bingham liquids characteristics. The values of yield stress, τ_y and fluid consistency factors, k , increase as the concentration increases.

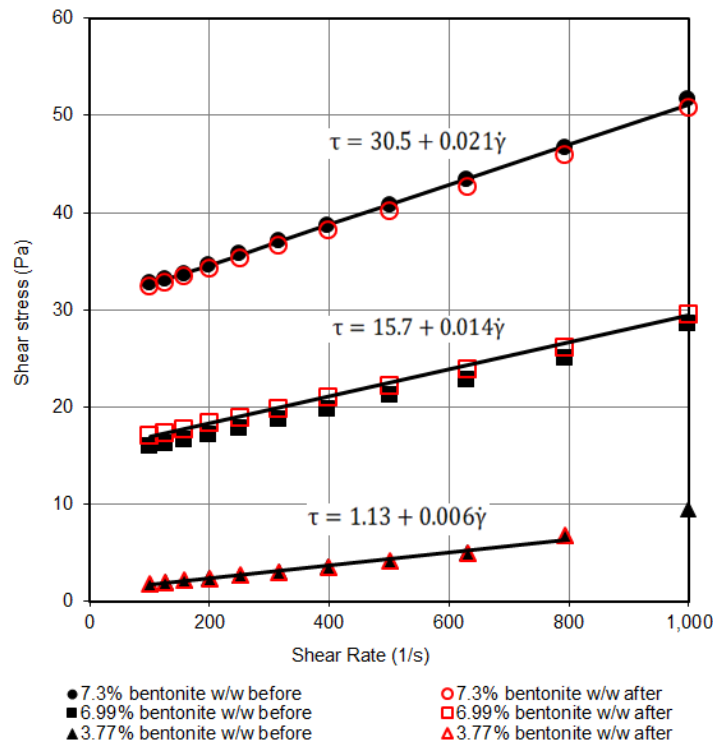


Figure 4.2 Rheograms for bentonite suspensions

4.2.3 CMC solutions

The rheograms for CMC solutions tested are illustrated in Figs. 4.3 and 4.4. Fig. 4.3 shows the shear diagram for 2.4% CMC. It has Newtonian fluid characteristics, as the fluid consistency index, n , is 1. Fig. 4.4 shows the rheograms for 7.5%, 6.58%, 5.21% and 2.81% CMC solutions; the solutions have power law behaviour.

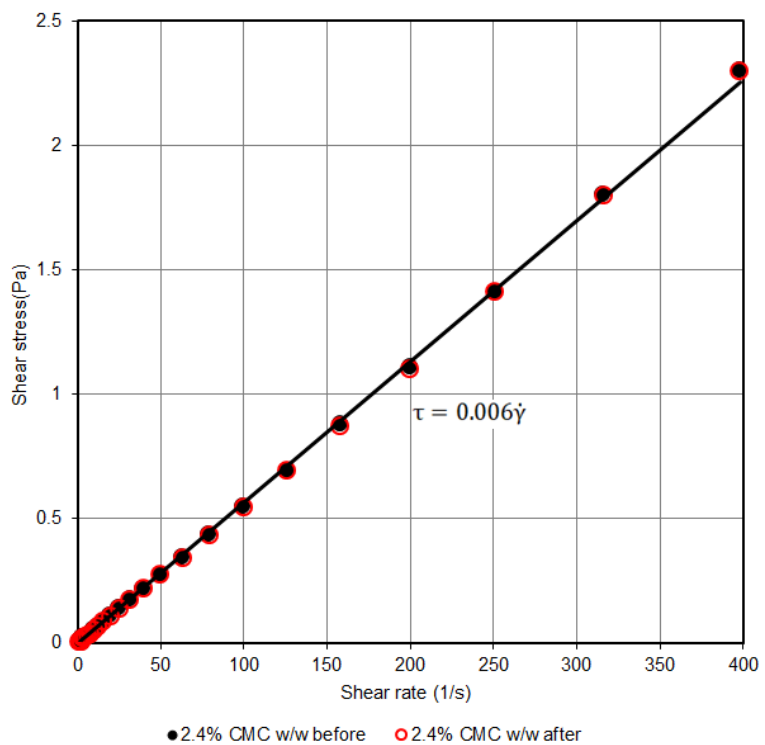


Figure 4.3 Rheogram for 2.4% CMC solution

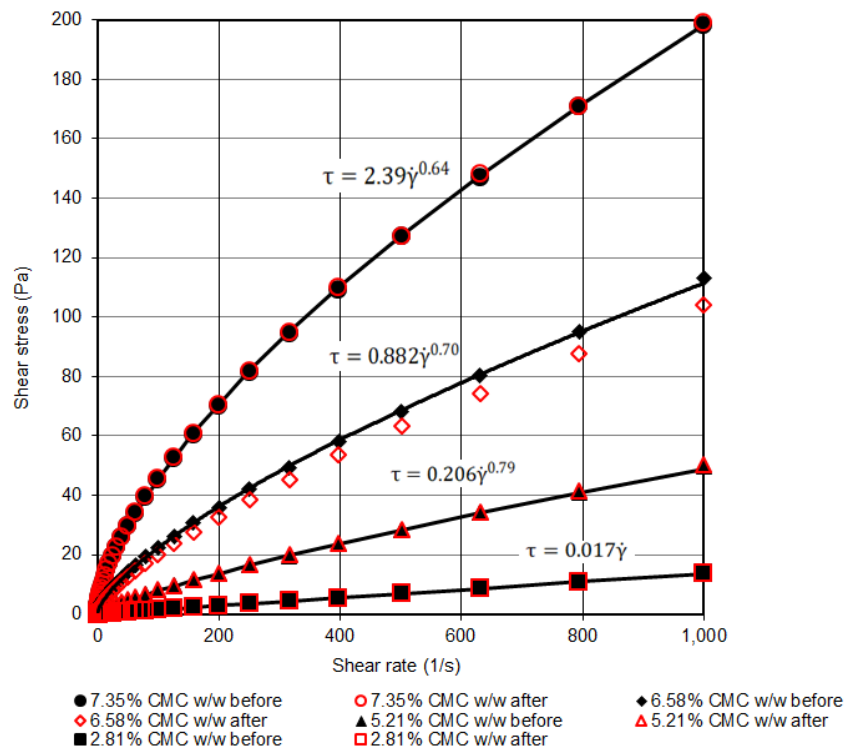


Figure 4.4 Rheograms for CMC solutions

4.2.4 Glycerine solutions

Glycerine solutions are Newtonian liquids. The viscosity increases steeply with increase in concentration. The shear diagrams for glycerine are shown in Fig. 4.5.

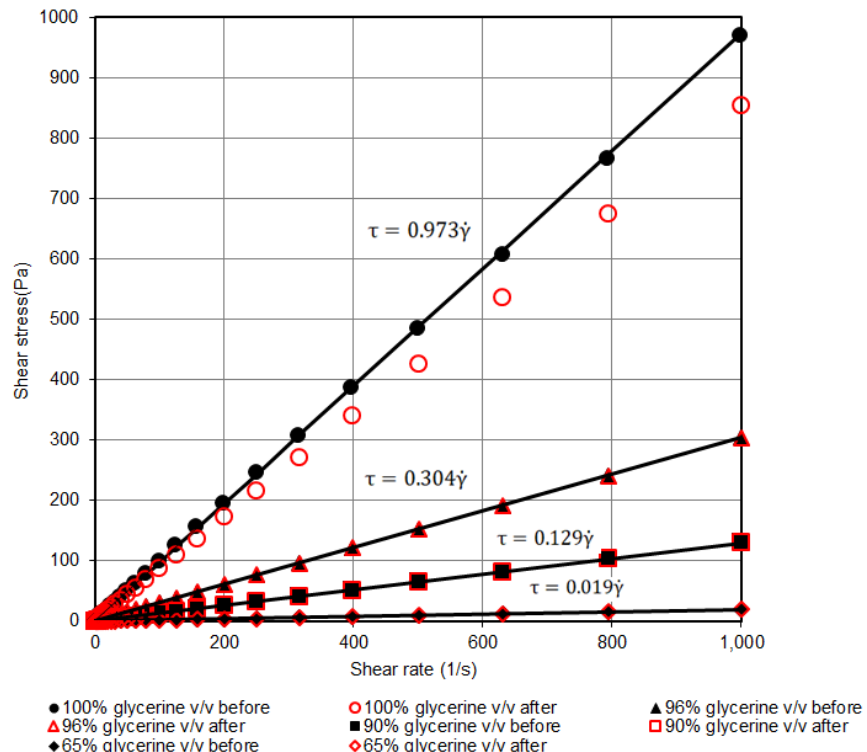


Figure 4.5 Rheograms for glycerine solutions

4.3 Effect of orifice shape (water results)

The water results are tabulated in Appendix B, C and D. Figures 4.6, 4.7, 4.8 and 4.9 show the comparison between circular, square and triangular orifices for 8 mm, 12 mm, 16 mm and 20 mm orifices, respectively. The C_d -head relationship indicates that there is no significant difference in C_d values for all the orifice shapes for the 8 mm hydraulic diameter.

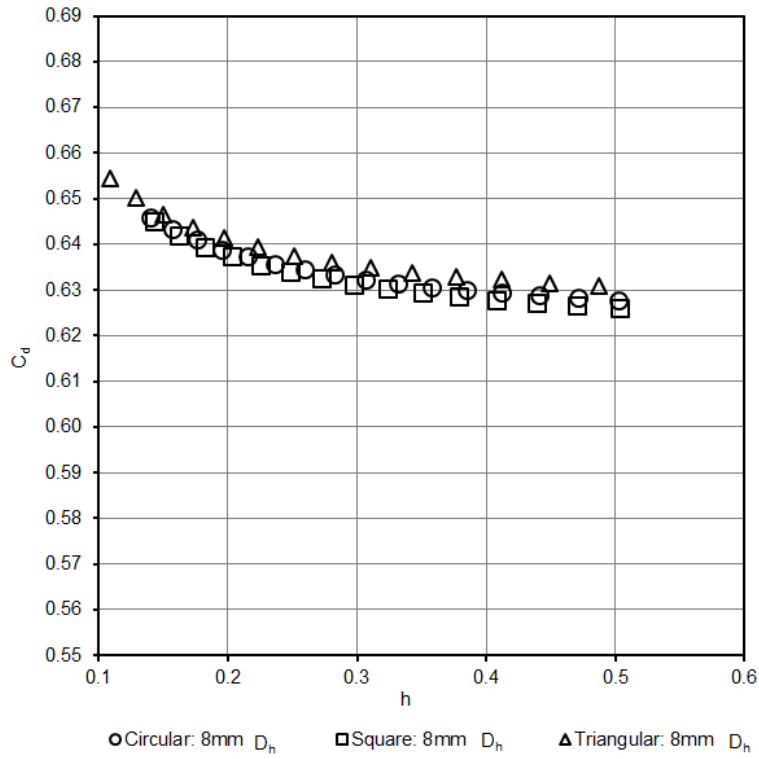


Figure 4.6 Water C_d versus head (m) for 8 mm hydraulic diameters orifices

The 12 mm hydraulic diameter square orifices show that square orifice and triangular orifice C_d values are above circular orifices by 3% and 2%, respectively (Fig. 4.7).

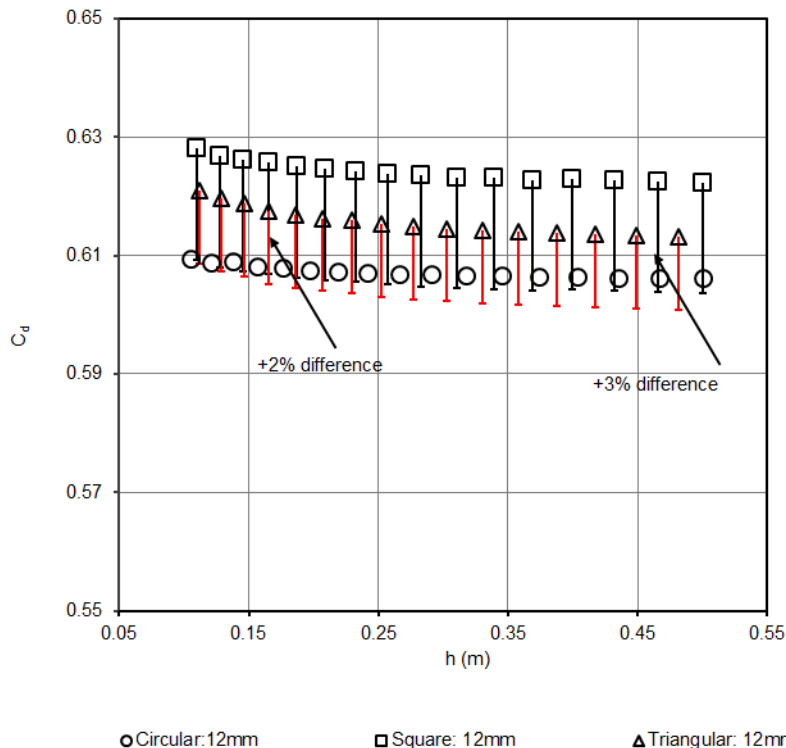


Figure 4.7 Water C_d versus head (m) for 12 mm hydraulic diameters orifices

Figure 4.8 shows hardly any difference between the 16 mm hydraulic diameter circular and square orifices C_d values; triangular orifices C_d values are +1.5% different from circular and square orifices.

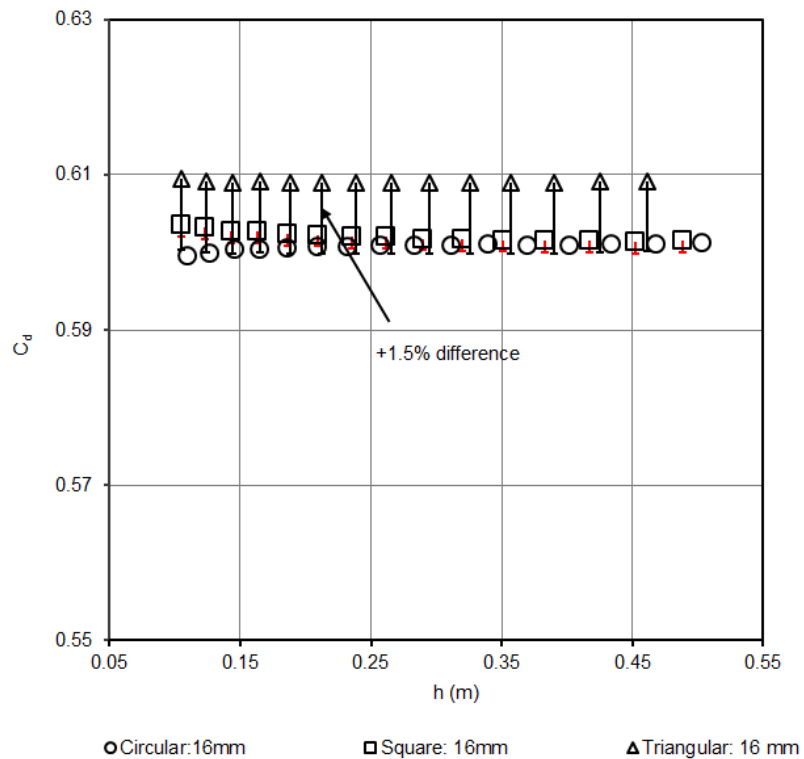


Figure 4.8 Water C_d versus head (m) for 16 mm hydraulic diameters orifices

The C_d versus head relationship for orifices with hydraulic diameter of 20 mm is illustrated in Fig. 4.9. The square and triangular orifices are 1 and 2% above the circular orifice.

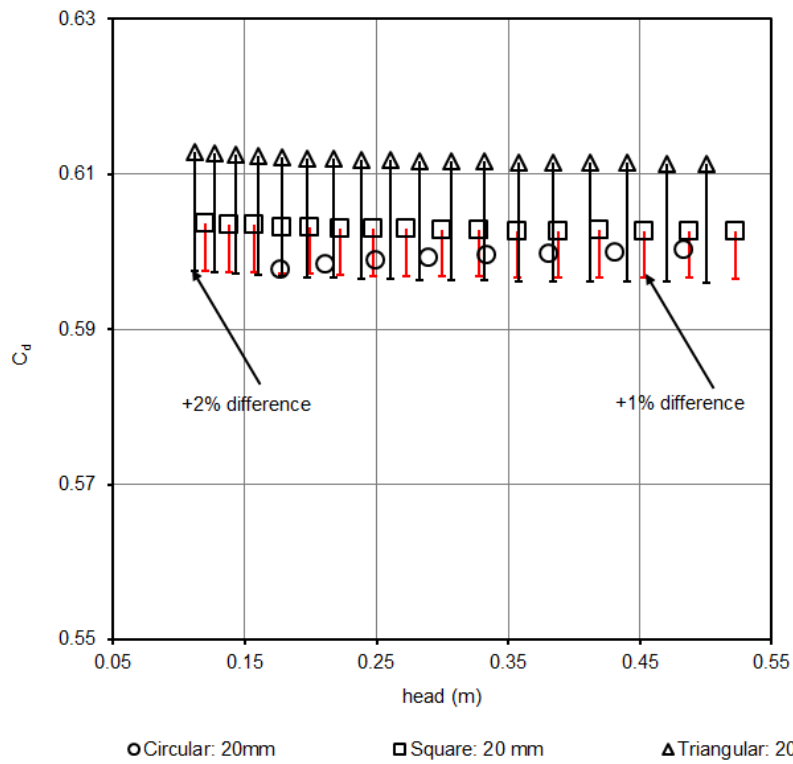


Figure 4.9 C_d versus head (m) for 20 mm hydraulic diameters orifices

4.4 Flow rate test

The flow rate test was carried out for all the test liquids. The results for glycerine and CMC solutions and kaolin and bentonite suspension are illustrated in Appendices E to T. Figures 4.10, 4.11 and 4.12 show the C_d - Re_2 relationship for circular, square and triangular orifice respectively, for all the liquids. The higher concentrations of the test liquids are in the laminar region and the C_d values increase with the increase in Reynolds numbers. For all the orifices, each liquid model has a unique behaviour in the laminar region and forming one curve with a constant C_d value in the turbulent region. This is due to the effect of viscosity for glycerine and CMC solutions, and viscosity and yield stress for kaolin and bentonite suspensions.

For circular orifices, glycerine solution had the lowest Re starting from $Re=12$, CMC at $Re=57$, kaolin at $Re=237$ and bentonite at $Re=332$. The highest Reynolds numbers obtained for the circular orifice is at $Re=61732$.

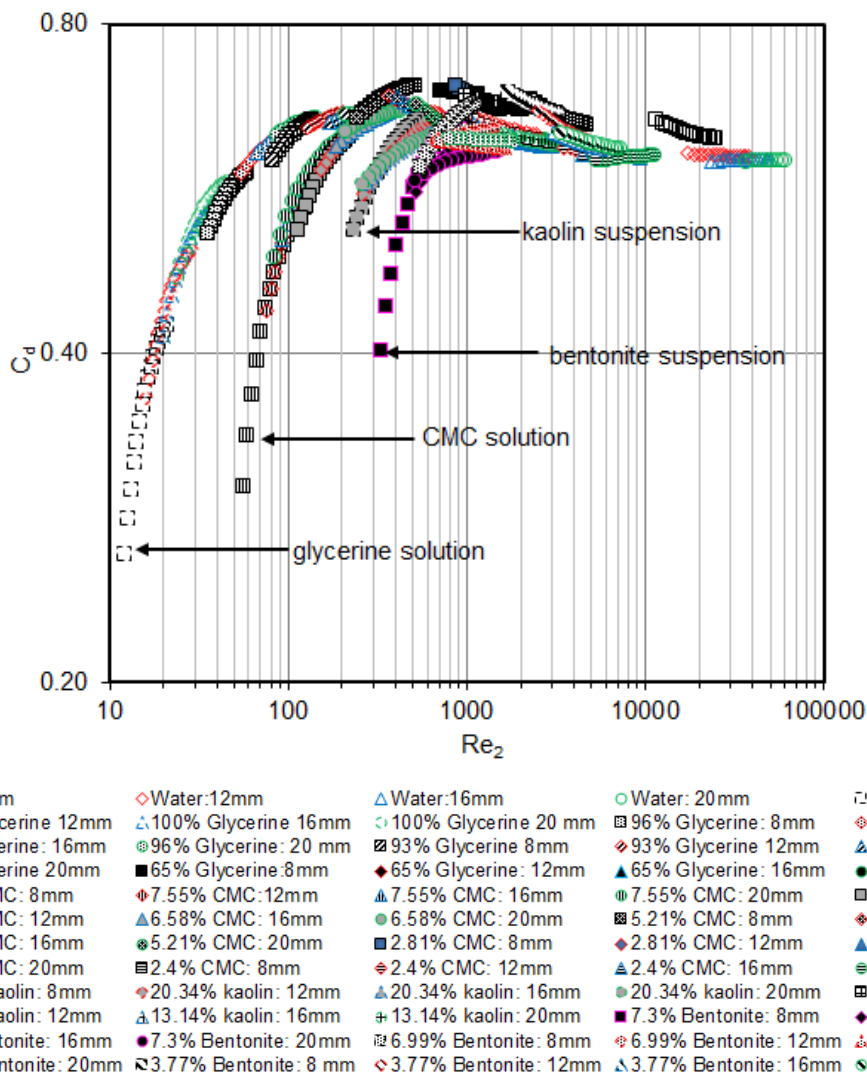


Figure 4.10 C_d versus Re_2 for circular orifices

The square orifices Reynolds number values started from $Re=11$ for the glycerine solution, $Re=53$ for the CMC solution, $Re=270$ for the kaolin suspension and $Re=342$ for the bentonite suspension. The highest Re value is 61732.

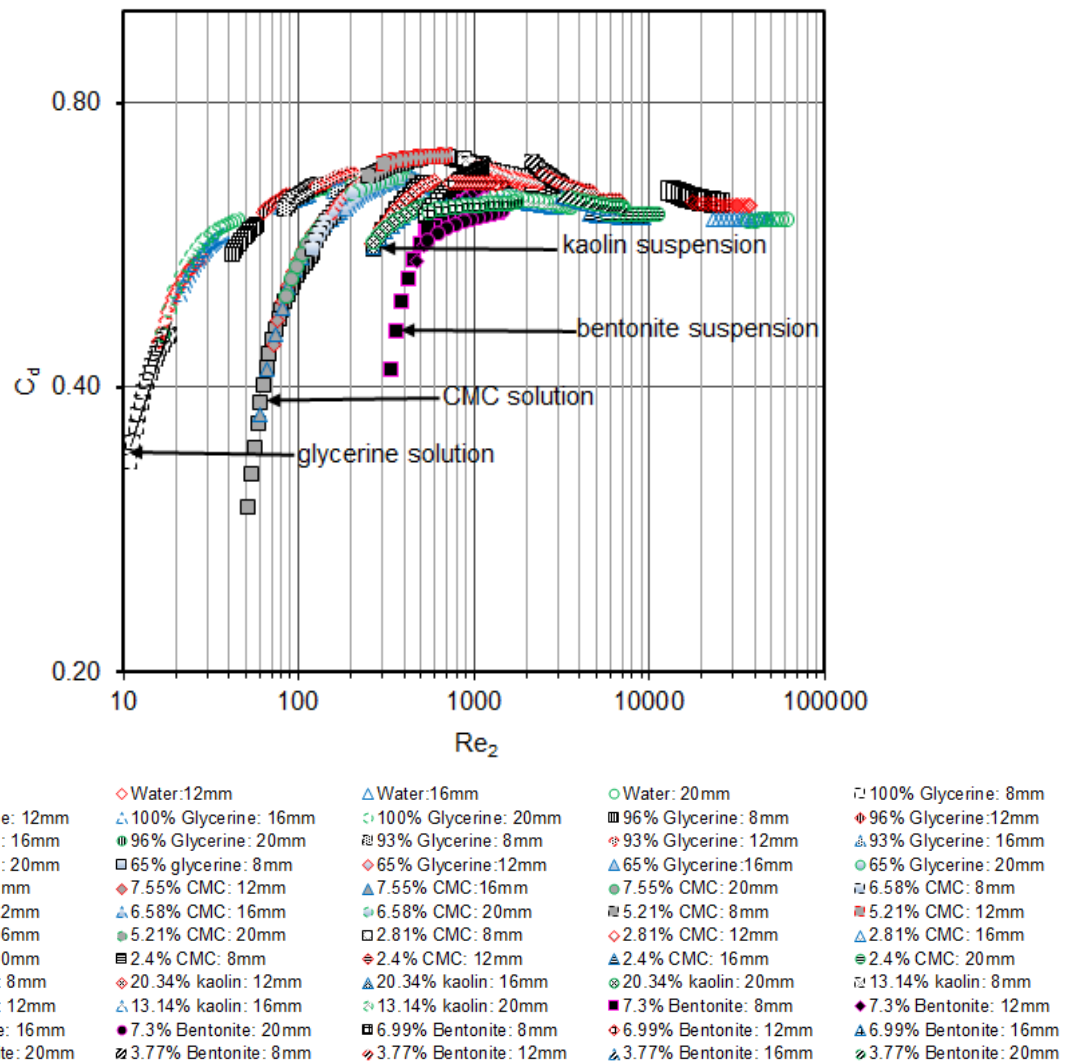


Figure 4.11 C_d versus Re_2 for square orifices

The lowest Reynolds numbers obtained for triangular orifices for glycerine solutions, CMC solutions, kaolin and bentonite suspensions are $Re=11$, $Re=56$, $Re=245$ and $Re=396$ respectively. The highest Reynolds number value obtained is at $Re=62608$.

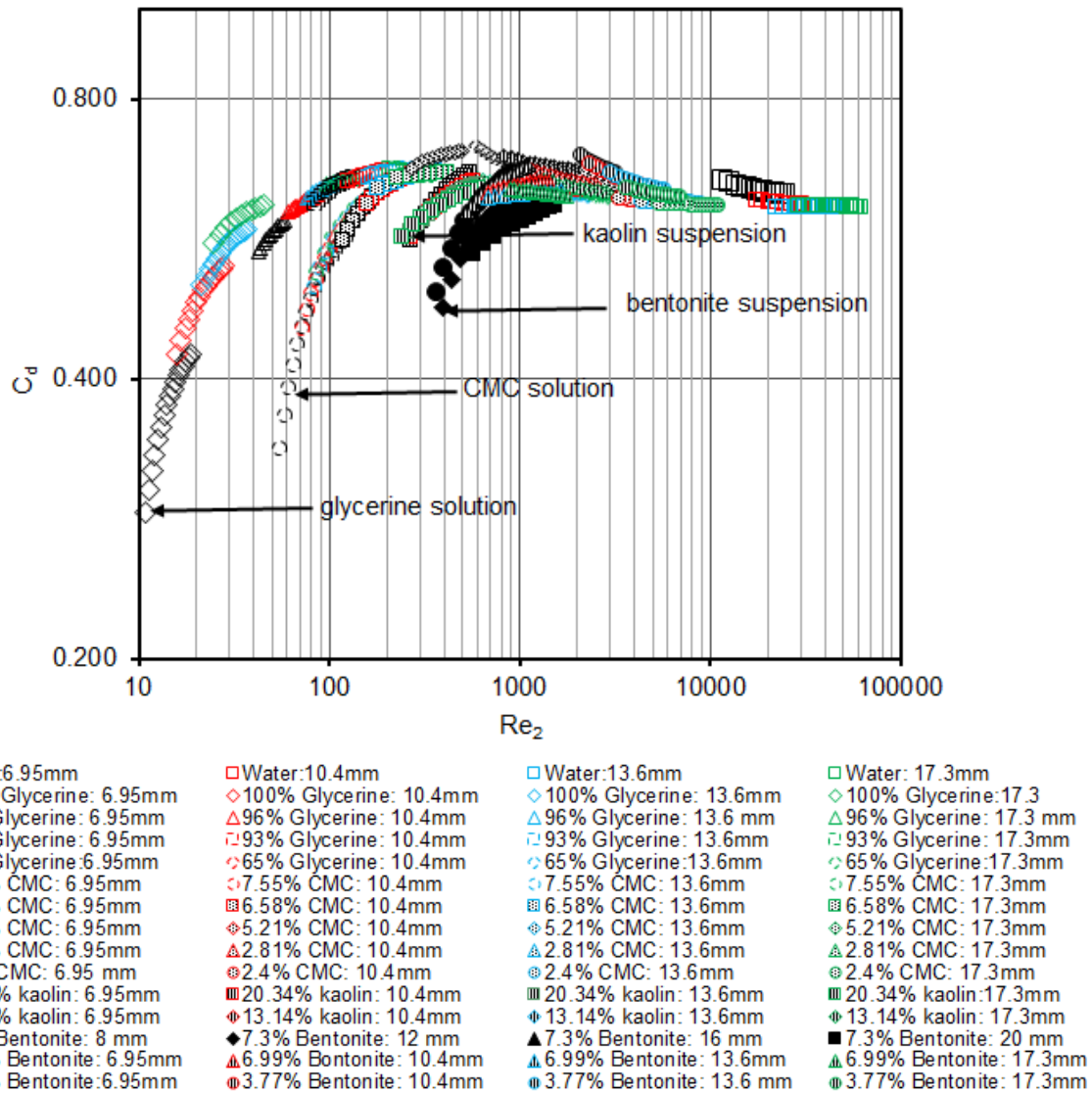


Figure 4.12 C_d versus Re_2 for triangular orifices

4.5 Effect of orifice shape (Newtonian and non-Newtonian liquids)

The C_d - Re_2 relationship for all the liquids and orifices is given in Fig. 4.13. The highly viscous glycerine Re values through all the orifices is at $Re=12$ for circular orifices and $Re=11$ for square and triangular orifices. The lowest Reynolds numbers values for CMC solutions for all the orifices are approximately at $Re=53$. For kaolin and bentonite suspensions, the Reynolds numbers for all the orifice shapes starts from approximate $Re=237$ and $Re=332$, respectively. The highest Re value obtained for all the orifice shapes is approximately at $Re=63000$. There is no difference in Re and average C_d values obtained in the turbulent region for Newtonian and non-Newtonian liquids and for circular square and triangular orifices. The average C_d value obtained is 0.64.

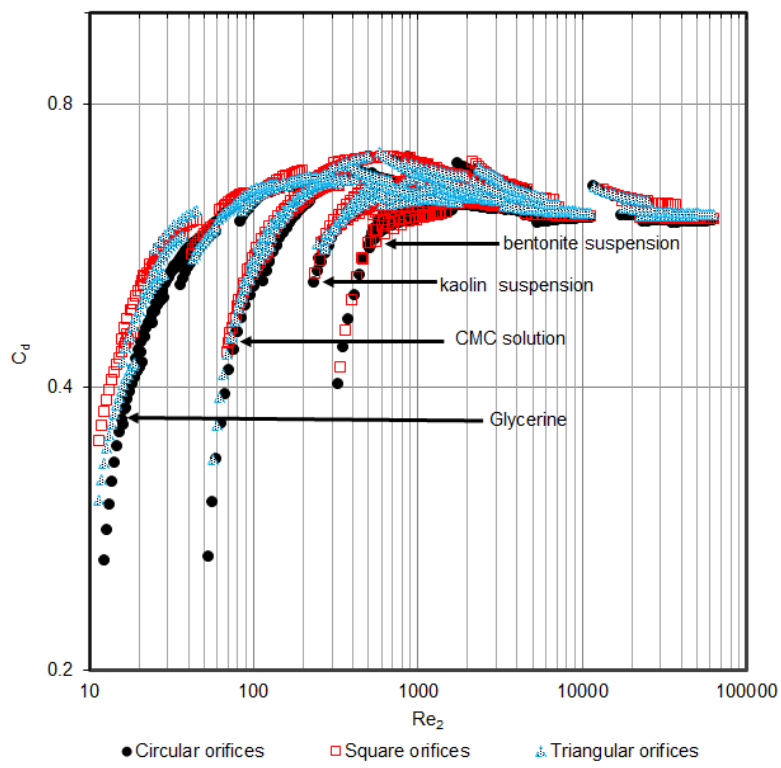


Figure 4.13 Cd-Re₂ relationship for Newtonian and non-Newtonian liquids for circular, square and triangular orifices

4.6 Metzner and Reed (1955) Reynolds number

The Metzner- Reed Reynolds number, Re_{MR} , was used to calculate the Reynolds number for CMC solutions through circular orifices to compare Re_{MR} with Re_2 . Figure 4.14 shows the C_d - Re relationship for CMC solutions. There is no significant difference between Re_{MR} and Re_2 for CMC solutions. The normal use of the Reynolds number that ‘best accounts for rheological behaviour’ and causes the results to coincide in orifices inserted in pipes does not do the same for flow from tanks through orifices.

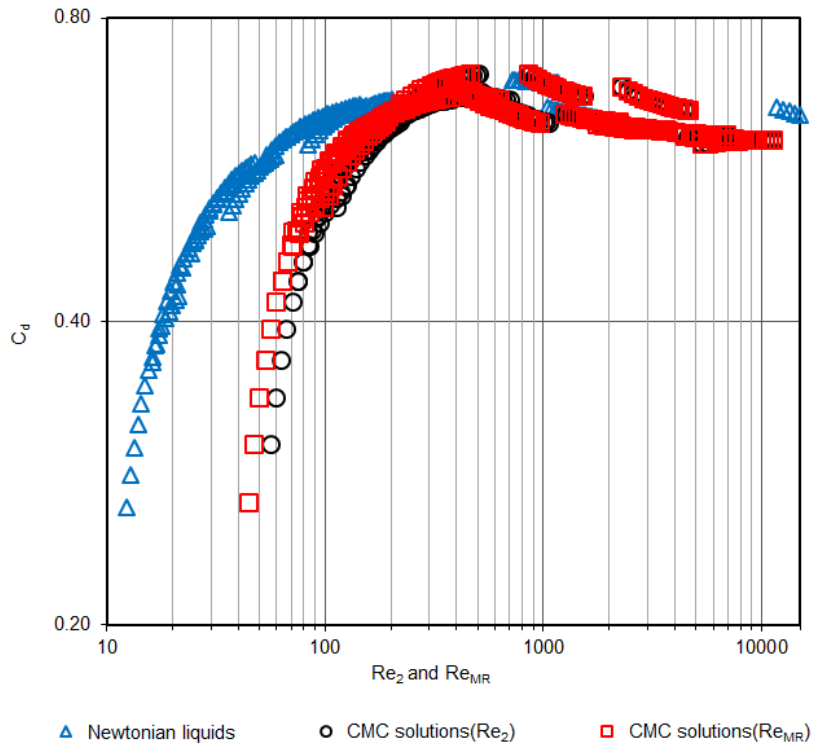


Figure 4.14 C_d versus Re_{MR} and Re_2 relationship for CMC solutions and Newtonian liquids through circular orifice

4.7 Conclusion

The rheological and physical parameters of the test liquids are presented in this chapter. The shear rates and temperature of the rheology tests were set to relate to the application shear rate and temperature of the flow of liquids through the orifices. The parameters obtained were used to calculate Reynolds numbers for the test liquids. The effect of the orifice shapes for water results was analysed and for the 8 mm diameter the effect of shape is insignificant. For the 12 mm, 16 mm and 20 mm orifices, however, the difference in C_d values is within $\pm 1.5\%$ between the orifice shapes. The flow rate tests for glycerine solutions, CMC solutions, kaolin and bentonite suspensions through orifices are illustrated and the C_d - Re_2 relationship is established. The C_d values in the laminar region increases with the increase in Re_2 and becomes constant in the turbulent region. Each liquid has a unique C_d - Re_2 relationship in the laminar region for all the orifice shapes. The Re values for the glycerine solutions start approximately at $Re=11$. CMC solutions, kaolin and bentonite solutions begin at approximate $Re=53$, $Re=232$ and $Re=330$, respectively, due to the effect of the liquids' viscosity and yield stress. The maximum Re_2 values obtained were $Re=63000$. The average C_d value in the turbulent region is 0.64. There was no significant effect of orifice shape for all the liquids in the turbulent region. The comparison was performed between Re_2 and Re_{MR} for CMC solutions. There was no difference in C_d values obtained when using the two definitions of Reynolds

numbers (Re_2 and Re_{MR}) for power law liquids and the C_d - Re relationship differs for Newtonian and power law liquids.

CHAPTER FIVE: DISCUSSION

5.1 Introduction

The results obtained for this study are discussed in relation to the results obtained by other researchers. The calibration results, the effect of orifice shape for water and all other tested liquids are discussed. Additionally, the effect of rheological properties of test liquids for flow through circular, square and triangular orifices is discussed.

5.2 Calibration results

In Fig. 5.1, the calibration results are compared to Dziubiński and Marcinkowski's (2006) average C_d value and the standard C_d value of 0.61 that is used for circular orifices for Newtonian liquids. The C_d values obtained were plotted against the generalised Reynolds number Re for Newtonian liquids and the values are within $\pm 4\%$ of that of Dziubiński and Marcinkowski (2006) average C_d value and the standard C_d value of 0.61 for Newtonian liquids. The exception is the data for the 8 mm hydraulic diameter orifices. The results show that the smaller orifice hydraulic diameters have the high C_d values, and the coefficient of discharge decreases as the orifice size increases. Similar behaviour was observed by Smith (1886) and Prohaska (2008).

The average C_d for circular, square and triangular orifices is 0.62 which agrees with the average C_d value reported by Dziubiński and Marcinkowski (2006) for flow through sharp crested orifice from tanks.

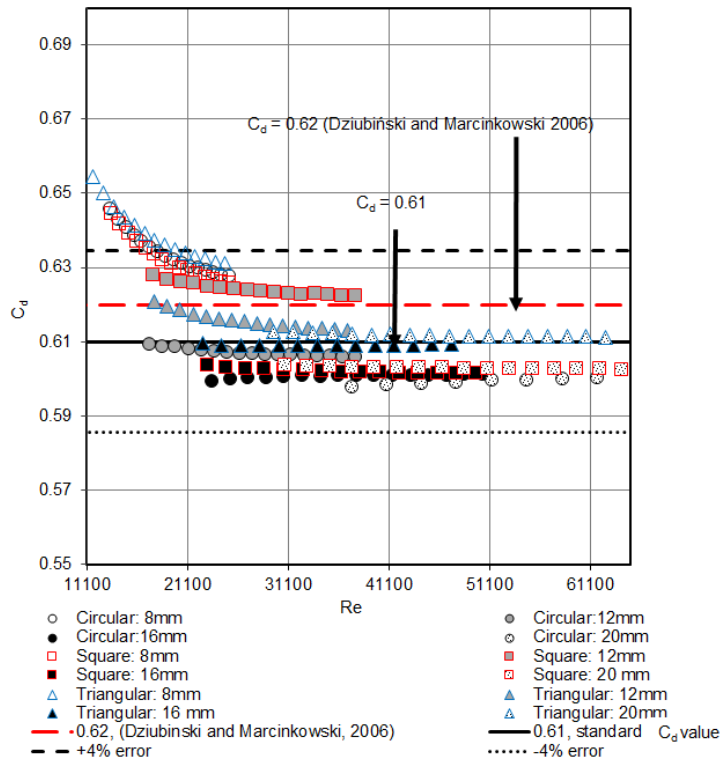
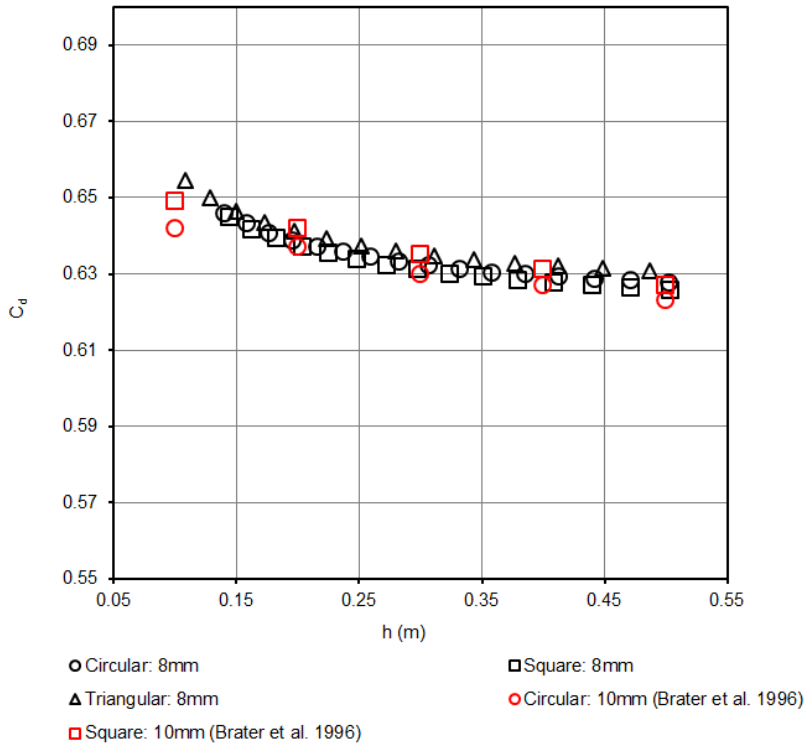


Figure 5.1 water C_d versus generalised Re for circular, square and triangular orifices

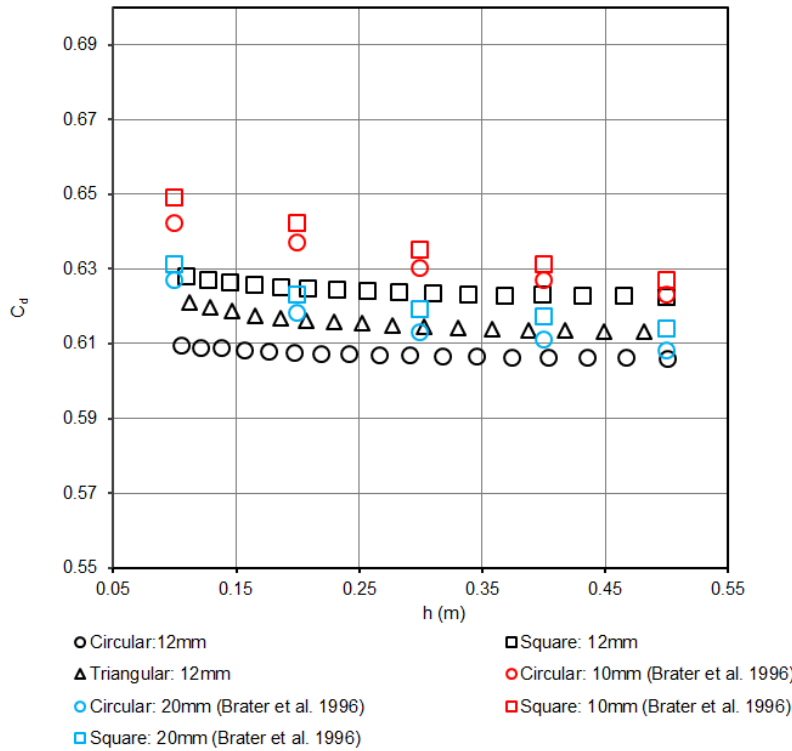
5.3 Effect of orifice shape (water results)

The water results through circular, square and triangular orifices are presented in Fig. 5.2. When comparing the relationship between the C_d values and the flow height for 8 mm hydraulic diameter orifices (circular, square and triangular) conducted in this study and the results presented by Brater *et al.* (1996) for circular and square orifices with hydraulic diameter of 10 mm, there is no difference in C_d values for all the orifices shapes and sizes for the current study and the results recorded by Brater *et al.* (1996).



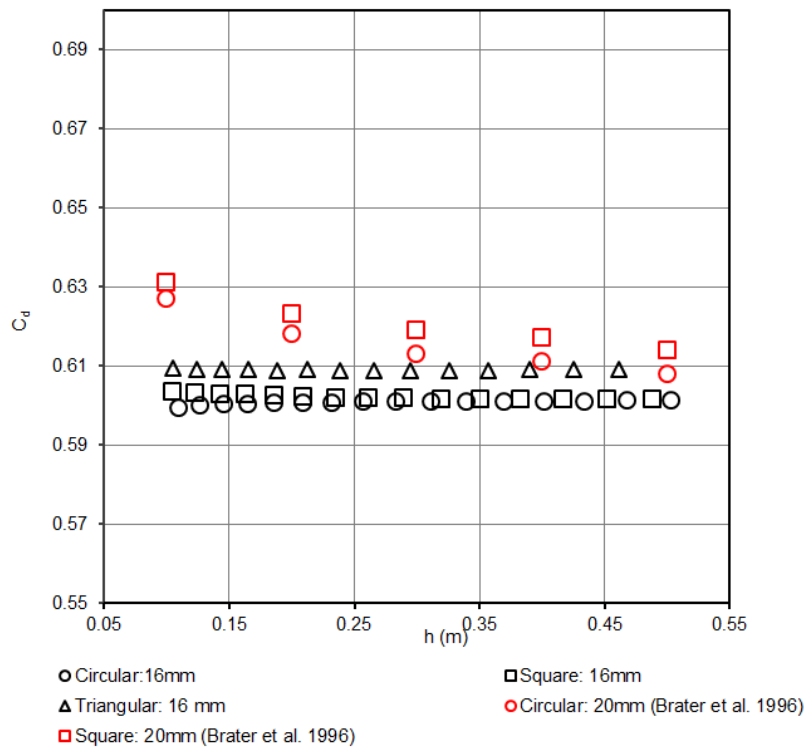
**Figure 5.2 water C_d versus head (m) for 8 mm and 10 mm hydraulic diameters
(This study; Brater et al., 1996)**

The available data from the previous studies do not include the 12 and 16 mm hydraulic diameter data. Therefore 10 mm and 20 mm hydraulic diameter data was used for comparison purpose. The 12 mm hydraulic diameter orifice results for this study are compared to 10 mm and 20 mm hydraulic diameter water results presented by Brater *et al.* (1996). Figure 5.3 shows that the 10 mm hydraulic diameter C_d values are higher than the 12 mm and 20 mm C_d values. The results recorded by Brater *et al.* (1996) show no significant difference between the circular and square orifices for 10 mm and 20 mm hydraulic diameters. For 12 mm hydraulic diameter orifices, however, the square orifices have higher C_d values compared to triangular and circular orifices, with circular orifices having the lowest C_d values.



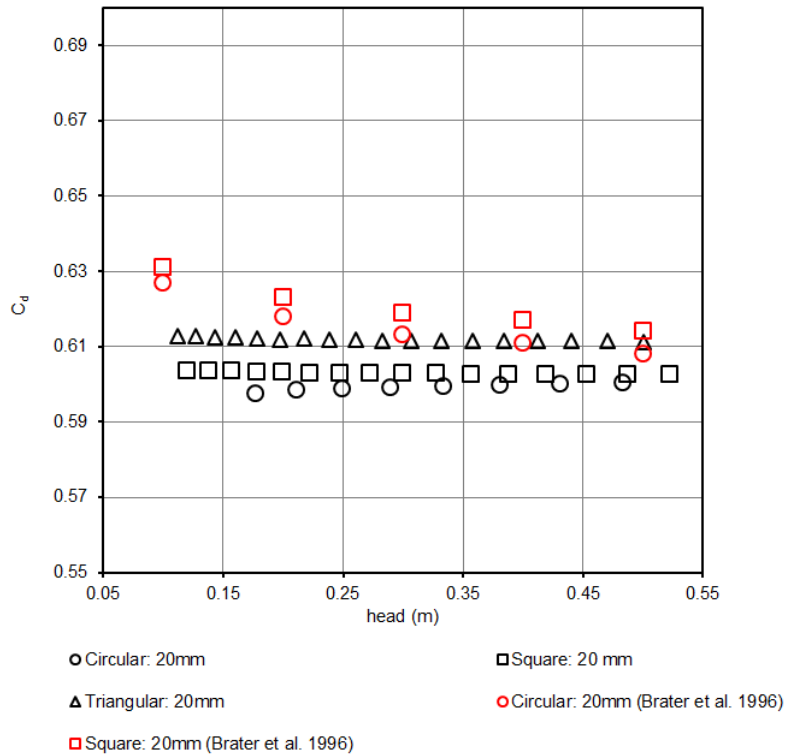
**Figure 5.3 water C_d versus head (m) for 10 mm, 12 mm and 20 mm hydraulic diameters
(This study; Brater et al., 1996)**

Figure 5.4 illustrates the 16 mm hydraulic diameter water results for this study compared to the 20 mm hydraulic diameter water results presented by Brater *et al.* (1996). The 16 mm hydraulic diameter results have lower C_d values compared to the 20 mm hydraulic diameter results given by Brater *et al.* (1996). There is no noticeable difference in C_d values between different orifice shapes for this study and the study by Brater *et al.* (1996).



**Figure 5.4 C_d versus head (m) for 16 mm and 20 mm hydraulic diameters
(This study; Brater et al., 1996)**

The 20 mm hydraulic diameter water results obtained in this study are compared to the results given by Brater *et al.* (1996) shown in Fig. 5.5. Brater *et al.* (1996) C_d values are higher than this study's C_d values. The circular and square orifice C_d values, however, do not differ. The triangular orifice C_d values are higher than those of circular and square values obtained for the current study.



**Figure 5.5 C_d versus head (m) for 20 mm hydraulic diameters
(This study; Brater *et al.*, 1996)**

Table 5.1 shows the average C_d values for this study and the average C_d values presented by King and Wisler (1992), Brater *et al.* (1996) and Dziubiński and Marcinkowski (2006). The orifice shapes with the same hydraulic diameter do not affect the flow rate in the turbulent region.

Table 5.1: Average C_d values for circular, square and triangular orifices

Author	Orifice Type	Hydraulic diameter (mm)	Average C_d value
This study	Circular	8	0.63
		12	0.61
		16	0.60
		20	0.60
This study	Square	8	0.64
		12	0.63
		16	0.60
		20	0.60
This study	Triangular	8	0.64
		12	0.62
		16	0.61
		20	0.61
Dziubiński & Marcinkowski (2006)	Circular	5, 8, 12.5, 17	0.62
Brater <i>et al.</i> (1996)	Circular	5	0.64
		10	0.62
		20	0.61
Brater <i>et al.</i> (1996)	Square	5	0.65
		10	0.63
		20	0.62
King & Wisler (1922)	Circular	-	0.60
King & Wisler (1922)	Square	-	0.61
King & Wisler (1922)	Triangular	-	0.61

5.4 Effect of orifice shape (Newtonian and non-Newtonian liquids)

The effect of orifice shape for gravitational flow of non-Newtonian liquids from tanks has only been studied by Khahledi *et al.* (2020) using the results obtained from this study. The study that used circular and triangular orifices and the test liquids were non-Newtonian was carried out by Ntamba Ntamba, (2011) albeit for pipe flow. The latter researcher tested water (Newtonian liquid), CMC solutions, kaolin and bentonite suspensions (non-Newtonian liquids). For pipe flow, the orifice shape did not influence the flow of Newtonian and non-Newtonian in laminar and transition flow as shown in Fig. 2.8.

For this study the circular, square and triangular orifices results are presented in Fig. 4.13. Considering the effect of orifice shape for highly viscous glycerine and high concentrations of non-Newtonian liquids, the Re values for Newtonian liquids through square orifices are less than the Re values through circular and triangular orifices in the laminar region, with the lowest Re value of 11 for square shape orifice and $Re=12$ for circular and triangular shaped orifices. It can therefore be concluded that there is no significant difference in Re and C_d values for orifices with different shapes with equal hydraulic diameters. There is no orifice shape effect for a liquid in the laminar, transition and turbulent region. Although there is no difference in the

flow for Newtonian and non-Newtonian liquids in pipe flow, for gravitational flows from tanks, however, Reynolds numbers differ for the various liquids in laminar and transition flows.

5.5 Flow behaviour of liquids through orifices

The test liquids that are used in this study represent Newtonian, power-law, Bingham and Herschel-Bulkley model liquids. The flow was through circular, square and triangular orifices from the base of the tank. The only available study that is similar to the current study was conducted by Dziubiński and Marcinkowski (2006) when they tested Newtonian and power law liquids through circular orifices.

The Reynolds number range for the current study for all orifices is between $Re=11$ and $Re=62608$. There are four flow trends in the laminar region. The highly viscous Newtonian liquids (different concentrations of glycerine) Re values start from $Re=11$; the power law (CMC) Re values start from $Re=53$; the yield-pseudoplastic liquids (kaolin suspensions) Re values start from $Re=237$ and Re for Bingham liquids (bentonite suspensions) started from $Re=332$. A similar trend was observed by Dziubiński and Marcinkowski (2006), as shown in Fig. 5.6, for the flow of Newtonian and non-Newtonian liquids through sharp crested circular orifices with an L/d of 0. For this work it is assumed that there is a difference in fluid flow trends because of the effect of viscosity and yield stress. For Dziubiński and Marcinkowski (2006), C_d values started from $Re=0.002$ for Newtonian liquids and $Re=0.017$ for non-Newtonian liquids. They used an orifice size of 5 mm diameter which is smaller than the smallest orifice (8 mm) used in this study. They indicated that the laminar region is within $Re \leq 10$. For this study the Reynolds numbers start at $Re=11$.

The C_d values for non-Newtonian liquids in the turbulent region coincide with the Newtonian C_d values. Therefore, the average C_d values for all the orifices and liquids in the turbulent region is approximately 0.64 which is a slight difference to the value of 0.67 reported by Dziubiński and Marcinkowski (2006) for non-Newtonian liquids. However, their results correspond to orifices with different L/d ratios.

Figure 5.6 shows a comparison between the current study and that of others including Lea (1942), Kiljanski (1993) and Dziubiński and Marcinkowski (2006). Each study is seen to have its own curve; thus, each orifice should be calibrated and analysed as per calibration results rendering it cumbersome for engineering design purposes. All the data presented except the current data have the C_d value below $Re=10$. Many researchers – Haldenwang (2003) for Fanning friction factor in open channels; Fester *et al.* (2008), for pressure loss coefficients in sudden pipe contractions; Ntamba Ntamba (2011) for pressure loss and discharge coefficient

through short square-edged orifices in pipes; Chowdhury and Fester (2012) and Chowdhury (2010) for pressure loss and discharge coefficient of sharp long square-edged orifices through pipes; and Khahledi *et al.* (2014) for coefficient of discharge over sharp crested weirs from tanks – demonstrated that the difficulty of different curves can be overcome by adequately accounting for the viscous properties of the liquids in the Reynolds number. However, Fig. 4.13 clearly shows that the use of the generalised Reynolds number utilising $8v/D$ as the effective shear rate, fails to do the same in the case of the discharge coefficient for gravitational flows from tanks in laminar flow. Marcinkowski & Dziubiński (2004) indicated that the flow may not be fully developed for flow of liquids through orifice fitted to a tank and the rheological properties of the liquids depend on the average shear rate in the entire orifice space. However, this is practical if the velocity is the same and D is proportional to d_h . However, the effect of friction with air has an effect on the liquid flow at the orifice exit. Therefore, a new Reynolds number to account for the effective shear rate as postulated by Della Valle *et al.* (2000) and Marcinkowski and Dziubiński (2004) and the incorporation of the yield stress is proposed in Chapter Six.

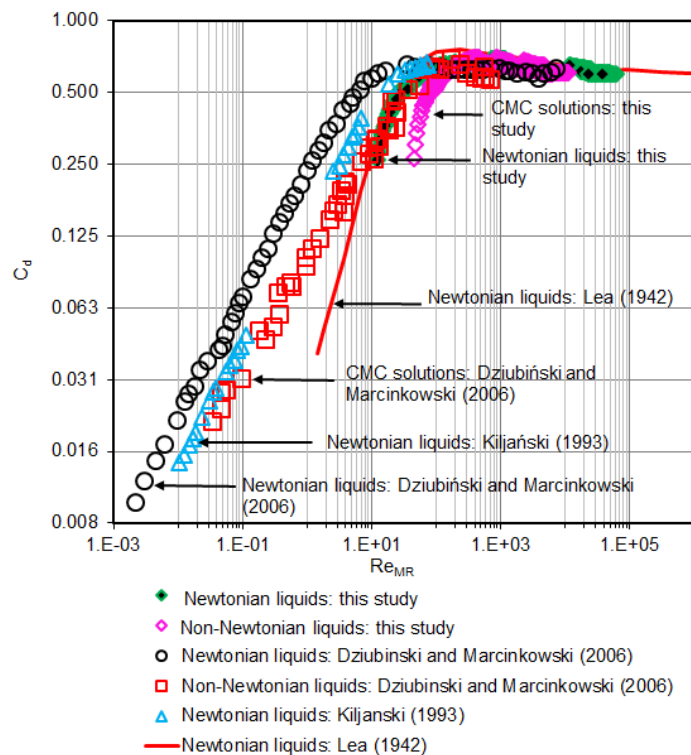


**Figure 5.6 C_d vs Re_{MR} for Newtonian and non-Newtonian liquids for L/d of 0
(This work; Lea, 1942; Kiljanski, 1993; Dziubiński & Marcinkowski, 2006)**

5.6 Conclusion

The calibration results are compared to the Dziubiński and Marcinkowski (2006) average C_d value and the standard C_d value of 0.61 commonly used for circular orifices for Newtonian liquids. Most C_d values for this study are within $\pm 4\%$ compared to the Dziubiński and Marcinkowski (2006) average C_d and the standard 0.61 C_d value. The average C_d value for Newtonian liquids and for all the orifice shapes is 0.62 which agrees with the average C_d value obtained by Dziubiński and Marcinkowski (2006) for Newtonian liquids. The smaller orifice hydraulic diameters have high C_d values, and as the orifice size increases the C_d values decrease. This agrees with the results reported by Smith (1886) and Prohaska (2008). The effect of orifice shape for water results has been discussed in comparison with the results reported by Brater *et al.* (1996). For these studies, there is no difference between circular, square and triangular orifices for orifices with equal hydraulic diameters. Similar behaviour has been observed by Brater *et al.* (1996) for circular and square orifices. For highly viscous glycerine and high concentrations of non-Newtonian liquids, the orifice shape does not have an effect. For the higher concentrations of the liquids, the results are in the laminar region and the C_d values increase with the increase in Re . Each fluid model has unique flow behaviour in the laminar region and that is assumed to be due to the effective shear rate in the orifice. The non-Newtonian C_d values coincide with Newtonian C_d values in the turbulent region, with a constant average C_d value of 0.64. This average C_d value is not far off from the average C_d value of 0.67 obtained by Dziubiński and Marcinkowski (2006) for non-Newtonian liquids. Dziubiński and Marcinkowski (2006) average C_d value was calculated from the results obtained from different L/d ratios. The Re range for this study is between $Re=11$ and $Re=63000$ for all the liquids and orifices. From the current results, it is evident that the generalised Reynolds number using the shear rate of 8 v/d does not account for the viscous properties of the liquids in the Reynolds number in the laminar region. This is in agreement with the suggestion by Della Valle *et al.* (2000) and Marcinkowski and Dziubiński (2004). As a consequence, a new Reynolds number to account for the effective shear rate and the yield stress is presented in Chapter Six.

CHAPTER SIX: MODEL PREDICTIONS

6.1 Introduction

The idea of an effective shear rate for flow through the orifice, as postulated by Della Valle *et al.* (2000) and Marcinkowski and Dziubiński (2004), is used to re-define the new Reynolds number for various liquids to consolidate the C_d -Re relationship to the Newtonian liquid curve. A single composite model is used to predict the relationship between C_d and Re for all liquids-orifices combinations used in this work. The procedure followed to determine the model prediction is explained in this chapter.

6.2 Model predictions

Considering the results obtained in this study and the research by Marcinkowski and Dziubiński (2004), it can be concluded that the viscosity and yield stress influence gravitational flow of liquids through orifices from tanks. The calculated average shear rate from the discharge of orifices from tanks is expected to be proportional to v/d but not $8v/d$ as it is commonly used in pipe flow (Della Valle *et al.*, 2000; Marcinkowski & Dziubiński, 2004).

Therefore, the effective average shear rate is assumed to be:

$$\dot{\gamma}_{\text{eff.}} = \frac{Fv}{d_h} \quad (6.1)$$

Where F is constant which is possibly smaller than 8, the value used for flow in a tube.

Therefore, the effective viscosity of the liquid is:

$$\mu_{\text{eff.}} = \frac{\tau}{\dot{\gamma}_{\text{eff}}} \quad (6.2)$$

Substituting the effective shear rate in the Herschel-Bulkley liquid model, the shear stress is given as:

$$\tau = \tau_y + k \dot{\gamma}_{\text{eff}}^n \quad (6.3)$$

Combining Eqns. 6.2 and 6.3

$$\mu_{\text{eff}} = \frac{\tau_y + k \dot{\gamma}_{\text{eff}}^n}{\dot{\gamma}_{\text{eff}}} \quad (6.4)$$

Thus

$$\mu_{\text{eff}} = \frac{\tau_y + k \left[\frac{F_v}{d_h} \right]^n}{\frac{F_v}{d_h}} \quad (6.5)$$

Or

$$\mu_{\text{eff}} = k \left(\frac{F_v}{d_h} \right)^{n-1} \left[\frac{\tau_y}{k \left(\frac{F_v}{d_h} \right)^n} + 1 \right] \quad (6.6)$$

But the Bingham number is given as:

$$Bn = \frac{\tau_y^B d_h}{\mu_B v} = \frac{\tau_y}{k \left(\frac{F_v}{d_h} \right)^n} \quad (6.7)$$

Therefore

$$\mu_{\text{eff}} = k \left(\frac{F_v}{d_h} \right)^{n-1} [1 + Bn] \quad (6.8)$$

The substitution of effective viscosity in the definition of Re is given as:

$$Re = \frac{\rho v d_h}{\mu} = \frac{\rho v d_h}{\mu_{eff}} = \frac{\rho v d_h}{k \left(\frac{F_v}{d_h} \right)^{n-1} (1+Bn)} \quad (6.9)$$

Therefore, the interim Re is:

$$Re_{(new)} = \frac{\rho v^{2-n} d_h^n}{k F^{n-1} (1+Bn)} \quad (6.10)$$

For the Bingham Model : n=1

For the power law model: Bn=0

And for Newtonian liquids: n=1 and Bn=0

Figure 6.1 illustrates the flow chart describing the steps taken to develop a consolidated C_d - Re_{new} correlation using this approach.

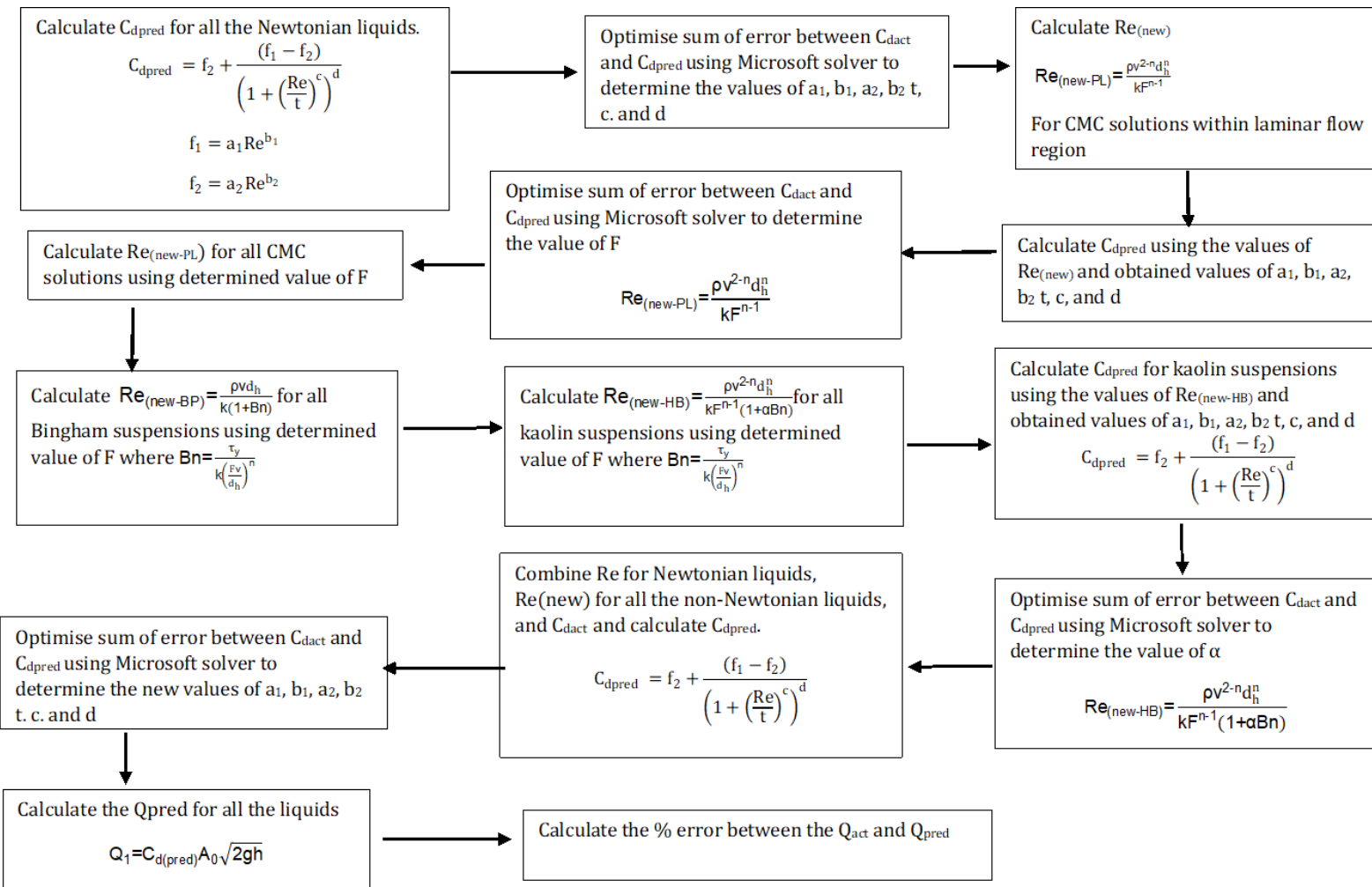


Figure 6.1 flow chart describing the steps taken to develop a consolidated C_d - Re_{new} correlation.

To determine the value of F, composite curve fitting (Eq. 2.64) as described by Patankar *et al.* (2002) was used to predict the fit for Newtonian liquids.

$$C_d = f_2 + \frac{(f_1 - f_2)}{\left(1 + \left(\frac{Re}{t}\right)^c\right)^d} \quad (2.76)$$

This fitting was applied to all the orifice shape results. f_1 for circular, square and triangular orifices was found to be $0.083Re^{0.49}$ and f_2 was 0.62. Eq. 2.83 was optimised, and the values obtained for t , c and d were 50, 1.26 and 1.43, respectively.

Therefore, the predicted C_d value for Newtonian liquids for circular, square and triangular orifices is as shown in Eq. 6.11. Figure 6.2 shows the relationship between the actual and predicted C_d values and Reynolds number for Newtonian liquids.

$$C_{dpred} = 0.62 + \frac{\left(0.083Re^{0.49} - 0.62\right)}{\left(1 + \left(\frac{Re}{50}\right)^{1.26}\right)^{1.43}} \quad (6.11)$$

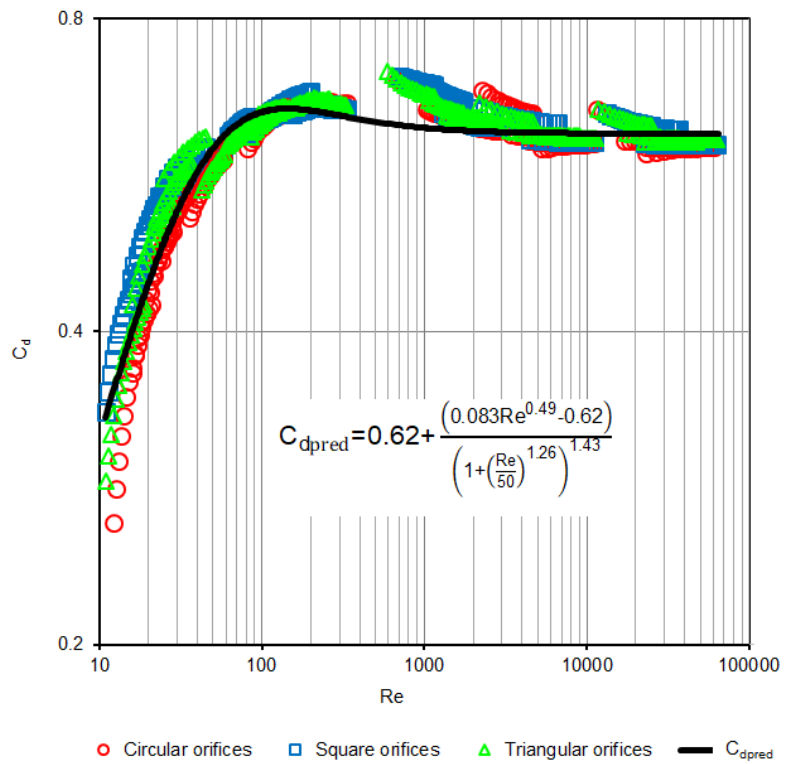


Figure 6.2 $C_d(\text{actual})$ and $C_d(\text{pred})$ versus Reynolds numbers for Newtonian liquids

The new Reynolds number (Re_{new}) Eq. 6.12 was calculated for power law liquids in the laminar flow region for each orifice shape. The data that was used was for 7.55% and 6.58% CMC solutions.

$$Re_{(\text{new-PL})} = \frac{\rho v^{2-n} d_h^n}{k F^{n-1}} \quad (6.12)$$

The Newtonian predicted C_d value in Eq. 6.11 was used to calculate the predicted C_d values for CMC solutions using the new Reynolds number (Eq. 6.12). The values of F were determined by the optimisation for the CMC solution in the laminar region for each orifice shape. The average F value for circular, square and triangular orifices and for all power law liquids was found to be 0.3.

The Re_{new} (eq. 6.10) values for all the liquids were calculated using the F value of 0.3. The Herschel–Bulkley and Bingham liquids were adjusted by the factor (α) to adjust the Re to Newtonian liquids as illustrated in Eq. 6.13.

$$Re_{(new-HB)} = \frac{\rho v^{2-n} d_h^n}{k F^{n-1} (1 + \alpha B_n)} \quad (6.13)$$

A Newtonian composite curve fitting was applied to kaolin and bentonite suspensions and the value of α was determined by the optimisation for all the orifice shapes. The average factor (α) of 0.2 was obtained for circular, square and triangular orifices. Thus for the Bingham liquids, the average factor (α) is 1.

The new Reynolds numbers were calculated for all non-Newtonian liquids using the following established Re_{new} equations:

For the Herschel-Bulkley model:

$$Re_{(new-HB)} = \frac{\rho v^{2-n} d_h^n}{k 0.3^{n-1} (1 + 0.2 B_n)} \quad (6.14)$$

For the Bingham model:

$$Re_{(new-BP)} = \frac{\rho v d_h}{k (1 + B_n)} \quad (6.15)$$

Where B_n is:

$$B_n = \frac{\tau_y}{k \left(\frac{0.3v}{d_h} \right)} \quad (6.16)$$

For the power law model:

$$Re_{(new-PL)} = \frac{\rho v^{2-n} d_h^n}{k 0.3^{n-1}} \quad (6.17)$$

The new fitting curve was established by applying a single composite equation to all the orifices data using the new Reynolds number values for non-Newtonian liquids. The values of f_1 and f_2 became $0.057Re^{0.58}$ and 0.61, respectively. After the non-linear optimisation method minimising the residual mean square of the single composite equation, the actual C_d and predicted C_d values versus Reynolds number curve was plotted (Fig. 6.3) and the combined C_d equation for circular, square and triangular orifices was established (Eq. 6.18) with 98% of the actual C_d values within a $\pm 10\%$ range when compared to the predicted C_d values (Fig. 6.4). Equation 6.18 is applicable for the following range of conditions: $8 \text{ mm} < d < 20 \text{ mm}$, $0 < L/d < 0.125$ and $11 < Re_2 < 63000$.

$$C_{d(pred)} = 0.61 + \frac{(0.057Re^{0.58} - 0.61)}{\left(1 + \left(\frac{Re}{80}\right)^{0.758}\right)^{1.98}} \quad (6.18)$$

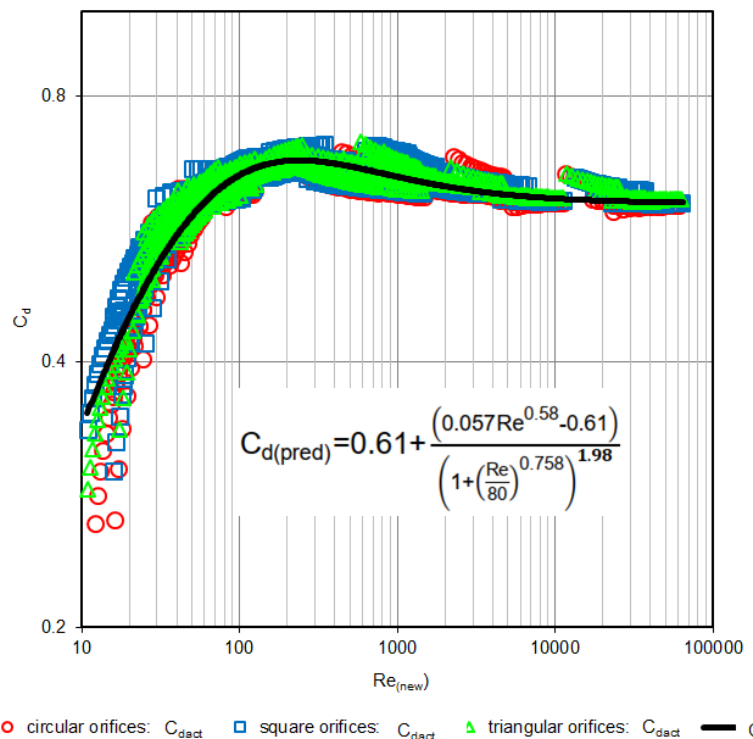


Figure 6.3 $C_{d(actual)}$ and $C_{d(pred)}$ versus Reynolds numbers (Re_{new-PL} , Re_{new-BP} , Re_{new-HB})

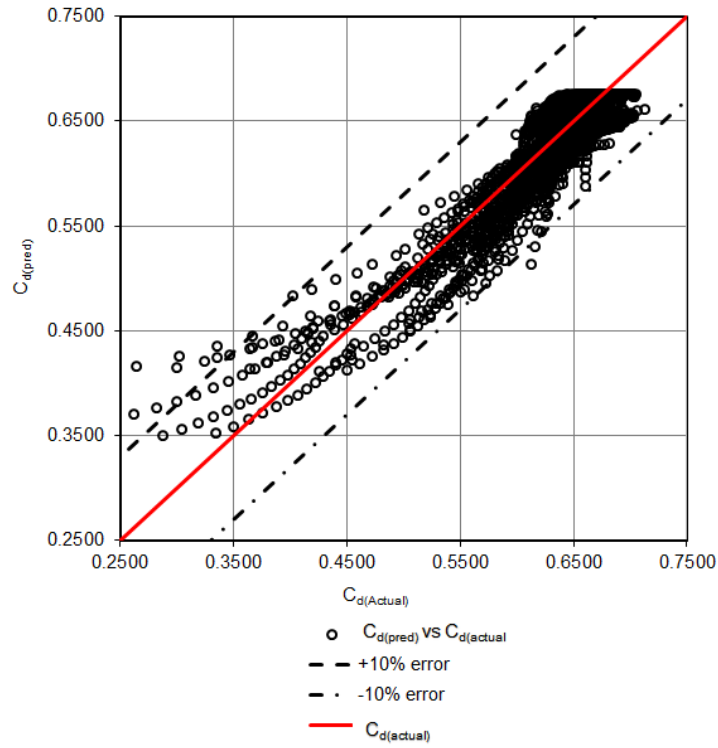


Figure 6.4 $C_{d(pred)}$ versus $C_{d(actual)}$

The predicted flow rate is expressed in Eq. 6.19. The error margins between the actual and predicted discharge for laminar, transition and turbulent flows are at $\pm 7\%$, $\pm 5\%$ and $\pm 2\%$, respectively, as shown in Figs. 6.5, 6.6 and 6.7.

$$Q_1 = C_{d(pred)} A_0 \sqrt{2gh} \quad (6.19)$$

This equation is applicable to orifices with an L/d of 0.125, 0.0833, 0.0625 and 0.05 fitted at the bottom of the tank, with the hydraulic diameters of 8 mm, 12 mm, 16mm and 20 mm respectively and for a Reynolds number range from 11 to 63000.

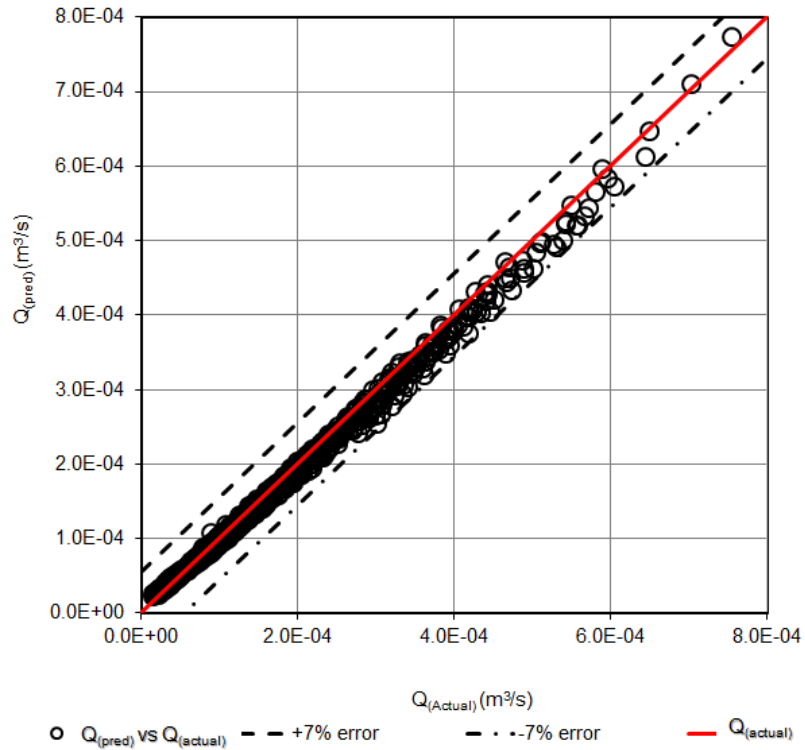


Figure 6.5 $Q_{(\text{pred})}$ versus $Q_{(\text{actual})}$ for laminar flow

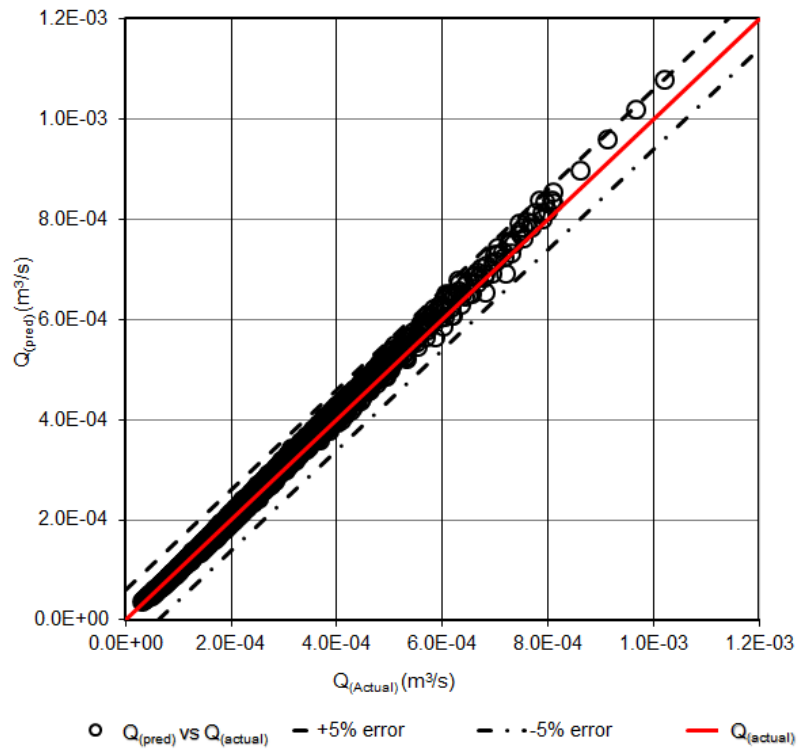


Figure 6.6 $Q_{(\text{pred})}$ versus $Q_{(\text{actual})}$ for transitional flow

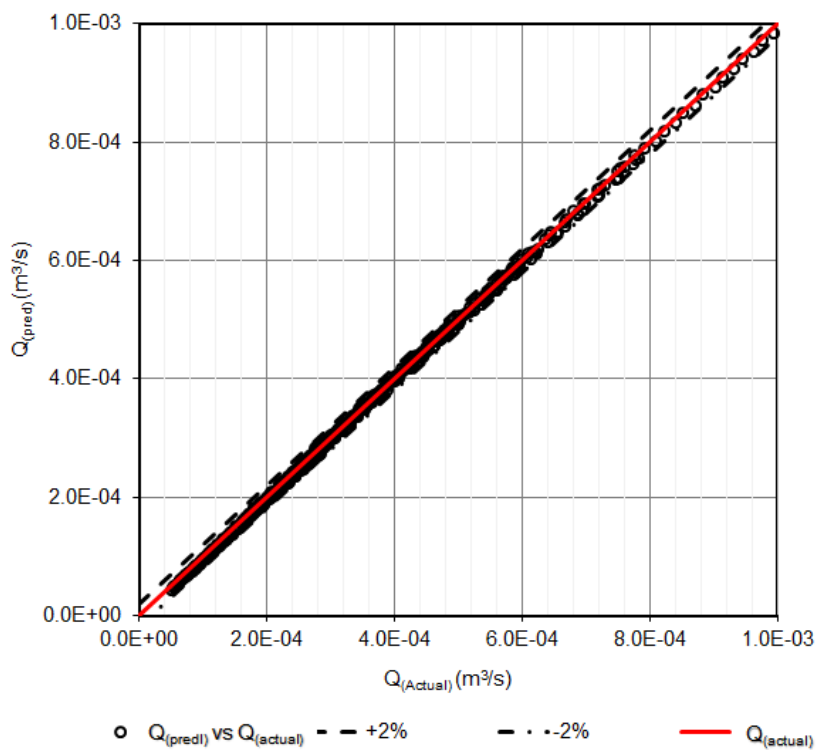


Figure 6.7 $Q_{(\text{pred})}$ versus $Q_{(\text{actual})}$ for turbulent flow

The new model captures the local maximum on the C_d -Re curve in the transition region between laminar and turbulent flow. During the onset of turbulence, the induced eddies increase the coefficient of discharge and that causes the local maximum (Alvi *et al.*, 1977). In order to validate the new model, the existing data must consist of rheology parameters, orifice diameter and flow rate. The Dziubiński & Marcinkowski (2006) data includes the rheological parameters of the tested liquids but the C_d -Re relationship curves do not separate each liquid concentration, and the diameter for each data point cannot be depicted because the curves were plotted according to L/d ratios. Therefore, the existing data could not be used to validate the new model.

The characteristic shear rate in an orifice fitted in a pipe is 26 times that fitted at the tank. The liquid discharged from a tank through an orifice exits to an open-air environment. Upon exit of the liquid from a tank, the jet is subjected to the effect of friction with air, and that slows down the jet. In pipe flow however the liquid exits to a motion medium that allows downstream mixing. The orifice flow in pipes depend on Beta ratio d/D and this is not the case in tank flow. Therefore, the shear rate through orifices from tanks will be lower than the shear rate in pipe flow.

6.3 Conclusion

The new Reynolds number equations were derived acknowledging that the shear rate is not $8v/d$ (Della Valle *et al.*, 2000; Marcinkowski & Dziubiński, 2004) in gravitational flows through orifices from tanks. The use of the Bingham number to account for the effect of yield stress was plausible. A single composite equation was applied to the data obtained for the Newtonian liquids for each orifice shape. The equation was used to determine the constants (F and α) which were used to calculate the new Re for non-Newtonian liquids for gravitational flow through orifice plates from the bottom of a tank. A single composite equation was applied to all the data for all the liquids and orifices (C_d values and Re values for Newtonian liquids and new Re values for non-Newtonian liquids). The C_d versus Re laminar flow relationship yielded $0.057Re^{0.58}$ and the average C_d value in the turbulent flow was found to be 0.61. New equations were developed to predict C_d values and discharge. The error margins between the actual and predicted discharge for laminar, transition and turbulent flows are at $\pm 7\%$, $\pm 5\%$ and

$\pm 2\%$, respectively. The new equations have the following limitations: $8 \text{ mm} < d < 20 \text{ mm}$, $0 < L/d < 0.125$ and $11 < Re_2 < 63000$.

CHAPTER SEVEN: SUMMARY, NEW CONTRIBUTIONS AND RECOMMENDATIONS

7.1 Introduction

This research focused on the flow rate measurement of Newtonian and non-Newtonian liquids through various orifice shapes from a tank as a function of the liquid flow properties and Reynolds number. The flow rate measurements of the different types and concentrations of Newtonian and non-Newtonian liquids through various sizes of circular, square and triangular orifices from a tank were carried out. The rheological properties of the test liquids were determined, and the viscosity model parameters evaluated. The C_d -Re relationship for Newtonian and non-Newtonian liquids for all the orifices was established and the discharge model developed. The limiting factors for this model are, $8 \text{ mm} < d < 20 \text{ mm}$, $0 < L/d < 0.125$ and $11 < Re_2 < 63000$.

7.2 Summary

Orifices are very popular in flow rate measurement and regulation of Newtonian liquids from tanks but not for non-Newtonian liquids. Non-Newtonian liquids are processed, transported and stored by various industries such as mining, food processing, chemical and medical related applications. As there can be leaks due to tank raptures, pinholes, corrosion that can affect tank levels, flow regulation and discharge, it is important to understand the factors that improve the efficiency and accuracy of flow regulation and measurement of the flow of Newtonian and non-Newtonian liquids through different shapes of sharp-edged orifices from a tank.

The current study and the work reported by King and Wisler (1992) and Brater *et al.* (1996) indicate that the various orifice shapes do not have any effect on the flow rate measurement of Newtonian liquids from tanks. The size, however, has an effect because as the orifice size increases, the C_d values decrease, also confirmed by Prohaska's study (2008).

Furthermore, this work concluded that the circular, square and triangular orifice shapes do not have any effect on the gravitational discharge of non-Newtonian liquids from a tank. The relationship between coefficient of discharge and Reynolds number obtained in this study for circular orifices was compared to that of Dziubiński and Marcinkowski (2006) for flow of Newtonian liquids and CMC solutions, and Lea (1942) and Kiljanski (1993) for the flow of highly viscous liquids. Each study had its own C_d -Re relationship. It is concluded, therefore, that each orifice result should be analysed as per its calibrated results. But as this is cumbersome for engineering design purposes, this needs to be improved.

With several types of liquids tested – Newtonian, power law, Bingham and Herschel-Bulkley – this research showed that each liquid formed a unique C_d -Re relationship in the laminar and transition flow region. Dziubiński and Marcinkowski (2006) data exhibited similar behaviour for the discharge of Newtonian and power law liquids through circular orifices from a tank.

7.3 New contributions

This current study established that sharp crested circular, square and triangular orifices with equal hydraulic diameters do not have an effect in the discharge of non-Newtonian liquids from tanks for the laminar, transitional and turbulent flow.

The new Reynolds number equations for power law, Bingham and the Herschel-Bulkley liquid models were derived acknowledging that the shear rate is not $8 v/d_h$ as indicated by Della Valle *et al.* (2000) and Marcinkowski and Dziubiński (2004).

Bingham and Herschel-Bulkley liquid models included the Bingham number to account for the yield stress to consolidate the data to Newtonian data.

The Herschel–Bulkley liquids were further adjusted by including a weighting factor of alpha to adjust the Re to Newtonian liquids.

A single composite equation was applied to the data obtained for Newtonian liquids for each orifice shape. The equation was used to determine the constants (F and α) which were used to calculate the new Re for non-Newtonian liquids for gravitational flow through orifice plates from the bottom of a tank.

A predictive C_d equation was established, and a new discharge equation derived. This equation can be used in process engineering and design for flow of non-Newtonian liquids through sharp crested orifices.

This is the first time that the relationship for the prediction of C_d for gravitational discharge of Newtonian and non-Newtonian liquids through different sizes of circular, square and triangular orifices from a tank has been presented. This includes both Newtonian and non-Newtonian liquids over a wide range of Reynolds numbers covering laminar, transitional and turbulent flow regions. The results, in the form of a large database, accentuate the existing database of similar but limited work by Dziubiński and Marcinkowski (2006). The mining, food processing, chemical processing and medical application industries will certainly benefit from this research.

Part of this research was published in the *19th International Conference on Transport & Sedimentation of Solid Particles* in 2019 in a paper entitled ***Non-Newtonian fluids discharge through circular and square orifices from a tank (Khahledi et al., 2019)***;

And a journal article published in the *Journal of Chemical Engineering Research and Design* entitled ***Non-Newtonian fluid flow from bottom of tank using orifices of different shapes (Khahledi et al., 2020)***.

Khahledi, M., Haldenwang, R., Chhabra, R. & Fester, V. 2020. Non-Newtonian fluid flow from bottom of tank using orifices of different shapes. *Chemical Engineering Research and Design*, 157:34-45. <https://doi.org/10.1016/j.cherd.2020.02.015>

7.4 Application in the industry

Non-Newtonian liquids are stored and transported using storage tanks and pipe networks. When designing the tank outlet through an orifice, estimating the orifice size and knowing the liquids rheological parameters, the Reynolds number of the liquids can be calculated. Figure 6.3 or eq. 6.18 can be used to obtain the C_d value and the discharge calculated. Depending on the expected discharge, the orifice size can be adjusted.

When there is a pinhole or tank rapture, the size of the hole and the liquids rheological parameters can be measured. The Re value would be determined, C_d value obtained and the discharge of the liquid calculated. This will help to determine the amount of the liquid discharged.

7.5 Recommendations

Recommendations for further research on this topic include the following:

The discharge of Newtonian and non-Newtonian liquids (power law, Bingham and Herschel-Bulkley liquids) using smaller sizes orifices (5 mm hydraulic diameter) that will produce the Reynolds number values below $Re=10$ can be studied. The literature reviewed classified the discharge below $Re=10$ to be laminar. This was not achieved within the scope of the current study. Therefore, circular, square and triangular orifices of 5 mm hydraulic diameters would be used to discharge water, glycerine solutions, CMC solutions, kaolin and bentonite suspensions.

According to this study and the work by Brater *et al.* (1996) and Prohaska (2008), it is concluded that the coefficient of discharge values increased with the decrease in orifice size for Newtonian liquids. Dziubiński and Marcinkowski (2006) employed different sizes of orifices but did not evaluate the effect of the size. Therefore, the effect of orifice size can be explored.

For validation of the influence of yield stress, more tests using yield stress liquids of different compositions should be studied.

During the liquid discharge from a rectangular tank, the liquids become stagnant at the bottom. Therefore, the discharge of non-Newtonian liquids through orifices from tanks using a pump can be investigated.

The discharge coefficient C_d includes flow end-effects as the minor (local) energy loss in the orifice and the reduction of the flow area (vena contracta). Further research can be conducted to distinguish the flow end-effects of different shapes of orifices.

REFERENCES 1

- Abou El-Azm Aly, A., Chong, A., Nicolleau, F. & Beck, S. 2010. Experimental study of the pressure drop after fractal-shaped orifices in turbulent pipe flows. *Experimental Thermal and Fluid Science*, 34:104-111.
- Abu-Jdayil. 2011. Rheology of sodium and calcium bentonite–water dispersions: Effect of electrolytes and aging time. *International Journal of Mineral Processing*, 98(3-4): 208-213.
- Abulnaga, B.E. 2002. *Slurry Systems Handbook*. USA: McGraw Hill, New York.
- Adam, N.J., De Cesare, G. & Schleiss, A. J. 2016. Head loss coefficient through sharp-edged orifices. *28th IAHR Symposium on Hydraulic Machinery and Systems*. Laboratory of Hydraulic Constructions, Ecole Polytechnique fédérale de Lausanne, Lausanne, Switzerland.
- Alvi, S.H., Sridharan, K. & Lakshman Rao, N.S. 1977. Nozzle flows at low and moderate Reynolds numbers. *Journal of the Indian Institute of Science*, 59(5):169-184.
- Bekkour, K., Leyama, M., Benchabane, A., Scrivener, O. 2005. Time-dependent rheological behavior of bentonite suspensions: An experimental study. *Journal of Rheology*, 49(1329): doi: 10.1122/1.2079267.
- Benslimane, A., Bekkour, K., François, P. & Bechir, H. 2016. Laminar and turbulent pipe flow of bentonite suspensions. *Journal of Petroleum Science and Engineering*, 139:85-93.
- Bevington, P.R. 1969. *Data Reduction and Error Analysis for the Physical Sciences*. McGraw-Hill, New York.
- Bingham, E.C. 1916. An investigation of the laws of plastic flow. Bureau standards. *Bulletin. US*, 36(4):591-612.
- Bird, R.B., Steward, W.E. & Lightfoot, E.N. 2002. *Transport Phenomena*. 2nd ed. John Wiley & Sons, New York.
- Bohra, L.K. 2004. Flow and pressure drop of highly viscous fluids in small aperture orifices. Unpublished MS thesis, School of Mechanical Engineering, Georgia Institute of Technology, Atlanta, United States of America.

Borutzky, W., Barnard, B. & Thoma, J. 2002. An orifice flow model for laminar and turbulent conditions. *Simulation Modelling Practice and Theory*, 10:41-152.

Bos, M.G. 1989. *Discharge Measurement Structures*. International Institute for Land Reclamation and Improvement, Wageningen, The Netherlands.

Bovey, H.T. 1901. *A treatise on hydraulics*. 2nd ed. John Wiley & Sons, New York.

Brater, E.F., King, H.W., Lindell, J.E. & Wei, C.Y. 1996. *Handbook of Hydraulics for the solution of Hydraulic Engineering Problems*. 7th ed. McGraw-Hill, New York.

Brinkworth, B.J. 1968. *An Introduction to experimentation*. English Universities Press, London.

Chhabra, R.P. & Richardson, J.F. 2008. *Non-Newtonian Flow and Applied Rheology in Engineering Applications*. 2nd ed. Elsevier Oxford, UK.

Chowdhury, M.R. & Fester, V. 2012. Modeling pressure losses for Newtonian and non-Newtonian laminar and turbulent flow in long square edged orifices. *Chemical Egineering Research and Design*, 90:863-869.

Csizmadia, P. & Till, S. 2018. The effect of rheology model of an activated sludge on to the predicted losses by an elbow. *Periodica Polytechnica Mechanical Engineering*, 62(4):305-311.

Dandwate, A., Mittal, S., Umale, O., Shelar, S. & Bajaj, R. 2016. Effect of Orifice Plate Shape on Performance Characteristics. *IOSR Journal of Mechanical and Civil Engineering*, 13(4):50-55.

Della Valle, D., Tanguy, P.A. & Carreau, P.J. 2000. Characterization of the extensional properties of complex fluids using an orifice flowmeter. *Journal of Non-Newtonian Fluid Mechanics*, 94:1-13.

Desouky, S.M. & Al-Awad, M.N. 1998. A new laminar-to-turbulent transition criterion for yield-pseudoplastic fluids. *Journal of Petroleum Science and Engineering*, 19:171-176.

Dietrich, N., Mayoufi, N., Poncin, S., Midoux, N. & Huai, Z. Li. 2013. Bubble formation at an orifice: A multiscale investigation. *Chemical Engineering Science*, 92:118-125.

Dziubinski, M. & Marcinkowski, A. 2006. Discharge of Newtonian and non-Newtonian liquids from tanks. *Chemical Egineering research and design*. 84(A12):1191-1198.

Elsaey, A., Abou El-Azm Aly, A. & Fuoad, M. 2014. CFD simulation of fractal-shaped orifices for flow measurement improvement. *Flow Measurement and Instrumentation*, 36:14-23.

Fester, V. Mbiya, B. & Slatter P. 2008. Energy losses of non-Newtonian fluids in sudden pipe contractions. *Chemical Engineering Journal*, 45:27-63.

Garcia, F., Garcia, J.C., Padrino, J.C., Mata, C., Trallero, J.C. & Joseph, D.D. 2003. Power law and composite power law friction factor correlations for laminar and turbulent gas-liquid flow in horizontal pipelines. *International Journal of Multiphase Flow*. 29:1605-1624.

Grose, R.D. 1985. Orifice Contraction Coefficients for Inviscid Incompressible Flow. *ASME Journal of Fluids Engineering*, 107(1):36-43.

Gutmark, E.J. & Grinstein, F.F. 1999. Flow control with noncircular jets. *Annual Review of Fluid Mechanics*, 31:239-272.

Haldenwang, R., Sutherland, A.P.N., Fester, V.G., Holm, R. & Chhabra, R.P. 2012. Sludge pipe flow Pressure drop prediction using composite power-law friction factor-Reynolds number correlation based on different non-Newtonian Reynolds numbers. *Water SA*. 38(4): 615-622.

Haldenwang, R. 2003. Flow of non-Newtonian fluids in open channels. Unpublished DTech thesis,Cape Technikon, Cape Town, South Africa.

Haldenwang, R., Slatter, P.T. & Chhabra, R.P. 2002. Laminar and transitional flow in open channels for non-Newtonian fluids. *Proceedings, Hydrotransport 15: 15th International Conference on the Hydraulic Transport of Solids in Pipes*, Banff, Canada, 755-768.

Hanafizadeh, P., Sattari, A., Hosseini-Doost, S.E., Nouri, A.G. & Ashjaee, M. 2018. Effect of orifice shape on bubble formation mechanism. *Meccanica*, 53:2461-2483.

Hershel, W.H. & Bulkley, R.I. 1926. Measurement of Consistency as Applied to Rubber-Benzine Solutions. *Proceedings of American-Society of Testing Materials*, 26:621-633.

Hicks, A. & Slaton, W. 2014. Determining the Coefficient of Discharge for a Draining Container. *The Physics Teacher*, 52:43-47.

Hodgson, J.L. 1929. The Laws of Similarity of Orifice and Nozzle Flows. *ASME Transactions*, 51:303-332.

Johansen, F.C. 1930. Flow through Pipe Orifices at Low Reynolds Numbers. *Proceedings of the Royal Society of London. Series A*, 126(801):231-245.

Joye, D.D. & Barret, B.C. 2003 The tank Drainage Problem Revisited: Do These Equations Actually Work? *The Canadian Journal of Chemical Engineering*, 81:1052-1057

Kestin, J. & Wakeham, W.A. 1988. *Transport properties of fluids: Thermal Conductivity, viscosity and diffusion coefficient*. Hemisphere, New York.

Khahledi, M., Haldenwang, R., Chhabra, R. & Fester, V. 2020. Non-Newtonian fluid flow from bottom of tank using orifices of different shapes. *Chemical Engineering Research and Design*, 157:34-45. <https://doi.org/10.1016/j.cherd.2020.02.015>

Khahledi, M., Haldenwang, R., Fester, V. & Chhabra, R. 2019. Non-Newtonian fluids discharge through circular and square orifices from a tank. *19th International Conference on Transport & Sedimentation of Solid Particles*, 113-119.

Khahledi, M., Haldenwang, R. & Chhabra, R. 2014. Flow rate measurement of non-Newtonian fluids through sharp crested notches. *ASCE Journal of Hydraulics Engineering*, 141(1):04014067.

Kiljanski, T. 1993. Discharge coefficient for free jets from orifices at low Reynolds number. *Transactions of the American Society of Mechanical Engineers*, 115:778-781.

King, H.W. & Wisler, C.O. 1922. *Hydraulics*. John Wiley & Sons, New York.

Kobo, N.S. 2009. Entropy analysis of a reactive variable viscosity channel flow. Unpublished Mtech thesis,Cape Peninsula University of Technology, Cape Town, South Africa.

Lazarus, J.H. & Nielson, I.D. 1978. A generalised correlation for friction head losses of settling mixtures in horizontal smooth pipelines. *Paper B1. Proceedings of the 5th International Conference on the Hydraulic Transport of Solids in Pipes, Hanover. Hydrotransport 5*.

Lea, F.C. 1942. *Hydraulics*. 6th ed. Longmans, New York.

Leinhard, J.H. 1984. Velocity Coefficients for Free Jets from Sharp-Edged Orifices. *Journal of Fluids Engineering*, 106:13-17.

Lichtarowicz, A., Duggins, R. K. & Markland, E. 1965. Discharge Coefficients for Incompressible, Non-Cavitating Flow through Long Orifices. *Journal of Mechanical Engineering Science*, 7(2):210-219.

Liu, S., Afacan, A. & Masliyah, J.H. 2001. A New Pressure Drop Model for Flow-Through Orifice Plates. *The Canadian Journal of Chemical Engineering*, 79:100-106.

Malkin, A. & Isayev. A. 2006. *Rheology Concepts, Methods, & Applications*. Chemtec Publishing, Toronto.

Marcinkowski, A. & Dziubiński, M. 2004. Discharge coefficient for discharge of non-Newtonian liquids from vessel. *Chemical and Process Engineering*, 25(3):1297-1302.

McCabe, W.L., Smith, J.C. & Harriott, P. 1993. *Unit operations of Chemical Engineering*. 5th ed. McGraw-Hill International Editions, Singapore.

McGuinness, P., Drenckhan, W. & Weaire, D. 2005. The optimal tap: three dimensional nozzle design. *Journal of Physics D: Applied Physics*, 38:3382-3386.

McNeil, D.A., Addlesee, A.J. & Stuart, A.D. 1999. An experimental study of viscous flows in contractions. *J. Loss Prevent. Process Ind*, 12:249-258.

McNeil, D.A., Addlesee, A.J. & Stuart, A.D. 2000. Newtonian and non-Newtonian viscous flows in nozzles. *In: Proceedings of the Institution of Mechanical Engineers, Part CJ. Mech. Eng. Sci.* 214:1425-1436.

McNeil, D.A. & Stuart, A.D. 2003. The effects of a highly viscous liquid phase on vertically upward two-phase flow in a pipe. *Int. J. Multiphas. Flow*, 29:1523-1549.

Medaugh, F.W. & Johnson, G.D. 1940, July. Investigation of the discharge and coefficients of small circular orifices. *Civil Engineering*, 7(7):422-424.

Merritt, H.E. 1967. *Hydraulic Control systems*. Wiley & Sons, New York.

Metzner, A.B. & Reed, J.C. 1955. Flow of non-Newtonian fluids-correlation of the laminar, transition and turbulent flow regions. *AIChE Journal*, 1:434-440.

Miller, R.W. 1983. *Flow Measurement Engineering Handbook*. McGraw-Hill, New York.

Mincks, L.M. 2002. Pressure Drop Characteristics of Viscous Fluid Flow across Orifices. Mechanical Engineering, Iowa State University, Ames, MS Thesis.

Mohajane, T. Khahledi, M. Haldenwang, R. Fester, V. & Chhabra, R. 2019. Effect of round orifice aspect ratio on non-Newtonian fluid discharge from tanks. *19th International Conference on Transport & Sedimentation of Solid Particles*, 129-136.

Neal, P. & Proctor, A. 2015. *Introduction to Geotechnical Engineering*.

Ntamba Ntamba, B.M.N. 2011. Non-Newtonian pressure loss and discharge coefficients for short square-edged orifice plates. Unpublished MTech thesis. Cape Peninsula University of Technology. Cape Town, South Africa.

Novák, O. & Koza, V. 2013. Measuring a Discharge Coefficient of an Orifice for an Unsteady Compressible Flow. *PALIVA*. 5(1):21-25.

Pal, R. 1993. Flow of Oil-in-Water Emulsions through Orifice and Venturi Meters. *Ind. Eng. Chem. Res.* 32:2012-2017.

Patankar, N.A., Joseph, D.D., Wang, J., Barree, R.D., Conway, M. & Asadi, M. 2002. Power law correlations for sediment transport in pressure driven channel flows. *International Journal Multiphase Flows*, 28:1269-1292.

Perry, R.H., Greene, D.W. & Maloney, J.O. 1997. *Perry's Chemical Engineers' Handbook*. 7th ed. McGraw-Hill, New York.

Poole, R.J. & Ridley, B.S. 2007. Development-length requirements for fully developed laminar pipe flow of inelastic non-Newtonian liquids. *Journal of Fluids Engineering*, 129:1281-1287.

Prohaska, D. 2008. *Investigation of the discharge coefficient for circular orifices in riser pipes*. Clemson University, South Carolina, pprohas@clemson.edu

Rajesh, K.R. Sakthikumar & R. Sivakumar, D. 2016. Interfacial oscillation of liquid jets discharging from non-circular orifices. *International Journal of Multiphase Flow*, 87:1-8.

Ramamurthy A.S., Udoysiara S.T. & Serraf S. 1986 Rectangular lateral orifices in open channel. *J Environ Eng ASCE*, 112(2):292–300.

Rashaida, A.A. 2005. Flow of non-Newtonian Bingham plastic fluid over a rotating disk. PhD thesis. University of Saskatchewan, Saskatoon, Saskatchewan, Canada.

Rituraj., Vacca, A. 2018. Modeling the flow of non-Newtonian fluids through sharp orifices. *Journal of Fluids Engineering*, 140:1-6.

Sahin, B. & Ceyhan, H. 1996. Numerical and Experimental Analysis of Laminar Flow through Square-Edged Orifice with Variable Thickness. *Transactions of the Institute of Measurement and Control*, 18(4):166-174.

Shah, M.S., Joshi, J. B., Kalsi, A.S., Prasad, C.S.R. & Shukla, D.S. 2012. Analysis of flow through an orifice meter: CFD simulation. *Chemical Engineering Science*, 71(2012):300-309.

Skelland, A.H.P. 1967. *Non-Newtonian flow and heat transfer*. Wiley & Sons, New York.

Slatter, P.T. 1997. The effect of the yield stress on the laminar/turbulent transition. *9th International Conference on Transport and Sedimentation of Solid Particles*. Cracow, 547–561.

Slatter, P.T. 1994. Transitional and turbulent flow of non-Newtonian slurries in pipes. Unpublished PhD thesis. University of Cape Town. Cape Town, South Africa.

Smith, H. 1886. *Hydraulics: the flow of water through orifices, over weirs, and through open conduits and pipes*. Wiley & Sons, New York.

Spencer, P.R. 2013. Investigation of Discharge Behaviour from a Sharp-Edged Circular Orifice in Both Weir and Orifice Flow Regimes Using an Unsteady Experimental Procedure. Electronic Thesis and Dissertation Repository. Paper 1565.

Sochi, T. 2009. Single-Phase Flow of Non-Newtonian Fluids in Porous Media. Technical report. London: Department of Physics and Astronomy, University College. [arXiv:0907.2399v1](https://arxiv.org/abs/0907.2399v1).

Stearns, R.F., Johnson, R.R., Jackson, R.M. & Larson, C.A. 1951. *Flow measurement with orifice meters*. Van Nostrand: Toronto.

Steffe, J.F. & Salas-Valerio, W.F. 1990. Orifice Discharge Coefficients for Power-Law Fluids. *Journal of Food Process Engineering*, 12(2):89-98.

Swamee, P.K. & Swamee, N. 2010. Discharge equation of a circular sharp-crested orifice. *Journal of Hydraulic Research*, 48(1):106-107.

Taylor, J.R. 1982. *An introduction to uncertainty analysis: the study of uncertainties in physical measurements*. University Science Books, Mill Valley.

The Scrubber Manual. 1995. The McIlvaine company, Northbrook, IL.

Thompson, R.L. & Soares, E.J. 2016. Viscoplastic dimensionless numbers. *Journal of Non-Newtonian Fluid Mechanics*, 238:57-64.

Triantafillopoulos, N. 1988. *Measurement of fluid rheology and interpretation of rheograms*. 2nd Ed. Michigan: Kaltec Scientific, Inc. Novi, USA.

Tullis, B.P., Olsen E.C. & Garadner, K. 2008. Reducing Detention Volumes with Improved Outlet Structure. *Journal of Irrigation and Drainage Engineering*, 134(6):824-830.

Tuğçe, Y. 2010. Scrutinization of flow characteristics through orifices. A Thesis submitted to the graduate school of applied sciences, Middle East Technical University, Ankara, Turkey.

Tuve, G. L. & Sprenkle, R. E. 1933. Orifice Discharge Coefficients for Viscous Liquids. *Instruments*, 6(1):210-206.

van Melick, P.A.J. & Geurts, B.J. 2013. Flow through a cylindrical pipe with a periodic array of fractal orifices. *Fluid dynamics research*, 45:1-21.

Wang, F. & Fang, T. 2015. Liquid jet breakup for non-circular orifices under low pressures. *International Journal of Multiphase Flow*, 72:248-262.

Witte, R. 1928. Flow Constants of the I. G. Measuring Devices for Water, Oil, Gas, and Steam. *Zeitschrift V. D. I.*, 1493-1502.

Wood, J.D. & Dickson, A.N., 1973. *Metering of oil-air mixtures with sharp-edged orifices*. Department of Mechanical Engineering Report, Heriot-Watt University, Riccarton, Edinburgh, UK.

Young, H.D. 1962. *Statistical Treatment of experimental data*. McGraw-Hill, New York.

APPENDICES

APPENDICES

APPENDIX A: Load cell calibration.....	158
APPENDIX B: Circular orifices calibration results (8 mm, 12 mm, 16 mm and 20 mm).....	161
APPENDIX C: Square orifices calibration results (8 mm, 12 mm, 16 mm and 20 mm)	169
APPENDIX D: Triangular orifices calibration results (8 mm, 12 mm, 16 mm and 20 mm).....	177
APPENDIX E: Water tests results (Q vs h).....	185
APPENDIX F: Water results standard deviation for 12 mm, 16 mm and 20 mm hydraulic diameter orifices	190
APPENDIX G: 100% glycerine solution	192
APPENDIX H: 96% glycerine solution	198
APPENDIX I: 93% glycerine solution	204
APPENDIX J: 65% glycerine solution	210
APPENDIX K: 7.55% CMC solution.....	217
APPENDIX L: 6.58% CMC solution	224
APPENDIX M: 5.21% CMC solution	230
APPENDIX N: 2.81% CMC solution	236
APPENDIX O: 2.4% CMC solution	242
APPENDIX P: 20.34% kaolin suspension.....	248
APPENDIX Q: 13.14% kaolin suspension	254
APPENDIX R: 7.3% bentonite suspension	260
APPENDIX S: 7.18% bentonite suspension	266
APPENDIX T: 3.77% bentonite suspension	273

APPENDIX A

Figure A.1 Load cell calibration (small weights)	158
Figure A.2 Static calibration from 88.02 kg including the tank weight (small weights)	159

Table A.1 Load cell calibration (small weights).....	158
Table A.2 Calibration from 88.02 kg including the tank using small weights.....	159
Table A.3 Effect of varying sampling rate and recorded load cell voltage.....	160

APPENDIX B

Table B.1 8 mm orifice (250 kg load cell).....	161
Table B.2 8 mm orifice (100 kg load cell).....	162
Table B.3 8 mm orifice (camera).....	162
Table B.4 12 mm orifice (250 kg load cell).....	163
Table B.5 12 mm orifice (100 kg load cell).....	164
Table B.6 12 mm orifice (camera).....	164
Table B.7 16 mm orifice (250 kg load cell).....	165
Table B.8 16 mm orifice (100 kg load cell).....	166
Table B.9 16 mm orifice (camera).....	166
Table B.10 20 mm orifice (250 kg load cell).....	167
Table B.11 20 mm orifice (100 kg load cell).....	167
Table B.12 20 mm orifice (camera).....	168

APPENDIX C

Table C.1 8 mm orifice (250 kg load cell)	169
Table C.2 8 mm orifice (100 kg load cell)	170
Table C.3 8 mm orifice (camera)	170
Table C.4 12 mm orifice (250 kg load cell)	171
Table C.5 12 mm orifice (100 kg load cell)	172
Table C.6 12 mm orifice (camera)	172
Table C.7 16 mm orifice (250 kg load cell)	173
Table C.8 16 mm orifice (100 kg load cell)	174
Table C.9 16 mm orifice (camera)	174
Table C.10 20 mm orifice (250 kg load cell)	175
Table C.11 20 mm orifice (100 kg load cell)	176
Table C.12 20 mm orifice (camera)	176

APPENDIX D

Table D.1 8 mm orifice (250 kg load cell)	177
Table D.2 8 mm orifice (100 kg load cell)	178
Table D.3 8 mm orifice (camera)	178
Table D.4 12 mm orifice (250 kg load cell)	179
Table D.5 12 mm orifice (100 kg load cell)	180
Table D.6 12 mm orifice (camera)	180
Table D.7 16 mm orifice (250 kg load cell)	181
Table D.8 16 mm orifice (100 kg load cell)	182
Table D.9 16 mm orifice (camera)	182
Table D.10 20 mm orifice (250 kg load cell)	183
Table D.11 20 mm orifice (100 kg load cell)	184
Table D.12 20 mm orifice (camera)	184

APPENDIX E

Figure E.1 Flow rate (m^3/s) versus head (m) for 12 mm hydraulic diameter for circular orifice.....	185
Figure E.2 Flow rate (m^3/s) versus head (m) for 12 mm hydraulic diameter for square orifice	185
Figure E.3 Flow rate (m^3/s) versus head (m) for 12 mm hydraulic diameter for triangular orifice	186
Figure E.4 Flow rate (m^3/s) versus head (m) for 16 mm hydraulic diameter for circular orifice.....	186
Figure E.5 Flow rate (m^3/s) versus head (m) for 16 mm hydraulic diameter for square orifice	187
Figure E.6 Flow rate (m^3/s) versus head (m) for 16 mm hydraulic diameter for triangular orifice	187
Figure E.7 Flow rate (m^3/s) versus head (m) for 20 mm hydraulic diameter for circular orifice.....	188
Figure E.8 Flow rate (m^3/s) versus head (m) for 20 mm hydraulic diameter for square orifice	188
Figure E.9 Flow rate (m^3/s) versus head (m) for 20 mm hydraulic diameter for triangular orifice	189

APPENDIX F

Figure F.1 Standard deviation versus average voltage (V) for 12 mm hydraulic diameter orifice.....	190
Figure F.2 Standard deviation versus average voltage (V) for 16 mm hydraulic diameter orifice.....	191
Figure F.3 Standard deviation versus average voltage (V) for 20 mm hydraulic diameter orifice.....	191

APPENDIX G

Table G.1 8 mm circular orifice results (100% glycerine)	192
Table G.2 12 mm circular orifice results (100% glycerine)	192
Table G.3 16 mm circular orifice results (100% glycerine)	193
Table G.4 20 mm circular orifice results (100% glycerine)	193
Table G.5 8 mm square orifice results (100% glycerine)	194
Table G.6 12 mm square orifice results (100% glycerine)	194
Table G.7 16 mm square orifice results (100% glycerine)	195
Table G.8 20 mm square orifice results (100% glycerine)	195
Table G.9 8 mm triangular orifice results (100% glycerine)	196
Table G.10 12 mm triangular orifice results (100% glycerine)	196
Table G.11 16 mm triangular orifice results (100% glycerine)	197
Table G.12 20 mm triangular orifice results (100% glycerine)	197

APPENDIX H

Table H.1 8 mm circular orifice results (96% glycerine)	198
Table H.2 12 mm circular orifice results (96% glycerine)	198
Table H.3 16 mm circular orifice results (96% glycerine)	199
Table H.4 20 mm circular orifice results (96% glycerine)	199
Table H.5 8 mm square orifice results (96% glycerine)	200
Table H.6 12 mm square orifice results (96% glycerine)	200
Table H.7 16 mm square orifice results (96% glycerine)	201
Table H.8 20 mm square orifice results (96% glycerine)	201
Table H.9 8 mm triangular orifice results (96% glycerine)	202
Table H.10 12 mm triangular orifice results (96% glycerine)	202
Table H.11 16 mm triangular orifice results (96% glycerine)	203
Table H.12 20 mm triangular orifice results (96% glycerine)	203

APPENDIX I

Table I.1 8 mm circular orifice results (93% glycerine)	204
Table I.2 12 mm circular orifice results (93% glycerine)	204
Table I.3 16mm circular orifice results (93% glycerine)	205
Table I.4 20 mm circular orifice results (93% glycerine)	205
Table I.5 8 mm square orifice results (93% glycerine)	206
Table I.6 12 mm square orifice results (93% glycerine)	206
Table I.7 16 mm square orifice results (93% glycerine)	207
Table I.8 20 mm square orifice results (93% glycerine)	207
Table I.9 8 mm triangular orifice results (93% glycerine)	208
Table I.10 12 mm triangular orifice results (93% glycerine)	208
Table I.11 16 mm triangular orifice results (93% glycerine)	209
Table I.12 20 mm triangular orifice results (93% glycerine)	209

APPENDIX J

Table J.1 8 mm circular orifice results (65% glycerine)	210
Table J.2 12 mm circular orifice results (65% glycerine)	211
Table J.3 16 mm circular orifice results (65% glycerine)	211
Table J.4 20 mm circular orifice results (65% glycerine)	212
Table J.5 8 mm square orifice results (65% glycerine)	212
Table J.6 12 mm square orifice results (65% glycerine)	213
Table J.7 16 mm square orifice results (65% glycerine)	213
Table J.8 20 mm square orifice results (65% glycerine)	214
Table J.9 8 mm triangular orifice results (65% glycerine)	214
Table J.10 12 mm triangular orifice results (65% glycerine)	215
Table J.11 16 mm triangular orifice results (65% glycerine)	215
Table J.12 20 mm triangular orifice results (65% glycerine)	216

APPENDIX K

Table K.1 8 mm circular orifice results (7.55% CMC)	217
Table K.2 12 mm circular orifice results (7.55% CMC)	218
Table K.3 16 mm circular orifice results (7.55% CMC)	218
Table K.4 20 mm circular orifice results (7.55% CMC)	219
Table K.5 8 mm square orifice results (7.55% CMC)	219
Table K.6 12 mm square orifice results (7.55% CMC)	220
Table K.7 16 mm square orifice results (7.55% CMC)	220
Table K.8 20 mm square orifice results (7.55% CMC)	221
Table K.9 8 mm triangular orifice results (7.55% CMC)	221
Table K.10 12 mm triangular orifice results (7.55% CMC)	222
Table K.11 16 mm triangular orifice results (7.55% CMC)	222
Table K.12 20 mm triangular orifice results (7.55% CMC)	223

APPENDIX K

Table L.1 8 mm circular orifice results (6.58% CMC)	224
Table L.2 12 mm circular orifice results (6.58% CMC)	224
Table L.3 16 mm circular orifice results (6.58% CMC)	225
Table L.4 20 mm circular orifice results (6.58% CMC)	225
Table L.5 8 mm square orifice results (6.58% CMC)	226
Table L.6 12 mm square orifice results (6.58% CMC)	226
Table L.7 16 mm square orifice results (6.58% CMC)	227
Table L.8 20 mm square orifice results (6.58% CMC)	227
Table L.9 8 mm triangular orifice results (6.58% CMC)	228
Table L.10 12 mm triangular orifice results (6.58% CMC)	228
Table L.11 16 mm triangular orifice results (6.58% CMC)	229
Table L.12 20 mm triangular orifice results (6.58% CMC)	229

APPENDIX M

Table M.1 8 mm circular orifice results (5.21% CMC)	230
Table M.2 12 mm circular orifice results (5.21% CMC)	230
Table M.3 16 mm circular orifice results (5.21% CMC)	231
Table M.4 20 mm circular orifice results (5.21% CMC)	231
Table M.5 8 mm square orifice results (5.21% CMC)	232
Table M.6 12 mm square orifice results (5.21% CMC)	232
Table M.7 16 mm square orifice results (5.21% CMC)	233
Table M.8 20 mm square orifice results (5.21% CMC)	233
Table M.9 8 mm triangular orifice results (5.21% CMC)	234
Table M.10 12 mm triangular orifice results (5.21% CMC)	234
Table M.11 16 mm triangular orifice results (5.21% CMC)	235
Table M.12 20 mm triangular orifice results (5.21% CMC)	235

APPENDIX N

Table N.1 8 mm circular orifice results (2.81% CMC)	236
Table N.2 12 mm circular orifice results (2.81% CMC)	236
Table N.3 16 mm circular orifice results (2.81% CMC)	237
Table N.4 20 mm circular orifice results (2.81% CMC)	237
Table N.5 8 mm square orifice results (2.81% CMC)	238
Table N.6 12 mm square orifice results (2.81% CMC)	238
Table N.7 16 mm square orifice results (2.81% CMC)	239
Table N.8 20 mm square orifice results (2.81% CMC)	239
Table N.9 8 mm triangular orifice results (2.81% CMC)	240
Table N.10 12 mm triangular orifice results (2.81% CMC)	240
Table N.11 16 mm triangular orifice results (2.81% CMC)	241
Table N.12 20 mm triangular orifice results (2.81% CMC)	241

APPENDIX O

Table O.1 8 mm circular orifice results (2.81% CMC)	242
Table O.2 12 mm circular orifice results (2.81% CMC)	242
Table O.3 16 mm circular orifice results (2.81% CMC)	243
Table O.4 20 mm circular orifice results (2.81% CMC)	243
Table O.5 8 mm square orifice results (2.81% CMC)	244
Table O.6 12 mm square orifice results (2.81% CMC)	244
Table O.7 16 mm square orifice results (2.81% CMC)	245
Table O.8 20 mm square orifice results (2.81% CMC)	245
Table O.9 8 mm triangular orifice results (2.81% CMC)	245
Table O.10 12 mm triangular orifice results (2.81% CMC)	246
Table O.11 16 mm triangular orifice results (2.81% CMC)	246
Table O.12 20 mm triangular orifice results (2.81% CMC)	247

APPENDIX P

Table P.1 8 mm circular orifice results (20.34% kaolin).....	248
Table P.2 12 mm circular orifice results (20.34% kaolin).....	249
Table P.3 16 mm circular orifice results (20.34% kaolin).....	249
Table P.4 20 mm circular orifice results (20.34% kaolin).....	250
Table P.5 8 mm square orifice results (20.34% kaolin)	250
Table P.6 12 mm square orifice results (20.34% kaolin)	251
Table P.7 16 mm square orifice results (20.34% kaolin)	251
Table P.8 20 mm square orifice results (20.34% kaolin)	252
Table P.9 8 mm triangular orifice results (20.34% kaolin)	252
Table P.10 12 mm triangular orifice results (20.34% kaolin)	253
Table M.11 16 mm triangular orifice results (20.34% kaolin).....	253
Table P.12 20 mm triangular orifice results (20.34% kaolin)	253

APPENDIX Q

Table Q.1 8 mm circular orifice results (13.14% kaolin)	254
Table Q.2 12 mm circular orifice results (13.14% kaolin)	255
Table Q.3 16 mm circular orifice results (13.14% kaolin)	255
Table Q.4 20 mm circular orifice results (13.14% kaolin)	256
Table Q.5 8 mm square orifice results (13.14% kaolin)	256
Table Q.6 12 mm square orifice results (13.14% kaolin)	257
Table Q.7 16 mm square orifice results (13.14% kaolin)	257
Table Q.8 20 mm square orifice results (13.14% kaolin)	258
Table Q.9 8 mm triangular orifice results (13.14% kaolin).....	258
Table Q.10 12 mm triangular orifice results (13.14% kaolin).....	259
Table Q.11 16 mm triangular orifice results (13.14% kaolin).....	259
Table Q.12 20 mm triangular orifice results (13.14% kaolin).....	259

APPENDIX R

Table R.1 8 mm circular orifice results (7.3% bentonite)	260
Table R.2 12 mm circular orifice results (7.3% bentonite)	260
Table R.3 16 mm circular orifice results (7.3% bentonite)	261
Table R.4 20 mm circular orifice results (7.3% bentonite)	261
Table R.5 8 mm square orifice results (7.3% bentonite).....	262
Table R.6 12 mm square orifice results (7.3% bentonite).....	262
Table R.7 16 mm square orifice results (7.3% bentonite).....	263
Table R.8 20 mm square orifice results (7.3% bentonite).....	263
Table R.9 8 mm triangular orifice results (7.3% bentonite).....	264
Table R.10 12 mm triangular orifice results (7.3% bentonite).....	264
Table R.11 16 mm triangular orifice results (7.3% bentonite).....	265
Table R.12 20 mm triangular orifice results (7.3% bentonite).....	265

APPENDIX S

Table S.1 8 mm circular orifice results (7.18% bentonite)	266
Table S.2 12 mm circular orifice results (7.18% bentonite)	267
Table S.3 16 mm circular orifice results (7.18% bentonite)	267
Table S.4 20 mm circular orifice results (7.18% bentonite)	268
Table S.5 8 mm square orifice results (7.18% bentonite).....	268
Table S.6 12 mm square orifice results (7.18% bentonite).....	269
Table S.7 16 mm square orifice results (7.18% bentonite).....	269
Table S.8 20 mm square orifice results (7.18% bentonite).....	270
Table S.9 8 mm triangular orifice results (7.18% bentonite).....	270
Table S.10 12 mm triangular orifice results (7.18% bentonite).....	271
Table S.11 16 mm triangular orifice results (7.18% bentonite).....	271
Table S.12 20 mm triangular orifice results (7.18% bentonite).....	272

APPENDIX T

Table T.1 8 mm circular orifice results (3.77% bentonite)	273
Table T.2 12 mm circular orifice results (3.77% bentonite)	274
Table T.3 16 mm circular orifice results (3.77% bentonite)	274
Table T.4 20 mm circular orifice results (3.77% bentonite)	275
Table T.5 8 mm square orifice results (3.77% bentonite)	275
Table T.6 12 mm square orifice results (3.77% bentonite)	276
Table T.7 16 mm square orifice results (3.77% bentonite)	276
Table T.8 20 mm square orifice results (3.77% bentonite)	277
Table T.9 8 mm triangular orifice results (3.77% bentonite)	277
Table T.10 12 mm triangular orifice results (3.77% bentonite)	278
Table T.11 16 mm triangular orifice results (3.77% bentonite)	278
Table T.12 20 mm triangular orifice results (3.77% bentonite)	279

APPENDIX A: Load cell calibration

Table A.1 Load cell calibration (small weights)

Weights kg	Loadcell Voltage V	Voltmeter V
39	2.724	2.723
39.009	2.723	2.725
39.019	2.724	2.727
39.019	2.726	2.731
39.028	2.725	2.728
39.029	2.726	2.729
39.037	2.726	2.729
39.038	2.727	2.731
39.047	2.728	2.731
39.056	2.729	2.732
39.134	2.735	2.739
39.134	2.733	2.738

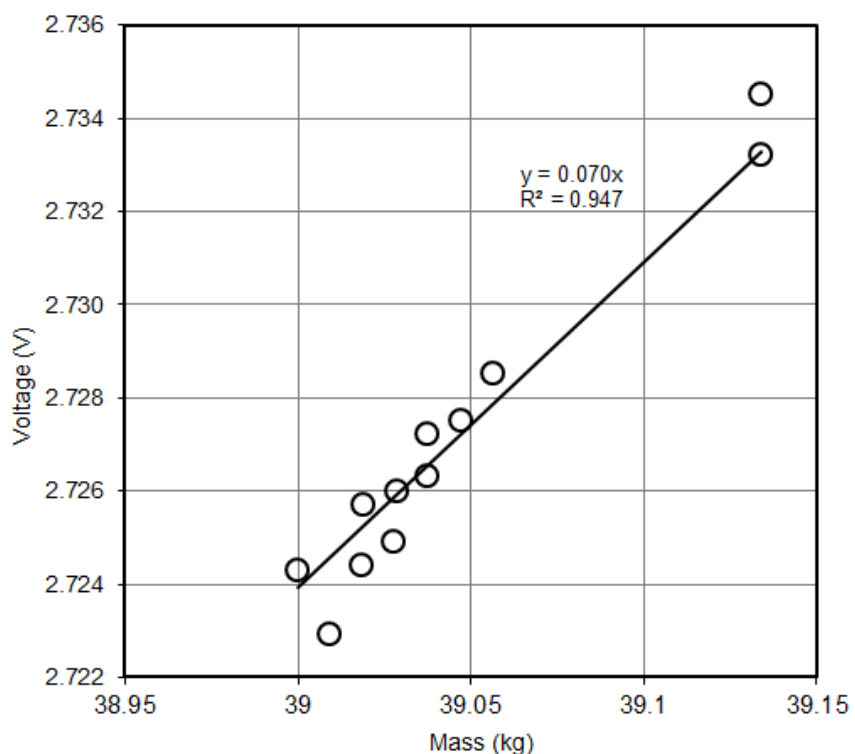


Figure A.1 Load cell calibration (small weights)

Table A.2 Calibration from 88.02 kg including the tank using small weights

Weights kg	Loadcell Voltage V	Voltmeter V
88.02	6.213	6.210
88.02	6.215	6.210
88.029	6.214	6.210
88.029	6.215	6.210
88.039	6.216	6.220
88.039	6.215	6.212
88.048	6.215	6.212
88.048	6.216	6.220
88.057	6.216	6.220
88.057	6.216	6.221
88.067	6.217	6.220
88.067	6.217	6.220
88.077	6.218	6.220
88.077	6.217	6.230
88.123	6.221	6.230

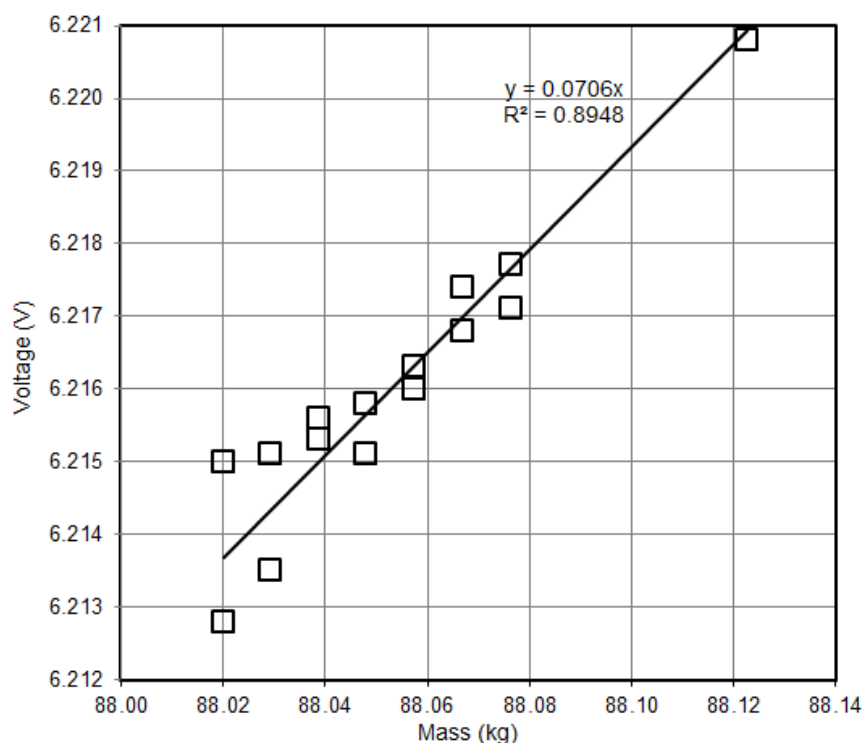


Figure A.2 Static calibration from 88.02 kg including the tank weight (small weights)

Table A.3 Effect of varying sampling rate and recorded load cell voltage

Sampling rate Hz	Voltage V
5	2.917
20	2.918
60	2.917
150	2.917
150	2.918
200	2.918
250	2.917
300	2.917
300	2.917
450	2.917
Standard Deviation	0.00026

APPENDIX B: Circular orifices calibration results (8 mm, 12 mm, 16 mm and 20 mm)

8 mm circular Orifice

WATER

Tank

length and width= 0.4 m
Area= 0.16 m²

Orifice:

diameter = 0.008 m
Area= 50.77E-6 m²
D_h= 0.008 m

Rheological and physical parameters

μ = 0.001 Pa.s
Density= 1000 kg/m³
g= 9.81 m/s²

Table B.1 8 mm orifice (250 kg load cell)

Time	Diff. Time	Mass in tank	Height	Diff.Height	Flow rate	Orifice		
						Velocity	C _d	Re
[s]		[kg]	[m]	[m]	[m ³ /s]	[m/s]		
8.325	0	85.577	0.535	0	0	0	0	0
58.33	50	80.493	0.503	0.032	0.0001	3.14	0.63	25259
108.3	100	75.529	0.472	0.063	97.053E-6	3.04	0.63	24468
158.3	150	70.753	0.442	0.093	94.011E-6	2.95	0.63	23682
208.3	200	66.132	0.413	0.122	90.970E-6	2.85	0.63	22896
258.3	250	61.667	0.385	0.149	87.928E-6	2.75	0.63	22109
308.3	300	57.389	0.359	0.176	84.886E-6	2.65	0.63	21328
358.3	350	53.222	0.333	0.202	81.845E-6	2.55	0.63	20540
408.3	400	49.182	0.307	0.227	78.803E-6	2.46	0.63	19745
458.3	450	45.310	0.283	0.252	75.762E-6	2.36	0.63	18951
508.3	500	41.584	0.260	0.275	72.720E-6	2.26	0.63	18155
558.3	550	38.027	0.238	0.297	69.678E-6	2.16	0.64	17362
608.3	600	34.615	0.216	0.319	66.637E-6	2.06	0.64	16564
658.3	650	31.383	0.196	0.339	63.595E-6	1.96	0.64	15772
708.3	700	28.259	0.177	0.358	60.554E-6	1.86	0.64	14967
758.3	750	25.306	0.158	0.377	57.512E-6	1.76	0.64	14163
808.3	800	22.515	0.141	0.394	54.470E-6	1.66	0.65	13359
858.3	850	19.885	0.124	0.411	51.429E-6	1.56	0.65	12555
908.3	900	17.371	0.109	0.426	48.387E-6	1.46	0.65	11734

Table B.2 8 mm orifice (100 kg load cell)

Time	Diff. Time	Mass in tank	Height	Diff. Height	Flow rate	Orifice Velocity	C_d	Re
[s]		[kg]	[m]	[m]	[m³/s]	[m/s]		
8.325	0.0	59.106	0.369	0	0	0	0	0
49.99	41.67	55.522	0.347	0.022	84.82E-6	2.61	0.64	20979
91.66	83.33	52.042	0.325	0.044	82.17E-6	2.53	0.64	20311
133.3	125.0	48.678	0.304	0.065	79.52E-6	2.44	0.64	19643
175.0	166.7	45.418	0.284	0.086	76.86E-6	2.36	0.64	18974
216.7	208.3	42.270	0.264	0.105	74.21E-6	2.28	0.64	18305
258.3	250.0	39.229	0.245	0.124	71.56E-6	2.19	0.64	17634
300.0	291.7	36.302	0.227	0.143	68.91E-6	2.11	0.64	16963
341.7	333.3	33.487	0.209	0.160	66.26E-6	2.03	0.64	16292
383.3	375.0	30.783	0.192	0.177	63.60E-6	1.94	0.64	15621
425.0	416.7	28.186	0.176	0.193	60.95E-6	1.86	0.65	14947
466.7	458.3	25.703	0.161	0.209	58.30E-6	1.78	0.65	14274
508.3	500.0	23.330	0.146	0.224	55.65E-6	1.69	0.65	13599
550.0	541.7	21.072	0.132	0.238	53.00E-6	1.61	0.65	12924
591.7	583.3	18.916	0.118	0.251	50.34E-6	1.52	0.65	12245
633.3	625.0	16.870	0.105	0.264	47.69E-6	1.44	0.65	11564
675.0	666.7	14.940	0.093	0.276	45.04E-6	1.35	0.66	10882
716.7	708.3	13.116	0.082	0.287	42.39E-6	1.27	0.66	10196
758.3	750.0	11.405	0.071	0.298	39.74E-6	1.18	0.66	9508

Table B.3 8 mm orifice (camera)

Cumulative								
Time	Time	Diff. Height	Height	Flow rate	Orifice Velocity	C_d	Re	
[s]	[s]	[m]	[m]	[m³/s]	[m/s]			
0	0	0	0.37	0	0	0	0	0
18.56	18.56	0.01	0.36	84.96E-6	2.66	0.63	21368	
18.56	37.12	0.02	0.35	83.87E-6	2.62	0.63	21069	
19.48	56.60	0.03	0.34	82.72E-6	2.58	0.63	20766	
19.48	76.08	0.04	0.33	81.58E-6	2.54	0.63	20458	
19.32	95.40	0.05	0.32	80.44E-6	2.51	0.63	20146	
20.08	115.5	0.06	0.31	79.26E-6	2.47	0.63	19828	
20.20	135.7	0.07	0.3	78.07E-6	2.43	0.63	19506	
20.88	156.6	0.08	0.29	76.84E-6	2.39	0.63	19178	
20.76	177.3	0.09	0.28	75.62E-6	2.34	0.64	18844	
21.36	198.7	0.10	0.27	74.37E-6	2.30	0.64	18505	
21.32	220.0	0.11	0.26	73.12E-6	2.26	0.64	18159	
22.16	242.2	0.12	0.25	71.81E-6	2.21	0.64	17806	
22.76	264.9	0.13	0.24	70.47E-6	2.17	0.64	17447	
22.96	287.9	0.14	0.23	69.13E-6	2.12	0.64	17079	
23.56	311.4	0.15	0.22	67.74E-6	2.08	0.64	16704	
23.88	335.3	0.16	0.21	66.34E-6	2.03	0.64	16320	
24.88	360.2	0.17	0.2	64.87E-6	1.98	0.65	15927	
25.00	385.2	0.18	0.19	63.40E-6	1.93	0.65	15523	
25.24	410.4	0.19	0.18	61.92E-6	1.88	0.65	15109	
26.80	437.2	0.2	0.17	60.35E-6	1.83	0.65	14684	
27.12	464.4	0.21	0.16	58.75E-6	1.77	0.65	14245	

12 mm circular orifice

WATER

Tank

Length and width= 0.4 m
Area= 0.160 m²

Orifice:

diameter = 0.012 m
Area= 113.9E-6 m
 D_h = 0.012 m

Other Parameters

μ = 0.0010 Pa.s
Density= 1000 kg/m³
 g = 9.81 m/s²

Table B.4 12 mm orifice (250 kg load cell)

Time [s]	Diff.Time [s]	Mass in tank [kg]	Height [m]	Diff.Height [m]	Orifice			C_d	Re
					Flow rate [m ³ /s]	Velocity [m/s]			
4.158	0	85.611	0.535	0	0	0	0	0	0
29.16	25	80.133	0.501	0.034	216.2E-6	3.13	0.61	37742	
54.16	50	74.815	0.468	0.067	209.0E-6	3.03	0.61	36468	
79.16	75	69.685	0.436	0.100	201.7E-6	2.92	0.61	35195	
104.2	100	64.729	0.405	0.131	194.4E-6	2.82	0.61	33921	
129.2	125	59.964	0.375	0.160	187.2E-6	2.71	0.61	32648	
154.2	150	55.368	0.346	0.189	179.9E-6	2.61	0.61	31372	
179.2	175	50.960	0.318	0.217	172.6E-6	2.50	0.61	30097	
204.2	200	46.750	0.292	0.243	165.4E-6	2.39	0.61	28828	
229.2	225	42.710	0.267	0.268	158.1E-6	2.29	0.61	27554	
254.2	250	38.848	0.243	0.292	150.8E-6	2.18	0.61	26278	
279.2	275	35.160	0.220	0.315	143.5E-6	2.08	0.61	25000	
304.2	300	31.668	0.198	0.337	136.3E-6	1.97	0.61	23726	
329.2	325	28.348	0.177	0.358	129.0E-6	1.86	0.61	22448	
354.2	350	25.215	0.158	0.377	121.7E-6	1.76	0.61	21171	
379.2	375	22.241	0.139	0.396	114.5E-6	1.65	0.61	19883	
404.2	400	19.510	0.122	0.413	107.2E-6	1.55	0.61	18623	
429.2	425	16.921	0.106	0.429	9.99E-05	1.44	0.61	17343	

Table B.5 12 mm orifice (100 kg load cell)

Time	Diff.Time	Mass in tank	Height	Diff.Height	Flow rate	Orifice Velocity	C _d	Re
[s]	[s]	[kg]	[m]	[m]	[m ³ /s]	[m/s]		
3.325	0	59.449	0.372	0	0	0	0	0
23.33	20	55.740	0.348	0.0232	182.7E-6	2.61	0.61	31478
43.33	40	52.145	0.326	0.0456	176.8E-6	2.53	0.61	30445
63.33	60	48.666	0.304	0.0674	170.9E-6	2.44	0.61	29412
83.33	80	45.308	0.283	0.0884	165.0E-6	2.36	0.61	28379
103.3	100	42.072	0.263	0.109	159.1E-6	2.27	0.62	27347
123.3	120	38.948	0.243	0.128	153.2E-6	2.19	0.62	26312
143.3	140	35.937	0.225	0.147	147.2E-6	2.10	0.62	25275
163.3	160	33.054	0.207	0.165	141.3E-6	2.01	0.62	24240
183.3	180	30.282	0.189	0.182	135.4E-6	1.93	0.62	23201
203.3	200	27.628	0.173	0.199	129.5E-6	1.84	0.62	22161
223.3	220	25.096	0.157	0.215	123.6E-6	1.75	0.62	21121
243.3	240	22.680	0.142	0.230	117.7E-6	1.67	0.62	20079
263.3	260	20.391	0.127	0.244	111.8E-6	1.58	0.62	19039
283.3	280	18.214	0.114	0.258	105.8E-6	1.49	0.62	17994

Table B.6 12 mm orifice (camera)

Cumulative								
Time	Time	Diff. Height	Height	Flow rate	Orifice Velocity	C _d	Re	
[s]	[s]	[m]	[m]	[m ³ /s]	[m/s]			
0.00	0.00	0	0.37	0	0	0	0	0
8.84	8.84	0.01	0.36	184.3E-6	2.66	0.61	31998	
8.72	17.56	0.02	0.35	181.8E-6	2.62	0.61	31551	
8.84	26.40	0.03	0.34	179.3E-6	2.58	0.61	31097	
8.80	35.20	0.04	0.33	176.7E-6	2.54	0.61	30636	
9.44	44.64	0.05	0.32	174.0E-6	2.51	0.61	30168	
9.16	53.80	0.06	0.31	171.4E-6	2.47	0.61	29693	
9.60	63.40	0.07	0.30	168.6E-6	2.43	0.61	29210	
9.72	73.12	0.08	0.29	165.8E-6	2.39	0.61	28719	
9.56	82.68	0.09	0.28	163.0E-6	2.34	0.61	28220	
9.84	92.52	0.10	0.27	160.2E-6	2.30	0.61	27711	
9.84	102.4	0.11	0.26	157.4E-6	2.26	0.61	27193	
10.16	112.5	0.12	0.25	154.4E-6	2.21	0.61	26665	
10.80	123.3	0.13	0.24	151.3E-6	2.17	0.61	26127	
10.80	134.1	0.14	0.23	148.2E-6	2.12	0.61	25576	
10.56	144.7	0.15	0.22	145.2E-6	2.08	0.61	25014	
11.60	156.3	0.16	0.21	141.8E-6	2.03	0.61	24439	
11.04	167.3	0.17	0.20	138.7E-6	1.98	0.61	23850	
12.00	179.3	0.18	0.19	135.2E-6	1.93	0.62	23246	
11.80	191.1	0.19	0.18	131.8E-6	1.88	0.62	22626	
12.08	203.2	0.20	0.17	128.3E-6	1.83	0.62	21989	
12.52	215.7	0.21	0.16	124.7E-6	1.77	0.62	21332	
11.60	227.3	0.22	0.15	121.4E-6	1.72	0.62	20655	
15.16	242.5	0.23	0.14	117.0E-6	1.66	0.62	19954	
13.64	256.1	0.24	0.13	113.1E-6	1.60	0.62	19229	
14.68	270.8	0.25	0.12	108.8E-6	1.53	0.62	18474	
15.08	285.9	0.26	0.11	104.5E-6	1.47	0.62	17688	
16.28	302.2	0.27	0.10	99.79E-6	1.40	0.63	16865	
15.60	317.8	0.28	0.09	95.29E-6	1.33	0.63	15999	

16 mm circular orifice

WATER

Tank

Length and width= 0.4 m
Area= 0.160 m²

Orifice:

diameter = 0.0160 m
Area= 202.1E-6 m²
 D_h = 0.0160 m

Other Parameters

μ = 0.0010 Pa.s
Density= 1000 kg/m³
 g = 9.81 m/s²

Table B.7 16 mm orifice (250 kg load cell)

Time [s]	Diff.Time [s]	Mass in tan [kg]	Height [m]	Diff.Height [m]	Flow rate [m ³ /s]	Orifice		
						Velocity [m/s]	C_d	Re
2.492	0	86.295	0.539	0	0	0	0	0
17.49	15	80.482	0.503	0.036	0.000382	3.14	0.60	50390
32.49	30	74.875	0.468	0.071	0.000368	3.03	0.60	48603
47.49	45	69.478	0.434	0.105	0.000354	2.92	0.60	46818
62.49	60	64.269	0.402	0.138	0.000341	2.81	0.60	45029
77.49	75	59.256	0.370	0.169	0.000327	2.70	0.60	43238
92.49	90	54.414	0.340	0.199	0.000314	2.58	0.60	41433
107.5	105	49.814	0.311	0.228	0.0003	2.47	0.60	39643
122.5	120	45.406	0.284	0.256	0.000287	2.36	0.60	37849
137.5	135	41.217	0.258	0.282	0.000273	2.25	0.60	36060
152.5	150	37.241	0.233	0.307	0.000259	2.14	0.60	34277
167.5	165	33.428	0.209	0.330	0.000246	2.02	0.60	32475
182.5	180	29.854	0.187	0.353	0.000232	1.91	0.60	30690
197.5	195	26.482	0.166	0.374	0.000219	1.80	0.60	28905
212.5	210	23.296	0.146	0.394	0.000205	1.69	0.60	27110

Table B.8 16 mm orifice (100 kg load cell)

Time [s]	Diff.Time [s]	Mass in tank [kg]	Height [m]	Diff.Height [m]	Flow rate [m ³ /s]	Orifice Velocity		
						C _d	Re	
2.075	0.0	59.124	0.370	0	0	0	0	0
14.58	12.5	55.061	0.344	0.025	319.9E-6	2.60	0.61	41679
27.08	25.0	51.137	0.320	0.050	308.4E-6	2.50	0.61	40166
39.58	37.5	47.355	0.296	0.074	296.9E-6	2.41	0.61	38652
52.08	50.0	43.721	0.273	0.096	285.4E-6	2.32	0.61	37140
64.58	62.5	40.228	0.251	0.118	273.9E-6	2.22	0.61	35625
77.08	75.0	36.867	0.230	0.139	262.4E-6	2.13	0.61	34104
89.58	87.5	33.659	0.210	0.159	250.9E-6	2.03	0.61	32587
102.1	100.0	30.591	0.191	0.178	239.5E-6	1.94	0.61	31067
114.6	112.5	27.668	0.173	0.197	228.0E-6	1.84	0.61	29545
127.1	125.0	24.890	0.156	0.214	216.5E-6	1.75	0.61	28022
139.6	137.5	22.253	0.139	0.230	205.0E-6	1.65	0.61	26496
152.1	150.0	19.763	0.124	0.246	193.5E-6	1.56	0.62	24970
164.6	162.5	17.414	0.109	0.261	182.0E-6	1.46	0.62	23439

Table B.9 16 mm orifice (camera)

Time [s]	Time [s]	Cumulative			Flow rate [m ³ /s]	Orifice Velocity [m/s]	C _d	Re
		Diff. Height [m]	Height [m]	Flow rate [m ³ /s]				
0.00	0.00	0.00	0.37	0	0	0	0	0
5.24	5.24	0.01	0.36	326.25E-6	2.66	0.61	42629	
4.40	9.64	0.02	0.35	322.22E-6	2.62	0.61	42033	
5.24	14.88	0.03	0.34	317.43E-6	2.58	0.61	41428	
4.84	19.72	0.04	0.33	313.00E-6	2.54	0.61	40814	
5.24	24.96	0.05	0.32	308.21E-6	2.51	0.61	40191	
5.48	30.44	0.06	0.31	303.20E-6	2.47	0.61	39558	
5.00	35.44	0.07	0.30	298.63E-6	2.43	0.61	38915	
5.60	41.04	0.08	0.29	293.51E-6	2.39	0.61	38261	
5.52	46.56	0.09	0.28	288.46E-6	2.34	0.61	37595	
5.64	52.20	0.10	0.27	283.30E-6	2.30	0.61	36918	
5.60	57.80	0.11	0.26	278.18E-6	2.26	0.61	36228	
5.68	63.48	0.12	0.25	272.98E-6	2.21	0.61	35524	
5.96	69.44	0.13	0.24	267.53E-6	2.17	0.61	34806	
6.20	75.64	0.14	0.23	261.86E-6	2.12	0.61	34074	
6.20	81.84	0.15	0.22	256.19E-6	2.08	0.61	33325	
6.20	88.04	0.16	0.21	250.52E-6	2.03	0.61	32558	
6.52	94.56	0.17	0.20	244.56E-6	1.98	0.61	31774	
6.80	101.4	0.18	0.19	238.34E-6	1.93	0.61	30969	
6.80	108.2	0.19	0.18	232.12E-6	1.88	0.61	30143	
6.56	114.7	0.20	0.17	226.12E-6	1.83	0.61	29294	
7.20	121.9	0.21	0.16	219.54E-6	1.77	0.61	28419	
7.56	129.5	0.22	0.15	212.62E-6	1.72	0.61	27517	
7.88	137.4	0.23	0.14	205.42E-6	1.66	0.61	26584	
7.68	145.0	0.24	0.13	198.39E-6	1.60	0.61	25617	
8.24	153.3	0.25	0.12	190.86E-6	1.53	0.62	24612	
8.52	161.8	0.26	0.11	183.06E-6	1.47	0.62	23564	
8.80	170.6	0.27	0.10	175.02E-6	1.40	0.62	22467	
9.80	180.4	0.28	0.09	166.05E-6	1.33	0.62	21314	
10.12	190.5	0.29	0.08	156.80E-6	1.25	0.62	20096	
10.04	200.6	0.30	0.07	147.62E-6	1.17	0.62	18798	
11.20	211.8	0.31	0.06	137.37E-6	1.08	0.63	17403	

20 mm circular orifice

WATER

Tank	
Length and width=	0.4 m
Area=	0.160 m ²
Orifice:	
diameter =	0.020 m
Area=	315.4E-6 m ²
D _h =	0.020 m
Other parameters	
μ =	0.0010 Pa.s
Density=	1000 kg/m ³
g=	9.81 m/s ²

Table B.10 20 mm orifice (250 kg load cell)

Time	Diff.Time	Mass in tank	Height	Diff.Height	Flow rate	Orifice Velocity	C _d	Re
[s]		[kg]	[m]	[m]	[m ³ /s]	[m/s]		
2.492	0	86.374	0.540	0				
17.492	15	77.384	0.484	0.056	0.000583	3.08	0.60	61732
32.492	30	68.912	0.431	0.109	0.000550	2.91	0.60	58255
47.492	45	60.902	0.381	0.159	0.000517	2.73	0.60	54765
62.492	60	53.384	0.334	0.206	0.000484	2.56	0.60	51273
77.492	75	46.386	0.290	0.250	0.000451	2.38	0.60	47795
92.492	90	39.867	0.249	0.291	0.000418	2.21	0.60	44309
107.492	105	33.836	0.211	0.328	0.000385	2.04	0.60	40820
122.492	120	28.334	0.177	0.363	0.000352	1.86	0.60	37354

Table B.11 20 mm orifice (100 kg load cell)

Time	Diff. Time	Mass in tank	Height	Diff.Height	Flow rate	Orifice Velocity	C _d	Re
[s]		[kg]	[m]	[m]	[m ³ /s]	[m/s]		
1.242	0.0	59.568	0.372	0	0	0	0	0
8.742	7.5	55.749	0.348	0.024	502.2E-6	2.61	0.61	52397
16.24	15.0	52.036	0.325	0.047	485.5E-6	2.53	0.61	50622
23.74	22.5	48.465	0.303	0.069	468.7E-6	2.44	0.61	48854
31.24	30.0	45.018	0.281	0.091	451.9E-6	2.35	0.61	47085
38.74	37.5	41.693	0.261	0.112	435.1E-6	2.26	0.61	45313
46.24	45.0	38.491	0.241	0.132	418.3E-6	2.17	0.61	43538
53.74	52.5	35.422	0.221	0.151	401.5E-6	2.08	0.61	41766
61.24	60.0	32.459	0.203	0.169	384.7E-6	2.00	0.61	39981
68.74	67.5	29.645	0.185	0.187	367.9E-6	1.91	0.61	38208
76.24	75.0	26.936	0.168	0.204	351.1E-6	1.82	0.61	36421
83.74	82.5	24.365	0.152	0.220	334.3E-6	1.73	0.61	34639
91.24	90.0	21.921	0.137	0.235	317.6E-6	1.64	0.61	32856
98.74	97.5	19.610	0.123	0.250	300.8E-6	1.55	0.61	31076
106.2	105.0	17.406	0.109	0.264	284.0E-6	1.46	0.62	29277

Table B.12 20 mm orifice (camera)

Cumulative							
Time	Time	Diff. Height	Height	Flow rate	Orifice Velocity	C_d	Re
[s]	[s]	[m]	[m]	[m³/s]	[m/s]		
0.00	0.00	0.00	0.37	0	0	0	0
3.12	3.12	0.01	0.36	508.1E-6	2.66	0.61	53260
3.28	6.40	0.02	0.35	500.9E-6	2.62	0.61	52515
3.40	9.80	0.03	0.34	493.5E-6	2.58	0.61	51759
3.00	12.80	0.04	0.33	486.9E-6	2.54	0.61	50992
3.52	16.32	0.05	0.32	479.3E-6	2.51	0.61	50214
3.24	19.56	0.06	0.31	472.2E-6	2.47	0.61	49423
3.16	22.72	0.07	0.30	465.3E-6	2.43	0.61	48619
3.72	26.44	0.08	0.29	457.2E-6	2.39	0.61	47802
3.36	29.80	0.09	0.28	449.8E-6	2.34	0.61	46971
3.72	33.52	0.10	0.27	441.7E-6	2.30	0.61	46124
3.36	36.88	0.11	0.26	434.4E-6	2.26	0.61	45262
4.16	41.04	0.12	0.25	425.3E-6	2.21	0.61	44383
3.76	44.80	0.13	0.24	417.1E-6	2.17	0.61	43486
3.84	48.64	0.14	0.23	408.7E-6	2.12	0.61	42571
3.84	52.48	0.15	0.22	400.3E-6	2.08	0.61	41635
4.36	56.84	0.16	0.21	390.8E-6	2.03	0.61	40678
4.04	60.88	0.17	0.20	382.0E-6	1.98	0.61	39697
4.20	65.08	0.18	0.19	372.8E-6	1.93	0.61	38692
4.44	69.52	0.19	0.18	363.1E-6	1.88	0.61	37660
4.20	73.72	0.20	0.17	354.0E-6	1.83	0.61	36599
4.48	78.20	0.21	0.16	344.2E-6	1.77	0.62	35506
4.52	82.72	0.22	0.15	334.3E-6	1.72	0.62	34379
5.00	87.72	0.23	0.14	323.4E-6	1.66	0.62	33213
4.88	92.60	0.24	0.13	312.8E-6	1.60	0.62	32005
5.52	98.12	0.25	0.12	300.7E-6	1.53	0.62	30749
5.56	103.68	0.26	0.11	288.6E-6	1.47	0.62	29440
5.76	109.44	0.27	0.10	276.0E-6	1.40	0.62	28070
6.00	115.44	0.28	0.09	262.9E-6	1.33	0.63	26630

APPENDIX C: Square orifices calibration results (8 mm, 12 mm, 16 mm and 20 mm)

D_h 8 mm orifice

WATER

Tank

Length and width= 0.4 m
Area= 0.16 m²

Orifice:

Breadth = 0.008 m
Length= 0.008 m
Area= 64.32E-6 m²
 D_h = 0.008 m

Other parameters

μ = 0.001 Pa.s
Density= 1000 kg/m³
 g = 9.81 m/s²

Table C.1 8 mm orifice (250 kg load cell)

Time [s]	Diff.Time [s]	Mass in tank [kg]	Height [m]	Diff.Height [m]	Flow rate [m ³ /s]	Orifice Velocity		
						C _d	Re	
8.325	0.00	86.013	0.54					
49.99	41.67	80.638	0.50	0.034	127.3E-6	3.14	0.63	25219
91.66	83.33	75.417	0.47	0.066	123.2E-6	3.04	0.63	24389
133.3	125.0	70.388	0.44	0.098	119.1E-6	2.94	0.63	23562
175.0	166.7	65.504	0.41	0.13	115.0E-6	2.83	0.63	22730
216.7	208.3	60.796	0.38	0.16	110.9E-6	2.73	0.63	21898
258.3	250.0	56.253	0.35	0.19	106.8E-6	2.63	0.63	21064
300.0	291.7	51.900	0.32	0.21	102.7E-6	2.52	0.63	20232
341.7	333.3	47.707	0.30	0.24	98.64E-6	2.42	0.63	19398
383.3	375.0	43.680	0.27	0.26	94.55E-6	2.31	0.64	18561
425.0	416.7	39.812	0.25	0.29	90.46E-6	2.21	0.64	17720
466.7	458.3	36.124	0.23	0.31	86.38E-6	2.10	0.64	16880
508.3	500.0	32.614	0.20	0.33	82.29E-6	2.00	0.64	16038
550.0	541.7	29.273	0.18	0.35	78.20E-6	1.89	0.64	15195
591.7	583.3	26.094	0.16	0.37	74.11E-6	1.79	0.64	14346
633.3	625.0	23.093	0.14	0.39	70.02E-6	1.68	0.65	13496

Table C.2 8 mm orifice (100 kg load cell)

Time [s]	Diff.Time [s]	Mass in tank [kg]	Height [m]	Diff.Height [m]	Flow rate [m ³ /s]	Orifice Velocity		
						C _d	Re	
8.325	0.00	59.260	0.370	0	0	0	0	0
49.99	41.67	54.731	0.342	0.028	106.6E-6	2.59	0.64	20777
91.66	83.33	50.378	0.315	0.056	102.4E-6	2.49	0.64	19933
133.3	125.0	46.202	0.289	0.082	98.12E-6	2.38	0.64	19089
175.0	166.7	42.201	0.264	0.107	93.87E-6	2.27	0.64	18244
216.7	208.3	38.384	0.240	0.130	89.62E-6	2.17	0.64	17400
258.3	250.0	34.735	0.217	0.153	85.37E-6	2.06	0.64	16552
300.0	291.7	31.268	0.195	0.175	81.12E-6	1.96	0.64	15704
341.7	333.3	27.975	0.175	0.196	76.86E-6	1.85	0.65	14854
383.3	375.0	24.855	0.155	0.215	72.61E-6	1.75	0.65	14001
425.0	416.7	21.917	0.137	0.233	68.36E-6	1.64	0.65	13148

Table C.3 8 mm orifice (camera)

Time [s]	Cumulative					Orifice Velocity [m/s]	C _d	Re
	Time [s]	Diff. Height [m]	Height [m]	Flow rate [m ³ /s]				
0.00	0.00	0.00	0.37	0	0	0	0	0
30.40	30.40	0.020	0.35	106.6E-6	2.62	0.63	21016	
30.32	60.72	0.040	0.33	103.7E-6	2.54	0.63	20407	
31.28	92.00	0.060	0.31	100.6E-6	2.47	0.63	19779	
32.28	124.3	0.080	0.29	97.47E-6	2.39	0.64	19130	
33.64	157.9	0.10	0.27	94.18E-6	2.30	0.64	18459	
34.36	192.3	0.12	0.25	90.83E-6	2.21	0.64	17762	
35.80	228.1	0.14	0.23	87.33E-6	2.12	0.64	17037	
37.64	265.7	0.16	0.21	83.66E-6	2.03	0.64	16279	
38.80	304.5	0.18	0.19	79.87E-6	1.93	0.64	15485	
40.60	345.1	0.20	0.17	75.91E-6	1.83	0.65	14647	
44.08	389.2	0.22	0.15	71.60E-6	1.72	0.65	13758	
46.00	435.2	0.24	0.13	67.11E-6	1.60	0.65	12808	
49.12	484.3	0.26	0.11	62.31E-6	1.47	0.66	11782	
54.88	539.2	0.28	0.09	56.96E-6	1.33	0.67	10657	

D_h 12 mm orifice

WATER

Tank

Length and width= 0.4 m
Area= 0.16 m²

Orifice:

Breadth = 0.012 m
Length= 0.012 m
Area= 144.5E-6 m²
D_h= 0.012 m

Other parameters

μ = 0.001 Pa.s
Density= 1000 kg/m³
g= 9.81 m/s²

Table C.4 12 mm orifice (250 kg load cell)

Time	Diff.Time	Mass in tank	Height	Diff.Height	Flow rate	Orifice Velocity								
						[s]	[s]	[kg]	[m]	[m]	[m ³ /s]	[m/s]	C _d	Re
2.492	0	59.268	0.37	0	0	0	0	0	0	0	0	0	0	0
17.49	15	55.604	0.35	0.023	240.6E-6	2.61	0.64	0.64	0.64	0.64	31387			
32.49	30	52.049	0.33	0.045	232.9E-6	2.53	0.64	0.64	0.64	0.64	30367			
47.49	45	48.619	0.30	0.067	225.2E-6	2.44	0.64	0.64	0.64	0.64	29349			
62.49	60	45.299	0.28	0.087	217.5E-6	2.36	0.64	0.64	0.64	0.64	28329			
77.49	75	42.092	0.26	0.11	209.8E-6	2.27	0.64	0.64	0.64	0.64	27308			
92.49	90	39.004	0.24	0.13	202.1E-6	2.19	0.64	0.64	0.64	0.64	26287			
107.5	105	36.026	0.23	0.15	194.4E-6	2.10	0.64	0.64	0.64	0.64	25264			
122.5	120	33.161	0.21	0.16	186.7E-6	2.02	0.64	0.64	0.64	0.64	24239			
137.5	135	30.424	0.19	0.18	179.0E-6	1.93	0.64	0.64	0.64	0.64	23217			
152.5	150	27.794	0.17	0.20	171.3E-6	1.85	0.64	0.64	0.64	0.64	22191			
167.5	165	25.285	0.16	0.21	163.6E-6	1.76	0.64	0.64	0.64	0.64	21165			
182.5	180	22.893	0.14	0.23	155.9E-6	1.68	0.64	0.64	0.64	0.64	20139			
197.5	195	20.620	0.13	0.24	148.2E-6	1.59	0.65	0.65	0.65	0.65	19113			
212.5	210	18.443	0.12	0.26	140.5E-6	1.50	0.65	0.65	0.65	0.65	18076			
227.5	225	16.399	0.10	0.27	132.8E-6	1.42	0.65	0.65	0.65	0.65	17045			
242.5	240	14.455	0.090	0.28	125.1E-6	1.33	0.65	0.65	0.65	0.65	16003			
257.5	255	12.639	0.079	0.29	117.4E-6	1.24	0.65	0.65	0.65	0.65	14964			
272.5	270	10.933	0.068	0.30	109.7E-6	1.16	0.66	0.66	0.66	0.66	13917			

Table C.5 12 mm orifice (100 kg load cell)

Time	Diff.Time	Mass in tank	Height	Diff.Height	Flow rate	Orifice Velocity	C _d	Re
[s]	[s]	[Kg]	[m]	[m]	[m ³ /s]	[m/s]		
3.325	0	85.756	0.54	0	0	0	0	0
23.33	20	80.000	0.50	0.036	282.6E-6	3.13	0.62	37648
43.33	40	74.433	0.47	0.071	272.6E-6	3.02	0.62	36314
63.33	60	69.073	0.43	0.10	262.7E-6	2.91	0.62	34982
83.33	80	63.903	0.40	0.14	252.8E-6	2.80	0.62	33648
103.3	100	59.010	0.37	0.17	242.8E-6	2.69	0.62	32334
123.3	120	54.236	0.34	0.20	232.9E-6	2.58	0.63	30998
143.3	140	49.684	0.31	0.23	223.0E-6	2.47	0.63	29669
163.3	160	45.317	0.28	0.25	213.1E-6	2.36	0.63	28335
183.3	180	41.147	0.26	0.28	203.1E-6	2.25	0.63	27000
203.3	200	37.182	0.23	0.30	193.2E-6	2.14	0.63	25666
223.3	220	33.419	0.21	0.33	183.3E-6	2.02	0.63	24333
243.3	240	29.858	0.19	0.35	173.4E-6	1.91	0.63	23000
263.3	260	26.479	0.17	0.37	163.4E-6	1.80	0.63	21659
283.3	280	23.327	0.15	0.39	153.5E-6	1.69	0.63	20329
303.3	300	20.361	0.13	0.41	143.6E-6	1.58	0.63	18993
323.3	320	17.578	0.11	0.43	133.7E-6	1.47	0.63	17648

Table C.6 12 mm orifice (camera)

Time	Time	Cumulative		Flow rate	Orifice Velocity	C _d	Re
[s]	[s]	[m]	[m]	[m ³ /s]	[m/s]		
0	0.0	0	0.37	0	0	0	0
5.44	5.44	0.01	0.36	245.5E-6	2.66	0.64	31945
6.68	12.1	0.02	0.35	242.2E-6	2.62	0.64	31498
6.64	18.8	0.03	0.34	238.9E-6	2.58	0.64	31045
6.20	25.0	0.04	0.33	235.8E-6	2.54	0.64	30585
6.96	31.9	0.05	0.32	232.4E-6	2.51	0.64	30118
7.64	39.6	0.06	0.31	228.6E-6	2.47	0.64	29644
6.72	46.3	0.07	0.30	225.3E-6	2.43	0.64	29162
7.48	53.8	0.08	0.29	221.6E-6	2.39	0.64	28672
7.36	61.1	0.09	0.28	217.9E-6	2.34	0.64	28173
7.64	68.8	0.10	0.27	214.1E-6	2.30	0.64	27665
7.32	76.1	0.11	0.26	210.5E-6	2.26	0.65	27148
7.64	83.7	0.12	0.25	206.7E-6	2.21	0.65	26621
8.00	91.7	0.13	0.24	202.8E-6	2.17	0.65	26083
7.92	99.6	0.14	0.23	198.9E-6	2.12	0.65	25534
8.12	107.8	0.15	0.22	194.8E-6	2.08	0.65	24973
8.24	116.0	0.16	0.21	190.8E-6	2.03	0.65	24399
8.44	124.4	0.17	0.20	186.6E-6	1.98	0.65	23811
8.80	133.2	0.18	0.19	182.2E-6	1.93	0.65	23208
8.60	141.8	0.19	0.18	178.0E-6	1.88	0.66	22589
8.72	150.6	0.20	0.17	173.7E-6	1.83	0.66	21952
9.60	160.2	0.21	0.16	168.9E-6	1.77	0.66	21297
9.20	169.4	0.22	0.15	164.4E-6	1.72	0.66	20621

D_h 16 mm orifice

WATER

Tank

Length and width= 0.4 m
Area= 0.16 m²

Orifice:

Breadth = 0.016 m
Length= 0.016 m
Area= 256.6E-6 m²
D_h= 0.016 m

Other Parameters

μ = 0.001 Pa.s
Density= 1000 kg/m³
g= 9.81 m/s²

Table C.7 16 mm orifice (250 kg load cell)

Time [s]	Diff.Time [s]	Mass in tank [kg]	Height [m]	Diff.Height [m]	Flow rate [m ³ /s]	Orifice		
						Velocity [m/s]	C _d	Re
2.075	0	84.296	0.53	0	0	0	0	0
14.58	12.5	78.181	0.49	0.038	479.1E-6	3.10	0.60	49602
27.08	25.0	72.327	0.45	0.075	460.8E-6	2.98	0.60	47709
39.58	37.5	66.673	0.42	0.11	442.5E-6	2.86	0.60	45807
52.08	50.0	61.255	0.38	0.14	424.2E-6	2.74	0.60	43906
64.58	62.5	56.071	0.35	0.18	405.9E-6	2.62	0.60	42007
77.08	75.0	51.107	0.32	0.21	387.5E-6	2.50	0.60	40105
89.58	87.5	46.379	0.29	0.24	369.2E-6	2.38	0.60	38204
102.1	100.0	41.866	0.26	0.27	350.9E-6	2.27	0.60	36298
114.6	112.5	37.602	0.24	0.29	332.6E-6	2.15	0.60	34400
127.1	125.0	33.545	0.21	0.32	314.3E-6	2.03	0.60	32491
139.6	137.5	29.734	0.19	0.34	296.0E-6	1.91	0.60	30590
152.1	150.0	26.147	0.16	0.36	277.6E-6	1.79	0.60	28686
164.6	162.5	22.804	0.14	0.38	259.3E-6	1.67	0.60	26789
177.1	175.0	19.672	0.12	0.40	241.0E-6	1.55	0.60	24881
189.6	187.5	16.771	0.10	0.42	222.7E-6	1.43	0.61	22973

Table C.8 16 mm orifice (100 kg load cell)

Time	Diff.Time	Mass in tank	Height	Diff.Height	Flow rate	Orifice Velocity	C _d	Re
[s]	[s]	[kg]	[m]	[m]	[m ³ /s]	[m/s]		
2.075	0	58.499	0.37	0	0	0	0	0
12.91	10.83	54.038	0.34	0.028	403.5E-6	2.57	0.61	41238
23.74	21.67	49.765	0.31	0.055	387.4E-6	2.47	0.61	39575
34.58	32.50	45.655	0.29	0.080	371.3E-6	2.37	0.61	37905
45.41	43.33	41.720	0.26	0.10	355.1E-6	2.26	0.61	36235
56.24	54.17	37.957	0.24	0.13	339.0E-6	2.16	0.61	34562
67.08	65.00	34.371	0.21	0.15	322.9E-6	2.05	0.61	32889
77.91	75.83	30.956	0.19	0.17	306.7E-6	1.95	0.61	31212
88.74	86.67	27.729	0.17	0.19	290.6E-6	1.84	0.61	29540
99.6	97.50	24.669	0.15	0.21	274.5E-6	1.74	0.61	27863
110.4	108.3	21.780	0.14	0.23	258.3E-6	1.63	0.62	26181
121.2	119.2	19.066	0.12	0.25	242.2E-6	1.53	0.62	24495
132.1	130.0	16.533	0.10	0.26	226.1E-6	1.42	0.62	22810
142.9	140.8	14.178	0.089	0.28	209.9E-6	1.32	0.62	21123

Table C.9 16 mm orifice (camera)

Cumulative								
Time	Time	Diff. Height	Height	Flow rate	Orifice Velocity	C _d	Re	
[s]	[s]	[m]	[m]	[m ³ /s]	[m/s]			
0.00	0.00	0.00	0.37	0	0	0	0	0
4.12	4.12	0.01	0.36	415.3E-6	2.66	0.61	42576	
3.88	8.00	0.02	0.35	409.4E-6	2.62	0.61	41980	
4.00	12.00	0.03	0.34	403.4E-6	2.58	0.61	41376	
3.76	15.76	0.04	0.33	397.8E-6	2.54	0.61	40763	
4.40	20.16	0.05	0.32	391.2E-6	2.51	0.61	40141	
4.12	24.28	0.06	0.31	385.0E-6	2.47	0.61	39509	
4.04	28.32	0.07	0.30	379.0E-6	2.43	0.61	38866	
4.40	32.72	0.08	0.29	372.4E-6	2.39	0.61	38213	
4.28	37.00	0.09	0.28	366.0E-6	2.34	0.61	37548	
4.36	41.36	0.10	0.27	359.4E-6	2.30	0.61	36872	
4.64	46.00	0.11	0.26	352.5E-6	2.26	0.61	36183	
4.52	50.52	0.12	0.25	345.7E-6	2.21	0.61	35480	
4.64	55.16	0.13	0.24	338.7E-6	2.17	0.61	34763	
4.56	59.72	0.14	0.23	331.9E-6	2.12	0.61	34031	
5.04	64.76	0.15	0.22	324.3E-6	2.08	0.61	33283	
4.92	69.68	0.16	0.21	317.0E-6	2.03	0.61	32518	
5.00	74.68	0.17	0.20	309.5E-6	1.98	0.61	31734	
5.20	79.88	0.18	0.19	301.7E-6	1.93	0.61	30931	
5.32	85.20	0.19	0.18	293.7E-6	1.88	0.61	30106	
5.44	90.64	0.20	0.17	285.5E-6	1.83	0.61	29257	
5.52	96.16	0.21	0.16	277.2E-6	1.77	0.61	28384	
6.60	102.8	0.22	0.15	267.3E-6	1.72	0.61	27483	
5.92	108.7	0.23	0.14	258.5E-6	1.66	0.61	26551	
6.52	115.2	0.24	0.13	248.7E-6	1.60	0.61	25585	
6.36	121.6	0.25	0.12	239.2E-6	1.53	0.61	24581	
6.72	128.3	0.26	0.11	229.1E-6	1.47	0.61	23535	
7.36	135.6	0.27	0.10	218.0E-6	1.40	0.61	22439	
7.52	143.2	0.28	0.09	206.8E-6	1.33	0.61	21288	
7.72	151	0.29	0.08	195.2E-6	1.25	0.61	20070	

D_h 20 mm orifice

WATER

Tank

Length and width= 0.4 m
Area= 0.16 m²

Orifice:

Breadth = 0.02 m
Length= 0.02 m
Area= 400.8E-6 m²
D_h= 0.02 m

Other parameters

μ = 0.001 Pa.s
Density= 1000 kg/m³
g= 9.81 m/s²

Table C.10 20 mm orifice (250 kg load cell)

Time [s]	Diff.Time [s]	Mass in tank [kg]	Height [m]	Diff.Height [m]	Flow rate [m ³ /s]	Orifice		
						Velocity [m/s]	C _d	Re
1.242	0.0	89.585	0.56	0	0	0	0	0
8.742	7.5	83.679	0.52	0.037	775.2E-6	3.20	0.60	64130
16.24	15.0	77.961	0.49	0.07	748.3E-6	3.09	0.60	61900
23.74	22.5	72.457	0.45	0.11	721.4E-6	2.98	0.60	59675
31.24	30.0	67.130	0.42	0.14	694.5E-6	2.87	0.60	57440
38.74	37.5	62.033	0.39	0.17	667.6E-6	2.76	0.60	55216
46.24	45.0	57.145	0.36	0.20	640.7E-6	2.65	0.60	52996
53.74	52.5	52.415	0.33	0.23	613.8E-6	2.54	0.60	50756
61.24	60.0	47.917	0.30	0.26	586.8E-6	2.42	0.60	48529
68.74	67.5	43.613	0.27	0.29	559.9E-6	2.31	0.60	46298
76.24	75.0	39.521	0.25	0.31	533.0E-6	2.20	0.60	44073
83.74	82.5	35.621	0.22	0.34	506.1E-6	2.09	0.60	41842
91.24	90.0	31.914	0.20	0.36	479.2E-6	1.98	0.60	39604
98.74	97.5	28.440	0.18	0.38	452.3E-6	1.87	0.60	37386
106.2	105.0	25.130	0.16	0.40	425.4E-6	1.76	0.60	35144
113.7	112.5	22.051	0.14	0.42	398.5E-6	1.64	0.60	32921
121.2	120.0	19.165	0.12	0.44	371.6E-6	1.53	0.60	30691

Table C.11 20 mm orifice (100 kg load cell)

Time	Diff.Time	Mass in tank	Height	Diff.Height	Flow rate	Orifice Velocity	C _d	Re
[s]	[s]	[kg]	[m]	[m]	[m ³ /s]	[m/s]		
0.825	0	64.337	0.40	0	0	0	0	0
7.492	6.667	59.836	0.37	0.028	663.1E-6	2.71	0.61	54230
14.16	13.33	55.492	0.35	0.055	638.8E-6	2.61	0.61	52224
20.83	20.00	51.339	0.32	0.081	614.5E-6	2.51	0.61	50232
27.49	26.67	47.312	0.30	0.11	590.3E-6	2.41	0.61	48221
34.16	33.33	43.462	0.27	0.13	566.0E-6	2.31	0.61	46218
40.83	40.00	39.773	0.25	0.15	541.7E-6	2.21	0.61	44213
47.49	46.67	36.234	0.23	0.18	517.4E-6	2.11	0.61	42200
54.16	53.33	32.857	0.21	0.20	493.1E-6	2.01	0.61	40185
60.83	60.00	29.644	0.19	0.22	468.9E-6	1.91	0.61	38170
67.49	66.67	26.601	0.17	0.24	444.6E-6	1.81	0.61	36158
74.16	73.33	23.716	0.15	0.25	420.3E-6	1.71	0.61	34141
80.83	80.00	20.994	0.13	0.27	396.0E-6	1.60	0.62	32122
87.49	86.67	18.437	0.12	0.29	371.8E-6	1.50	0.62	30103
94.16	93.33	16.035	0.10	0.30	347.5E-6	1.40	0.62	28073
100.8	100.0	13.808	0.086	0.32	323.2E-6	1.30	0.62	26050
107.5	106.7	11.746	0.073	0.33	298.9E-6	1.20	0.62	24027

Table C.12 20 mm orifice (camera)

Cumulative								
Time	Time	Diff. Height	Height	Flow rate	Orifice Velocity	C _d	Re	
[s]	[s]	[m]	[m]	[m ³ /s]	[m/s]			
0.00	0.0	0	0.37	0	0	0	0	0
2.04	2.04	0.01	0.36	649.4E-6	2.66	0.61	53207	
2.20	4.24	0.02	0.35	641.5E-6	2.62	0.61	52462	
2.48	6.72	0.03	0.34	632.7E-6	2.58	0.61	51707	
2.56	9.28	0.04	0.33	623.6E-6	2.54	0.61	50941	
3.00	12.3	0.05	0.32	612.9E-6	2.51	0.61	50164	
2.52	14.8	0.06	0.31	603.9E-6	2.47	0.61	49374	
2.56	17.4	0.07	0.3	594.8E-6	2.43	0.61	48571	
2.64	20.0	0.08	0.29	585.3E-6	2.39	0.61	47754	
2.96	23.0	0.09	0.28	574.8E-6	2.34	0.61	46924	
2.92	25.9	0.1	0.27	564.4E-6	2.30	0.61	46078	
2.64	28.5	0.11	0.26	555.0E-6	2.26	0.61	45217	
3.04	31.6	0.12	0.25	544.1E-6	2.21	0.61	44339	
2.64	34.2	0.13	0.24	534.7E-6	2.17	0.61	43443	
3.48	37.7	0.14	0.23	522.3E-6	2.12	0.61	42528	
3.00	40.7	0.15	0.22	511.6E-6	2.08	0.61	41593	
3.12	43.8	0.16	0.21	500.5E-6	2.03	0.62	40637	
3.32	47.1	0.17	0.2	488.7E-6	1.98	0.62	39658	
3.24	50.4	0.18	0.19	477.1E-6	1.93	0.62	38654	
3.32	53.7	0.19	0.18	465.3E-6	1.88	0.62	37623	
3.64	57.3	0.2	0.17	452.3E-6	1.83	0.62	36563	
3.24	60.6	0.21	0.16	440.8E-6	1.77	0.62	35471	
3.24	63.8	0.22	0.15	429.2E-6	1.72	0.62	34345	
4.28	68.1	0.23	0.14	413.9E-6	1.66	0.62	33180	
4.36	72.4	0.24	0.13	398.4E-6	1.60	0.62	31973	
4.16	76.6	0.25	0.12	383.6E-6	1.53	0.62	30719	
3.92	80.5	0.26	0.11	369.6E-6	1.47	0.63	29411	
4.36	84.9	0.27	0.1	354.1E-6	1.40	0.63	28042	
4.56	89.4	0.28	0.09	337.8E-6	1.33	0.63	26603	
5.00	94.4	0.29	0.08	320.0E-6	1.25	0.64	25082	

APPENDIX D: Triangular orifices calibration results (8 mm, 12 mm, 16 mm and 20 mm)

D_h 8 mm orifice

WATER

Tank

Length and width= 0.4 m
 Area= 0.16 m²

Orifice:

Breadth = 6.95E-3 m
 Length= 12.04E-3 m
 Area= 83.68E-6 m²
 h= 13.9E-3 m
 D_h= 0.008 m

Other parameters

μ = 0.001 Pa.s
 Density= 1000 kg/m³
 g= 9.81 m/s²

Table D.1 8 mm orifice (250 kg load cell)

Time [s]	Diff.Time [s]	Mass in tank [kg]	Height [m]	Diff.Height [m]	Flow rate [m ³ /s]	Orifice Velocity		
						C _d	Re	
6.658	0	84.295	0.53	0	0.00	0.00	0	
44.99	38.33	77.910	0.49	0.040	163.2E-6	3.09	0.63	24805
83.33	76.67	71.783	0.45	0.078	156.8E-6	2.97	0.63	23810
121.7	115.0	65.895	0.41	0.11	150.4E-6	2.84	0.63	22812
160.0	153.3	60.278	0.38	0.15	144.0E-6	2.72	0.63	21818
198.3	191.7	54.878	0.34	0.18	137.6E-6	2.59	0.63	20818
236.7	230.0	49.729	0.31	0.22	131.2E-6	2.47	0.63	19818
275.0	268.3	44.824	0.28	0.25	124.8E-6	2.34	0.64	18815
313.3	306.7	40.167	0.25	0.28	118.4E-6	2.22	0.64	17811
351.7	345.0	35.731	0.22	0.30	112.0E-6	2.09	0.64	16798
390.0	383.3	31.565	0.20	0.33	105.6E-6	1.97	0.64	15789
428.3	421.7	27.651	0.17	0.35	99.16E-6	1.84	0.64	14778
466.7	460.0	23.983	0.15	0.38	92.76E-6	1.71	0.65	13763
505.0	498.3	20.554	0.13	0.40	86.36E-6	1.59	0.65	12741
543.3	536.7	17.382	0.11	0.42	79.96E-6	1.46	0.65	11716

Table D.2 8 mm orifice (100 kg load cell)

Time [s]	Diff.Time [s]	Mass in tank [kg]	Height [m]	Diff.Height [m]	Orifice			C_d	Re
					Flow rate [m³/s]	Velocity [m/s]			
5	0	59.415	0.37	0	0	0	0	0	0
35	30	55.161	0.34	0.027	139.2E-6	2.60	0.64	20872	
65	60	51.067	0.32	0.052	134.0E-6	2.50	0.64	20082	
95	90	47.128	0.29	0.077	128.9E-6	2.40	0.64	19292	
125	120	43.337	0.27	0.10	123.7E-6	2.31	0.64	18500	
155	150	39.701	0.25	0.12	118.5E-6	2.21	0.64	17707	
185	180	36.219	0.23	0.14	113.4E-6	2.11	0.64	16913	
215	210	32.899	0.21	0.17	108.2E-6	2.01	0.64	16119	
245	240	29.728	0.19	0.19	103.1E-6	1.91	0.65	15322	
275	270	26.713	0.17	0.20	97.90E-6	1.81	0.65	14525	
305	300	23.854	0.15	0.22	92.74E-6	1.71	0.65	13725	
335	330	21.157	0.13	0.24	87.58E-6	1.61	0.65	12926	
365	360	18.606	0.12	0.26	82.42E-6	1.51	0.65	12122	
395	390	16.207	0.10	0.27	77.26E-6	1.41	0.65	11313	

Table D.3 8 mm orifice (camera)

Time [s]	Time [s]	Cumulative			Flow rate [m³/s]	Orifice Velocity [m/s]	C_d	Re
		Diff. Height [m]	Height [m]	[m³/s]				
0	0	0	0.37	000.0E+0	0	0	0	0
22.36	22.36	0.02	0.35	138.5E-6	2.62	0.63	21030	
22.96	45.32	0.04	0.33	134.8E-6	2.54	0.63	20420	
24.52	69.84	0.06	0.31	130.9E-6	2.47	0.63	19792	
24.68	94.52	0.08	0.29	126.9E-6	2.39	0.64	19143	
25.68	120.2	0.10	0.27	122.8E-6	2.30	0.64	18471	
25.76	146.0	0.12	0.25	118.7E-6	2.21	0.64	17774	
27.92	173.9	0.14	0.23	114.3E-6	2.12	0.64	17048	
28.80	202.7	0.16	0.21	109.7E-6	2.03	0.65	16290	
29.64	232.3	0.18	0.19	104.9E-6	1.93	0.65	15495	
31.16	263.5	0.20	0.17	99.93E-6	1.83	0.65	14656	
32.56	299.7	0.22	0.15	94.14E-6	1.72	0.66	13767	
36.24	332.3	0.24	0.13	88.94E-6	1.60	0.67	12817	
38.96	368.5	0.26	0.11	83.14E-6	1.47	0.68	11790	
41.96	407.5	0.28	0.09	76.92E-6	1.33	0.69	10664	

D_h 12 mm orifice

WATER

Tank:

Lenth and width=	0.4 m
Area=	0.16 m ²

Orifice:

Breadth =	0.0104 m
Length=	0.018 m
Area=	187.3E-6 m ²
h=	0.0208 m
D _h =	0.012 m

Other parameters

μ=	0.001 Pa.s
Density=	1000 kg/m ³
g=	9.81 m/s ²

Table D.4 12 mm orifice (250 kg load cell)

Time [s]	Diff.Time [s]	Mass in tank [kg]	Height [m]	Diff.Height [m]	Flow rate [m ³ /s]	Orifice Velocity		
						C _d	Re	
2.492	0	82.377	0.51	0	0	0	0	0
17.49	15	77.004	0.48	0.034	352.9E-6	3.07	0.61	36902
32.49	30	71.809	0.45	0.066	340.9E-6	2.97	0.61	35635
47.49	45	66.784	0.42	0.097	328.8E-6	2.86	0.61	34366
62.49	60	61.940	0.39	0.13	316.8E-6	2.76	0.61	33096
77.49	75	57.269	0.36	0.16	304.8E-6	2.65	0.61	31824
92.49	90	52.791	0.33	0.18	292.7E-6	2.54	0.61	30554
107.5	105	48.491	0.30	0.21	280.7E-6	2.44	0.61	29283
122.5	120	44.364	0.28	0.24	268.7E-6	2.33	0.61	28010
137.5	135	40.421	0.25	0.26	256.6E-6	2.23	0.62	26736
152.5	150	36.650	0.23	0.29	244.6E-6	2.12	0.62	25458
167.5	165	33.093	0.21	0.31	232.5E-6	2.01	0.62	24191
182.5	180	29.697	0.19	0.33	220.5E-6	1.91	0.62	22916
197.5	195	26.487	0.17	0.35	208.5E-6	1.80	0.62	21643
212.5	210	23.425	0.15	0.37	196.4E-6	1.69	0.62	20353
227.5	225	20.583	0.13	0.39	184.4E-6	1.59	0.62	19079
242.5	240	17.906	0.11	0.40	172.3E-6	1.48	0.62	17795

Table D.5 12 mm orifice (100 kg load cell)

Time	Diff.Time	Mass in tank	Height	Diff.Height	Flow rate	Orifice Velocity	C _d	Re
[s]	[s]	[kg]	[m]	[m]	[m ³ /s]	[m/s]		
2.075	0	59.665	0.37	0	0	0	0	0
14.58	12.5	55.789	0.35	0.024	305.7E-6	2.62	0.62	31410
27.08	25.0	52.031	0.33	0.048	295.4E-6	2.53	0.62	30334
39.58	37.5	48.413	0.30	0.070	285.1E-6	2.44	0.62	29260
52.08	50.0	44.909	0.28	0.092	274.8E-6	2.35	0.63	28181
64.58	62.5	41.539	0.26	0.11	264.5E-6	2.26	0.63	27103
77.08	75.0	38.300	0.24	0.13	254.2E-6	2.17	0.63	26025
89.58	87.5	35.175	0.22	0.15	243.9E-6	2.08	0.63	24941
102.1	100.0	32.198	0.20	0.17	233.6E-6	1.99	0.63	23862
114.6	112.5	29.339	0.18	0.19	223.3E-6	1.90	0.63	22778
127.1	125.0	26.621	0.17	0.21	213.0E-6	1.81	0.63	21697
139.6	137.5	24.021	0.15	0.22	202.7E-6	1.72	0.63	20610
152.1	150.0	21.551	0.13	0.24	192.4E-6	1.63	0.63	19522
164.6	162.5	19.213	0.12	0.25	182.1E-6	1.53	0.63	18433

Table D.6 12 mm orifice (camera)

Cumulative								
Time	Time	Diff. Height	Height	Flow rate	Orifice Velocity	C _d	Re	
[s]	[s]	[m]	[m]	[m ³ /s]	[m/s]			
0	0	0	0.37	0	0	0	0	0
9.32	9.32	0.02	0.35	301.4E-6	2.62	0.61	31469	
10.96	20.28	0.04	0.33	293.2E-6	2.54	0.62	30557	
11.12	31.40	0.06	0.31	285.0E-6	2.47	0.62	29616	
11.36	42.76	0.08	0.29	276.5E-6	2.39	0.62	28645	
11.64	54.40	0.10	0.27	267.9E-6	2.30	0.62	27640	
12.24	66.64	0.12	0.25	258.8E-6	2.21	0.62	26596	
12.72	79.36	0.14	0.23	249.3E-6	2.12	0.63	25510	
13.08	92.4	0.16	0.21	239.6E-6	2.03	0.63	24376	
13.52	106.0	0.18	0.19	229.5E-6	1.93	0.63	23186	
14.40	120.4	0.20	0.17	218.8E-6	1.83	0.64	21932	
15.12	136.7	0.22	0.15	206.6E-6	1.72	0.64	20601	
16.36	151.8	0.24	0.13	195.4E-6	1.60	0.65	19179	

D_h 16 mm orifice

WATER

Tank

Length and width= 0.4 m
Area= 0.16 m²

Orifice:

Breadth = 0.0136 m
Length= 0.0236 m
Area= 320.96E-6 m²
h= 0.0272 m
D_h= 0.016 m

Other parameters

μ = 0.001 Pa.s
Density= 1000 kg/m³
g= 9.81 m/s²

Table D.7 16 mm orifice (250 kg load cell)

Time [s]	Diff.Time	Mass in tank [kg]	Height [m]	Diff.Height [m]	Flow rate [m ³ /s]	Orifice		
						Velocity [m/s]	C _d	Re
1.658	0	79.863	0.50	0	0	0	0	0
11.66	10	73.810	0.46	0.038	588.3E-6	3.01	0.61	47245
21.66	20	68.009	0.43	0.074	564.6E-6	2.89	0.61	45350
31.66	30	62.465	0.39	0.11	541.0E-6	2.77	0.61	43463
41.66	40	57.147	0.36	0.14	517.4E-6	2.65	0.61	41571
51.66	50	52.041	0.33	0.17	493.7E-6	2.53	0.61	39671
61.66	60	47.170	0.29	0.20	470.1E-6	2.41	0.61	37769
71.66	70	42.544	0.27	0.23	446.4E-6	2.28	0.61	35869
81.66	80	38.152	0.24	0.26	422.8E-6	2.16	0.61	33967
91.66	90	34.002	0.21	0.29	399.1E-6	2.04	0.61	32067
101.7	100	30.100	0.19	0.31	375.5E-6	1.92	0.61	30171
111.7	110	26.416	0.17	0.33	351.9E-6	1.80	0.61	28264
121.7	120	22.992	0.14	0.36	328.2E-6	1.68	0.61	26368
131.7	130	19.796	0.12	0.38	304.6E-6	1.56	0.61	24468
141.7	140	16.819	0.11	0.39	280.9E-6	1.44	0.61	22553

Table D.8 16 mm orifice (100 kg load cell)

Time [s]	Diff.Time [s]	Mass in tank [kg]	Height [m]	Diff.Height [m]	Flow rate [m ³ /s]	Orifice Velocity [m/s]	C _d	Re
1.242	0	59.570	0.37	0	0	0	0	0
8.742	7.5	55.614	0.35	0.025	519.9E-6	2.61	0.62	41010
16.24	15.0	51.776	0.32	0.049	501.9E-6	2.52	0.62	39570
23.74	22.5	48.097	0.30	0.072	483.8E-6	2.43	0.62	38138
31.24	30.0	44.521	0.28	0.094	465.8E-6	2.34	0.62	36693
38.74	37.5	41.106	0.26	0.12	447.8E-6	2.25	0.62	35257
46.24	45.0	37.809	0.24	0.14	429.7E-6	2.15	0.62	33814
53.74	52.5	34.659	0.22	0.16	411.7E-6	2.06	0.62	32375
61.24	60.0	31.633	0.20	0.17	393.7E-6	1.97	0.62	30929
68.74	67.5	28.740	0.18	0.19	375.6E-6	1.88	0.62	29481
76.24	75.0	25.989	0.16	0.21	357.6E-6	1.79	0.62	28034
83.74	82.5	23.375	0.15	0.23	339.6E-6	1.69	0.62	26587
91.24	90.0	20.895	0.13	0.24	321.5E-6	1.60	0.63	25138
98.74	97.5	18.555	0.12	0.26	303.5E-6	1.51	0.63	23688
106.2	105.0	16.345	0.10	0.27	285.5E-6	1.42	0.63	22232

Table D.9 16 mm orifice (camera)

Cumulative								
Time [s]	Time [s]	Diff. Height [m]	Height [m]	Flow rate [m ³ /s]	Orifice Velocity [m/s]	C _d	Re	
0	0	0	0.37	0	0	0	0	0
5.52	5.52	0.02	0.35	510.6E-6	2.62	0.61	41152	
5.80	11.3	0.04	0.33	498.2E-6	2.54	0.61	39959	
6.48	17.8	0.06	0.31	484.4E-6	2.47	0.61	38729	
7.56	25.4	0.08	0.29	468.3E-6	2.39	0.61	37459	
6.56	31.9	0.10	0.27	454.3E-6	2.30	0.61	36144	
7.12	39.0	0.12	0.25	439.1E-6	2.21	0.62	34780	
7.56	46.6	0.14	0.23	423.0E-6	2.12	0.62	33360	
7.36	54.0	0.16	0.21	407.3E-6	2.03	0.63	31876	
8.24	62.2	0.18	0.19	389.7E-6	1.93	0.63	30320	
8.88	71.1	0.20	0.17	370.8E-6	1.83	0.63	28680	
8.44	80.7	0.22	0.15	350.2E-6	1.72	0.64	26940	
9.64	89.2	0.24	0.13	332.2E-6	1.60	0.65	25080	

D_h 20 mm orifice

WATER

Tank:

Length and width= 0.4 m
Area= 0.16 m²

Orifice:

Breadth = 0.0173 m
Length= 0.03 m
Area= 518.3E-6 m²
h= 0.0346 m
D_h= 0.02 m

Other parameters

μ = 0.001 Pa.s
Density= 1000 kg/m³
g= 9.81 m/s²

Table D.10 20 mm orifice (250 kg load cell)

Time [s]	Diff.Time [s]	Mass in tank [kg]	Height [m]	Diff.Height [m]	Flow rate [m ³ /s]	Orifice Velocity		
						C _d	Re	
0.825	0	85.118	0.53	0	0	0	0	0
5.825	5	80.103	0.50	0.031	992.9E-6	3.13	0.61	62608
10.83	10	75.190	0.47	0.062	962.2E-6	3.04	0.61	60657
15.83	15	70.459	0.44	0.092	931.5E-6	2.94	0.61	58718
20.83	20	65.868	0.41	0.12	900.7E-6	2.84	0.61	56773
25.83	25	61.453	0.38	0.15	870.0E-6	2.75	0.61	54837
30.83	30	57.190	0.36	0.17	839.3E-6	2.65	0.61	52901
35.83	35	53.054	0.33	0.20	808.5E-6	2.55	0.61	50952
40.83	40	49.096	0.31	0.23	777.8E-6	2.45	0.61	49015
45.83	45	45.289	0.28	0.25	747.1E-6	2.36	0.61	47076
50.83	50	41.622	0.26	0.27	716.3E-6	2.26	0.61	45130
55.83	55	38.117	0.24	0.29	685.6E-6	2.16	0.61	43188
60.83	60	34.753	0.22	0.31	654.8E-6	2.06	0.61	41238
65.83	65	31.577	0.20	0.33	624.1E-6	1.97	0.61	39309
70.83	70	28.523	0.18	0.35	593.4E-6	1.87	0.61	37360
75.83	75	25.628	0.16	0.37	562.6E-6	1.77	0.61	35413
80.83	80	22.890	0.14	0.39	531.9E-6	1.68	0.61	33468
85.83	85	20.312	0.13	0.41	501.2E-6	1.58	0.61	31527
90.83	90	17.887	0.11	0.42	470.4E-6	1.48	0.61	29585

Table D.11 20 mm orifice (100 kg load cell)

Time	Diff.Time	Mass in tank	Height	Diff.Height	Flow rate	Orifice Velocity	C _d	Re
[s]	[s]	[kg]	[m]	[m]	[m ³ /s]	[m/s]		
0.825	0	58.383	0.36	0	0	0.00	0.00	0
5.825	5	54.164	0.34	0.026	827.0E-6	2.58	0.62	51483
10.83	10	50.121	0.31	0.052	795.8E-6	2.48	0.62	49524
15.83	15	46.216	0.29	0.076	764.6E-6	2.38	0.62	47556
20.83	20	42.476	0.27	0.099	733.4E-6	2.28	0.62	45591
25.83	25	38.880	0.24	0.12	702.2E-6	2.18	0.62	43618
30.83	30	35.454	0.22	0.14	670.9E-6	2.09	0.62	41652
35.83	35	32.170	0.20	0.16	639.7E-6	1.99	0.62	39677
40.83	40	29.044	0.18	0.18	608.5E-6	1.89	0.62	37699
45.83	45	26.073	0.16	0.20	577.3E-6	1.79	0.62	35719
50.83	50	23.277	0.15	0.22	546.1E-6	1.69	0.62	33749
55.83	55	20.616	0.13	0.24	514.9E-6	1.59	0.62	31762
60.83	60	18.127	0.11	0.25	483.6E-6	1.49	0.63	29783
65.83	65	15.788	0.099	0.27	452.4E-6	1.39	0.63	27796
70.83	70	13.602	0.085	0.28	421.2E-6	1.29	0.63	25799
75.83	75	11.576	0.072	0.29	390.0E-6	1.19	0.63	23800

Table D.12 20 mm orifice (camera)

Time	Cumulative					Orifice Velocity	C _d	Re
	Time	Diff. Height	Height	Flow rate				
[s]	[s]	[m]	[m]	[m ³ /s]	[m/s]			
0	0	0	0.37	0	0	0	0	0
4.04	4.04	0.02	0.35	813.4E-6	2.62	0.60	52348	
4.04	8.08	0.04	0.33	791.8E-6	2.54	0.60	50830	
4.12	12.20	0.06	0.31	769.9E-6	2.47	0.60	49266	
4.48	16.68	0.08	0.29	746.0E-6	2.39	0.60	47650	
4.04	20.72	0.10	0.27	724.5E-6	2.30	0.61	45978	
4.12	24.84	0.12	0.25	702.5E-6	2.21	0.61	44242	
5.00	29.84	0.14	0.23	675.9E-6	2.12	0.61	42435	
4.64	34.48	0.16	0.21	651.2E-6	2.03	0.62	40548	
5.04	39.52	0.18	0.19	624.3E-6	1.93	0.62	38569	
5.20	44.72	0.2	0.17	596.6E-6	1.83	0.63	36483	
5.52	50.84	0.22	0.15	564.0E-6	1.72	0.63	34270	
6.12	56.36	0.24	0.13	534.6E-6	1.60	0.65	31903	
6.36	62.48	0.26	0.11	502.0E-6	1.47	0.66	29347	
7.16	68.84	0.28	0.09	468.1E-6	1.33	0.68	26545	

APPENDIX E: Water tests results (Q vs h)

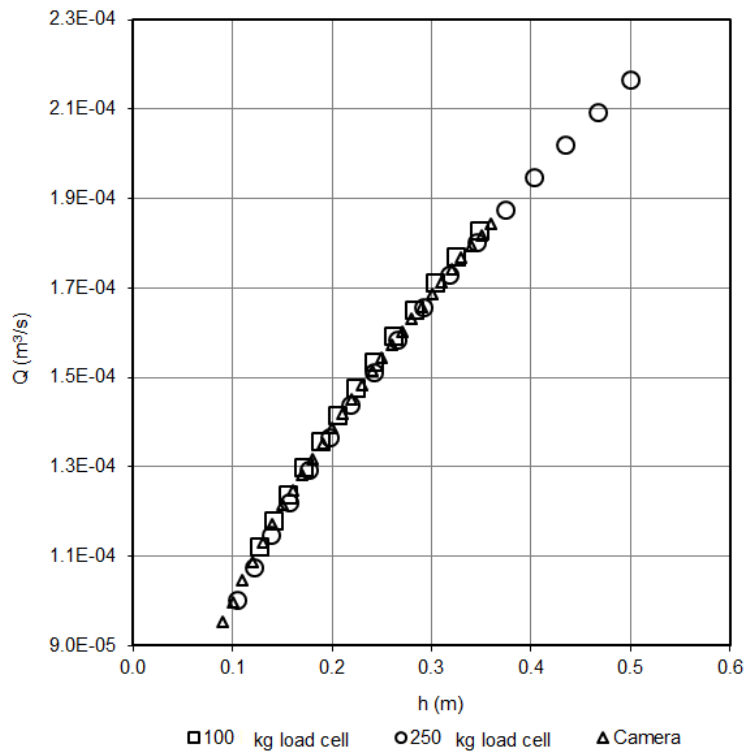


Figure E.1 Flow rate (m^3/s) versus head (m) for 12 mm hydraulic diameter for circular orifice

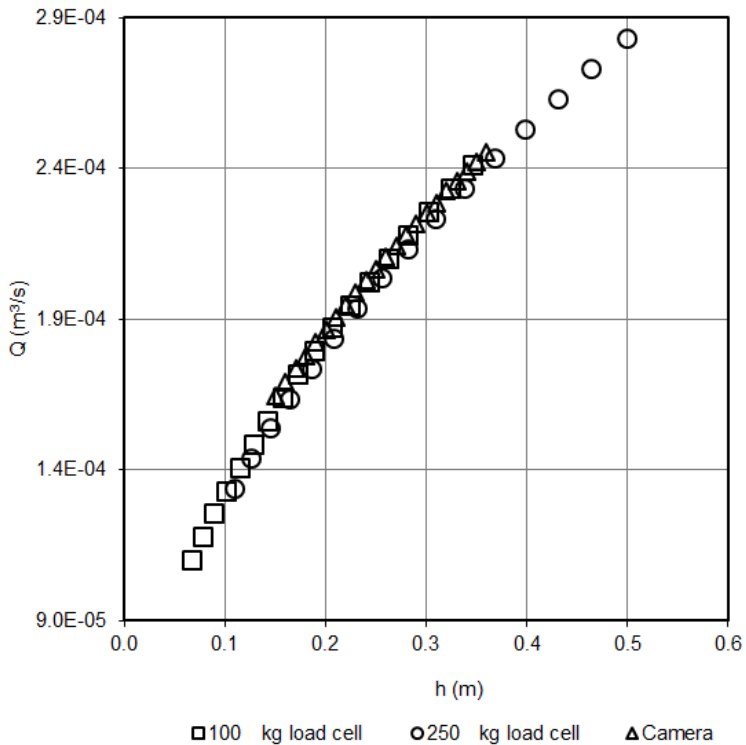


Figure E.2 Flow rate (m^3/s) versus head (m) for 12 mm hydraulic diameter for square orifice

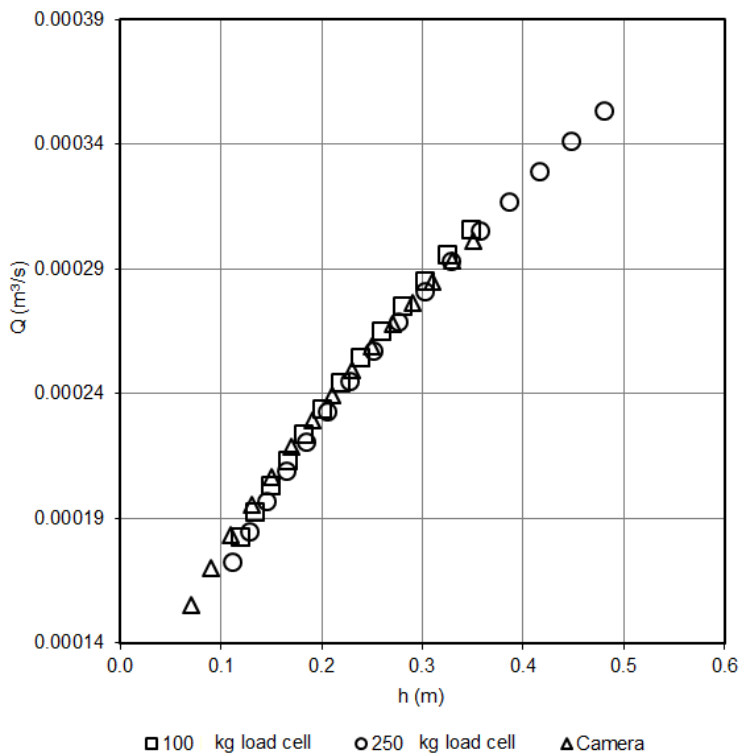


Figure E.3 Flow rate (m^3/s) versus head (m) for 12 mm hydraulic diameter for triangular orifice

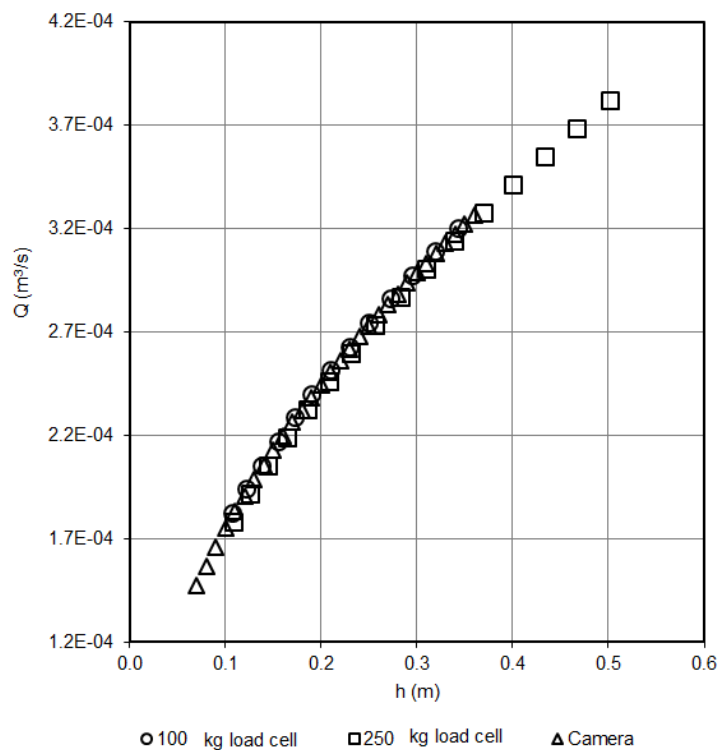


Figure E.4 Flow rate (m^3/s) versus head (m) for 16 mm hydraulic diameter for circular orifice

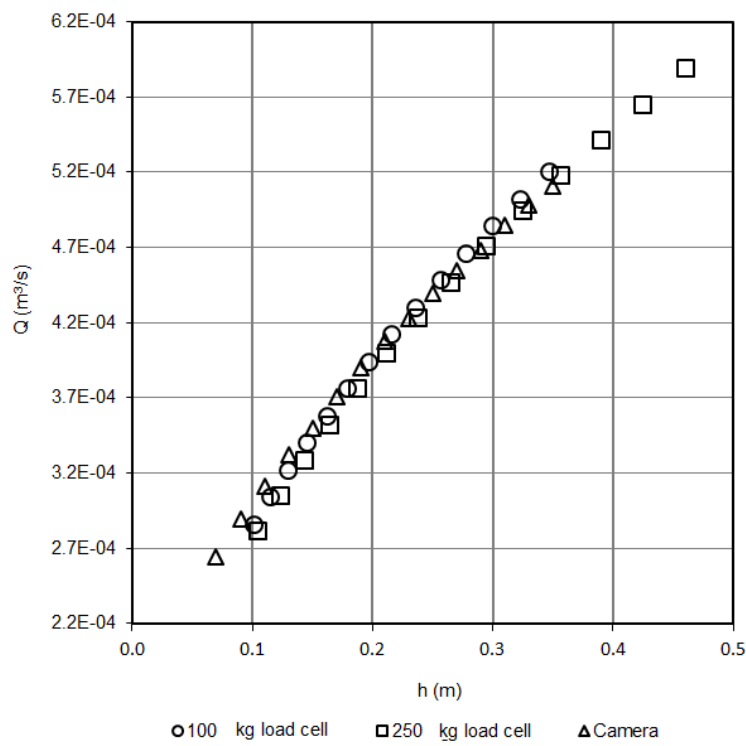


Figure E.5 Flow rate (m^3/s) versus head (m) for 16 mm hydraulic diameter for square orifice

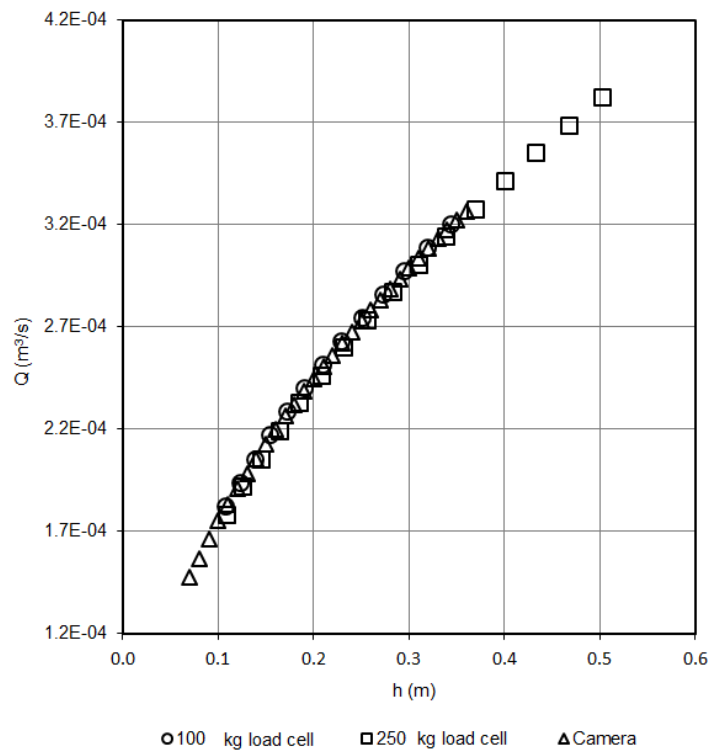


Figure E.6 Flow rate (m^3/s) versus head (m) for 16 mm hydraulic diameter for triangular orifice

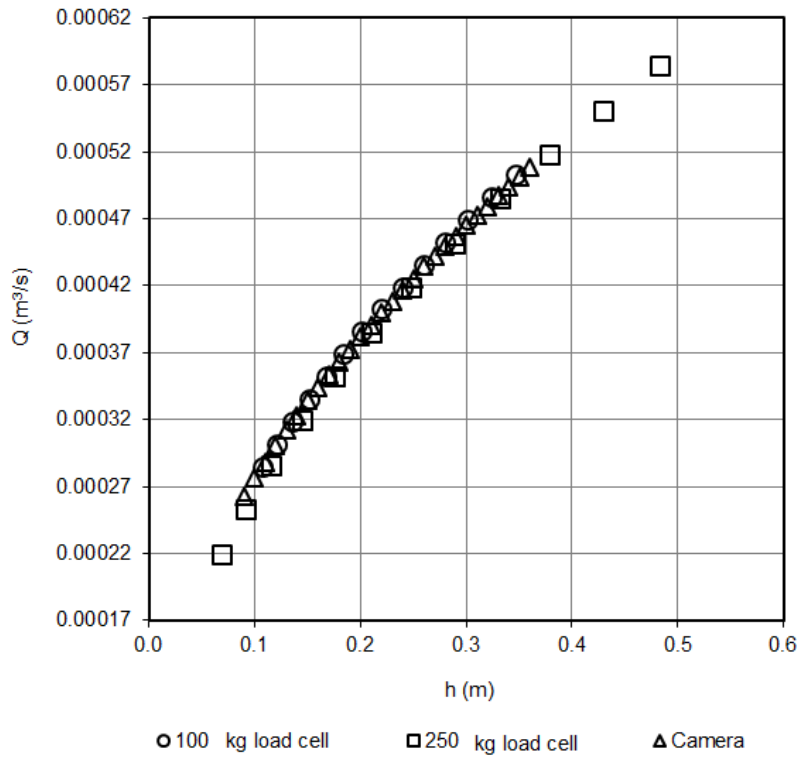


Figure E.7 Flow rate (m^3/s) versus head (m) for 20 mm hydraulic diameter for circular orifice

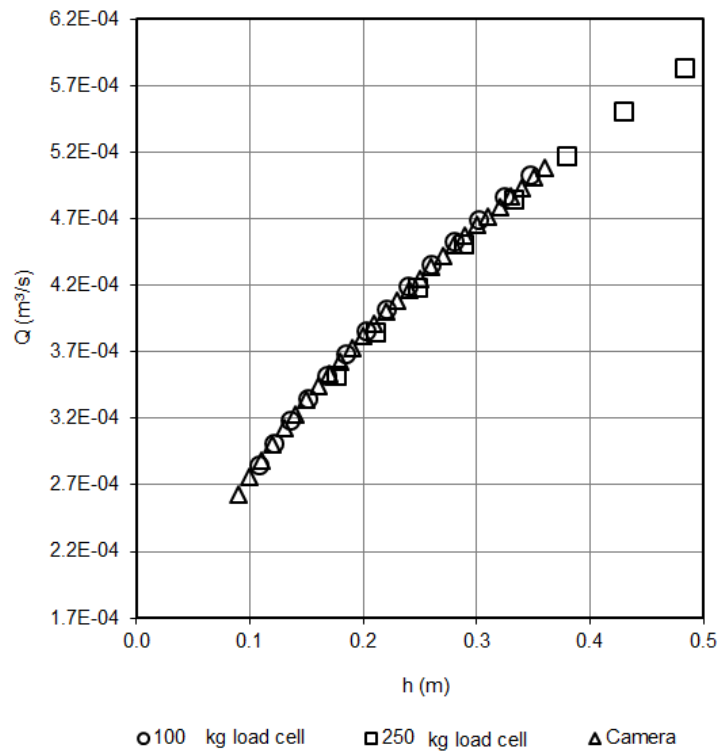


Figure E.8 Flow rate (m^3/s) versus head (m) for 20 mm hydraulic diameter for square orifice

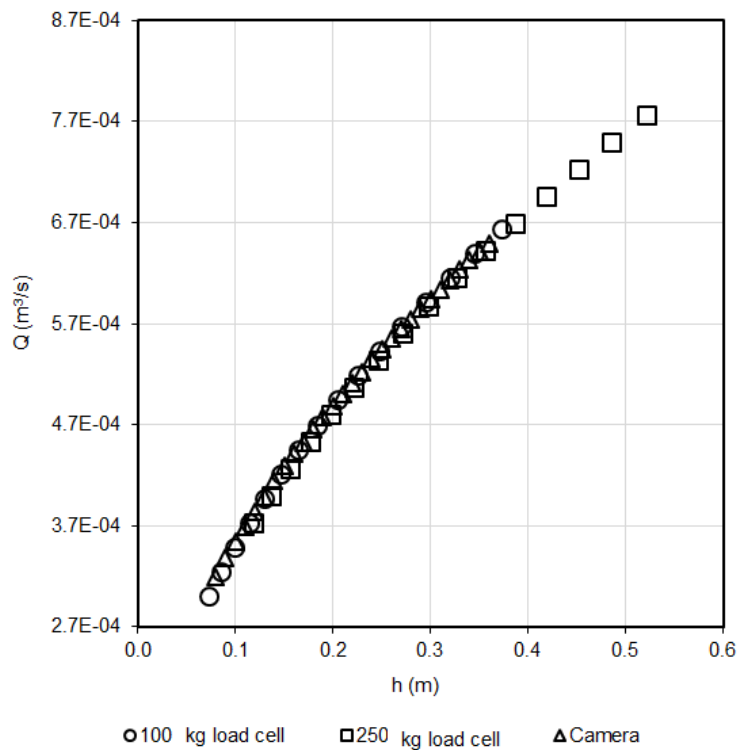


Figure E.9 Flow rate (m^3/s) versus head (m) for 20 mm hydraulic diameter for triangular orifice

APPENDIX F: Water results standard deviation for 12 mm, 16 mm and 20 mm hydraulic diameter orifices

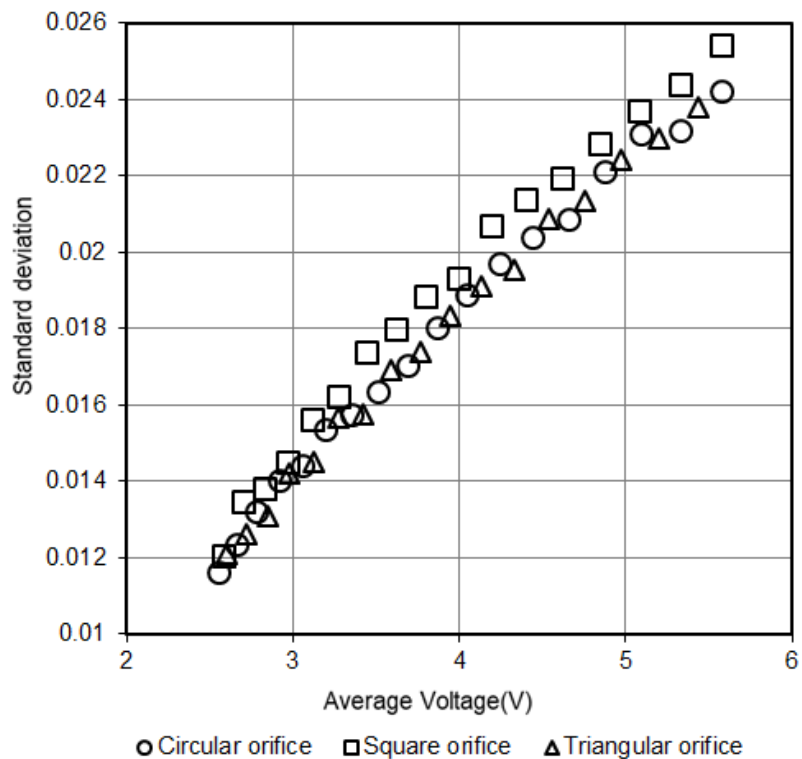


Figure F.1 Standard deviation versus average voltage (V) for 12 mm hydraulic diameter orifice

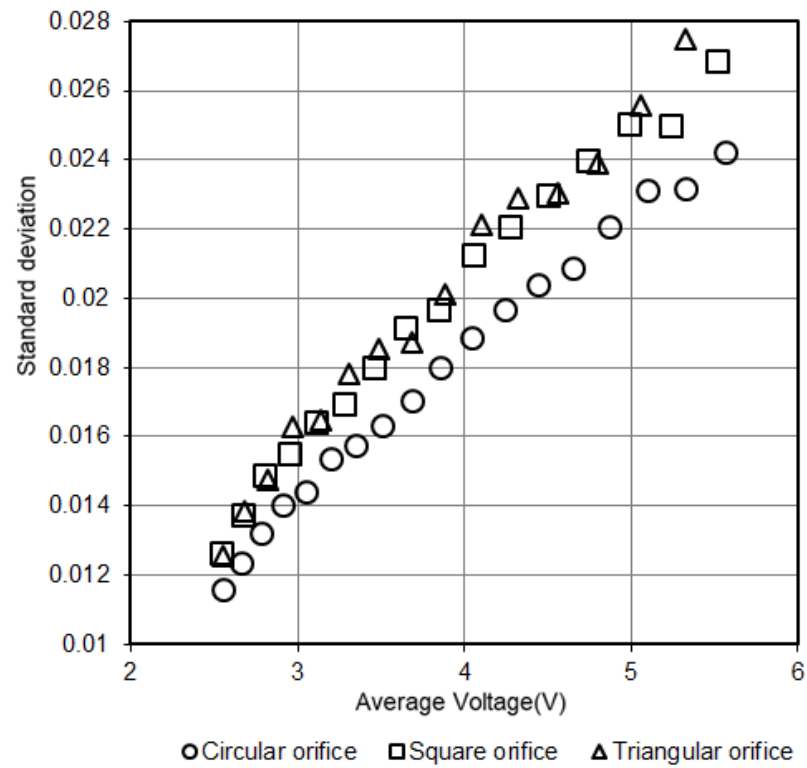


Figure F.2 Standard deviation versus average voltage (V) for 16 mm hydraulic diameter orifice

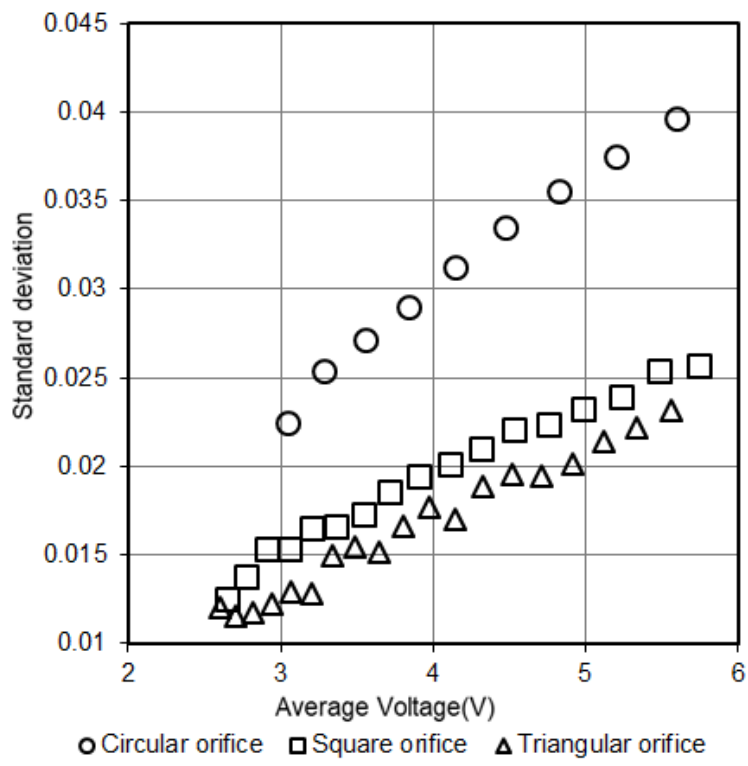


Figure F.3 Standard deviation versus average voltage (V) for 20 mm hydraulic diameter orifice

APPENDIX G: 100% glycerine solution

D_h 8 mm orifices

$$\begin{aligned}\mu &= 0.973 \text{ Pa.s} \\ \text{Density} &= 1258 \text{ kg/m}^3 \\ g &= 9.81 \text{ m/s}^2\end{aligned}$$

Circular orifices

Table G.1 8 mm circular orifice results (100% glycerine)

Time [s]	Diff.time [s]	Mass in tank [kg]	Height [m]	Diff.Height [m]	Flow rate [m ³ /s]	Orifice		
						Velocity [m/s]	C _d	Re
8.325	0	36.484	0.23	0	0.00	0.00	0.00	0
58.33	50	34.140	0.21	0.015	44.02E-6	2.05	0.42	21
108.3	100	31.919	0.20	0.029	42.14E-6	1.98	0.42	21
158.3	150	29.826	0.19	0.042	40.26E-6	1.91	0.41	20
208.3	200	27.850	0.17	0.054	38.38E-6	1.85	0.41	19
258.3	250	25.982	0.16	0.066	36.50E-6	1.78	0.40	19
308.3	300	24.229	0.15	0.077	34.61E-6	1.72	0.40	18
358.3	350	22.567	0.14	0.087	32.73E-6	1.66	0.39	17
408.3	400	21.006	0.13	0.097	30.85E-6	1.60	0.38	17
458.3	450	19.543	0.12	0.11	28.97E-6	1.55	0.37	16
508.3	500	18.163	0.11	0.11	27.09E-6	1.49	0.36	16
558.3	550	16.867	0.11	0.12	25.21E-6	1.44	0.35	15
608.3	600	15.664	0.098	0.13	23.32E-6	1.39	0.33	14
658.3	650	14.526	0.091	0.14	21.44E-6	1.33	0.32	14
708.3	700	13.467	0.084	0.14	19.56E-6	1.29	0.30	13
758.3	750	12.476	0.078	0.15	17.68E-6	1.24	0.28	13
808.3	800	11.554	0.072	0.16	15.80E-6	1.19	0.26	12

Table G.2 12 mm circular orifice results (100% glycerine)

Time [s]	Diff.Time [s]	Mass in tank [kg]	Height [m]	Diff.Height [m]	Flow rate [m ³ /s]	Orifice		
						Velocity [m/s]	C _d	Re
2.492	0.00	36.780	0.18	0.00				
17.49	15	34.754	0.17	0.010	104.3E-6	1.84	0.50	29
32.49	30	32.781	0.16	0.020	100.7E-6	1.79	0.49	28
47.49	45	30.906	0.15	0.029	97.05E-6	1.74	0.49	27
62.49	60	29.103	0.14	0.038	93.45E-6	1.68	0.49	26
77.49	75	27.369	0.14	0.047	89.85E-6	1.63	0.48	25
92.49	90	25.708	0.13	0.055	86.25E-6	1.58	0.48	25
107.5	105	24.123	0.12	0.063	82.65E-6	1.53	0.47	24
122.5	120	22.614	0.11	0.070	79.04E-6	1.48	0.47	23
137.5	135	21.159	0.11	0.078	75.44E-6	1.44	0.46	22
152.5	150	19.796	0.098	0.084	71.84E-6	1.39	0.45	22
167.5	165	18.479	0.092	0.091	68.24E-6	1.34	0.45	21
182.5	180	17.227	0.086	0.097	64.64E-6	1.30	0.44	20
197.5	195	16.054	0.080	0.103	61.04E-6	1.25	0.43	19
212.5	210	14.929	0.074	0.109	57.44E-6	1.21	0.42	19
227.5	225	13.867	0.069	0.114	53.83E-6	1.16	0.41	18
242.5	240	12.875	0.064	0.119	50.23E-6	1.12	0.39	17
257.5	255	11.935	0.059	0.123	46.63E-6	1.08	0.38	17
272.5	270	11.053	0.055	0.128	43.03E-6	1.04	0.36	16

Table G.3 16 mm circular orifice results (100% glycerine)

Time	Diff.Time	Mass in tank	Height	Diff.Height	Flow rate	Orifice Velocity	C _d	Re
[s]	[s]	[kg]	[m]	[m]	[m ³ /s]	[m/s]		
1.658	0	36.736	0.18	0	0	0.00	0.00	0
11.66	10	34.105	0.17	0.013	201.1E-6	1.82	0.55	38
21.66	20	31.602	0.16	0.026	192.4E-6	1.76	0.54	36
31.66	30	29.223	0.15	0.037	183.8E-6	1.69	0.54	35
41.66	40	26.954	0.13	0.049	175.1E-6	1.62	0.53	34
51.66	50	24.814	0.12	0.059	166.4E-6	1.56	0.53	32
61.66	60	22.786	0.11	0.069	157.8E-6	1.49	0.52	31
71.66	70	20.862	0.10	0.079	149.1E-6	1.43	0.52	30
81.66	80	19.068	0.095	0.088	140.5E-6	1.36	0.51	28
91.66	90	17.369	0.086	0.096	131.8E-6	1.30	0.50	27
101.7	100	15.770	0.078	0.104	123.1E-6	1.24	0.49	26
111.7	110	14.282	0.071	0.112	114.5E-6	1.18	0.48	24
121.7	120	12.894	0.064	0.118	105.8E-6	1.12	0.47	23
131.7	130	11.607	0.058	0.125	97.15E-6	1.06	0.45	22
141.7	140	10.406	0.052	0.131	88.49E-6	1.01	0.43	21
151.7	150	9.294	0.046	0.136	79.82E-6	0.95	0.42	20

Table G.4 20 mm circular orifice results (100% glycerine)

Time	Diff.Time	Mass in tank	Height	Diff.Height	Flow rate	Orifice Velocity	C _d	Re
[s]	[s]	[kg]	[m]	[m]	[m ³ /s]	[m/s]		
0.825	0	36.545	0.182	0	0	0.00	0.00	0
5.825	5	34.415	0.171	0.011	332.0E-6	1.83	0.57	47
10.83	10	32.323	0.161	0.021	320.6E-6	1.78	0.57	46
15.83	15	30.320	0.151	0.031	309.2E-6	1.72	0.57	45
20.83	20	28.391	0.141	0.041	297.8E-6	1.66	0.57	43
25.83	25	26.546	0.132	0.050	286.4E-6	1.61	0.56	42
30.83	30	24.774	0.123	0.058	275.0E-6	1.55	0.56	40
35.83	35	23.077	0.115	0.067	263.6E-6	1.50	0.56	39
40.83	40	21.445	0.107	0.075	252.2E-6	1.45	0.55	37
45.83	45	19.880	0.099	0.083	240.8E-6	1.39	0.55	36
50.83	50	18.388	0.091	0.090	229.4E-6	1.34	0.54	35
55.83	55	16.991	0.084	0.097	218.0E-6	1.29	0.54	33
60.83	60	15.641	0.078	0.104	206.6E-6	1.23	0.53	32
65.83	65	14.375	0.071	0.110	195.2E-6	1.18	0.52	31
70.83	70	13.169	0.065	0.116	183.8E-6	1.13	0.51	29
75.83	75	12.034	0.060	0.122	172.4E-6	1.08	0.50	28
80.83	80	10.974	0.055	0.127	161.0E-6	1.03	0.49	27
85.83	85	9.965	0.050	0.132	149.6E-6	0.99	0.48	26
90.83	90	9.014	0.045	0.137	138.2E-6	0.94	0.47	24

Square orifices

Table G.5 8 mm square orifice results (100% glycerine)

Time	Diff.Time	Mass in tank	Height	Diff.Height	Flow rate	Orifice Velocity	C _d	Re
[s]	[s]	[kg]	[m]	[m]	[m ³ /s]	[m/s]		
4.992	0	35.311	0.175	0				
34.99	30	33.265	0.165	0.010	52.86E-6	1.80	0.46	19
64.99	60	31.275	0.155	0.020	50.86E-6	1.75	0.45	18
94.99	90	29.378	0.146	0.029	48.87E-6	1.69	0.45	18
125	120	27.560	0.137	0.039	46.88E-6	1.64	0.44	17
155	150	25.824	0.128	0.047	44.89E-6	1.59	0.44	16
185	180	24.169	0.120	0.055	42.90E-6	1.53	0.43	16
215	210	22.610	0.112	0.063	40.90E-6	1.48	0.43	15
245	240	21.116	0.105	0.071	38.91E-6	1.43	0.42	15
275	270	19.701	0.098	0.078	36.92E-6	1.39	0.41	14
305	300	18.357	0.091	0.084	34.93E-6	1.34	0.41	14
335	330	17.084	0.085	0.091	32.94E-6	1.29	0.40	13
365	360	15.880	0.079	0.097	30.94E-6	1.24	0.39	13
395	390	14.742	0.073	0.102	28.95E-6	1.20	0.38	12
425	420	13.676	0.068	0.107	26.96E-6	1.15	0.36	12
455	450	12.662	0.063	0.113	24.97E-6	1.11	0.35	12
485	480	11.723	0.058	0.117	22.98E-6	1.07	0.33	11

Table G.6 12 mm square orifice results (100% glycerine)

Time	Diff.Time	Mass in tank	Height	Diff.Height	Flow rate	Orifice Velocity	C _d	Re
[s]	[s]	[kg]	[m]	[m]	[m ³ /s]	[m/s]		
1.658	0	35.3	0.175	0	0	0	0	0
11.66	10	33.5	0.166	0.009	143.8E-6	1.81	0.55	28
21.66	20	31.7	0.157	0.018	139.3E-6	1.76	0.55	27
31.66	30	29.9	0.149	0.027	134.8E-6	1.71	0.55	27
41.66	40	28.3	0.140	0.035	130.2E-6	1.66	0.54	26
51.66	50	26.7	0.132	0.043	125.7E-6	1.61	0.54	25
61.66	60	25.1	0.125	0.051	121.2E-6	1.56	0.54	24
71.66	70	23.6	0.117	0.058	116.7E-6	1.52	0.53	24
81.66	80	22.2	0.110	0.065	112.1E-6	1.47	0.53	23
91.66	90	20.8	0.103	0.072	107.6E-6	1.42	0.52	22
101.7	100	19.5	0.097	0.079	103.1E-6	1.38	0.52	21
111.7	110	18.2	0.091	0.085	98.56E-6	1.33	0.51	21
121.7	120	17.0	0.085	0.091	94.04E-6	1.29	0.51	20
131.7	130	15.9	0.079	0.097	89.51E-6	1.24	0.50	19
141.7	140	14.8	0.073	0.102	84.99E-6	1.20	0.49	19
151.7	150	13.7	0.068	0.107	80.46E-6	1.16	0.48	18
161.7	160	12.7	0.063	0.112	75.94E-6	1.11	0.47	17
171.7	170	11.8	0.059	0.117	71.41E-6	1.07	0.46	17
181.7	180	10.9	0.054	0.121	66.89E-6	1.03	0.45	16

Table G.7 16 mm square orifice results (100% glycerine)

Time [s]	Diff.Height [s]	Mass in tank [kg]	Height [m]	Diff.Height [m]	Flow rate [m ³ /s]	Orifice Velocity		
						C _d	Re	
0.825	0	34.9	0.173	0	0	0	0	0
5.825	5	33.2	0.165	0.009	268.5E-6	1.80	0.58	37
10.83	10	31.5	0.157	0.017	260.9E-6	1.75	0.58	36
15.83	15	29.9	0.149	0.025	253.3E-6	1.71	0.58	35
20.83	20	28.3	0.141	0.033	245.6E-6	1.66	0.58	34
25.83	25	26.8	0.133	0.040	238.0E-6	1.62	0.57	33
30.83	30	25.3	0.126	0.048	230.3E-6	1.57	0.57	33
35.83	35	23.9	0.119	0.055	222.7E-6	1.53	0.57	32
40.83	40	22.5	0.112	0.061	215.1E-6	1.48	0.57	31
45.83	45	21.2	0.105	0.068	207.4E-6	1.44	0.56	30
50.83	50	19.9	0.099	0.074	199.8E-6	1.39	0.56	29
55.83	55	18.7	0.093	0.081	192.2E-6	1.35	0.55	28
60.83	60	17.5	0.087	0.086	184.5E-6	1.31	0.55	27
65.83	65	16.4	0.081	0.092	176.9E-6	1.26	0.55	26
70.83	70	15.3	0.076	0.097	169.3E-6	1.22	0.54	25
75.83	75	14.2	0.071	0.103	161.6E-6	1.18	0.53	24
80.83	80	13.2	0.066	0.108	154.0E-6	1.14	0.53	24
85.83	85	12.3	0.061	0.112	146.4E-6	1.09	0.52	23
90.83	90	11.4	0.057	0.117	138.7E-6	1.05	0.51	22
95.83	95	10.5	0.052	0.121	131.1E-6	1.01	0.50	21

Table G.8 20 mm square orifice results (100% glycerine)

Time [s]	Diff.Time [s]	Mass in tank [kg]	Height [m]	Diff.Height [m]	Flow rate [m ³ /s]	Orifice Velocity		
						C _d	Re	
0.825	0	34.587	0.172	0				
5.825	5	31.830	0.158	0.014	423.9E-6	1.76	0.60	46
10.83	10	29.205	0.145	0.027	404.9E-6	1.69	0.60	44
15.83	15	26.698	0.133	0.039	385.9E-6	1.61	0.60	42
20.83	20	24.331	0.121	0.051	366.8E-6	1.54	0.59	40
25.83	25	22.086	0.110	0.062	347.8E-6	1.47	0.59	38
30.83	30	19.942	0.099	0.073	328.8E-6	1.39	0.59	36
35.83	35	17.949	0.089	0.083	309.8E-6	1.32	0.58	34
40.83	40	16.083	0.080	0.092	290.8E-6	1.25	0.58	32
45.83	45	14.312	0.071	0.101	271.8E-6	1.18	0.57	31
50.83	50	12.663	0.063	0.109	252.8E-6	1.11	0.57	29
55.83	55	11.150	0.055	0.116	233.8E-6	1.04	0.56	27
60.83	60	9.747	0.048	0.123	214.8E-6	0.97	0.55	25
65.83	65	8.446	0.042	0.130	195.8E-6	0.91	0.54	23
70.83	70	7.283	0.036	0.136	176.8E-6	0.84	0.52	22
75.83	75	6.233	0.031	0.141	157.8E-6	0.78	0.50	20
80.83	80	5.294	0.026	0.146	138.8E-6	0.72	0.48	19
85.83	85	4.433	0.022	0.150	119.7E-6	0.66	0.45	17

Triangular orifices

Table G.9 8 mm triangular orifice results (100% glycerine)

Time	Diff.Time	Mass in tank	Height	Diff.Height	Flow rate	Orifice Velocity	C _d	Re
[s]	[s]	[kg]	[m]	[m]	[m ³ /s]	[m/s]		
4.158	0	36.1	0.180	0	0	0	0	0
29.16	25	34.0	0.169	0.011	64.68E-6	1.82	0.42	19
54.16	50	31.9	0.159	0.021	62.21E-6	1.76	0.42	18
79.16	75	30.0	0.149	0.030	59.75E-6	1.71	0.42	18
104.2	100	28.2	0.140	0.040	57.28E-6	1.66	0.41	17
129.2	125	26.4	0.131	0.048	54.81E-6	1.60	0.41	17
154.2	150	24.7	0.123	0.057	52.34E-6	1.55	0.40	16
179.2	175	23.1	0.115	0.065	49.87E-6	1.50	0.40	16
204.2	200	21.6	0.107	0.072	47.40E-6	1.45	0.39	15
229.2	225	20.2	0.100	0.079	44.93E-6	1.40	0.38	15
254.2	250	18.8	0.094	0.086	42.46E-6	1.36	0.37	14
279.2	275	17.6	0.087	0.092	40.00E-6	1.31	0.37	14
304.2	300	16.3	0.081	0.098	37.53E-6	1.26	0.36	13
329.2	325	15.2	0.076	0.104	35.06E-6	1.22	0.34	13
354.2	350	14.1	0.070	0.109	32.59E-6	1.17	0.33	12
379.2	375	13.1	0.065	0.114	30.12E-6	1.13	0.32	12
404.2	400	12.2	0.060	0.119	27.65E-6	1.09	0.30	11
429.2	425	11.3	0.056	0.124	25.18E-6	1.05	0.29	11

Table G.10 12 mm triangular orifice results (100% glycerine)

Time	Diff.Time	Mass in tank	Height	Diff.Height	Flow rate	Orifice Velocity	C _d	Re
[s]	[s]	[kg]	[m]	[m]	[m ³ /s]	[m/s]		
0.825	0	35.925	0.178	0	0	0	0	0
5.825	5	33.799	0.168	0.011	337.4E-6	1.82	0.58	37
10.83	10	31.714	0.158	0.021	325.6E-6	1.76	0.58	36
15.83	15	29.701	0.148	0.031	313.8E-6	1.70	0.57	35
20.83	20	27.781	0.138	0.040	301.9E-6	1.65	0.57	33
25.83	25	25.910	0.129	0.050	290.1E-6	1.59	0.57	32
30.83	30	24.156	0.120	0.058	278.2E-6	1.53	0.56	31
35.83	35	22.455	0.112	0.067	266.4E-6	1.48	0.56	30
40.83	40	20.829	0.103	0.075	254.6E-6	1.42	0.56	29
45.83	45	19.290	0.096	0.083	242.7E-6	1.37	0.55	28
50.83	50	17.824	0.089	0.090	230.9E-6	1.32	0.55	27
55.83	55	16.413	0.082	0.097	219.1E-6	1.26	0.54	26
60.83	60	15.084	0.075	0.104	207.2E-6	1.21	0.53	25
65.83	65	13.835	0.069	0.110	195.4E-6	1.16	0.52	24
70.83	70	12.645	0.063	0.116	183.5E-6	1.11	0.52	23
75.83	75	11.515	0.057	0.121	171.7E-6	1.06	0.50	22

Table G.11 16 mm triangular orifice results (100% glycerine)

Time	Diff.Time	Mass in tank	Height	Diff.Height	Flow rate	Orifice Velocity	C _d	Re
[s]	[s]	[kg]	[m]	[m]	[m ³ /s]	[m/s]		
1.658	0	36.164	0.180	0	0	0	0	0
11.66	10	33.840	0.168	0.012	179.7E-6	1.82	0.53	28
21.66	20	31.602	0.157	0.023	172.7E-6	1.76	0.53	27
31.66	30	29.458	0.146	0.033	165.7E-6	1.69	0.52	26
41.66	40	27.413	0.136	0.043	158.7E-6	1.63	0.52	25
51.66	50	25.468	0.127	0.053	151.7E-6	1.58	0.51	24
61.66	60	23.609	0.117	0.062	144.7E-6	1.52	0.51	24
71.66	70	21.838	0.108	0.071	137.7E-6	1.46	0.50	23
81.66	80	20.159	0.100	0.080	130.7E-6	1.40	0.50	22
91.66	90	18.575	0.092	0.087	123.6E-6	1.35	0.49	21
101.7	100	17.076	0.085	0.095	116.6E-6	1.29	0.48	20
111.7	110	15.642	0.078	0.102	109.6E-6	1.23	0.47	19
121.7	120	14.307	0.071	0.109	102.6E-6	1.18	0.46	18
131.7	130	13.055	0.065	0.115	95.6E-6	1.13	0.45	18
141.7	140	11.870	0.059	0.121	88.6E-6	1.08	0.44	17
151.7	150	10.775	0.054	0.126	81.6E-6	1.02	0.43	16

Table G.12 20 mm triangular orifice results (100% glycerine)

Time	Diff.Time	Mass in tank	Height	Diff.Height	Flow rate	Orifice Velocity	C _d	Re
[s]	[s]	[kg]	[m]	[m]	[m ³ /s]	[m/s]		
0.408	0.0	34.395	0.171	0	0	0	0	0
4.575	4.167	31.396	0.156	0.015	558.6E-6	1.75	0.62	45
8.742	8.333	28.527	0.142	0.029	530.6E-6	1.67	0.61	43
12.91	12.50	25.808	0.128	0.043	502.6E-6	1.59	0.61	41
17.08	16.67	23.256	0.116	0.055	474.6E-6	1.51	0.61	39
21.24	20.83	20.850	0.104	0.067	446.6E-6	1.43	0.60	37
25.41	25.00	18.588	0.092	0.079	418.6E-6	1.35	0.60	35
29.58	29.17	16.469	0.082	0.089	390.7E-6	1.27	0.59	33
33.74	33.33	14.487	0.072	0.099	362.7E-6	1.19	0.59	31
37.91	37.50	12.649	0.063	0.108	334.7E-6	1.11	0.58	29
42.08	41.67	10.983	0.055	0.116	306.7E-6	1.03	0.57	27
46.24	45.83	9.429	0.047	0.124	278.7E-6	0.96	0.56	25

APPENDIX H: 96% glycerine solution

Rheological and physical Parameters

$$\begin{aligned}\mu &= 0.304 \text{ Pa.s} \\ \text{Density} &= 1248 \text{ kg/m}^3 \\ g &= 9.81 \text{ m/s}^2\end{aligned}$$

Circular orifices

Table H.1 8 mm circular orifice results (96% glycerine)

Time	Diff.Time	Mass in tank	Height	Diff.Height	Flow rate	Orifice Velocity	C_d	Re
[s]	[s]	[kg]	[m]	[m]	[m³/s]	[m/s]		
4.158	0	34.490	0.173	0	0	0.00	0.00	0
29.16	25	32.790	0.164	0.009	53.26E-6	1.79	0.58	59
54.16	50	31.145	0.156	0.017	51.72E-6	1.75	0.58	58
79.16	75	29.560	0.148	0.025	50.19E-6	1.70	0.58	56
104.2	100	28.010	0.140	0.032	48.65E-6	1.66	0.58	55
129.2	125	26.519	0.133	0.040	47.11E-6	1.61	0.57	53
154.2	150	25.066	0.126	0.047	45.57E-6	1.57	0.57	52
179.2	175	23.678	0.119	0.054	44.04E-6	1.53	0.57	50
204.2	200	22.332	0.112	0.061	42.50E-6	1.48	0.57	49
229.2	225	21.037	0.105	0.067	40.96E-6	1.44	0.56	47
254.2	250	19.772	0.099	0.074	39.42E-6	1.39	0.56	46
279.2	275	18.581	0.093	0.080	37.89E-6	1.35	0.55	45
304.2	300	17.419	0.087	0.085	36.35E-6	1.31	0.55	43
329.2	325	16.311	0.082	0.091	34.81E-6	1.27	0.54	42
354.2	350	15.240	0.076	0.096	33.27E-6	1.22	0.54	40
379.2	375	14.228	0.071	0.101	31.74E-6	1.18	0.53	39
404.2	400	13.256	0.066	0.106	30.20E-6	1.14	0.52	38
429.2	425	12.328	0.062	0.111	28.66E-6	1.10	0.51	36

Table H.2 12 mm circular orifice results (96% glycerine)

Time	Diff.Time	Mass in tank	Height	Diff.Height	Flow rate	Orifice Velocity	C_d	Re
[s]	[s]	[kg]	[m]	[m]	[m³/s]	[m/s]		
2.075	0	34.582	0.173	0	0	0	0	0
14.58	13	32.561	0.163	0.010	128.3E-6	1.79	0.63	88
27.08	25	30.576	0.153	0.020	124.0E-6	1.73	0.63	86
39.58	38	28.664	0.144	0.030	119.7E-6	1.68	0.63	83
52.08	50	26.852	0.134	0.039	115.5E-6	1.62	0.62	80
64.58	63	25.071	0.126	0.048	111.2E-6	1.57	0.62	78
77.08	75	23.385	0.117	0.056	106.9E-6	1.52	0.62	75
89.58	88	21.736	0.109	0.064	102.6E-6	1.46	0.62	72
102.1	100	20.178	0.101	0.072	98.37E-6	1.41	0.61	70
114.6	113	18.668	0.093	0.080	94.10E-6	1.35	0.61	67
127.1	125	17.240	0.086	0.087	89.82E-6	1.30	0.61	64
139.6	138	15.875	0.080	0.094	85.55E-6	1.25	0.60	62
152.1	150	14.569	0.073	0.100	81.28E-6	1.20	0.60	59
164.6	163	13.326	0.067	0.106	77.01E-6	1.14	0.59	57
177.1	175	12.165	0.061	0.112	72.74E-6	1.09	0.58	54

Table H.3 16 mm circular orifice results (96% glycerine)

Time [s]	Diff.Time [s]	Mass in tank [kg]	Height [m]	Diff.Height [m]	Orifice			C_d	Re
					Flow rate [m³/s]	Velocity [m/s]			
1.242	0	33.856	0.170	0	0	0	0	0	0
8.742	8	31.672	0.159	0.011	230.0E-6	1.76	0.65	116	
16.24	15	29.535	0.148	0.022	221.8E-6	1.70	0.64	112	
23.74	23	27.528	0.138	0.032	213.5E-6	1.64	0.64	108	
31.24	30	25.556	0.128	0.042	205.3E-6	1.58	0.64	104	
38.74	38	23.663	0.119	0.051	197.1E-6	1.52	0.64	100	
46.24	45	21.855	0.109	0.060	188.8E-6	1.47	0.64	96	
53.74	53	20.139	0.101	0.069	180.6E-6	1.41	0.64	93	
61.24	60	18.476	0.093	0.077	172.4E-6	1.35	0.63	89	
68.74	68	16.903	0.085	0.085	164.2E-6	1.29	0.63	85	
76.24	75	15.404	0.077	0.092	155.9E-6	1.23	0.63	81	
83.74	83	13.977	0.070	0.100	147.7E-6	1.17	0.62	77	
91.24	90	12.663	0.063	0.106	139.5E-6	1.12	0.62	73	
98.74	98	11.385	0.057	0.113	131.2E-6	1.06	0.61	70	
106.2	105	10.168	0.051	0.119	123.0E-6	1.00	0.61	66	

Table H.4 20 mm circular orifice results (96% glycerine)

Time [s]	Diff.Time [s]	Mass in tank [kg]	Height [m]	Diff.Height [m]	Orifice			C_d	Re
					Flow rate [m³/s]	Velocity [m/s]			
0.825	0	33.6	0.168	0	0	0	0	0	0
5.825	5	31.3	0.157	0.011	363.0E-6	1.75	0.66	144	
10.83	10	29.1	0.146	0.023	349.3E-6	1.69	0.66	139	
15.83	15	26.9	0.135	0.033	335.6E-6	1.63	0.65	134	
20.83	20	24.9	0.125	0.044	322.0E-6	1.56	0.65	129	
25.83	25	22.9	0.115	0.054	308.3E-6	1.50	0.65	123	
30.83	30	21.1	0.106	0.063	294.6E-6	1.44	0.65	118	
35.83	35	19.3	0.096	0.072	281.0E-6	1.38	0.65	113	
40.83	40	17.5	0.088	0.081	267.3E-6	1.31	0.65	108	
45.83	45	15.9	0.080	0.089	253.6E-6	1.25	0.64	103	
50.83	50	14.4	0.072	0.096	240.0E-6	1.19	0.64	98	
55.83	55	12.9	0.065	0.104	226.3E-6	1.13	0.64	93	
60.83	60	11.6	0.058	0.110	212.6E-6	1.07	0.63	88	

Square orifices

Table H.5 8 mm square orifice results (96% glycerine)

Time	Diff.Time	Mass in tank	Height	Diff.Height	Flow rate	Orifice Velocity	C_d	Re
[s]	[s]	[kg]	[m]	[m]	[m³/s]	[m/s]		
3.325	0	34.045	0.170	0	0	0	0	0
23.33	20	32.322	0.162	0.009	68.16E-6	1.78	0.59	59
43.33	40	30.654	0.154	0.017	66.10E-6	1.74	0.59	57
63.33	60	29.014	0.145	0.025	64.05E-6	1.69	0.59	56
83.33	80	27.442	0.137	0.033	62.00E-6	1.64	0.59	54
103.3	100	25.931	0.130	0.041	59.95E-6	1.60	0.58	53
123.3	120	24.447	0.122	0.048	57.89E-6	1.55	0.58	51
143.3	140	23.033	0.115	0.055	55.84E-6	1.50	0.58	50
163.3	160	21.674	0.109	0.062	53.79E-6	1.46	0.57	48
183.3	180	20.353	0.102	0.069	51.74E-6	1.41	0.57	47
203.3	200	19.080	0.096	0.075	49.68E-6	1.37	0.56	45
223.3	220	17.873	0.090	0.081	47.63E-6	1.33	0.56	44
243.3	240	16.703	0.084	0.087	45.58E-6	1.28	0.55	42

Table H.6 12 mm square orifice results (96% glycerine)

Time	Diff.Height	Mass in tank	Height	Diff.Height	Flow rate	Orifice Velocity	C_d	Re
[s]	[s]	[kg]	[m]	[m]	[m³/s]	[m/s]		
1.242	0	33.873	0.170	0	0	0	0	0
8.742	8	32.299	0.162	0.008	165.3E-6	1.78	0.64	88
16.24	15	30.789	0.154	0.015	161.0E-6	1.74	0.64	86
23.74	23	29.299	0.147	0.023	156.7E-6	1.70	0.64	84
31.24	30	27.833	0.139	0.030	152.4E-6	1.65	0.64	82
38.74	38	26.418	0.132	0.037	148.1E-6	1.61	0.64	80
46.24	45	25.079	0.126	0.044	143.8E-6	1.57	0.63	77
53.74	53	23.751	0.119	0.051	139.5E-6	1.53	0.63	75
61.24	60	22.446	0.112	0.057	135.2E-6	1.49	0.63	73
68.74	68	21.202	0.106	0.063	130.9E-6	1.44	0.63	71
76.24	75	20.023	0.100	0.069	126.6E-6	1.40	0.62	69
83.74	83	18.830	0.094	0.075	122.3E-6	1.36	0.62	67
91.24	90	17.722	0.089	0.081	118.0E-6	1.32	0.62	65
98.74	98	16.622	0.083	0.086	113.7E-6	1.28	0.62	63

Table H.7 16 mm square orifice results (96% glycerine)

Time	Diff.Time	Mass in tank	Height	Diff.Height	Flow rate	Orifice Velocity	C _d	Re
[s]	[s]	[kg]	[m]	[m]	[m ³ /s]	[m/s]		
0.825	0	33.098	0.166	0	0	0	0	0
5.825	5	31.259	0.157	0.009	288.5E-6	1.75	0.64	115
10.83	10	29.489	0.148	0.018	279.8E-6	1.70	0.64	112
15.83	15	27.768	0.139	0.027	271.1E-6	1.65	0.64	109
20.83	20	26.121	0.131	0.035	262.3E-6	1.60	0.64	105
25.83	25	24.498	0.123	0.043	253.6E-6	1.55	0.64	102
30.83	30	22.942	0.115	0.051	244.8E-6	1.50	0.64	99
35.83	35	21.436	0.107	0.058	236.1E-6	1.45	0.63	95
40.83	40	20.001	0.100	0.066	227.3E-6	1.40	0.63	92
45.83	45	18.615	0.093	0.073	218.6E-6	1.35	0.63	89
50.83	50	17.263	0.086	0.079	209.8E-6	1.30	0.63	86
55.83	55	15.978	0.080	0.086	201.1E-6	1.25	0.63	82
60.83	60	14.764	0.074	0.092	192.4E-6	1.20	0.62	79

Table H.8 20 mm square orifice results (96% glycerine)

Time	Diff.Time	Mass in tank	Height	Diff.Height	Flow rate	Orifice Velocity	C _d	Re
[s]	[s]	[kg]	[m]	[m]	[m ³ /s]	[m/s]		
0.408	0.0	33.207	0.166	0				
2.908	2.5	31.751	0.159	0.007	460.4E-6	1.77	0.65	145
5.408	5.0	30.322	0.152	0.014	449.6E-6	1.73	0.65	142
7.908	7.5	28.959	0.145	0.021	438.8E-6	1.69	0.65	139
10.41	10.0	27.585	0.138	0.028	428.0E-6	1.65	0.65	135
12.91	12.5	26.275	0.132	0.035	417.2E-6	1.61	0.65	132
15.41	15.0	25.019	0.125	0.041	406.4E-6	1.57	0.65	129
17.91	17.5	23.725	0.119	0.047	395.5E-6	1.53	0.65	125
20.41	20.0	22.555	0.113	0.053	384.7E-6	1.49	0.64	122
22.91	22.5	21.332	0.107	0.059	373.9E-6	1.45	0.64	119
25.41	25.0	20.171	0.101	0.065	363.1E-6	1.41	0.64	116
27.91	27.5	19.071	0.096	0.071	352.3E-6	1.37	0.64	113
30.41	30.0	17.995	0.090	0.076	341.5E-6	1.33	0.64	109
32.91	32.5	16.943	0.085	0.081	330.7E-6	1.29	0.64	106
35.41	35.0	15.943	0.080	0.086	319.9E-6	1.25	0.64	103
37.91	37.5	14.947	0.075	0.091	309.1E-6	1.21	0.64	100

Triangular orifices

Table H.9 8 mm triangular orifice results (96% glycerine)

Time [s]	Diff.Time [s]	Mass in tank [kg]	Height [m]	Diff.Height [m]	Flow rate [m ³ /s]	Orifice		
						Velocity [m/s]	C _d	Re
2.492	0	33.7	0.169	0	0	0	0	0
17.49	15	32.0	0.160	0.008	87.73E-6	1.77	0.59	58
32.49	30	30.4	0.152	0.016	85.12E-6	1.73	0.59	57
47.49	45	28.8	0.144	0.024	82.51E-6	1.68	0.59	55
62.49	60	27.3	0.137	0.032	79.90E-6	1.64	0.58	54
77.49	75	25.8	0.129	0.039	77.29E-6	1.59	0.58	52
92.49	90	24.4	0.122	0.046	74.68E-6	1.55	0.58	51
107.5	105	23.0	0.115	0.053	72.07E-6	1.50	0.57	50
122.5	120	21.7	0.109	0.060	69.46E-6	1.46	0.57	48
137.5	135	20.4	0.102	0.066	66.85E-6	1.42	0.56	47
152.5	150	19.2	0.096	0.072	64.24E-6	1.37	0.56	45
167.5	165	18.0	0.090	0.078	61.63E-6	1.33	0.55	44
182.5	180	16.9	0.085	0.084	59.02E-6	1.29	0.55	42

Table H.10 12 mm triangular orifice results (96% glycerine)

Time [s]	Diff.Time [s]	Mass in tank [kg]	Height [m]	Diff.Height [m]	Flow rate [m ³ /s]	Orifice		
						Velocity [m/s]	C _d	Re
0.825	0	33.4	0.167	0	0	0	0	0
5.825	5	32.1	0.161	0.007	209.9E-6	1.78	0.63	88
10.83	10	30.8	0.154	0.013	205.3E-6	1.74	0.63	86
15.83	15	29.5	0.148	0.020	200.7E-6	1.70	0.63	84
20.83	20	28.3	0.142	0.026	196.0E-6	1.67	0.63	82
25.83	25	27.1	0.136	0.032	191.4E-6	1.63	0.63	80
30.83	30	25.9	0.130	0.038	186.8E-6	1.60	0.63	79
35.83	35	24.8	0.124	0.043	182.1E-6	1.56	0.62	77
40.83	40	23.6	0.118	0.049	177.5E-6	1.52	0.62	75
45.83	45	22.5	0.113	0.055	172.9E-6	1.49	0.62	73
50.83	50	21.5	0.108	0.060	168.2E-6	1.45	0.62	72
55.83	55	20.4	0.102	0.065	163.6E-6	1.42	0.62	70
60.83	60	19.4	0.097	0.070	159.0E-6	1.38	0.61	68
65.83	65	18.5	0.092	0.075	154.3E-6	1.35	0.61	66
70.83	70	17.5	0.088	0.080	149.7E-6	1.31	0.61	65
75.83	75	16.6	0.083	0.084	145.1E-6	1.28	0.61	63
80.83	80	15.7	0.079	0.089	140.4E-6	1.24	0.60	61

Table H.11 16 mm triangular orifice results (96% glycerine)

Time	Diff.Time	Mass in tank	Height	Diff.Height	Flow rate	Orifice Velocity	C _d	Re
[s]	[s]	[kg]	[m]	[m]	[m ³ /s]	[m/s]		
0.617	0.00	33.137	0.166	0	0	0	0	0
4.367	3.75	31.377	0.157	0.009	367.8E-6	1.76	0.65	113
8.117	7.50	29.684	0.149	0.017	357.0E-6	1.71	0.65	110
11.87	11.25	28.052	0.140	0.025	346.3E-6	1.66	0.65	107
15.62	15.00	26.454	0.132	0.033	335.5E-6	1.61	0.65	104
19.37	18.75	24.903	0.125	0.041	324.8E-6	1.56	0.65	101
23.12	22.50	23.410	0.117	0.049	314.0E-6	1.52	0.65	98
26.87	26.25	21.966	0.110	0.056	303.3E-6	1.47	0.64	95
30.62	30.00	20.577	0.103	0.063	292.5E-6	1.42	0.64	92
34.37	33.75	19.214	0.096	0.070	281.8E-6	1.37	0.64	89
38.12	37.50	17.934	0.090	0.076	271.0E-6	1.33	0.64	86
41.87	41.25	16.699	0.084	0.082	260.2E-6	1.28	0.63	83
45.62	45.00	15.499	0.078	0.088	249.5E-6	1.23	0.63	80
49.37	48.75	14.358	0.072	0.094	238.7E-6	1.19	0.63	77

Table H.12 20 mm triangular orifice results (96% glycerine)

Time	Diff.Time	Mass in tank	Height	Diff.Height	Flow rate	Orifice Velocity	C _d	Re
[s]	[s]	[kg]	[m]	[m]	[m ³ /s]	[m/s]		
0.408	0.0	30.817	0.154	0	0	0	0	0
2.908	2.5	29.031	0.145	0.009	576.5E-6	1.69	0.66	139
5.408	5.0	27.259	0.137	0.018	558.0E-6	1.64	0.66	134
7.908	7.5	25.549	0.128	0.026	539.6E-6	1.58	0.66	130
10.41	10.0	23.846	0.119	0.035	521.2E-6	1.53	0.66	126
12.91	12.5	22.260	0.111	0.043	502.8E-6	1.48	0.66	121
15.41	15.0	20.730	0.104	0.051	484.3E-6	1.43	0.65	117
17.91	17.5	19.263	0.096	0.058	465.9E-6	1.38	0.65	113
20.41	20.0	17.838	0.089	0.065	447.5E-6	1.32	0.65	109
22.91	22.5	16.448	0.082	0.072	429.1E-6	1.27	0.65	104
25.41	25.0	15.182	0.076	0.078	410.6E-6	1.22	0.65	100
27.91	27.5	13.881	0.070	0.085	392.2E-6	1.17	0.65	96

APPENDIX I: 93% glycerine solution

Other Parameters

μ =	0.129 Pa.s
Density=	1242 kg/m ³
g =	9.81 m/s ²

Circular orifices

Table I.1 8 mm circular orifice results (93% glycerine)

Time [s]	Diff.Time [s]	Mass in tank [kg]	Height [m]	Diff.Height [m]	Flow rate [m ³ /s]	Orifice Velocity		
						Velocity [m/s]	C_d	Re
4.158	0	33.41	0.168	0	0	0	0	0
29.16	25	31.56	0.159	0.009	58.50E-6	1.77	0.65	136
54.16	50	29.78	0.150	0.018	56.66E-6	1.71	0.65	132
79.16	75	28.04	0.141	0.027	54.82E-6	1.66	0.65	128
104.2	100	26.37	0.133	0.035	52.98E-6	1.61	0.65	125
129.2	125	24.76	0.125	0.044	51.14E-6	1.56	0.64	121
154.2	150	23.21	0.117	0.051	49.30E-6	1.51	0.64	117
179.2	175	21.69	0.109	0.059	47.46E-6	1.46	0.64	113
204.2	200	20.25	0.102	0.066	45.62E-6	1.41	0.64	109
229.2	225	18.85	0.095	0.073	43.78E-6	1.36	0.63	105
254.2	250	17.53	0.088	0.080	41.94E-6	1.32	0.63	102
279.2	275	16.25	0.082	0.086	40.10E-6	1.27	0.62	98
304.2	300	15.04	0.076	0.092	38.26E-6	1.22	0.62	94
329.2	325	13.88	0.070	0.098	36.42E-6	1.17	0.61	90
354.2	350	12.78	0.064	0.104	34.58E-6	1.12	0.61	87
379.2	375	11.73	0.059	0.109	32.74E-6	1.08	0.60	83

Table I.2 12 mm circular orifice results (93% glycerine)

Time [s]	Diff.Time [s]	Mass in tank [kg]	Height [m]	Diff.Height [m]	Flow rate [m ³ /s]	Orifice Velocity		
						Velocity [m/s]	C_d	Re
1.658	0	32.715	0.165	0	0	0	0	0
11.66	10	31.064	0.156	0.008	132.3E-6	1.75	0.66	202
21.66	20	29.444	0.148	0.016	128.7E-6	1.71	0.66	197
31.66	30	27.840	0.140	0.025	125.0E-6	1.66	0.66	192
41.66	40	26.331	0.133	0.032	121.4E-6	1.61	0.66	186
51.66	50	24.841	0.125	0.040	117.7E-6	1.57	0.66	181
61.66	60	23.397	0.118	0.047	114.1E-6	1.52	0.66	176
71.66	70	22.019	0.111	0.054	110.4E-6	1.47	0.66	170
81.66	80	20.638	0.104	0.061	106.8E-6	1.43	0.66	165
91.66	90	19.359	0.097	0.067	103.1E-6	1.38	0.66	160
101.7	100	18.110	0.091	0.073	99.49E-6	1.34	0.65	155
111.7	110	16.892	0.085	0.080	95.84E-6	1.29	0.65	149
121.7	120	15.706	0.079	0.086	92.19E-6	1.25	0.65	144
131.7	130	14.581	0.073	0.091	88.53E-6	1.20	0.65	139
141.7	140	13.528	0.068	0.097	84.88E-6	1.16	0.65	134
151.7	150	12.479	0.063	0.102	81.23E-6	1.11	0.64	128

Table I.3 16mm circular orifice results (93% glycerine)

Time	Diff.Time	Mass in tank	Height	Diff.Height	Flow rate	Orifice Velocity	C_d	Re
[s]	[s]	[kg]	[m]	[m]	[m³/s]	[m/s]		
0.825	0	33.667	0.169	0	0	0	0	0
7.492	6.667	31.652	0.159	0.010	237.4E-6	1.77	0.66	272
14.16	13.33	29.715	0.150	0.020	229.8E-6	1.71	0.66	264
20.83	20.00	27.855	0.140	0.029	222.3E-6	1.66	0.66	255
27.49	26.67	26.014	0.131	0.039	214.7E-6	1.60	0.66	247
34.16	33.33	24.308	0.122	0.047	207.1E-6	1.55	0.66	239
40.83	40.00	22.612	0.114	0.056	199.6E-6	1.49	0.66	230
47.49	46.67	21.008	0.106	0.064	192.0E-6	1.44	0.66	222
54.16	53.33	19.443	0.098	0.072	184.4E-6	1.39	0.66	213
60.83	60.00	17.928	0.090	0.079	176.9E-6	1.33	0.66	205
67.49	66.67	16.489	0.083	0.086	169.3E-6	1.28	0.66	197
74.16	73.33	15.119	0.076	0.093	161.7E-6	1.22	0.66	188
80.83	80.00	13.805	0.069	0.100	154.2E-6	1.17	0.65	180
87.49	86.67	12.591	0.063	0.106	146.6E-6	1.11	0.65	172

Table I.4 20 mm circular orifice results (93% glycerine)

Time	Diff.Time	Mass in tank	Height	Diff.Height	Flow rate	Orifice Velocity	C_d	Re
[s]	[s]	[kg]	[m]	[m]	[m³/s]	[m/s]		
0.825	0	33.3	0.167	0	0	0	0.66	337
5.825	5	31.0	0.156	0.012	364.7E-6	1.75	0.66	324
10.83	10	28.8	0.145	0.023	351.3E-6	1.69	0.66	312
15.83	15	26.6	0.134	0.033	337.9E-6	1.62	0.66	300
20.83	20	24.6	0.124	0.044	324.5E-6	1.56	0.66	287
25.83	25	22.6	0.114	0.054	311.1E-6	1.49	0.66	275
30.83	30	20.7	0.104	0.063	297.7E-6	1.43	0.66	263
35.83	35	18.9	0.095	0.073	284.3E-6	1.36	0.66	250
40.83	40	17.1	0.086	0.081	270.9E-6	1.30	0.66	238
45.83	45	15.5	0.078	0.089	257.6E-6	1.24	0.66	226
50.83	50	14.0	0.070	0.097	244.2E-6	1.17	0.66	214
55.83	55	12.5	0.063	0.105	230.8E-6	1.11	0.66	

Square orifices

Table I.5 8 mm square orifice results (93% glycerine)

Time [s]	Diff.Time [s]	Mass in tank [kg]	Height [m]	Diff.Height [m]	Orifice			
					Flow rate [m ³ /s]	Velocity [m/s]	C _d	Re
3.325	0	33.0	0.166	0				
23.33	20	31.1	0.156	0.009	74.02E-6	1.75	0.66	135
43.33	40	29.3	0.147	0.019	71.68E-6	1.70	0.66	131
63.33	60	27.5	0.139	0.027	69.34E-6	1.65	0.65	127
83.33	80	25.8	0.130	0.036	67.00E-6	1.60	0.65	123
103.3	100	24.2	0.122	0.044	64.65E-6	1.55	0.65	119
123.3	120	22.6	0.114	0.052	62.31E-6	1.49	0.65	115
143.3	140	21.1	0.106	0.060	59.97E-6	1.44	0.65	111
163.3	160	19.6	0.099	0.067	57.62E-6	1.39	0.64	107
183.3	180	18.3	0.092	0.074	55.28E-6	1.34	0.64	103
203.3	200	16.9	0.085	0.081	52.94E-6	1.29	0.64	99
223.3	220	15.6	0.079	0.087	50.59E-6	1.24	0.63	96
243.3	240	14.4	0.072	0.094	48.25E-6	1.19	0.63	92
263.3	260	13.2	0.066	0.099	45.91E-6	1.14	0.62	88
283.3	280	12.1	0.061	0.105	43.57E-6	1.09	0.62	84

Table I.6 12 mm square orifice results (93% glycerine)

Time [s]	Diff.Height [s]	Mass in tank [kg]	Height [m]	Diff.Height [m]	Orifice			
					Flow rate [m ³ /s]	Velocity [m/s]	C _d	Re
1.658	0	32.8	0.165	0.000	0	0	0	0
11.66	10	30.6	0.154	0.011	170.3E-6	1.74	0.68	201
21.66	20	28.5	0.144	0.021	164.2E-6	1.68	0.68	194
31.66	30	26.5	0.134	0.031	158.1E-6	1.62	0.68	187
41.66	40	24.6	0.124	0.041	151.9E-6	1.56	0.67	180
51.66	50	22.8	0.115	0.050	145.8E-6	1.50	0.67	173
61.66	60	21.0	0.106	0.059	139.6E-6	1.44	0.67	166
71.66	70	19.3	0.097	0.068	133.5E-6	1.38	0.67	159
81.66	80	17.7	0.089	0.076	127.4E-6	1.32	0.67	152
91.66	90	16.1	0.081	0.084	121.2E-6	1.26	0.66	146
101.7	100	14.7	0.074	0.091	115.1E-6	1.20	0.66	139
111.7	110	13.3	0.067	0.098	108.9E-6	1.14	0.66	132
121.7	120	12.0	0.060	0.105	102.8E-6	1.09	0.65	125

Table I.7 16 mm square orifice results (93% glycerine)

Time	Diff.Time	Mass in tank	Height	Diff.Height	Flow rate	Orifice Velocity	C _d	Re
[s]	[s]	[kg]	[m]	[m]	[m ³ /s]	[m/s]		
0.825	0	32.6	0.164	0				
5.825	5	30.7	0.155	0.009	295.3E-6	1.74	0.66	268
10.83	10	28.9	0.145	0.018	286.3E-6	1.69	0.66	260
15.83	15	27.1	0.137	0.027	277.2E-6	1.64	0.66	252
20.83	20	25.5	0.128	0.036	268.2E-6	1.59	0.66	244
25.83	25	23.8	0.120	0.044	259.2E-6	1.53	0.66	236
30.83	30	22.2	0.112	0.052	250.2E-6	1.48	0.66	228
35.83	35	20.7	0.104	0.060	241.2E-6	1.43	0.66	220
40.83	40	19.2	0.097	0.067	232.1E-6	1.38	0.66	212
45.83	45	17.8	0.090	0.074	223.1E-6	1.33	0.66	204
50.83	50	16.4	0.083	0.081	214.1E-6	1.27	0.65	196
55.83	55	15.2	0.076	0.087	205.1E-6	1.22	0.65	188
60.83	60	13.9	0.070	0.094	196.0E-6	1.17	0.65	180
65.83	65	12.7	0.064	0.100	187.0E-6	1.12	0.65	172
70.83	70	11.6	0.058	0.105	178.0E-6	1.07	0.65	165
75.83	75	10.5	0.053	0.111	169.0E-6	1.02	0.65	157

Table I.8 20 mm square orifice results (93% glycerine)

Time	Diff.Time	Mass in tank	Height	Diff.Height	Flow rate	Orifice Velocity	C _d	Re
[s]	[s]	[kg]	[m]	[m]	[m ³ /s]	[m/s]		
0.408	0.0	32.5	0.163	0	0	0	0	0
2.908	2.5	31.0	0.156	0.007	458.5E-6	1.75	0.65	337
5.408	5.0	29.6	0.149	0.014	448.0E-6	1.71	0.65	329
7.908	7.5	28.3	0.142	0.021	437.5E-6	1.67	0.65	321
10.41	10.0	26.9	0.135	0.028	427.0E-6	1.63	0.65	313
12.91	12.5	25.7	0.129	0.034	416.6E-6	1.59	0.65	306
15.41	15.0	24.3	0.122	0.041	406.1E-6	1.55	0.65	298
17.91	17.5	23.1	0.116	0.047	395.6E-6	1.51	0.65	290
20.41	20.0	21.9	0.110	0.053	385.1E-6	1.47	0.65	283
22.91	22.5	20.7	0.104	0.059	374.6E-6	1.43	0.65	275
25.41	25.0	19.5	0.098	0.065	364.2E-6	1.39	0.65	267
27.91	27.5	18.4	0.093	0.071	353.7E-6	1.35	0.65	259
30.41	30.0	17.4	0.087	0.076	343.2E-6	1.31	0.65	252
32.91	32.5	16.3	0.082	0.082	332.7E-6	1.27	0.65	244
35.41	35.0	15.3	0.077	0.086	322.2E-6	1.23	0.65	236
37.91	37.5	14.3	0.072	0.092	311.8E-6	1.19	0.65	228
40.41	40.0	13.4	0.067	0.096	301.3E-6	1.15	0.65	221
42.91	42.5	12.5	0.063	0.101	290.8E-6	1.11	0.65	213
45.41	45.0	11.5	0.058	0.105	280.3E-6	1.07	0.66	205

Triangular orifices

Table I.9 8 mm triangular orifice results (93% glycerine)

Time [s]	Diff.Time [s]	Mass in tank [kg]	Height [m]	Diff.Height [m]	Flow rate [m ³ /s]	Orifice		
						Velocity [m/s]	C _d	Re
2.492	0	32.7	0.165	0				
17.49	15	30.9	0.156	0.009	95.92E-6	1.75	0.66	135
32.49	30	29.1	0.147	0.018	92.93E-6	1.70	0.65	131
47.49	45	27.5	0.138	0.027	89.94E-6	1.65	0.65	127
62.49	60	25.8	0.130	0.035	86.95E-6	1.60	0.65	123
77.49	75	24.2	0.122	0.043	83.96E-6	1.55	0.65	119
92.49	90	22.7	0.114	0.051	80.96E-6	1.50	0.65	115
107.5	105	21.2	0.107	0.058	77.97E-6	1.45	0.64	111
122.5	120	19.8	0.099	0.065	74.98E-6	1.40	0.64	108
137.5	135	18.4	0.093	0.072	71.99E-6	1.35	0.64	104
152.5	150	17.1	0.086	0.079	69.00E-6	1.30	0.64	100
167.5	165	15.8	0.080	0.085	66.01E-6	1.25	0.63	96
182.5	180	14.6	0.074	0.091	63.02E-6	1.20	0.63	93
197.5	195	13.5	0.068	0.097	60.02E-6	1.15	0.62	89
212.5	210	12.4	0.062	0.102	57.03E-6	1.11	0.62	85

Table I.10 12 mm triangular orifice results (93% glycerine)

Time [s]	Diff.Time [s]	Mass in tank [kg]	Height [m]	Diff.Height [m]	Flow rate [m ³ /s]	Orifice		
						Velocity [m/s]	C _d	Re
1.242	0.0	32.5	0.163	0	0	0	0	0
8.742	7.5	30.4	0.153	0.010	216.6E-6	1.73	0.67	200
16.24	15.0	28.4	0.143	0.020	209.1E-6	1.67	0.67	193
23.74	22.5	26.5	0.133	0.030	201.7E-6	1.62	0.67	187
31.24	30.0	24.7	0.124	0.039	194.2E-6	1.56	0.66	180
38.74	37.5	22.9	0.115	0.048	186.8E-6	1.50	0.66	173
46.24	45.0	21.2	0.107	0.057	179.4E-6	1.45	0.66	167
53.74	52.5	19.6	0.098	0.065	171.9E-6	1.39	0.66	160
61.24	60.0	18.0	0.091	0.073	164.5E-6	1.33	0.66	154
68.74	67.5	16.5	0.083	0.080	157.1E-6	1.28	0.66	147
76.24	75.0	15.1	0.076	0.088	149.6E-6	1.22	0.65	141
83.74	82.5	13.7	0.069	0.094	142.2E-6	1.16	0.65	134
91.24	90.0	12.4	0.062	0.101	134.7E-6	1.11	0.65	128

Table I.11 16 mm triangular orifice results (93% glycerine)

Time [s]	Diff.Time [s]	Mass in tank [kg]	Height [m]	Diff.Height [m]	Flow rate [m ³ /s]	Orifice Velocity		
						C _d	Re	
0.408	0.000	32.375	0.163	0	372.2E-6	1.73	0.67	261
4.575	4.167	30.401	0.153	0.010	360.2E-6	1.68	0.67	253
8.742	8.333	28.527	0.144	0.019	348.1E-6	1.62	0.67	245
12.91	12.50	26.687	0.134	0.029	336.0E-6	1.57	0.67	236
17.08	16.67	24.909	0.125	0.038	324.0E-6	1.51	0.67	228
21.24	20.83	23.202	0.117	0.046	311.9E-6	1.46	0.67	220
25.41	25.00	21.575	0.109	0.054	299.8E-6	1.40	0.67	212
29.58	29.17	19.972	0.101	0.062	287.8E-6	1.35	0.66	204
33.74	33.33	18.460	0.093	0.070	275.7E-6	1.30	0.66	195
37.91	37.50	17.018	0.086	0.077	263.6E-6	1.24	0.66	187
42.08	41.67	15.621	0.079	0.084	251.5E-6	1.19	0.66	179
46.24	45.83	14.235	0.072	0.091	239.5E-6	1.13	0.66	171
50.41	50.00	12.962	0.065	0.098	227.4E-6	1.08	0.66	163
54.58	54.17	11.831	0.060	0.103				

Table I.12 20 mm triangular orifice results (93% glycerine)

Time [s]	Diff.Time [s]	Mass in tank [kg]	Height [m]	Diff.Height [m]	Flow rate [m ³ /s]	Orifice Velocity		
						C _d	Re	
0.408	0.0	31.836	0.160	0	0	0	0	0
2.908	2.5	29.953	0.151	0.009	588.4E-6	1.72	0.66	330
5.408	5.0	28.179	0.142	0.018	570.9E-6	1.67	0.66	320
7.908	7.5	26.423	0.133	0.027	553.4E-6	1.62	0.66	310
10.41	10.0	24.740	0.124	0.036	535.8E-6	1.56	0.66	300
12.91	12.5	23.094	0.116	0.044	518.3E-6	1.51	0.66	290
15.41	15.0	21.536	0.108	0.052	500.8E-6	1.46	0.66	280
17.91	17.5	19.977	0.101	0.060	483.3E-6	1.40	0.66	269
20.41	20.0	18.545	0.093	0.067	465.8E-6	1.35	0.66	260
22.91	22.5	17.087	0.086	0.074	448.2E-6	1.30	0.67	249
25.41	25.0	15.710	0.079	0.081	430.7E-6	1.25	0.67	239
27.91	27.5	14.417	0.073	0.088	413.2E-6	1.19	0.67	229
30.41	30.0	13.173	0.066	0.094	395.7E-6	1.14	0.67	219
32.91	32.5	11.974	0.060	0.100	378.2E-6	1.09	0.67	209

APPENDIX J: 65% glycerine solution

Other Parameters

μ = 0.0193 Pa.s
 Density= 1179 kg/m³
 g = 9.81 m/s²

Circular orifices

Table J.1 8 mm circular orifice results (65% glycerine)

Time [s]	Diff.Time [s]	Mass in tank [kg]	Height [m]	Diff.Height [m]	Flow rate [m ³ /s]	Orifice		
						Velocity [m/s]	C_d	Re
4.158	0	56.911	0.302	0	0	0	0	0
29.16	25	54.435	0.289	0.013	83.26E-6	2.38	0.69	1169
54.16	50	52.015	0.276	0.026	81.40E-6	2.33	0.69	1143
79.16	75	49.646	0.263	0.039	79.55E-6	2.27	0.69	1116
104.2	100	47.328	0.251	0.051	77.69E-6	2.22	0.69	1090
129.2	125	45.071	0.239	0.063	75.83E-6	2.17	0.69	1064
154.2	150	42.861	0.227	0.074	73.97E-6	2.11	0.69	1037
179.2	175	40.713	0.216	0.086	72.12E-6	2.06	0.69	1011
204.2	200	38.610	0.205	0.097	70.26E-6	2.00	0.69	985
229.2	225	36.565	0.194	0.108	68.40E-6	1.95	0.69	958
254.2	250	34.573	0.183	0.118	66.54E-6	1.90	0.69	932
279.2	275	32.636	0.173	0.129	64.69E-6	1.84	0.69	905
304.2	300	30.754	0.163	0.139	62.83E-6	1.79	0.69	879
329.2	325	28.922	0.153	0.148	60.97E-6	1.73	0.69	852
354.2	350	27.161	0.144	0.158	59.11E-6	1.68	0.69	826
379.2	375	25.442	0.135	0.167	57.26E-6	1.63	0.69	799
404.2	400	23.783	0.126	0.176	55.40E-6	1.57	0.69	773
429.2	425	22.187	0.118	0.184	53.54E-6	1.52	0.69	746
454.2	450	20.641	0.109	0.192	51.68E-6	1.47	0.69	720
479.2	475	19.150	0.102	0.200	49.83E-6	1.41	0.70	693

Table J.2 12 mm circular orifice results (65% glycerine)

Time [s]	Diff.Time [s]	Mass in tank [kg]	Height [m]	Diff.Height [m]	Flow rate [m ³ /s]	Velocity [m/s]	Orifice Velocity	C _d	Re
2.075	0	56.777	0.301	0					
14.58	12.5	54.206	0.287	0.014	172.4E-6	2.37	0.64	1747	
27.08	25.0	51.688	0.274	0.027	168.5E-6	2.32	0.64	1706	
39.58	37.5	49.234	0.261	0.040	164.5E-6	2.26	0.64	1665	
52.08	50.0	46.837	0.248	0.053	160.6E-6	2.21	0.64	1624	
64.58	62.5	44.497	0.236	0.065	156.6E-6	2.15	0.64	1583	
77.08	75.0	42.218	0.224	0.077	152.7E-6	2.10	0.64	1542	
89.58	87.5	39.999	0.212	0.089	148.8E-6	2.04	0.64	1501	
102.1	100.0	37.832	0.201	0.100	144.8E-6	1.98	0.64	1460	
114.6	112.5	35.723	0.189	0.112	140.9E-6	1.93	0.64	1418	
127.1	125.0	33.684	0.179	0.122	137.0E-6	1.87	0.64	1377	
139.6	137.5	31.687	0.168	0.133	133.0E-6	1.82	0.64	1336	
152.1	150.0	29.771	0.158	0.143	129.1E-6	1.76	0.64	1295	
164.6	162.5	27.900	0.148	0.153	125.2E-6	1.70	0.65	1253	
177.1	175.0	26.078	0.138	0.163	121.2E-6	1.65	0.65	1212	
189.6	187.5	24.320	0.129	0.172	117.3E-6	1.59	0.65	1170	
202.1	200.0	22.627	0.120	0.181	113.4E-6	1.53	0.65	1129	
214.6	212.5	20.969	0.111	0.190	109.4E-6	1.48	0.65	1087	
227.1	225.0	19.367	0.103	0.198	105.5E-6	1.42	0.65	1044	

Table J.3 16 mm circular orifice results (65% glycerine)

Time [s]	Diff.Time [s]	Mass in tank [kg]	Height [m]	Diff.Height [m]	Flow rate [m ³ /s]	Velocity [m/s]	Orifice Velocity	C _d	Re
1.658	0	56.383	0.299	0	0	0	0	0	0
11.66	10	52.823	0.280	0.019	297.5E-6	2.34	0.63	2298	
21.66	20	49.369	0.262	0.037	287.9E-6	2.27	0.63	2221	
31.66	30	46.022	0.244	0.055	278.2E-6	2.19	0.63	2145	
41.66	40	42.815	0.227	0.072	268.6E-6	2.11	0.63	2069	
51.66	50	39.703	0.211	0.088	258.9E-6	2.03	0.63	1992	
61.66	60	36.708	0.195	0.104	249.3E-6	1.95	0.63	1915	
71.66	70	33.839	0.179	0.120	239.6E-6	1.88	0.63	1839	
81.66	80	31.062	0.165	0.134	229.9E-6	1.80	0.63	1762	
91.66	90	28.403	0.151	0.148	220.3E-6	1.72	0.63	1685	
101.7	100	25.870	0.137	0.162	210.6E-6	1.64	0.64	1608	
111.7	110	23.438	0.124	0.175	201.0E-6	1.56	0.64	1530	
121.7	120	21.138	0.112	0.187	191.3E-6	1.48	0.64	1453	
131.7	130	18.934	0.100	0.199	181.7E-6	1.40	0.64	1376	

Table J.4 20 mm circular orifice results (65% glycerine)

Time [s]	Diff.Time [s]	Mass in tank [kg]	Height [m]	Diff.Height [m]	Orifice			C_d	Re
					Flow rate [m³/s]	Velocity [m/s]			
0.825	0	56.672	0.300		0	0	0	0	0
5.825	5	53.905	0.286	0.015	464.3E-6	2.37	0.62	2900	
10.83	10	51.212	0.272	0.029	452.8E-6	2.31	0.62	2826	
15.83	15	48.557	0.257	0.043	441.3E-6	2.25	0.62	2752	
20.83	20	45.999	0.244	0.057	429.8E-6	2.19	0.62	2679	
25.83	25	43.502	0.231	0.070	418.3E-6	2.13	0.62	2605	
30.83	30	41.064	0.218	0.083	406.8E-6	2.07	0.62	2531	
35.83	35	38.707	0.205	0.095	395.2E-6	2.01	0.62	2457	
40.83	40	36.409	0.193	0.107	383.7E-6	1.95	0.63	2383	
45.83	45	34.185	0.181	0.119	372.2E-6	1.89	0.63	2309	
50.83	50	32.026	0.170	0.131	360.7E-6	1.83	0.63	2235	
55.83	55	29.922	0.159	0.142	349.2E-6	1.76	0.63	2160	
60.83	60	27.900	0.148	0.153	337.7E-6	1.70	0.63	2086	
65.83	65	25.962	0.138	0.163	326.2E-6	1.64	0.63	2012	
70.83	70	24.053	0.128	0.173	314.6E-6	1.58	0.63	1937	
75.83	75	22.238	0.118	0.183	303.1E-6	1.52	0.63	1863	
80.83	80	20.493	0.109	0.192	291.6E-6	1.46	0.63	1788	
85.83	85	18.804	0.100	0.201	280.1E-6	1.40	0.63	1713	
90.83	90	17.181	0.091	0.209	268.6E-6	1.34	0.64	1637	

Square orifices

Table J.5 8 mm square orifice results (65% glycerine)

Time [s]	Diff.Time [s]	Mass in tank [kg]	Height [m]	Diff.Height [m]	Orifice			C_d	Re
					Flow rate [m³/s]	Velocity [m/s]			
4.158	0	57.1	0.303	0					
29.16	25	53.9	0.286	0.017	105.0E-6	2.37	0.69	1161	
54.16	50	50.9	0.270	0.033	102.0E-6	2.30	0.69	1128	
79.16	75	47.9	0.254	0.049	99.09E-6	2.23	0.69	1094	
104.2	100	45.0	0.239	0.064	96.16E-6	2.16	0.69	1061	
129.2	125	42.3	0.224	0.079	93.23E-6	2.10	0.69	1028	
154.2	150	39.6	0.210	0.093	90.30E-6	2.03	0.69	994	
179.2	175	36.9	0.196	0.107	87.36E-6	1.96	0.69	961	
204.2	200	34.4	0.182	0.120	84.43E-6	1.89	0.69	927	
229.2	225	32.0	0.169	0.133	81.50E-6	1.82	0.69	894	
254.2	250	29.6	0.157	0.146	78.57E-6	1.75	0.70	860	
279.2	275	27.3	0.145	0.158	75.64E-6	1.69	0.70	826	
304.2	300	25.1	0.133	0.169	72.70E-6	1.62	0.70	793	
329.2	325	23.0	0.122	0.180	69.77E-6	1.55	0.70	759	
354.2	350	21.0	0.112	0.191	66.84E-6	1.48	0.70	725	

Table J.6 12 mm square orifice results (65% glycerine)

Time	Diff.Time	Mass in tank	Height	Diff.Height	Flow rate	Orifice Velocity	C _d	Re
[s]	[s]	[kg]	[m]	[m]	[m ³ /s]	[m/s]		
1.658	0	57.3	0.304	0	0	0	0	0
11.66	10	54.6	0.289	0.014	228.7E-6	2.38	0.66	1750
21.66	20	51.9	0.275	0.029	223.3E-6	2.32	0.66	1707
31.66	30	49.3	0.262	0.042	217.9E-6	2.27	0.67	1664
41.66	40	46.8	0.248	0.056	212.5E-6	2.21	0.67	1620
51.66	50	44.3	0.235	0.069	207.1E-6	2.15	0.67	1577
61.66	60	41.9	0.222	0.082	201.7E-6	2.09	0.67	1533
71.66	70	39.6	0.210	0.094	196.3E-6	2.03	0.67	1490
81.66	80	37.3	0.198	0.106	190.9E-6	1.97	0.67	1446
91.66	90	35.1	0.186	0.118	185.5E-6	1.91	0.67	1403
101.7	100	32.9	0.174	0.129	180.1E-6	1.85	0.67	1359
111.7	110	30.8	0.163	0.141	174.7E-6	1.79	0.68	1315
121.7	120	28.8	0.153	0.151	169.3E-6	1.73	0.68	1271
131.7	130	26.8	0.142	0.162	163.9E-6	1.67	0.68	1227
141.7	140	24.9	0.132	0.172	158.5E-6	1.61	0.68	1183
151.7	150	23.1	0.122	0.182	153.1E-6	1.55	0.68	1138
161.7	160	21.3	0.113	0.191	147.7E-6	1.49	0.69	1093
171.7	170	19.6	0.104	0.200	142.3E-6	1.43	0.69	1049

Table J.7 16 mm square orifice results (65% glycerine)

Time	Diff.Time	Mass in tank	Height	Diff.Height	Flow rate	Orifice Velocity	C _d	Re
[s]	[s]	[kg]	[m]	[m]	[m ³ /s]	[m/s]		
0.825	0	56.8	0.301	0	0	0	0	0
9.158	8	53.0	0.281	0.020	378.4E-6	2.35	0.63	2299
17.49	17	49.4	0.262	0.039	365.5E-6	2.27	0.63	2219
25.83	25	45.9	0.243	0.058	352.7E-6	2.18	0.63	2138
34.16	33	42.5	0.225	0.076	339.9E-6	2.10	0.63	2057
42.49	42	39.2	0.208	0.093	327.0E-6	2.02	0.63	1976
50.83	50	36.0	0.191	0.110	314.2E-6	1.94	0.63	1895
59.16	58	33.0	0.175	0.126	301.4E-6	1.85	0.63	1814
67.49	67	30.1	0.160	0.142	288.5E-6	1.77	0.64	1733
75.83	75	27.3	0.145	0.156	275.7E-6	1.69	0.64	1651
84.16	83	24.7	0.131	0.170	262.9E-6	1.60	0.64	1569
92.49	92	22.2	0.118	0.184	250.0E-6	1.52	0.64	1487
100.8	100	19.8	0.105	0.196	237.2E-6	1.43	0.64	1404
109.2	108	17.5	0.093	0.208	224.3E-6	1.35	0.65	1322

Table J.8 20 mm square orifice results (65% glycerine)

Time	Diff.Time	Mass in tank	Height	Diff.Height	Flow rate	Orifice		
						Velocity	C _d	Re
[s]	[s]	[kg]	[m]	[m]	[m ³ /s]	[m/s]		
0.825	0	56.9	0.302	0	0	0	0	0
5.825	5	53.3	0.283	0.019	592.5E-6	2.36	0.63	2881
10.83	10	49.9	0.265	0.037	573.7E-6	2.28	0.63	2787
15.83	15	46.6	0.247	0.055	554.9E-6	2.20	0.63	2693
20.83	20	43.4	0.230	0.072	536.0E-6	2.12	0.63	2598
25.83	25	40.3	0.213	0.088	517.2E-6	2.05	0.63	2504
30.83	30	37.3	0.198	0.104	498.4E-6	1.97	0.63	2408
35.83	35	34.4	0.182	0.119	479.5E-6	1.89	0.63	2313
40.83	40	31.6	0.168	0.134	460.7E-6	1.81	0.63	2218
45.83	45	29.0	0.154	0.148	441.9E-6	1.74	0.64	2123
50.83	50	26.4	0.140	0.162	423.0E-6	1.66	0.64	2027
55.83	55	24.0	0.127	0.175	404.2E-6	1.58	0.64	1931
60.83	60	21.6	0.115	0.187	385.4E-6	1.50	0.64	1835
65.83	65	19.4	0.103	0.199	366.5E-6	1.42	0.64	1738
70.83	70	17.3	0.092	0.210	347.7E-6	1.34	0.65	1642

Triangular orifices**Table J.9 8 mm triangular orifice results (65% glycerine)**

Time	Diff.Time	Mass in tank	Height	Diff.Height	Flow rate	Orifice		
						Velocity	C _d	Re ₂
[s]	[s]	[kg]	[m]	[m]	[m ³ /s]	[m/s]		
4.158	0	56.546	0.300	0	0	0	0	0
29.16	25	52.603	0.279	0.021	131.6E-6	2.34	0.67	1147
54.16	50	48.800	0.259	0.041	126.9E-6	2.25	0.67	1105
79.16	75	45.135	0.239	0.061	122.3E-6	2.17	0.67	1063
104.2	100	41.604	0.221	0.079	117.7E-6	2.08	0.68	1020
129.2	125	38.207	0.203	0.097	113.0E-6	1.99	0.68	978
154.2	150	34.944	0.185	0.115	108.4E-6	1.91	0.68	935
179.2	175	31.811	0.169	0.131	103.8E-6	1.82	0.68	892
204.2	200	28.823	0.153	0.147	99.13E-6	1.73	0.68	849
229.2	225	25.956	0.138	0.162	94.49E-6	1.64	0.69	806
254.2	250	23.232	0.123	0.177	89.86E-6	1.55	0.69	762
279.2	275	20.640	0.109	0.190	85.22E-6	1.47	0.70	719
304.2	300	18.193	0.096	0.203	80.59E-6	1.38	0.70	675
329.2	325	15.918	0.084	0.215	75.95E-6	1.29	0.71	631
354.2	350	13.783	0.073	0.227	71.32E-6	1.20	0.71	587

Table J.10 12 mm triangular orifice results (65% glycerine)

Time [s]	Diff.Time [s]	Mass in tank [kg]	Height [m]	Diff.Height [m]	Flow rate [m ³ /s]	Orifice Velocity		
						C _d	Re ₂	
1.658	0	56.488	0.300	0	0	0	0	0
11.66	10	53.066	0.281	0.018	285.7E-6	2.35	0.65	1724
21.66	20	49.746	0.264	0.036	276.9E-6	2.27	0.65	1669
31.66	30	46.537	0.247	0.053	268.2E-6	2.20	0.65	1615
41.66	40	43.425	0.230	0.069	259.4E-6	2.13	0.65	1560
51.66	50	40.423	0.214	0.085	250.7E-6	2.05	0.65	1505
61.66	60	37.516	0.199	0.101	241.9E-6	1.98	0.65	1450
71.66	70	34.724	0.184	0.115	233.2E-6	1.90	0.66	1395
81.66	80	32.021	0.170	0.130	224.5E-6	1.83	0.66	1339
91.66	90	29.431	0.156	0.143	215.7E-6	1.75	0.66	1284
101.7	100	26.940	0.143	0.157	207.0E-6	1.67	0.66	1228
111.7	110	24.550	0.130	0.169	198.2E-6	1.60	0.66	1173
121.7	120	22.271	0.118	0.181	189.5E-6	1.52	0.66	1117
131.7	130	20.075	0.106	0.193	180.7E-6	1.45	0.67	1060

Table J.11 16 mm triangular orifice results (65% glycerine)

Time [s]	Diff.Time [s]	Mass in tank [kg]	Height [m]	Diff.Height [m]	Flow rate [m ³ /s]	Orifice Velocity		
						C _d	Re ₂	
0.825	0	57.130	0.303	0	0	0	0	0
5.825	5	54.223	0.288	0.015	484.1E-6	2.38	0.64	2279
10.83	10	51.396	0.273	0.030	471.5E-6	2.31	0.64	2219
15.83	15	48.639	0.258	0.045	458.9E-6	2.25	0.64	2159
20.83	20	45.949	0.244	0.059	446.4E-6	2.19	0.64	2098
25.83	25	43.344	0.230	0.073	433.8E-6	2.12	0.64	2038
30.83	30	40.811	0.216	0.087	421.2E-6	2.06	0.64	1977
35.83	35	38.363	0.203	0.100	408.7E-6	2.00	0.64	1917
40.83	40	35.986	0.191	0.112	396.1E-6	1.93	0.64	1857
45.83	45	33.668	0.179	0.124	383.5E-6	1.87	0.64	1796
50.83	50	31.427	0.167	0.136	370.9E-6	1.81	0.64	1735
55.83	55	29.278	0.155	0.148	358.4E-6	1.75	0.64	1675
60.83	60	27.191	0.144	0.159	345.8E-6	1.68	0.64	1614
65.83	65	25.188	0.134	0.169	333.2E-6	1.62	0.64	1553
70.83	70	23.230	0.123	0.180	320.7E-6	1.55	0.64	1492
75.83	75	21.364	0.113	0.190	308.1E-6	1.49	0.64	1431
80.83	80	19.563	0.104	0.199	295.5E-6	1.43	0.65	1369

Table J.12 20 mm triangular orifice results (65% glycerine)

Time [s]	Diff.Time [s]	Mass in tank [kg]	Height [m]	Diff.Height [m]	Flowrate [m ³ /s]	Orifice Velocity [m/s]	C _d	Re ₂
0.408	0.00	57.179	0.303	0	772.2E-6	2.36	0.63	2875
4.575	4.167	53.326	0.283	0.020	745.4E-6	2.27	0.63	2773
8.742	8.333	49.602	0.263	0.040	718.6E-6	2.19	0.63	2670
12.91	12.50	45.993	0.244	0.059	691.8E-6	2.10	0.63	2568
17.08	16.67	42.543	0.226	0.078	665.0E-6	2.02	0.64	2465
21.24	20.83	39.209	0.208	0.095	638.2E-6	1.94	0.64	2363
25.41	25.00	36.011	0.191	0.112	611.4E-6	1.85	0.64	2260
29.58	29.17	32.937	0.175	0.129	584.6E-6	1.77	0.64	2156
33.74	33.33	29.999	0.159	0.144	557.8E-6	1.68	0.64	2053
37.91	37.50	27.188	0.144	0.159	531.0E-6	1.60	0.64	1950
42.08	41.67	24.522	0.130	0.173	504.2E-6	1.51	0.64	1845
46.24	45.83	21.970	0.116	0.187	477.4E-6	1.43	0.65	1742
50.41	50.00	19.576	0.104	0.199				

APPENDIX K: 7.55% CMC solution

Rheological and physical Parameters

$n=n'=$	0.64
$k=$	2.388 Pa.s ⁿ
$k'=$	2.598 Pa.s ⁿ
Density=	1043 kg/m ³
$g=$	9.81 m/s ²

Circular orifices

Table K.1 8 mm circular orifice results (7.55% CMC)

Time [s]	Diff.Time [s]	Mass in tank [kg]	Height [m]	Diff.Height [m]	Flow rate [m ³ /s]	Orifice Velocity [m/s]	Orifice		
							C_d	Re_{MR}	Re_2
8.325	0	45.984	0.276	0	0	0	0	0	0
58.33	50	42.592	0.255	0.020	61.66E-6	2.24	0.54	107	126
108.3	100	39.389	0.236	0.040	58.61E-6	2.15	0.54	101	120
158.3	150	36.372	0.218	0.058	55.56E-6	2.07	0.53	96	113
208.3	200	33.530	0.201	0.075	52.51E-6	1.99	0.52	91	107
258.3	250	30.860	0.185	0.091	49.46E-6	1.90	0.51	86	101
308.3	300	28.391	0.170	0.105	46.42E-6	1.83	0.50	81	96
358.3	350	26.075	0.156	0.119	43.37E-6	1.75	0.49	76	90
408.3	400	23.928	0.143	0.132	40.32E-6	1.68	0.47	72	85
458.3	450	21.953	0.132	0.144	37.27E-6	1.61	0.46	68	80
508.3	500	20.124	0.121	0.155	34.22E-6	1.54	0.44	64	76
558.3	550	18.449	0.111	0.165	31.18E-6	1.47	0.42	60	71
608.3	600	16.909	0.101	0.174	28.13E-6	1.41	0.39	57	67
658.3	650	15.511	0.093	0.183	25.08E-6	1.35	0.37	54	64
708.3	700	14.242	0.085	0.190	22.03E-6	1.29	0.34	51	60
758.3	750	13.087	0.078	0.197	18.98E-6	1.24	0.30	48	57
808.3	800	12.040	0.072	0.203	15.94E-6	1.19	0.26	45	53

Table K.2 12 mm circular orifice results (7.55% CMC)

Time	Diff.Time	Mass in tank	Height	Diff.Height	Flow rate	Orifice									
						[s]	[s]	[kg]	[m]	[m]	[m ³ /s]	[m/s]	C _d	Re _{MR}	Re ₂
2.492	0	45.314	0.272	0	0	0	0	0	0	0	0	0	0	0	0
17.49	15	42.846	0.257	0.015	154.3E-6	2.24	0.60	139	164						
32.49	30	40.468	0.243	0.029	148.9E-6	2.18	0.60	133	158						
47.49	45	38.167	0.229	0.043	143.6E-6	2.12	0.60	128	152						
62.49	60	35.955	0.215	0.056	138.3E-6	2.06	0.59	123	146						
77.49	75	33.834	0.203	0.069	132.9E-6	1.99	0.59	118	140						
92.49	90	31.800	0.191	0.081	127.6E-6	1.93	0.58	113	134						
107.5	105	29.842	0.179	0.093	122.3E-6	1.87	0.57	108	128						
122.5	120	27.972	0.168	0.104	116.9E-6	1.81	0.57	104	123						
137.5	135	26.190	0.157	0.115	111.6E-6	1.75	0.56	99	117						
152.5	150	24.507	0.147	0.125	106.3E-6	1.70	0.55	95	112						
167.5	165	22.895	0.137	0.134	100.9E-6	1.64	0.54	91	107						
182.5	180	21.358	0.128	0.144	95.61E-6	1.58	0.53	86	102						
197.5	195	19.904	0.119	0.152	90.27E-6	1.53	0.52	82	97						
212.5	210	18.538	0.111	0.160	84.94E-6	1.48	0.51	78	93						
227.5	225	17.245	0.103	0.168	79.61E-6	1.42	0.49	75	88						
242.5	240	16.032	0.096	0.175	74.28E-6	1.37	0.48	71	84						
257.5	255	14.895	0.089	0.182	68.94E-6	1.32	0.46	68	80						
272.5	270	13.837	0.083	0.189	63.61E-6	1.28	0.44	64	76						

Table K.3 16 mm circular orifice results (7.55% CMC)

Time	Diff.Time	Mass in tank	Height	Diff.Height	Flow rate	Orifice									
						[s]	[s]	[kg]	[m]	[m]	[m ³ /s]	[m/s]	C _d	Re _{MR}	Re ₂
1.658	0	45.312	0.272	0	0	0	0	0	0	0	0	0	0	0	0
11.66	10	42.299	0.254	0.0181	282.2E-6	2.23	0.63	165	196						
21.66	20	39.411	0.236	0.0354	270.7E-6	2.15	0.62	157	186						
31.66	30	36.640	0.220	0.0520	259.2E-6	2.08	0.62	150	177						
41.66	40	34.004	0.204	0.0678	247.7E-6	2.00	0.61	142	169						
51.66	50	31.475	0.189	0.0829	236.1E-6	1.92	0.61	135	160						
61.66	60	29.078	0.174	0.0973	224.6E-6	1.85	0.60	128	152						
71.66	70	26.796	0.161	0.1110	213.1E-6	1.78	0.59	121	143						
81.66	80	24.646	0.148	0.1239	201.5E-6	1.70	0.59	114	135						
91.66	90	22.609	0.136	0.1361	190.0E-6	1.63	0.58	108	128						
101.7	100	20.690	0.124	0.1476	178.5E-6	1.56	0.57	102	120						
111.7	110	18.888	0.113	0.1584	167.0E-6	1.49	0.55	95	113						
121.7	120	17.205	0.103	0.1685	155.4E-6	1.42	0.54	90	106						
131.7	130	15.636	0.094	0.1779	143.9E-6	1.36	0.53	84	99						
141.7	140	14.176	0.085	0.1866	132.4E-6	1.29	0.51	79	93						

Table K.4 20 mm circular orifice results (7.55% CMC)

Time	Diff.Time	Mass in tank	Height	Diff.Height	Flow rate	Orifice Velocity	C_d	Re_{MR}	Re_2
[s]	[s]	[kg]	[m]	[m]	[m³/s]	[m/s]			
0.825	0.00	45.341	0.272	0	0	0	0	0	0
7.492	6.67	42.163	0.253	0.019	447.3E-6	2.23	0.64	190	225
14.16	13.33	39.117	0.234	0.037	428.7E-6	2.14	0.63	181	214
20.83	20.00	36.196	0.217	0.055	410.0E-6	2.06	0.63	171	203
27.49	26.67	33.415	0.200	0.071	391.4E-6	1.98	0.63	162	192
34.16	33.33	30.746	0.184	0.087	372.8E-6	1.90	0.62	153	181
40.83	40.00	28.221	0.169	0.103	354.2E-6	1.82	0.62	145	171
47.49	46.67	25.821	0.155	0.117	335.5E-6	1.74	0.61	136	161
54.16	53.33	23.556	0.141	0.131	316.9E-6	1.66	0.60	128	151
60.83	60.00	21.423	0.128	0.143	298.3E-6	1.59	0.60	120	142
67.49	66.67	19.422	0.116	0.155	279.6E-6	1.51	0.59	112	133
74.16	73.33	17.542	0.105	0.167	261.0E-6	1.44	0.58	105	124
80.83	80.00	15.799	0.095	0.177	242.4E-6	1.36	0.56	97	115
87.49	86.67	14.176	0.085	0.187	223.8E-6	1.29	0.55	91	107
94.16	93.33	12.686	0.076	0.196	205.1E-6	1.22	0.53	84	99
100.8	100.0	11.316	0.068	0.204	186.5E-6	1.15	0.51	78	92
107.5	106.7	10.055	0.060	0.211	167.9E-6	1.09	0.49	72	85

Square orifices

Table K.5 8 mm square orifice results (7.55% CMC)

Time	Diff.Time	Mass in tank	Height	Diff.Height	Flow rate	Orifice Velocity	C_d	Re_2
[s]	[s]	[kg]	[m]	[m]	[m³/s]	[m/s]		
4.158	0	43.283	0.259	0	0	0	0	0
29.16	25	41.159	0.247	0.013	78.61E-6	2.20	0.56	123
54.16	50	39.097	0.234	0.025	76.08E-6	2.14	0.55	119
79.16	75	37.106	0.222	0.037	73.54E-6	2.09	0.55	115
104.2	100	35.210	0.211	0.048	71.00E-6	2.03	0.54	111
129.2	125	33.367	0.200	0.059	68.46E-6	1.98	0.54	107
154.2	150	31.602	0.189	0.070	65.93E-6	1.93	0.53	103
179.2	175	29.930	0.179	0.080	63.39E-6	1.88	0.53	99
204.2	200	28.311	0.170	0.090	60.85E-6	1.82	0.52	96
229.2	225	26.773	0.160	0.099	58.31E-6	1.77	0.51	92
254.2	250	25.289	0.152	0.108	55.78E-6	1.72	0.50	88
279.2	275	23.886	0.143	0.116	53.24E-6	1.68	0.49	85
304.2	300	22.560	0.135	0.124	50.70E-6	1.63	0.48	82
329.2	325	21.291	0.128	0.132	48.16E-6	1.58	0.47	79
354.2	350	20.084	0.120	0.139	45.63E-6	1.54	0.46	76
379.2	375	18.937	0.113	0.146	43.09E-6	1.49	0.45	73
404.2	400	17.870	0.107	0.152	40.55E-6	1.45	0.43	70
429.2	425	16.851	0.101	0.158	38.01E-6	1.41	0.42	67
454.2	450	15.897	0.095	0.164	35.48E-6	1.37	0.40	64
479.2	475	14.977	0.090	0.170	32.94E-6	1.33	0.39	62
504.2	500	14.131	0.085	0.175	30.40E-6	1.29	0.37	60
529.2	525	13.327	0.080	0.180	27.86E-6	1.25	0.35	57
554.2	550	12.581	0.075	0.184	25.32E-6	1.22	0.32	55
579.2	575	11.889	0.071	0.188	22.79E-6	1.18	0.30	53

Table K.6 12 mm square orifice results (7.55% CMC)

Time	Diff.Time	Mass in tank	Height	Diff.Height	Flow rate	Orifice Velocity	C _d	Re ₂
[s]	[s]	[kg]	[m]	[m]	[m ³ /s]	[m/s]		
2.492	0	43.63	0.262	0	0	0	0	0
17.49	15	40.49	0.243	0.019	194.9E-6	2.18	0.62	158
32.49	30	37.49	0.225	0.037	185.9E-6	2.10	0.61	150
47.49	45	34.63	0.208	0.054	177.0E-6	2.02	0.61	142
62.49	60	31.95	0.191	0.070	168.0E-6	1.94	0.60	134
77.49	75	29.39	0.176	0.085	159.0E-6	1.86	0.59	127
92.49	90	26.97	0.162	0.100	150.1E-6	1.78	0.58	120
107.5	105	24.71	0.148	0.113	141.1E-6	1.70	0.57	113
122.5	120	22.57	0.135	0.126	132.1E-6	1.63	0.56	106
137.5	135	20.60	0.123	0.138	123.2E-6	1.56	0.55	100
152.5	150	18.74	0.112	0.149	114.2E-6	1.48	0.53	93
167.5	165	17.02	0.102	0.159	105.3E-6	1.41	0.51	88
182.5	180	15.44	0.093	0.169	96.30E-6	1.35	0.49	82
197.5	195	13.97	0.084	0.178	87.34E-6	1.28	0.47	77
212.5	210	12.65	0.076	0.186	78.38E-6	1.22	0.44	72

Table K.7 16 mm square orifice results (7.55% CMC)

Time	Diff.Time	Mass in tank	Height	Diff.Height	Flow rate	Orifice Velocity	C _d	Re ₂
[s]	[s]	[kg]	[m]	[m]	[m ³ /s]	[m/s]		
1.658	0.00	42.991	0.258	0	0	0	0	0
11.66	10	39.306	0.236	0.022	341.8E-6	2.15	0.62	186
21.66	20	35.799	0.215	0.043	323.9E-6	2.05	0.62	174
31.66	30	32.509	0.195	0.063	306.0E-6	1.96	0.61	163
41.66	40	29.380	0.176	0.082	288.1E-6	1.86	0.60	152
51.66	50	26.474	0.159	0.099	270.1E-6	1.76	0.60	142
61.66	60	23.765	0.142	0.115	252.2E-6	1.67	0.59	132
71.66	70	21.243	0.127	0.130	234.3E-6	1.58	0.58	122
81.66	80	18.929	0.113	0.144	216.4E-6	1.49	0.57	113
91.66	90	16.772	0.101	0.157	198.5E-6	1.40	0.55	104
101.7	100	14.799	0.089	0.169	180.6E-6	1.32	0.53	96
111.7	110	13.041	0.078	0.180	162.7E-6	1.24	0.51	88
121.7	120	11.428	0.068	0.189	144.8E-6	1.16	0.49	80
131.7	130	9.992	0.060	0.198	126.9E-6	1.08	0.46	73
141.7	140	8.721	0.052	0.205	109.0E-6	1.01	0.42	67
151.7	150	7.616	0.046	0.212	91.07E-6	0.95	0.37	61

Table K.8 20 mm square orifice results (7.55% CMC)

Time	Diff.Time	Mass in tank	Height	Diff.Height	Flow rate	Orifice Velocity	C _d	Re ₂
[s]	[s]	[kg]	[m]	[m]	[m ³ /s]	[m/s]		
0.825	0	43.572	0.261	0	555.2E-6	2.19	0.63	219
5.825	5	40.641	0.244	0.018	532.9E-6	2.11	0.63	209
10.83	10	37.801	0.227	0.035	510.5E-6	2.03	0.63	198
15.83	15	35.092	0.210	0.051	488.2E-6	1.95	0.62	188
20.83	20	32.465	0.195	0.067	465.8E-6	1.88	0.62	178
25.83	25	29.974	0.180	0.081	443.5E-6	1.80	0.61	169
30.83	30	27.597	0.165	0.096	421.1E-6	1.73	0.61	159
35.83	35	25.349	0.152	0.109	398.8E-6	1.65	0.60	150
40.83	40	23.224	0.139	0.122	376.4E-6	1.58	0.60	141
45.83	45	21.187	0.127	0.134	354.1E-6	1.51	0.59	132
50.83	50	19.293	0.116	0.146	331.7E-6	1.43	0.58	124
55.83	55	17.509	0.105	0.156	309.4E-6	1.36	0.57	115
60.83	60	15.836	0.095	0.166	287.0E-6	1.30	0.55	108
65.83	65	14.284	0.086	0.176	264.7E-6	1.23	0.54	100
70.83	70	12.852	0.077	0.184	242.3E-6	1.16	0.52	93
75.83	75	11.526	0.069	0.192	220.0E-6	1.10	0.50	86
80.83	80	10.290	0.062	0.199				

Triangular orifices

Table K.9 8 mm triangular orifice results (7.55% CMC)

Time	Diff.Time	Mass in tank	Height	Diff.Height	Flow rate	Orifice Velocity	C _d	Re ₂
[s]	[s]	[kg]	[m]	[m]	[m ³ /s]	[m/s]		
4.158	0	45.187	0.271	0	0	0	0	0
29.16	25	42.327	0.254	0.017	105.5E-6	2.23	0.57	126
54.16	50	39.588	0.237	0.034	101.1E-6	2.16	0.56	120
79.16	75	36.984	0.222	0.049	96.66E-6	2.09	0.55	115
104.2	100	34.504	0.207	0.064	92.23E-6	2.01	0.55	109
129.2	125	32.160	0.193	0.078	87.80E-6	1.94	0.54	104
154.2	150	29.934	0.179	0.091	83.37E-6	1.88	0.53	99
179.2	175	27.826	0.167	0.104	78.94E-6	1.81	0.52	94
204.2	200	25.849	0.155	0.116	74.51E-6	1.74	0.51	90
229.2	225	23.984	0.144	0.127	70.08E-6	1.68	0.50	85
254.2	250	22.236	0.133	0.138	65.65E-6	1.62	0.49	81
279.2	275	20.615	0.124	0.147	61.22E-6	1.56	0.47	77
304.2	300	19.075	0.114	0.156	56.79E-6	1.50	0.45	73
329.2	325	17.660	0.106	0.165	52.36E-6	1.44	0.43	69
354.2	350	16.346	0.098	0.173	47.93E-6	1.39	0.41	66
379.2	375	15.123	0.091	0.180	43.50E-6	1.33	0.39	62
404.2	400	13.993	0.084	0.187	39.07E-6	1.28	0.36	59
429.2	425	12.958	0.078	0.193	34.64E-6	1.23	0.34	56

Table K.10 12 mm triangular orifice results (7.55% CMC)

Time [s]	Diff.Time [s]	Mass in tank [kg]	Height [m]	Diff.Height [m]	Flow rate [m ³ /s]	Orifice Velocity		
						C _d	Re ₂	
1.658	0	43.883	0.263	0	0	0	0	0
11.66	10	41.161	0.247	0.016	252.1E-6	2.20	0.61	159
21.66	20	38.571	0.231	0.032	242.3E-6	2.13	0.61	153
31.66	30	36.081	0.216	0.047	232.6E-6	2.06	0.60	146
41.66	40	33.711	0.202	0.061	222.8E-6	1.99	0.60	139
51.66	50	31.442	0.188	0.075	213.0E-6	1.92	0.59	133
61.66	60	29.285	0.176	0.087	203.2E-6	1.86	0.58	127
71.66	70	27.216	0.163	0.100	193.4E-6	1.79	0.58	120
81.66	80	25.246	0.151	0.112	183.6E-6	1.72	0.57	114
91.66	90	23.418	0.140	0.123	173.8E-6	1.66	0.56	109
101.7	100	21.641	0.130	0.133	164.1E-6	1.60	0.55	103
111.7	110	20.008	0.120	0.143	154.3E-6	1.53	0.54	98
121.7	120	18.436	0.110	0.153	144.5E-6	1.47	0.52	92
131.7	130	16.980	0.102	0.161	134.7E-6	1.41	0.51	87
141.7	140	15.618	0.094	0.169	124.9E-6	1.36	0.49	83
151.7	150	14.347	0.086	0.177	115.1E-6	1.30	0.47	78
161.7	160	13.177	0.079	0.184	105.4E-6	1.24	0.45	73

Table K.11 16 mm triangular orifice results (7.55% CMC)

Time [s]	Diff.Time [s]	Mass in tank [kg]	Height [m]	Diff.Height [m]	Flow rate [m ³ /s]	Orifice Velocity		
						C _d	Re ₂	[m ³ /s]
1.242	0	43.481	0.261	0	0	0	0	0
8.742	8	39.943	0.239	0.021	441.3E-6	2.17	0.63	186
16.24	15	36.580	0.219	0.041	418.9E-6	2.07	0.63	175
23.74	23	33.378	0.200	0.061	396.5E-6	1.98	0.62	164
31.24	30	30.370	0.182	0.079	374.2E-6	1.89	0.62	154
38.74	38	27.525	0.165	0.096	351.8E-6	1.80	0.61	144
46.24	45	24.867	0.149	0.112	329.4E-6	1.71	0.60	134
53.74	53	22.386	0.134	0.126	307.0E-6	1.62	0.59	125
61.24	60	20.066	0.120	0.140	284.6E-6	1.54	0.58	116
68.74	68	17.938	0.108	0.153	262.2E-6	1.45	0.56	108
76.24	75	15.966	0.096	0.165	239.9E-6	1.37	0.55	99
83.74	83	14.188	0.085	0.176	217.5E-6	1.29	0.52	92
91.24	90	12.547	0.075	0.185	195.1E-6	1.21	0.50	84

Table K.12 20 mm triangular orifice results (7.55% CMC)

Time [s]	Diff.Time [s]	Mass in tank [kg]	Height [m]	Diff.Height [m]	Flow rate [m ³ /s]	Orifice Velocity		
						C _d	Re ₂	
0.825	0	43.464	0.260	0	0	0	0	0
5.825	5	39.665	0.238	0.023	722.0E-6	2.16	0.64	215
10.83	10	35.967	0.216	0.045	683.3E-6	2.06	0.64	201
15.83	15	32.492	0.195	0.066	644.7E-6	1.95	0.64	188
20.83	20	29.244	0.175	0.085	606.0E-6	1.85	0.63	175
25.83	25	26.194	0.157	0.104	567.4E-6	1.76	0.62	162
30.83	30	23.314	0.140	0.121	528.7E-6	1.66	0.62	150
35.83	35	20.649	0.124	0.137	490.0E-6	1.56	0.61	138
40.83	40	18.209	0.109	0.151	451.4E-6	1.46	0.60	127
45.83	45	15.969	0.096	0.165	412.7E-6	1.37	0.58	116
50.83	50	13.908	0.083	0.177	374.1E-6	1.28	0.56	106
55.83	55	12.064	0.072	0.188	335.4E-6	1.19	0.54	96
60.83	60	10.409	0.062	0.198	296.8E-6	1.11	0.52	87

APPENDIX L: 6.58% CMC solution

Rheological and physical Parameters

n=	0.700
k=	0.882 Pa.s ⁿ
k'=	0.947 Pa.s ⁿ
Density=	1037 kg/m ³
g=	9.81 m/s ²

Circular orifices

Table L.1 8 mm circular orifice results (6.58% CMC)

Time [s]	Diff.Time [s]	Mass in tank [kg]	Height [m]	Diff.Height [m]	Flow rate [m ³ /s]	Orifice Velocity			
						Velocity [m/s]	C _d	Re _{MR}	Re ₂
4.158	0.00	47.434	0.286	0.000	0	0	0	0	0
37.49	33.33	44.826	0.270	0.016	73.57E-6	2.30	0.63	192	222
70.83	66.67	42.321	0.255	0.031	71.10E-6	2.24	0.63	185	214
104.2	100.0	39.904	0.241	0.045	68.62E-6	2.17	0.62	178	206
137.5	133.3	37.575	0.226	0.059	66.15E-6	2.11	0.62	171	198
170.8	166.7	35.320	0.213	0.073	63.67E-6	2.04	0.61	165	190
204.2	200.0	33.170	0.200	0.086	61.20E-6	1.98	0.61	158	182
237.5	233.3	31.095	0.187	0.098	58.73E-6	1.92	0.60	152	175
270.8	266.7	29.120	0.176	0.110	56.25E-6	1.86	0.60	145	167
304.2	300.0	27.228	0.164	0.122	53.78E-6	1.79	0.59	139	160
337.5	333.3	25.411	0.153	0.133	51.30E-6	1.73	0.58	133	153
370.8	366.7	23.680	0.143	0.143	48.83E-6	1.67	0.57	127	146
404.2	400.0	22.029	0.133	0.153	46.35E-6	1.61	0.57	121	140
437.5	433.3	20.479	0.123	0.162	43.88E-6	1.56	0.56	116	133
470.8	466.7	18.992	0.114	0.171	41.40E-6	1.50	0.54	110	127
504.2	500.0	17.603	0.106	0.180	38.93E-6	1.44	0.53	105	121
537.5	533.3	16.276	0.098	0.188	36.45E-6	1.39	0.52	100	115

Table L.2 12 mm circular orifice results (6.58% CMC)

Time [s]	Diff.Height [s]	Mass in tank [Kg]	Height [m]	Diff.Height [m]	Flow rate [m ³ /s]	Orifice Velocity			
						Velocity [m/s]	C _d	Re	Re ₂
2.492	0	50.851	0.306	0	0	0	0	0	0
17.49	15	48.029	0.289	0.017	178.2E-6	2.38	0.66	267	308
32.49	30	45.298	0.273	0.033	172.5E-6	2.31	0.65	257	296
47.49	45	42.661	0.257	0.049	166.9E-6	2.25	0.65	247	285
62.49	60	40.094	0.242	0.065	161.2E-6	2.18	0.65	237	274
77.49	75	37.653	0.227	0.080	155.5E-6	2.11	0.65	228	263
92.49	90	35.273	0.213	0.094	149.9E-6	2.04	0.64	218	252
107.5	105	32.993	0.199	0.108	144.2E-6	1.98	0.64	209	241
122.5	120	30.781	0.186	0.121	138.6E-6	1.91	0.64	200	230
137.5	135	28.678	0.173	0.134	132.9E-6	1.84	0.63	191	220
152.5	150	26.658	0.161	0.146	127.2E-6	1.78	0.63	182	210
167.5	165	24.726	0.149	0.157	121.6E-6	1.71	0.62	173	200
182.5	180	22.882	0.138	0.169	115.9E-6	1.64	0.62	165	190
197.5	195	21.143	0.127	0.179	110.3E-6	1.58	0.61	156	180
212.5	210	19.442	0.117	0.189	104.6E-6	1.52	0.61	148	171
227.5	225	17.864	0.108	0.199	98.95E-6	1.45	0.60	140	162
242.5	240	16.360	0.099	0.208	93.29E-6	1.39	0.59	132	153

Table L.3 16 mm circular orifice results (6.58% CMC)

Time [s]	Diff.Time [s]	Mass in tank [kg]	Height [m]	Diff.Height [m]	Flow rate [m ³ /s]	Orifice Velocity		
						C _d	Re _{MR}	Re ₂
1.658	0	50.090	0.302	0	0	0	0	0
11.66	10	46.760	0.282	0.020	315.4E-6	2.35	0.66	320
21.66	20	43.553	0.262	0.039	303.6E-6	2.27	0.66	306
31.66	30	40.471	0.244	0.058	291.7E-6	2.19	0.66	292
41.66	40	37.515	0.226	0.076	279.9E-6	2.11	0.66	278
51.66	50	34.656	0.209	0.093	268.1E-6	2.02	0.66	264
61.66	60	31.945	0.193	0.109	256.3E-6	1.94	0.65	250
71.66	70	29.351	0.177	0.125	244.5E-6	1.86	0.65	237
81.66	80	26.868	0.162	0.140	232.6E-6	1.78	0.65	224
91.66	90	24.503	0.148	0.154	220.8E-6	1.70	0.64	211
101.7	100	22.302	0.134	0.167	209.0E-6	1.62	0.64	198
111.7	110	20.188	0.122	0.180	197.2E-6	1.55	0.63	186
121.7	120	18.207	0.110	0.192	185.4E-6	1.47	0.63	174
131.7	130	16.346	0.099	0.203	173.5E-6	1.39	0.62	162
								187

Table L.4 20 mm circular orifice results (6.58% CMC)

Time [s]	Diff.Time [s]	Mass in tank [kg]	Height [m]	Diff.Height [m]	Flow rate [m ³ /s]	Orifice Velocity		
						C _d	Re _{MR}	Re ₂
0.825	0	50.472	0.304	0	0	0	0	0
5.825	5	47.854	0.288	0.0158	500.1E-6	2.38	0.67	380
10.83	10	45.309	0.273	0.0311	486.0E-6	2.31	0.67	367
15.83	15	42.794	0.258	0.0463	471.9E-6	2.25	0.67	354
20.83	20	40.435	0.244	0.0605	457.8E-6	2.19	0.66	341
25.83	25	38.066	0.229	0.0748	443.7E-6	2.12	0.66	328
30.83	30	35.818	0.216	0.0883	429.5E-6	2.06	0.66	315
35.83	35	33.622	0.203	0.102	415.4E-6	1.99	0.66	302
40.83	40	31.472	0.190	0.115	401.3E-6	1.93	0.66	290
45.83	45	29.426	0.177	0.127	387.2E-6	1.87	0.66	277
50.83	50	27.497	0.166	0.138	373.1E-6	1.80	0.66	265
55.83	55	25.578	0.154	0.150	359.0E-6	1.74	0.65	253
60.83	60	23.763	0.143	0.161	344.8E-6	1.68	0.65	241
65.83	65	22.005	0.133	0.172	330.7E-6	1.61	0.65	229
70.83	70	20.318	0.122	0.182	316.6E-6	1.55	0.65	218
75.83	75	18.724	0.113	0.191	302.5E-6	1.49	0.64	207
80.83	80	17.181	0.104	0.201	288.4E-6	1.43	0.64	195
85.83	85	15.746	0.095	0.209	274.3E-6	1.36	0.64	185
								213

Square orifices

Table L.5 8 mm square orifice results (6.58% CMC)

Time [s]	Diff.Time [s]	Mass in tank [kg]	Height [m]	Diff.Height [m]	Flow rate [m ³ /s]	Orifice Velocity [m/s]	C _d	Re ₂
4.158	0	50.123	0.302	0	0	0	0	0
29.16	25	47.497	0.286	0.016	99.24E-6	2.37	0.65	230
54.16	50	44.959	0.271	0.031	96.13E-6	2.31	0.65	222
79.16	75	42.507	0.256	0.046	93.02E-6	2.24	0.65	214
104.2	100	40.121	0.242	0.060	89.91E-6	2.18	0.64	206
129.2	125	37.841	0.228	0.074	86.80E-6	2.12	0.64	198
154.2	150	35.633	0.215	0.087	83.69E-6	2.05	0.63	191
179.2	175	33.497	0.202	0.100	80.58E-6	1.99	0.63	183
204.2	200	31.473	0.190	0.112	77.48E-6	1.93	0.62	176
229.2	225	29.493	0.178	0.124	74.37E-6	1.87	0.62	169
254.2	250	27.608	0.166	0.136	71.26E-6	1.81	0.61	161
279.2	275	25.808	0.156	0.147	68.15E-6	1.75	0.61	155
304.2	300	24.081	0.145	0.157	65.04E-6	1.69	0.60	148
329.2	325	22.438	0.135	0.167	61.93E-6	1.63	0.59	141
354.2	350	20.871	0.126	0.176	58.82E-6	1.57	0.58	135
379.2	375	19.376	0.117	0.185	55.71E-6	1.51	0.57	128
404.2	400	17.953	0.108	0.194	52.60E-6	1.46	0.56	122

Table L.6 12 mm square orifice results (6.58% CMC)

Time [s]	Diff.Time [s]	Mass in tank [kg]	Height [m]	Diff.Height [m]	Flow rate [m ³ /s]	Orifice Velocity [m/s]	C _d	Re ₂
1.658	0	48.831	0.294	0	0	0	0	0
11.66	10	46.419	0.280	0.015	230.0E-6	2.34	0.68	300
21.66	20	44.050	0.265	0.029	223.4E-6	2.28	0.68	290
31.66	30	41.756	0.252	0.043	216.9E-6	2.22	0.68	281
41.66	40	39.560	0.238	0.056	210.4E-6	2.16	0.67	271
51.66	50	37.404	0.225	0.069	203.9E-6	2.10	0.67	261
61.66	60	35.328	0.213	0.081	197.4E-6	2.04	0.67	252
71.66	70	33.312	0.201	0.094	190.9E-6	1.98	0.67	242
81.66	80	31.371	0.189	0.105	184.3E-6	1.93	0.66	233
91.66	90	29.489	0.178	0.117	177.8E-6	1.87	0.66	224
101.7	100	27.694	0.167	0.127	171.3E-6	1.81	0.66	215
111.7	110	25.928	0.156	0.138	164.8E-6	1.75	0.65	206
121.7	120	24.287	0.146	0.148	158.3E-6	1.69	0.65	197
131.7	130	22.659	0.137	0.158	151.7E-6	1.64	0.64	189
141.7	140	21.121	0.127	0.167	145.2E-6	1.58	0.64	180
151.7	150	19.646	0.118	0.176	138.7E-6	1.52	0.63	172
161.7	160	18.245	0.110	0.184	132.2E-6	1.47	0.62	164
171.7	170	16.894	0.102	0.192	125.7E-6	1.41	0.62	156

Table L.7 16 mm square orifice results (6.58% CMC)

Time	Diff.Time	Mass in tank	Height	Diff.Height	Flow rate	Orifice Velocity	C _d	Re ₂
[s]	[s]	[kg]	[m]	[m]	[m ³ /s]	[m/s]		
0.825	0	48.724	0.294	0	0	0	0	0
5.825	5	46.622	0.281	0.013	400.9E-6	2.35	0.67	368
10.83	10	44.579	0.269	0.025	391.3E-6	2.30	0.66	358
15.83	15	42.544	0.256	0.037	381.8E-6	2.24	0.66	347
20.83	20	40.630	0.245	0.049	372.2E-6	2.19	0.66	337
25.83	25	38.707	0.233	0.060	362.7E-6	2.14	0.66	327
30.83	30	36.838	0.222	0.072	353.2E-6	2.09	0.66	316
35.83	35	35.024	0.211	0.083	343.6E-6	2.04	0.66	306
40.83	40	33.269	0.201	0.093	334.1E-6	1.98	0.66	296
45.83	45	31.590	0.190	0.103	324.5E-6	1.93	0.65	286
50.83	50	29.939	0.180	0.113	315.0E-6	1.88	0.65	276
55.83	55	28.309	0.171	0.123	305.5E-6	1.83	0.65	266
60.83	60	26.754	0.161	0.132	295.9E-6	1.78	0.65	257
65.83	65	25.254	0.152	0.141	286.4E-6	1.73	0.65	247
70.83	70	23.758	0.143	0.150	276.8E-6	1.68	0.64	238
75.83	75	22.354	0.135	0.159	267.3E-6	1.63	0.64	229
80.83	80	21.020	0.127	0.167	257.7E-6	1.58	0.64	220
85.83	85	19.676	0.119	0.175	248.2E-6	1.53	0.63	210
90.83	90	18.433	0.111	0.183	238.7E-6	1.48	0.63	202
95.83	95	17.221	0.104	0.190	229.1E-6	1.43	0.63	193
100.8	100	16.063	0.097	0.197	219.6E-6	1.38	0.62	184

Table L.8 20 mm square orifice results (6.58% CMC)

Time	Diff.Time	Mass in tank	Height	Diff.Height	Flow rate	Orifice Velocity	C _d	Re ₂
[s]	[s]	[kg]	[m]	[m]	[m ³ /s]	[m/s]		
0.825	0	48.447	0.292	0	0	0	0	0
5.825	5	45.217	0.273	0.019	618.4E-6	2.31	0.67	422
10.83	10	42.096	0.254	0.038	595.7E-6	2.23	0.67	403
15.83	15	39.080	0.236	0.056	573.1E-6	2.15	0.67	384
20.83	20	36.153	0.218	0.074	550.5E-6	2.07	0.66	365
25.83	25	33.418	0.201	0.091	527.9E-6	1.99	0.66	347
30.83	30	30.735	0.185	0.107	505.3E-6	1.91	0.66	329
35.83	35	28.188	0.170	0.122	482.7E-6	1.83	0.66	311
40.83	40	25.778	0.155	0.137	460.1E-6	1.75	0.66	293
45.83	45	23.465	0.141	0.151	437.5E-6	1.67	0.66	276
50.83	50	21.285	0.128	0.164	414.9E-6	1.59	0.65	259
55.83	55	19.222	0.116	0.176	392.3E-6	1.51	0.65	242
60.83	60	17.254	0.104	0.188	369.7E-6	1.43	0.65	226
65.83	65	15.397	0.093	0.199	347.1E-6	1.35	0.64	210

Triangular orifices

Table L.9 8 mm triangular orifice results (6.58% CMC)

Time	Diff.Time	Mass in tank	Height	Diff.Height	Flow rate	Orifice Velocity	C_d	Re_2
[s]	[s]	[kg]	[m]	[m]	[m³/s]	[m/s]		
4.158	0	48.128	0.290	0	0	0	0	0
29.16	25	44.810	0.270	0.020	125.2E-6	2.30	0.65	221
54.16	50	41.629	0.251	0.039	119.9E-6	2.22	0.65	211
79.16	75	38.586	0.233	0.058	114.7E-6	2.14	0.64	201
104.2	100	35.678	0.215	0.075	109.4E-6	2.05	0.64	191
129.2	125	32.899	0.198	0.092	104.2E-6	1.97	0.63	181
154.2	150	30.276	0.182	0.108	98.94E-6	1.89	0.62	172
179.2	175	27.791	0.167	0.123	93.68E-6	1.81	0.62	162
204.2	200	25.431	0.153	0.137	88.43E-6	1.73	0.61	153
229.2	225	23.215	0.140	0.150	83.18E-6	1.66	0.60	144
254.2	250	21.127	0.127	0.163	77.93E-6	1.58	0.59	136
279.2	275	19.161	0.115	0.175	72.68E-6	1.51	0.58	127
304.2	300	17.328	0.104	0.186	67.42E-6	1.43	0.56	119

Table L.10 12 mm triangular orifice results (6.58% CMC)

Time	Diff.Time	Mass in tank	Height	Diff.Height	Flow rate	Orifice Velocity	C_d	Re_2
[s]	[s]	[kg]	[m]	[m]	[m³/s]	[m/s]		
1.658	0	49.321	0.297	0	0	0	0	0
11.66	10	46.229	0.279	0.019	292.3E-6	2.34	0.67	300
21.66	20	43.249	0.261	0.037	281.8E-6	2.26	0.67	287
31.66	30	40.381	0.243	0.054	271.4E-6	2.19	0.66	274
41.66	40	37.635	0.227	0.070	260.9E-6	2.11	0.66	262
51.66	50	34.977	0.211	0.086	250.4E-6	2.03	0.66	250
61.66	60	32.437	0.195	0.102	240.0E-6	1.96	0.65	238
71.66	70	29.989	0.181	0.117	229.5E-6	1.88	0.65	226
81.66	80	27.670	0.167	0.130	219.1E-6	1.81	0.65	215
91.66	90	25.457	0.153	0.144	208.6E-6	1.74	0.64	203
101.7	100	23.339	0.141	0.157	198.2E-6	1.66	0.64	192
111.7	110	21.342	0.129	0.169	187.7E-6	1.59	0.63	181
121.7	120	19.454	0.117	0.180	177.3E-6	1.52	0.62	171
131.7	130	17.665	0.106	0.191	166.8E-6	1.45	0.62	160

Table L.11 16 mm triangular orifice results (6.58% CMC)

Time	Diff.Time	Mass in tank	Height	Diff.Height	Flow rate	Orifice Velocity	C_d	Re_2
[s]	[s]	[Kg]	[m]	[m]	[m³/s]	[m/s]		
0.825	0.00	49.680	0.299	0	0	0	0	0
7.492	6.667	46.190	0.278	0.021	501.3E-6	2.34	0.67	361
14.16	13.33	42.786	0.258	0.042	481.6E-6	2.25	0.67	344
20.83	20.00	39.521	0.238	0.061	461.9E-6	2.16	0.67	326
27.49	26.67	36.391	0.219	0.080	442.2E-6	2.07	0.66	309
34.16	33.33	33.408	0.201	0.098	422.5E-6	1.99	0.66	293
40.83	40.00	30.530	0.184	0.115	402.8E-6	1.90	0.66	276
47.49	46.67	27.835	0.168	0.132	383.1E-6	1.81	0.66	260
54.16	53.33	25.250	0.152	0.147	363.4E-6	1.73	0.66	244
60.83	60.00	22.804	0.137	0.162	343.7E-6	1.64	0.65	228
67.49	66.67	20.487	0.123	0.176	324.0E-6	1.56	0.65	213
74.16	73.33	18.326	0.110	0.189	304.3E-6	1.47	0.64	198
80.83	80.00	16.307	0.098	0.201	284.6E-6	1.39	0.64	184

Table L.12 20 mm triangular orifice results (6.58% CMC)

Time	Diff.Time	Mass in tank	Height	Diff.Height	Flow rate	Orifice Velocity	C_d	Re_2
[s]	[s]	[Kg]	[m]	[m]	[m³/s]	[m/s]		
0.825	0	48.755	0.294	0	0	0	0	0
5.825	5	44.585	0.269	0.025	791.7E-6	2.30	0.67	418
10.83	10	40.569	0.245	0.049	754.6E-6	2.19	0.66	393
15.83	15	36.742	0.221	0.072	717.5E-6	2.08	0.66	368
20.83	20	33.118	0.200	0.094	680.4E-6	1.98	0.66	344
25.83	25	29.701	0.179	0.115	643.4E-6	1.87	0.66	321
30.83	30	26.431	0.159	0.135	606.3E-6	1.77	0.66	297
35.83	35	23.385	0.141	0.153	569.2E-6	1.66	0.66	275
40.83	40	20.536	0.124	0.170	532.1E-6	1.56	0.66	252
45.83	45	17.893	0.108	0.186	495.0E-6	1.45	0.66	231

APPENDIX M: 5.21% CMC solution

Rheological and physical Parameters

n=	0.79
k=	0.209 Pa.s ⁿ
k'=	0.220 Pa.s ⁿ
Density=	1029 kg/m ³
g=	9.81 m/s ²

Circular orifices

Table M.1 8 mm circular orifice results (5.21% CMC)

Time [s]	Diff.Time [s]	Mass in tank [kg]	Height [m]	Diff.Height [m]	Flow rate [m ³ /s]	Orifice Velocity [m/s]	Orifice		
							C _d	Re _{MR}	Re ₂
4.158	0.00	55.660	0.338	0	0	0	0	0	0
37.49	33.33	52.552	0.319	0.019	89.23E-6	2.50	0.70	465	515
70.83	66.67	49.530	0.301	0.037	86.49E-6	2.43	0.70	449	497
104.2	100.0	46.603	0.283	0.055	83.75E-6	2.36	0.70	433	479
137.5	133.3	43.787	0.266	0.072	81.01E-6	2.28	0.70	417	462
170.8	166.7	41.054	0.249	0.089	78.27E-6	2.21	0.70	401	444
204.2	200.0	38.417	0.233	0.105	75.53E-6	2.14	0.70	385	426
237.5	233.3	35.871	0.218	0.120	72.79E-6	2.07	0.69	369	409
270.8	266.7	33.422	0.203	0.135	70.05E-6	2.00	0.69	354	392
304.2	300.0	31.057	0.189	0.149	67.32E-6	1.92	0.69	339	375
337.5	333.3	28.800	0.175	0.163	64.58E-6	1.85	0.69	323	358
370.8	366.7	26.632	0.162	0.176	61.84E-6	1.78	0.68	308	342
404.2	400.0	24.559	0.149	0.189	59.10E-6	1.71	0.68	294	325
437.5	433.3	22.572	0.137	0.201	56.36E-6	1.64	0.68	279	309
470.8	466.7	20.690	0.126	0.212	53.62E-6	1.57	0.67	265	293
504.2	500.0	18.890	0.115	0.223	50.88E-6	1.50	0.67	251	277
537.5	533.3	17.195	0.104	0.234	48.14E-6	1.43	0.66	237	262
570.8	566.7	15.593	0.095	0.243	45.40E-6	1.36	0.66	223	247

Table M.2 12 mm circular orifice results (5.21% CMC)

Time [s]	Diff.Height [s]	Mass in tank [kg]	Height [m]	Diff.Height [m]	Flow rate [m ³ /s]	Orifice Velocity [m/s]	Orifice		
							C _d	Re _{MR}	Re ₂
2.492	0	56.390	0.342	0	0	0	0	0	0
17.49	15	53.431	0.324	0.018	190.2E-6	2.52	0.66	639	707
32.49	30	50.534	0.307	0.036	185.2E-6	2.45	0.66	618	684
47.49	45	47.717	0.290	0.053	180.2E-6	2.38	0.66	597	660
62.49	60	44.976	0.273	0.069	175.2E-6	2.31	0.66	576	637
77.49	75	42.333	0.257	0.085	170.1E-6	2.25	0.67	555	614
92.49	90	39.733	0.241	0.101	165.1E-6	2.18	0.67	534	591
107.5	105	37.211	0.226	0.116	160.1E-6	2.11	0.67	513	568
122.5	120	34.779	0.211	0.131	155.1E-6	2.04	0.67	493	546
137.5	135	32.417	0.197	0.146	150.1E-6	1.97	0.67	472	523
152.5	150	30.109	0.183	0.160	145.1E-6	1.89	0.67	452	500
167.5	165	27.908	0.169	0.173	140.1E-6	1.82	0.67	432	478
182.5	180	25.774	0.156	0.186	135.1E-6	1.75	0.68	411	455
197.5	195	23.726	0.144	0.198	130.1E-6	1.68	0.68	391	433
212.5	210	21.777	0.132	0.210	125.0E-6	1.61	0.68	371	411
227.5	225	19.889	0.121	0.222	120.0E-6	1.54	0.68	352	389
242.5	240	18.116	0.110	0.232	1.15E-04	1.47	0.69	332	368

Table M.3 16 mm circular orifice results (5.21% CMC)

Time	Diff.Time	Mass in tank	Height	Diff.Height	Flow rate	Orifice Velocity	C _d	Re _{MR}	Re ₂
[s]	[s]	[kg]	[m]	[m]	[m ³ /s]	[m/s]			
1.658	0	54.508	0.331	0	0	0	0	0	0
11.66	10	51.169	0.311	0.020	319.2E-6	2.47	0.64	781	864
21.66	20	47.952	0.291	0.040	309.6E-6	2.39	0.64	751	831
31.66	30	44.815	0.272	0.059	300.0E-6	2.31	0.64	721	798
41.66	40	41.800	0.254	0.077	290.4E-6	2.23	0.64	691	765
51.66	50	38.836	0.236	0.095	280.8E-6	2.15	0.65	661	732
61.66	60	36.003	0.219	0.112	271.2E-6	2.07	0.65	631	699
71.66	70	33.254	0.202	0.129	261.6E-6	1.99	0.65	602	666
81.66	80	30.609	0.186	0.145	252.0E-6	1.91	0.65	572	634
91.66	90	28.046	0.170	0.161	242.4E-6	1.83	0.66	543	601
101.7	100	25.596	0.155	0.176	232.8E-6	1.75	0.66	514	569
111.7	110	23.250	0.141	0.190	223.2E-6	1.66	0.66	485	536
121.7	120	20.972	0.127	0.204	213.6E-6	1.58	0.67	455	504
131.7	130	18.849	0.114	0.217	204.0E-6	1.50	0.67	427	473
141.7	140	16.816	0.102	0.229	194.4E-6	1.42	0.68	399	441
151.7	150	14.891	0.090	0.241	184.8E-6	1.33	0.69	370	410

Table M.4 20 mm circular orifice results (5.21% CMC)

Time	Diff.Time	Mass in tank	Height	Diff.Height	Flow rate	Orifice Velocity	C _d	Re _{MR}	Re ₂
[s]	[s]	[kg]	[m]	[m]	[m ³ /s]	[m/s]			
0.825	0	57.294	0.348	0	0	0	0	0	0
5.825	5	54.673	0.332	0.016	505.5E-6	2.55	0.63	969	1073
10.83	10	52.071	0.316	0.032	494.2E-6	2.49	0.63	941	1042
15.83	15	49.544	0.301	0.047	483.0E-6	2.43	0.63	913	1011
20.83	20	47.066	0.286	0.062	471.7E-6	2.37	0.63	885	980
25.83	25	44.644	0.271	0.077	460.5E-6	2.31	0.63	858	949
30.83	30	42.321	0.257	0.091	449.2E-6	2.25	0.63	830	919
35.83	35	40.024	0.243	0.105	438.0E-6	2.18	0.64	803	888
40.83	40	37.805	0.230	0.118	426.7E-6	2.12	0.64	776	858
45.83	45	35.623	0.216	0.132	415.5E-6	2.06	0.64	748	828
50.83	50	33.508	0.203	0.144	404.3E-6	2.00	0.64	721	798
55.83	55	31.451	0.191	0.157	393.0E-6	1.94	0.64	694	768
60.83	60	29.447	0.179	0.169	381.8E-6	1.87	0.65	667	738
65.83	65	27.507	0.167	0.181	370.5E-6	1.81	0.65	640	708
70.83	70	25.598	0.155	0.192	359.3E-6	1.75	0.65	613	678
75.83	75	23.769	0.144	0.204	348.0E-6	1.68	0.66	586	648
80.83	80	21.988	0.134	0.214	336.8E-6	1.62	0.66	559	619
85.83	85	20.288	0.123	0.225	325.5E-6	1.55	0.66	532	589
90.83	90	18.639	0.113	0.235	314.3E-6	1.49	0.67	506	560
95.83	95	17.037	0.103	0.244	303.1E-6	1.42	0.67	479	530

Square orifices

Table M.5 8 mm square orifice results (5.21% CMC)

Time	Diff.Time	Mass in tank	Height	Diff.Height	Flow rate	Orifice Velocity	C _d	Re ₂
[s]	[s]	[kg]	[m]	[m]	[m ³ /s]	[m/s]		
4.158	0	55.686	0.338	0	0	0	0	0
29.16	25	52.759	0.320	0.018	112.8E-6	2.51	0.70	509
54.16	50	49.914	0.303	0.035	109.6E-6	2.44	0.70	492
79.16	75	47.130	0.286	0.052	106.3E-6	2.37	0.70	475
104.2	100	44.431	0.270	0.068	103.1E-6	2.30	0.70	459
129.2	125	41.815	0.254	0.084	99.9E-6	2.23	0.70	442
154.2	150	39.270	0.238	0.100	96.7E-6	2.16	0.69	426
179.2	175	36.811	0.224	0.115	93.4E-6	2.09	0.69	409
204.2	200	34.493	0.209	0.129	90.2E-6	2.03	0.69	394
229.2	225	32.215	0.196	0.143	87.0E-6	1.96	0.69	378
254.2	250	30.010	0.182	0.156	83.8E-6	1.89	0.69	362
279.2	275	27.878	0.169	0.169	80.5E-6	1.82	0.69	346
304.2	300	25.847	0.157	0.181	77.32E-6	1.75	0.69	331
329.2	325	23.884	0.145	0.193	74.10E-6	1.69	0.68	315
354.2	350	22.031	0.134	0.204	70.88E-6	1.62	0.68	300
379.2	375	20.250	0.123	0.215	67.65E-6	1.55	0.68	285
404.2	400	18.555	0.113	0.225	64.43E-6	1.49	0.67	271
429.2	425	16.954	0.103	0.235	61.21E-6	1.42	0.67	256

Table M.6 12 mm square orifice results (5.21% CMC)

Time	Diff.Time	Mass in tank	Height	Diff.Height	Flow rate	Orifice Velocity	C _d	Re ₂
[s]	[s]	[kg]	[m]	[m]	[m ³ /s]	[m/s]		
2.492	0	55.830	0.339	0	0	0	0	0
17.49	15	51.877	0.315	0.024	252.5E-6	2.49	0.70	694
32.49	30	48.087	0.292	0.047	242.9E-6	2.39	0.70	663
47.49	45	44.413	0.270	0.069	233.3E-6	2.30	0.70	632
62.49	60	40.889	0.248	0.091	223.7E-6	2.21	0.70	601
77.49	75	37.493	0.228	0.111	214.1E-6	2.11	0.70	570
92.49	90	34.259	0.208	0.131	204.5E-6	2.02	0.70	540
107.5	105	31.159	0.189	0.150	194.9E-6	1.93	0.70	510
122.5	120	28.202	0.171	0.168	185.3E-6	1.83	0.70	480
137.5	135	25.417	0.154	0.185	175.7E-6	1.74	0.70	451
152.5	150	22.778	0.138	0.201	166.1E-6	1.65	0.70	422
167.5	165	20.296	0.123	0.216	156.5E-6	1.55	0.70	393
182.5	180	17.965	0.109	0.230	146.9E-6	1.46	0.69	365
197.5	195	15.777	0.096	0.243	137.3E-6	1.37	0.69	338
212.5	210	13.750	0.083	0.256	127.7E-6	1.28	0.69	311

Table M.7 16 mm square orifice results (5.21% CMC)

Time	Diff.Time	Mass in tank	Height	Diff.Height	Flow rate	Orifice Velocity	C _d	Re ₂
[s]	[s]	[kg]	[m]	[m]	[m ³ /s]	[m/s]		
0.825	0	54.391	0.330	0	0	0	0	0
5.825	5	52.248	0.317	0.013	408.2E-6	2.49	0.64	874
10.83	10	50.177	0.305	0.026	400.4E-6	2.44	0.64	853
15.83	15	48.142	0.292	0.038	392.6E-6	2.39	0.64	832
20.83	20	46.161	0.280	0.050	384.8E-6	2.35	0.64	811
25.83	25	44.131	0.268	0.062	377.0E-6	2.29	0.64	790
30.83	30	42.246	0.257	0.074	369.2E-6	2.24	0.64	769
35.83	35	40.351	0.245	0.085	361.4E-6	2.19	0.64	748
40.83	40	38.532	0.234	0.096	353.6E-6	2.14	0.64	727
45.83	45	36.723	0.223	0.107	345.8E-6	2.09	0.64	707
50.83	50	34.959	0.212	0.118	338.0E-6	2.04	0.65	686
55.83	55	33.276	0.202	0.128	330.2E-6	1.99	0.65	666
60.83	60	31.600	0.192	0.138	322.4E-6	1.94	0.65	645
65.83	65	29.940	0.182	0.148	314.6E-6	1.89	0.65	624
70.83	70	28.326	0.172	0.158	306.8E-6	1.84	0.65	604
75.83	75	26.779	0.163	0.168	299.0E-6	1.79	0.65	584
80.83	80	25.246	0.153	0.177	291.3E-6	1.73	0.65	563
85.83	85	23.758	0.144	0.186	283.5E-6	1.68	0.66	543
90.83	90	22.343	0.136	0.195	275.7E-6	1.63	0.66	523
95.83	95	20.911	0.127	0.203	267.9E-6	1.58	0.66	503
100.8	100	19.597	0.119	0.211	260.1E-6	1.53	0.66	483
105.8	105	18.275	0.111	0.219	252.3E-6	1.48	0.67	463
110.8	110	16.961	0.103	0.227	244.5E-6	1.42	0.67	443

Table M.8 20 mm square orifice results (5.21% CMC)

Time	Diff.Time	Mass in tank	Height	Diff.Height	Flow rate	Orifice Velocity	C _d	Re ₂
[s]	[s]	[kg]	[m]	[m]	[m ³ /s]	[m/s]		
0.825	0	52.464	0.319	0	0	0	0	0
5.825	5	49.246	0.299	0.020	618.4E-6	2.42	0.64	1006
10.83	10	46.133	0.280	0.038	599.1E-6	2.34	0.64	967
15.83	15	43.070	0.262	0.057	579.9E-6	2.27	0.64	928
20.83	20	40.183	0.244	0.075	560.6E-6	2.19	0.64	890
25.83	25	37.300	0.226	0.092	541.4E-6	2.11	0.64	851
30.83	30	34.578	0.210	0.109	522.1E-6	2.03	0.64	813
35.83	35	31.930	0.194	0.125	502.9E-6	1.95	0.64	774
40.83	40	29.365	0.178	0.140	483.6E-6	1.87	0.65	736
45.83	45	26.959	0.164	0.155	464.4E-6	1.79	0.65	699
50.83	50	24.624	0.150	0.169	445.1E-6	1.71	0.65	662
55.83	55	22.388	0.136	0.183	425.9E-6	1.63	0.65	625
60.83	60	20.232	0.123	0.196	406.6E-6	1.55	0.65	588
65.83	65	18.192	0.110	0.208	387.4E-6	1.47	0.66	551

Triangular orifices

Table M.9 8 mm triangular orifice results (5.21% CMC)

Time [s]	Diff.Time [s]	Mass in tank [kg]	Height [m]	Diff.Height [m]	Flow rate [m ³ /s]	Orifice Velocity		
						C _d	Re ₂	
4.158	0	55.024	0.334	0	0	0	0	0
29.16	25	51.232	0.311	0.023	145.5E-6	2.47	0.70	498
54.16	50	47.567	0.289	0.045	139.9E-6	2.38	0.70	476
79.16	75	44.038	0.267	0.067	134.4E-6	2.29	0.70	454
104.2	100	40.662	0.247	0.087	128.8E-6	2.20	0.70	433
129.2	125	37.395	0.227	0.107	123.2E-6	2.11	0.70	411
154.2	150	34.293	0.208	0.126	117.7E-6	2.02	0.70	390
179.2	175	31.326	0.190	0.144	112.1E-6	1.93	0.69	370
204.2	200	28.517	0.173	0.161	106.6E-6	1.84	0.69	349
229.2	225	25.841	0.157	0.177	101.0E-6	1.75	0.69	329
254.2	250	23.322	0.142	0.192	95.42E-6	1.67	0.68	309
279.2	275	20.953	0.127	0.207	89.86E-6	1.58	0.68	290
304.2	300	18.713	0.114	0.220	84.29E-6	1.49	0.67	271

Table M.10 12 mm triangular orifice results (5.21% CMC)

Time [s]	Diff.Time [s]	Mass in tank [kg]	Height [m]	Diff.Height [m]	Flow rate [m ³ /s]	Orifice Velocity		
						C _d	Re ₂	
1.658	0	55.068	0.334	0	0	0	0	0
11.66	10	51.858	0.315	0.019	308.3E-6	2.49	0.66	689
21.66	20	48.737	0.296	0.038	299.3E-6	2.41	0.66	664
31.66	30	45.705	0.278	0.057	290.3E-6	2.33	0.66	639
41.66	40	42.756	0.260	0.075	281.4E-6	2.26	0.67	613
51.66	50	39.905	0.242	0.092	272.4E-6	2.18	0.67	588
61.66	60	37.139	0.225	0.109	263.4E-6	2.10	0.67	563
71.66	70	34.502	0.209	0.125	254.4E-6	2.03	0.67	539
81.66	80	31.918	0.194	0.141	245.4E-6	1.95	0.67	514
91.66	90	29.427	0.179	0.156	236.5E-6	1.87	0.67	489
101.7	100	27.031	0.164	0.170	227.5E-6	1.79	0.68	465
111.7	110	24.727	0.150	0.184	218.5E-6	1.72	0.68	440
121.7	120	22.524	0.137	0.198	209.5E-6	1.64	0.68	416
131.7	130	20.425	0.124	0.210	200.6E-6	1.56	0.69	392
141.7	140	18.442	0.112	0.222	191.6E-6	1.48	0.69	369

Table M.11 16 mm triangular orifice results (5.21% CMC)

Time [s]	Diff.Time [s]	Mass in tank [kg]	Height [m]	Diff.Height [m]	Flow rate [m ³ /s]	Orifice Velocity		
						C _d	Re ₂	
1.242	0.0	53.157	0.323	0	0	0	0	
8.742	7.5	49.172	0.299	0.024	501.4E-6	2.42	0.65	
16.24	15.0	45.388	0.276	0.047	482.7E-6	2.33	0.65	
23.74	22.5	41.740	0.253	0.069	463.9E-6	2.23	0.65	
31.24	30.0	38.214	0.232	0.091	445.2E-6	2.13	0.65	
38.74	37.5	34.853	0.212	0.111	426.4E-6	2.04	0.65	
46.24	45.0	31.649	0.192	0.131	407.7E-6	1.94	0.65	
53.74	52.5	28.578	0.174	0.149	388.9E-6	1.85	0.66	
61.24	60.0	25.663	0.156	0.167	370.2E-6	1.75	0.66	
68.74	67.5	22.849	0.139	0.184	351.4E-6	1.65	0.66	
76.24	75.0	20.215	0.123	0.200	332.7E-6	1.55	0.67	
83.74	82.5	17.703	0.107	0.215	313.9E-6	1.45	0.67	

Table M.12 20 mm triangular orifice results (5.21% CMC)

Time [s]	Diff.Time [s]	Mass in tank [kg]	Height [m]	Diff.Height [m]	Flow rate [m ³ /s]	Orifice Velocity		
						C _d	Re ₂	
0.825	0	52.974	0.322	0	0	0	0	
5.825	5	48.757	0.296	0.026	801.6E-6	2.41	0.64	
10.83	10	44.724	0.272	0.050	769.0E-6	2.31	0.64	
15.83	15	40.855	0.248	0.074	736.3E-6	2.21	0.64	
20.83	20	37.168	0.226	0.096	703.7E-6	2.10	0.65	
25.83	25	33.601	0.204	0.118	671.0E-6	2.00	0.65	
30.83	30	30.244	0.184	0.138	638.4E-6	1.90	0.65	
35.83	35	27.019	0.164	0.158	605.8E-6	1.79	0.65	
40.83	40	23.994	0.146	0.176	573.1E-6	1.69	0.65	
45.83	45	21.123	0.128	0.193	540.5E-6	1.59	0.66	
50.83	50	18.457	0.112	0.210	507.8E-6	1.48	0.66	

APPENDIX N: 2.81% CMC solution

Rheological and physical parameters

$$n=n'=0.969$$

$$k=0.017$$

$$\text{Pa.s}^n$$

$$k'=0.017$$

$$\text{Pa.s}^n$$

$$\text{Density}=1016$$

$$\text{kg/m}^3$$

$$g=9.81$$

$$\text{m/s}^2$$

Circular orifices

Table N.1 8 mm circular orifice results (2.81% CMC)

Time [s]	Diff.Time [s]	Mass in tank [kg]	Height [m]	Diff.Height [m]	Flow rate [m³/s]	Orifice Velocity			
						C _d	Re _{MR}	Re ₂	
4.158	0.00	53.882	0.331	0	0	0	0	0	0
37.49	33.33	51.007	0.314	0.018	84.05E-6	2.48	0.67	1523	1546
70.83	66.67	48.196	0.296	0.035	81.83E-6	2.41	0.67	1479	1502
104.2	100.0	45.478	0.280	0.052	79.61E-6	2.34	0.67	1436	1458
137.5	133.3	42.821	0.263	0.068	77.38E-6	2.27	0.67	1392	1413
170.8	166.7	40.231	0.247	0.084	75.16E-6	2.20	0.67	1348	1368
204.2	200.0	37.730	0.232	0.099	72.94E-6	2.13	0.67	1304	1324
237.5	233.3	35.288	0.217	0.114	70.72E-6	2.06	0.68	1260	1279
270.8	266.7	32.929	0.202	0.129	68.50E-6	1.99	0.68	1216	1234
304.2	300.0	30.640	0.188	0.143	66.28E-6	1.92	0.68	1171	1189
337.5	333.3	28.423	0.175	0.157	64.05E-6	1.85	0.68	1127	1144
370.8	366.7	26.286	0.162	0.170	61.83E-6	1.78	0.68	1082	1099
404.2	400.0	24.223	0.149	0.182	59.61E-6	1.71	0.69	1038	1054
437.5	433.3	22.247	0.137	0.195	57.39E-6	1.64	0.69	993	1008
470.8	466.7	20.345	0.125	0.206	55.17E-6	1.57	0.69	948	963
504.2	500.0	18.534	0.114	0.217	52.94E-6	1.50	0.70	904	918
537.5	533.3	16.790	0.103	0.228	50.72E-6	1.42	0.70	859	872

Table N.2 12 mm circular orifice results (2.81% CMC)

Time [s]	Diff.Time [s]	Mass in tank [kg]	Height [m]	Diff.Height [m]	Flow rate [m³/s]	Orifice Velocity			
						C _d	Re _{MR}	Re ₂	
0.825	0	53.237	0.327	0	0	0	0	0	0
5.825	5	50.776	0.312	0.015	482.3E-6	2.48	0.62	3683	3739
10.83	10	48.363	0.297	0.030	470.8E-6	2.42	0.62	3592	3647
15.83	15	45.984	0.283	0.045	459.3E-6	2.36	0.62	3499	3553
20.83	20	43.716	0.269	0.059	447.8E-6	2.30	0.62	3409	3462
25.83	25	41.433	0.255	0.073	436.3E-6	2.24	0.62	3317	3367
30.83	30	39.246	0.241	0.086	424.8E-6	2.18	0.62	3225	3275
35.83	35	37.117	0.228	0.099	413.3E-6	2.12	0.62	3134	3182
40.83	40	35.020	0.215	0.112	401.8E-6	2.06	0.62	3041	3088
45.83	45	33.026	0.203	0.124	390.4E-6	2.00	0.62	2951	2996
50.83	50	31.072	0.191	0.136	378.9E-6	1.94	0.62	2859	2903
55.83	55	29.193	0.180	0.148	367.4E-6	1.88	0.62	2769	2812
60.83	60	27.329	0.168	0.159	355.9E-6	1.82	0.62	2676	2718
65.83	65	25.565	0.157	0.170	344.4E-6	1.76	0.62	2586	2626
70.83	70	23.868	0.147	0.181	332.9E-6	1.70	0.62	2496	2534
75.83	75	22.173	0.136	0.191	321.4E-6	1.64	0.62	2403	2440
80.83	80	20.576	0.127	0.201	309.9E-6	1.58	0.62	2312	2348
85.83	85	19.038	0.117	0.210	298.4E-6	1.52	0.62	2222	2256
90.83	90	17.530	0.108	0.220	286.9E-6	1.45	0.63	2129	2162

Table N.3 16 mm circular orifice results (2.81% CMC)

Time	Diff.Time	Mass in tank	Height	Diff.Height	Flow rate	Orifice Velocity	C _d	Re _{MR}	Re ₂
[s]	[s]	[kg]	[m]	[m]	[m ³ /s]	[m/s]			
1.242	0	53.413	0.328	0	0	0	0	0	0
8.742	8	51.033	0.314	0.015	309.9E-6	2.48	0.62	2976	3021
16.24	15	48.700	0.299	0.029	302.8E-6	2.42	0.62	2905	2949
23.74	23	46.431	0.286	0.043	295.8E-6	2.37	0.62	2834	2878
31.24	30	44.196	0.272	0.057	288.7E-6	2.31	0.62	2763	2806
38.74	38	42.025	0.258	0.070	281.7E-6	2.25	0.62	2692	2734
46.24	45	39.893	0.245	0.083	274.6E-6	2.19	0.62	2621	2661
53.74	53	37.826	0.233	0.096	267.6E-6	2.14	0.62	2550	2589
61.24	60	35.829	0.220	0.108	260.5E-6	2.08	0.62	2480	2518
68.74	68	33.855	0.208	0.120	253.4E-6	2.02	0.62	2408	2445
76.24	75	31.936	0.196	0.132	246.4E-6	1.96	0.62	2337	2373
83.74	83	30.100	0.185	0.143	239.3E-6	1.91	0.62	2267	2302
91.24	90	28.290	0.174	0.154	232.3E-6	1.85	0.62	2196	2229
98.74	98	26.545	0.163	0.165	225.2E-6	1.79	0.62	2125	2157
106.2	105	24.863	0.153	0.176	218.1E-6	1.73	0.62	2054	2086
113.7	113	23.212	0.143	0.186	211.1E-6	1.67	0.62	1983	2013
121.2	120	21.651	0.133	0.195	204.0E-6	1.62	0.62	1913	1942
128.7	128	20.124	0.124	0.205	197.0E-6	1.56	0.63	1842	1870
136.2	135	18.648	0.115	0.214	189.9E-6	1.50	0.63	1771	1799

Table N.4 20 mm circular orifice results (2.81% CMC)

Time	Diff.Time	Mass in tank	Height	Diff.Height	Flow rate	Orifice Velocity	C _d	Re	Re ₂
[s]	[s]	[kg]	[m]	[m]	[m ³ /s]	[m/s]			
0.825	0	53.237	0.327	0	0	0	0	0	0
5.825	5	50.776	0.312	0.015	482.3E-6	2.48	0.62	3683	3739
10.83	10	48.363	0.297	0.030	470.8E-6	2.42	0.62	3592	3647
15.83	15	45.984	0.283	0.045	459.3E-6	2.36	0.62	3499	3553
20.83	20	43.716	0.269	0.059	447.8E-6	2.30	0.62	3409	3462
25.83	25	41.433	0.255	0.073	436.3E-6	2.24	0.62	3317	3367
30.83	30	39.246	0.241	0.086	424.8E-6	2.18	0.62	3225	3275
35.83	35	37.117	0.228	0.099	413.3E-6	2.12	0.62	3134	3182
40.83	40	35.020	0.215	0.112	401.8E-6	2.06	0.62	3041	3088
45.83	45	33.026	0.203	0.124	390.4E-6	2.00	0.62	2951	2996
50.83	50	31.072	0.191	0.136	378.9E-6	1.94	0.62	2859	2903
55.83	55	29.193	0.180	0.148	367.4E-6	1.88	0.62	2769	2812
60.83	60	27.329	0.168	0.159	355.9E-6	1.82	0.62	2676	2718
65.83	65	25.565	0.157	0.170	344.4E-6	1.76	0.62	2586	2626
70.83	70	23.868	0.147	0.181	332.9E-6	1.70	0.62	2496	2534
75.83	75	22.173	0.136	0.191	321.4E-6	1.64	0.62	2403	2440
80.83	80	20.576	0.127	0.201	309.9E-6	1.58	0.62	2312	2348
85.83	85	19.038	0.117	0.210	298.4E-6	1.52	0.62	2222	2256
90.83	90	17.530	0.108	0.220	286.9E-6	1.45	0.63	2129	2162

Square orifices

Table N.5 8 mm square orifice results (2.81% CMC)

Time [s]	Diff.Time [s]	Mass in tank [kg]	Height [m]	Diff.Height [m]	Flow rate [m³/s]	Orifice		
						Velocity [m/s]	C _d	Re ₂
4.158	0	53.650	0.330	0	0	0	0	0
29.16	25	50.940	0.313	0.017	105.6E-6	2.48	0.66	1542
54.16	50	48.288	0.297	0.033	103.0E-6	2.41	0.66	1500
79.16	75	45.702	0.281	0.049	100.4E-6	2.35	0.66	1458
104.2	100	43.177	0.265	0.064	97.75E-6	2.28	0.67	1416
129.2	125	40.723	0.250	0.079	95.15E-6	2.22	0.67	1374
154.2	150	38.326	0.236	0.094	92.55E-6	2.15	0.67	1331
179.2	175	36.025	0.222	0.108	89.94E-6	2.08	0.67	1290
204.2	200	33.780	0.208	0.122	87.34E-6	2.02	0.67	1248
229.2	225	31.585	0.194	0.136	84.74E-6	1.95	0.67	1205
254.2	250	29.473	0.181	0.149	82.14E-6	1.89	0.68	1163
279.2	275	27.423	0.169	0.161	79.53E-6	1.82	0.68	1120
304.2	300	25.440	0.156	0.173	76.93E-6	1.75	0.68	1078
329.2	325	23.518	0.145	0.185	74.33E-6	1.68	0.69	1035
354.2	350	21.651	0.133	0.197	71.73E-6	1.62	0.69	992
379.2	375	19.853	0.122	0.208	69.12E-6	1.55	0.69	949
404.2	400	18.121	0.111	0.218	66.52E-6	1.48	0.70	905

Table N.6 12 mm square orifice results (2.81% CMC)

Time [s]	Diff.Time [s]	Mass in tank [kg]	Height [m]	Diff.Height [m]	Flow rate [m³/s]	Orifice		
						Velocity [m/s]	C _d	Re ₂
1.658	0	52.308	0.322	0	0	0	0	0
11.66	10	49.915	0.307	0.015	231.2E-6	2.45	0.65	2258
21.66	20	47.602	0.293	0.029	226.0E-6	2.40	0.65	2204
31.66	30	45.329	0.279	0.043	220.9E-6	2.34	0.65	2149
41.66	40	43.100	0.265	0.057	215.7E-6	2.28	0.65	2094
51.66	50	40.952	0.252	0.070	210.6E-6	2.22	0.66	2039
61.66	60	38.832	0.239	0.083	205.4E-6	2.16	0.66	1984
71.66	70	36.766	0.226	0.096	200.3E-6	2.11	0.66	1929
81.66	80	34.763	0.214	0.108	195.1E-6	2.05	0.66	1874
91.66	90	32.820	0.202	0.120	190.0E-6	1.99	0.66	1820
101.7	100	30.885	0.190	0.132	184.8E-6	1.93	0.66	1763
111.7	110	29.049	0.179	0.143	179.7E-6	1.87	0.66	1709
121.7	120	27.234	0.167	0.154	174.5E-6	1.81	0.67	1653
131.7	130	25.517	0.157	0.165	169.4E-6	1.75	0.67	1598
141.7	140	23.808	0.146	0.175	164.2E-6	1.69	0.67	1542
151.7	150	22.162	0.136	0.185	159.1E-6	1.64	0.67	1486
161.7	160	20.596	0.127	0.195	153.9E-6	1.58	0.68	1431
171.7	170	19.034	0.117	0.205	148.8E-6	1.52	0.68	1374
181.7	180	17.538	0.108	0.214	143.6E-6	1.45	0.68	1317

Table N.7 16 mm square orifice results (2.81% CMC)

Time	Diff.Time	Mass in tank	Height	Diff.Height	Flow rate	Orifice Velocity	C _d	Re ₂
[s]	[s]	[kg]	[m]	[m]	[m ³ /s]	[m/s]		
1.242	0	52.027	0.320	0	0	0	0	0
8.742	8	49.006	0.301	0.019	388.50E-6	2.43	0.62	2955
16.24	15	46.118	0.284	0.036	377.00E-6	2.36	0.62	2864
23.74	23	43.257	0.266	0.054	365.50E-6	2.28	0.62	2771
31.24	30	40.508	0.249	0.071	354.00E-6	2.21	0.62	2679
38.74	38	37.867	0.233	0.087	342.50E-6	2.14	0.62	2588
46.24	45	35.275	0.217	0.103	331.00E-6	2.06	0.63	2495
53.74	53	32.819	0.202	0.118	319.49E-6	1.99	0.63	2404
61.24	60	30.412	0.187	0.133	307.99E-6	1.92	0.63	2311
68.74	68	28.154	0.173	0.147	296.49E-6	1.84	0.63	2221
76.24	75	25.897	0.159	0.161	284.99E-6	1.77	0.63	2128
83.74	83	23.815	0.146	0.173	273.49E-6	1.70	0.63	2038
91.24	90	21.738	0.134	0.186	261.99E-6	1.62	0.63	1944
98.74	98	19.785	0.122	0.198	250.49E-6	1.54	0.63	1852
106.2	105	17.919	0.110	0.210	238.99E-6	1.47	0.63	1760
113.7	113	16.121	0.099	0.221	227.49E-6	1.39	0.64	1666

Table N.8 20 mm square orifice results (2.81% CMC)

Time	Diff.Time	Mass in tank	Height	Diff.Height	Flow rate	Orifice Velocity	C _d	Re ₂
[s]	[s]	[kg]	[m]	[m]	[m ³ /s]	[m/s]		
0.825	1.65	51.375	0.316	0	0	0	0	0
5.825	6.65	48.260	0.297	0.019	599.7E-6	2.41	0.62	3639
10.83	11.65	45.257	0.278	0.038	581.1E-6	2.34	0.62	3521
15.83	16.65	42.363	0.260	0.055	562.6E-6	2.26	0.62	3403
20.83	21.65	39.543	0.243	0.073	544.0E-6	2.18	0.62	3284
25.83	26.65	36.821	0.226	0.089	525.5E-6	2.11	0.62	3166
30.83	31.65	34.200	0.210	0.106	506.9E-6	2.03	0.62	3048
35.83	36.65	31.678	0.195	0.121	488.4E-6	1.95	0.62	2930
40.83	41.65	29.232	0.180	0.136	469.8E-6	1.88	0.62	2811
45.83	46.65	26.915	0.165	0.150	451.3E-6	1.80	0.62	2694
50.83	51.65	24.663	0.152	0.164	432.8E-6	1.72	0.63	2575
55.83	56.65	22.491	0.138	0.178	414.2E-6	1.65	0.63	2456
60.83	61.65	20.470	0.126	0.190	395.7E-6	1.57	0.63	2339
65.83	66.65	18.460	0.114	0.202	377.1E-6	1.49	0.63	2218
70.83	71.65	16.601	0.102	0.214	358.6E-6	1.42	0.63	2100

Triangular orifices

Table N.9 8 mm triangular orifice results (2.81% CMC)

Time [s]	Diff.Time [s]	Mass in tank [kg]	Height [m]	Diff.Height [m]	Flow rate [m ³ /s]	Orifice Velocity		
						C _d	Re ₂	
4.158	0	52.829	0.325	0	0	0	0	0
29.16	25	49.329	0.303	0.022	135.4E-6	2.44	0.66	1517
54.16	50	45.935	0.282	0.042	130.9E-6	2.35	0.66	1463
79.16	75	42.681	0.262	0.062	126.4E-6	2.27	0.67	1408
104.2	100	39.504	0.243	0.082	121.9E-6	2.18	0.67	1353
129.2	125	36.457	0.224	0.101	117.5E-6	2.10	0.67	1298
154.2	150	33.544	0.206	0.119	113.0E-6	2.01	0.67	1244
179.2	175	30.737	0.189	0.136	108.5E-6	1.93	0.67	1189
204.2	200	28.042	0.172	0.152	104.1E-6	1.84	0.68	1134
229.2	225	25.459	0.157	0.168	99.60E-6	1.75	0.68	1079
254.2	250	22.980	0.141	0.184	95.13E-6	1.67	0.68	1024
279.2	275	20.615	0.127	0.198	90.66E-6	1.58	0.69	968
304.2	300	18.343	0.113	0.212	86.19E-6	1.49	0.69	911

Table N.10 12 mm triangular orifice results (2.81% CMC)

Time [s]	Diff.Time [s]	Mass in tank [kg]	Height [m]	Diff.Height [m]	Flow rate [m ³ /s]	Orifice Velocity		
						C _d	Re ₂	
1.658	0	54.148	0.333	0	0	0	0	0
11.66	10	51.084	0.314	0.019	296.8E-6	2.48	0.64	2283
21.66	20	48.121	0.296	0.037	288.4E-6	2.41	0.64	2214
31.66	30	45.214	0.278	0.055	279.9E-6	2.34	0.64	2144
41.66	40	42.420	0.261	0.072	271.5E-6	2.26	0.64	2075
51.66	50	39.693	0.244	0.089	263.1E-6	2.19	0.64	2005
61.66	60	37.086	0.228	0.105	254.6E-6	2.12	0.64	1936
71.66	70	34.524	0.212	0.121	246.2E-6	2.04	0.64	1866
81.66	80	32.074	0.197	0.136	237.7E-6	1.97	0.65	1796
91.66	90	29.705	0.183	0.150	229.3E-6	1.89	0.65	1727
101.7	100	27.412	0.169	0.164	220.8E-6	1.82	0.65	1657
111.7	110	25.218	0.155	0.178	212.4E-6	1.74	0.65	1587
121.7	120	23.106	0.142	0.191	203.9E-6	1.67	0.65	1517
131.7	130	21.065	0.130	0.203	195.5E-6	1.59	0.65	1447
141.7	140	19.126	0.118	0.215	187.1E-6	1.52	0.66	1376
151.7	150	17.259	0.106	0.227	178.6E-6	1.44	0.66	1305

Table N.11 16 mm triangular orifice results (2.81% CMC)

Time	Diff.Time	Mass in tank	Height	Diff.Height	Flow rate	Orifice Velocity	C _d	Re ₂
[s]	[s]	[kg]	[m]	[m]	[m ³ /s]	[m/s]		
1.242	0.0	53.693	0.330	0	0	0	0	0
8.742	7.5	49.836	0.306	0.024	498.5E-6	2.45	0.63	2924
16.24	15.0	46.105	0.283	0.047	479.8E-6	2.36	0.63	2809
23.74	22.5	42.521	0.261	0.069	461.1E-6	2.26	0.63	2694
31.24	30.0	39.083	0.240	0.090	442.5E-6	2.17	0.63	2580
38.74	37.5	35.753	0.220	0.110	423.8E-6	2.08	0.64	2464
46.24	45.0	32.583	0.200	0.130	405.2E-6	1.98	0.64	2349
53.74	52.5	29.588	0.182	0.148	386.5E-6	1.89	0.64	2235
61.24	60.0	26.724	0.164	0.166	367.8E-6	1.80	0.64	2121
68.74	67.5	23.973	0.147	0.183	349.2E-6	1.70	0.64	2005
76.24	75.0	21.410	0.132	0.199	330.5E-6	1.61	0.64	1892
83.74	82.5	18.924	0.116	0.214	311.9E-6	1.51	0.64	1775

Table N.12 20 mm triangular orifice results (2.81% CMC)

Time	Diff.Time	Mass in tank	Height	Diff.Height	Flow rate	Orifice Velocity	C _d	Re ₂
[s]	[s]	[kg]	[m]	[m]	[m ³ /s]	[m/s]		
0.825	0	51.358	0.316	0	0	0	0	0
5.825	5	47.320	0.291	0.025	782.2E-6	2.39	0.63	3595
10.83	10	43.417	0.267	0.049	749.9E-6	2.29	0.63	3439
15.83	15	39.704	0.244	0.072	717.7E-6	2.19	0.63	3284
20.83	20	36.128	0.222	0.094	685.4E-6	2.09	0.63	3128
25.83	25	32.733	0.201	0.115	653.2E-6	1.99	0.63	2973
30.83	30	29.466	0.181	0.135	621.0E-6	1.89	0.64	2816
35.83	35	26.418	0.162	0.153	588.7E-6	1.79	0.64	2662
40.83	40	23.492	0.144	0.171	556.5E-6	1.68	0.64	2506
45.83	45	20.754	0.128	0.188	524.2E-6	1.58	0.64	2351
50.83	50	18.171	0.112	0.204	492.0E-6	1.48	0.64	2195
55.83	55	15.765	0.097	0.219	459.8E-6	1.38	0.64	2040

APPENDIX O: 2.4% CMC solution

Rheological and physical parameters

n=	1
k=	0.006 Pa.s ⁿ
Density=	1014 kg/m ³
g=	9.81 m/s ²

Circular orifices

Table O.1 8 mm circular orifice results (2.81% CMC)

Time [s]	Diff.Time [s]	Mass in tank [kg]	Height [m]	Diff.Height [m]	Flow rate [m ³ /s]	Orifice Velocity		
						C _d	Re	
8.325	0	90.120	0.555	0	0	0	0	0
58.33	50	84.736	0.522	0.033	105.1E-6	3.20	0.65	4715
108.3	100	79.498	0.490	0.065	101.9E-6	3.10	0.65	4567
158.3	150	74.438	0.459	0.097	98.69E-6	3.00	0.65	4420
208.3	200	69.525	0.429	0.127	95.50E-6	2.90	0.65	4271
258.3	250	64.754	0.399	0.156	92.32E-6	2.80	0.65	4122
308.3	300	60.148	0.371	0.185	89.14E-6	2.70	0.65	3973
358.3	350	55.715	0.343	0.212	85.95E-6	2.60	0.65	3824
408.3	400	51.417	0.317	0.239	82.77E-6	2.49	0.65	3673
458.3	450	47.283	0.291	0.264	79.58E-6	2.39	0.66	3522
508.3	500	43.328	0.267	0.288	76.40E-6	2.29	0.66	3372
558.3	550	39.536	0.244	0.312	73.22E-6	2.19	0.66	3221
608.3	600	35.888	0.221	0.334	70.03E-6	2.08	0.66	3069
658.3	650	32.439	0.200	0.356	66.85E-6	1.98	0.66	2917
708.3	700	29.145	0.180	0.376	63.66E-6	1.88	0.67	2765
758.3	750	26.018	0.160	0.395	60.48E-6	1.77	0.67	2613
808.3	800	22.991	0.142	0.414	57.30E-6	1.67	0.68	2456
858.3	850	20.224	0.125	0.431	54.11E-6	1.56	0.68	2304

Table O.2 12 mm circular orifice results (2.81% CMC)

Time [s]	Diff.Time [s]	Mass in tank [kg]	Height [m]	Diff.Height [m]	Flow rate [m ³ /s]	Orifice Velocity		
						C _d	Re	
4.158	0.00	89.387	0.551	0	0	0	0	0
37.49	33.33	81.832	0.504	0.0466	218.7E-6	3.15	0.61	6939
70.83	66.67	74.612	0.460	0.0911	208.9E-6	3.00	0.61	6626
104.2	100.0	67.712	0.417	0.134	199.1E-6	2.86	0.61	6312
137.5	133.3	61.167	0.377	0.174	189.3E-6	2.72	0.61	5999
170.8	166.7	54.938	0.339	0.212	179.5E-6	2.58	0.61	5686
204.2	200.0	48.994	0.302	0.249	169.7E-6	2.43	0.61	5369
237.5	233.3	43.436	0.268	0.283	159.8E-6	2.29	0.61	5056
270.8	266.7	38.202	0.235	0.315	150.0E-6	2.15	0.61	4741
304.2	300.0	33.290	0.205	0.346	140.2E-6	2.01	0.61	4426
337.5	333.3	28.712	0.177	0.374	130.4E-6	1.86	0.61	4110
370.8	366.7	24.470	0.151	0.400	120.6E-6	1.72	0.62	3795
404.2	400.0	20.579	0.127	0.424	110.8E-6	1.58	0.62	3480

Table O.3 16 mm circular orifice results (2.81% CMC)

Time	Diff.Time	Mass in tank	Height	Diff.Height	Flow rate	Orifice Velocity	C _d	Re
[s]	[s]	[kg]	[m]	[m]	[m ³ /s]	[m/s]		
3.325	0	91.474	0.564	0	0	0	0	0
23.33	20	83.446	0.514	0.049	388.0E-6	3.18	0.60	9335
43.33	40	75.748	0.467	0.097	369.8E-6	3.03	0.60	8894
63.33	60	68.437	0.422	0.142	351.6E-6	2.88	0.60	8454
83.33	80	61.495	0.379	0.185	333.4E-6	2.73	0.60	8014
103.3	100	54.919	0.339	0.225	315.1E-6	2.58	0.61	7573
123.3	120	48.709	0.300	0.264	296.9E-6	2.43	0.61	7132
143.3	140	42.874	0.264	0.300	278.7E-6	2.28	0.61	6691
163.3	160	37.402	0.231	0.333	260.5E-6	2.13	0.61	6250
183.3	180	32.318	0.199	0.365	242.3E-6	1.98	0.61	5810
203.3	200	27.593	0.170	0.394	224.0E-6	1.83	0.61	5368
223.3	220	23.245	0.143	0.421	205.8E-6	1.68	0.61	4927
243.3	240	19.235	0.119	0.445	187.6E-6	1.53	0.61	4482

Table O.4 20 mm circular orifice results (2.81% CMC)

Time	Diff.Time	Mass in tank	Height	Diff.Height	Flow rate	Orifice Velocity	C _d	Re
[s]	[s]	[kg]	[m]	[m]	[m ³ /s]	[m/s]		
1.658	0	85.017	0.524	0	0	0	0	0
11.66	10	78.948	0.487	0.037	589.5E-6	3.09	0.60	11345
21.66	20	73.100	0.451	0.073	567.1E-6	2.97	0.60	10916
31.66	30	67.432	0.416	0.108	544.6E-6	2.86	0.60	10485
41.66	40	62.030	0.382	0.142	522.2E-6	2.74	0.60	10056
51.66	50	56.872	0.351	0.173	499.7E-6	2.62	0.60	9629
61.66	60	51.905	0.320	0.204	477.2E-6	2.51	0.60	9199
71.66	70	47.183	0.291	0.233	454.8E-6	2.39	0.60	8770
81.66	80	42.687	0.263	0.261	432.3E-6	2.27	0.60	8342
91.66	90	38.411	0.237	0.287	409.9E-6	2.16	0.60	7913
101.7	100	34.361	0.212	0.312	387.4E-6	2.04	0.60	7484
111.7	110	30.547	0.188	0.336	364.9E-6	1.92	0.60	7057
121.7	120	26.946	0.166	0.358	342.5E-6	1.81	0.60	6628
131.7	130	23.635	0.146	0.378	320.0E-6	1.69	0.60	6207
141.7	140	20.494	0.126	0.398	297.5E-6	1.57	0.60	5780
151.7	150	17.580	0.108	0.416	275.1E-6	1.46	0.60	5353

Square orifices

Table O.5 8 mm square orifice results (2.81% CMC)

Time	Diff.Time	Mass in tank	Height	Diff.Height	Flow rate	Orifice Velocity	C _d	Re
[s]	[s]	[kg]	[m]	[m]	[m ³ /s]	[m/s]		
8.325	0	87.890	0.542	0	0	0	0	0
58.33	50	81.273	0.501	0.041	128.4E-6	3.14	0.64	4606
108.3	100	74.896	0.462	0.080	123.3E-6	3.01	0.64	4422
158.3	150	68.794	0.424	0.118	118.3E-6	2.88	0.64	4238
208.3	200	62.912	0.388	0.154	113.2E-6	2.76	0.64	4053
258.3	250	57.300	0.353	0.189	108.2E-6	2.63	0.64	3868
308.3	300	51.932	0.320	0.222	103.1E-6	2.51	0.64	3682
358.3	350	46.830	0.289	0.253	98.0E-6	2.38	0.64	3497
408.3	400	41.989	0.259	0.283	93.0E-6	2.25	0.64	3311
458.3	450	37.406	0.231	0.311	87.9E-6	2.13	0.64	3125
508.3	500	33.059	0.204	0.338	82.9E-6	2.00	0.64	2938
558.3	550	28.984	0.179	0.363	77.8E-6	1.87	0.65	2751
608.3	600	25.165	0.155	0.387	72.8E-6	1.74	0.65	2563
658.3	650	21.646	0.133	0.408	67.7E-6	1.62	0.65	2377
708.3	700	18.328	0.113	0.429	62.7E-6	1.49	0.65	2188

Table O.6 12 mm square orifice results (2.81% CMC)

Time	Diff.Time	Mass in tank	Height	Diff.Height	Flow rate	Orifice Velocity	C _d	Re
[s]	[s]	[kg]	[m]	[m]	[m ³ /s]	[m/s]		
4.158	0	85.344	0.526	0	0	0	0	0
29.16	25	78.070	0.481	0.045	280.6E-6	3.07	0.63	6767
54.16	50	71.103	0.438	0.088	268.0E-6	2.93	0.63	6458
79.16	75	64.482	0.397	0.129	255.3E-6	2.79	0.63	6150
104.2	100	58.163	0.359	0.168	242.7E-6	2.65	0.63	5840
129.2	125	52.182	0.322	0.204	230.0E-6	2.51	0.63	5532
154.2	150	46.503	0.287	0.239	217.3E-6	2.37	0.63	5222
179.2	175	41.158	0.254	0.272	204.7E-6	2.23	0.64	4913
204.2	200	36.115	0.223	0.303	192.0E-6	2.09	0.64	4602
229.2	225	31.422	0.194	0.332	179.4E-6	1.95	0.64	4293
254.2	250	27.023	0.167	0.359	166.7E-6	1.81	0.64	3981
279.2	275	22.957	0.142	0.385	154.1E-6	1.67	0.64	3669
304.2	300	19.213	0.118	0.408	141.4E-6	1.52	0.64	3357

Table O.7 16 mm square orifice results (2.81% CMC)

Time [s]	Diff.Time [s]	Mass in tank [kg]	Height [m]	Diff.Height [m]	Flow rate [m ³ /s]	Orifice Velocity		
						C _d	Re	
2.492	0	88.752	0.547	0	0	0	0	0
17.49	15	81.166	0.500	0.047	487.7E-6	3.13	0.61	9195
32.49	30	73.917	0.456	0.091	465.5E-6	2.99	0.61	8775
47.49	45	66.998	0.413	0.134	443.3E-6	2.85	0.61	8354
62.49	60	60.435	0.373	0.175	421.1E-6	2.70	0.61	7935
77.49	75	54.195	0.334	0.213	398.9E-6	2.56	0.61	7514
92.49	90	48.286	0.298	0.249	376.7E-6	2.42	0.61	7092
107.5	105	42.731	0.263	0.284	354.6E-6	2.27	0.61	6672
122.5	120	37.504	0.231	0.316	332.4E-6	2.13	0.61	6251
137.5	135	32.613	0.201	0.346	310.2E-6	1.99	0.61	5829
152.5	150	28.061	0.173	0.374	288.0E-6	1.84	0.61	5407
167.5	165	23.867	0.147	0.400	265.8E-6	1.70	0.61	4986
182.5	180	19.980	0.123	0.424	243.6E-6	1.55	0.61	4562

Table O.8 20 mm square orifice results (2.81% CMC)

Time [s]	Diff.Time [s]	Mass in tank [kg]	Height [m]	Diff.Height [m]	Flow rate [m ³ /s]	Orifice Velocity		
						C _d	Re	
1.658	3.32	86.645	0.534	0	0	0	0	0
11.66	13.32	78.880	0.486	0.048	752.11E-6	3.09	0.61	11328
21.66	23.32	71.427	0.440	0.094	715.79E-6	2.94	0.61	10780
31.66	33.32	64.340	0.397	0.137	679.47E-6	2.79	0.61	10231
41.66	43.32	57.633	0.355	0.179	643.15E-6	2.64	0.61	9683
51.66	53.32	51.296	0.316	0.218	606.83E-6	2.49	0.61	9135
61.66	63.32	45.328	0.279	0.255	570.51E-6	2.34	0.61	8587
71.66	73.32	39.715	0.245	0.289	534.19E-6	2.19	0.61	8038
81.66	83.32	34.496	0.213	0.321	497.87E-6	2.04	0.61	7491
91.66	93.32	29.636	0.183	0.351	461.55E-6	1.89	0.61	6944
101.7	103.3	25.135	0.155	0.379	425.23E-6	1.74	0.61	6395
111.7	113.3	21.006	0.129	0.405	388.91E-6	1.59	0.61	5846

Triangular orifices

Table O.9 8 mm triangular orifice results (2.81% CMC)

Time [s]	Diff.Time [s]	Mass in tank [kg]	Height [m]	Diff.Height [m]	Flow rate [m ³ /s]	Orifice Velocity		
						C _d	Re ₂	
8.325	0.00	88.147	0.543	0	0	0	0	0
49.99	41.67	80.977	0.499	0.044	166.8E-6	3.13	0.64	4601
91.66	83.33	74.132	0.457	0.086	159.8E-6	2.99	0.64	4402
133.3	125.0	67.469	0.416	0.127	152.7E-6	2.86	0.64	4200
175.0	166.7	61.182	0.377	0.166	145.6E-6	2.72	0.64	3999
216.7	208.3	55.173	0.340	0.203	138.5E-6	2.58	0.64	3798
258.3	250.0	49.469	0.305	0.238	131.4E-6	2.45	0.64	3596
300.0	291.7	44.061	0.272	0.272	124.3E-6	2.31	0.64	3394
341.7	333.3	38.964	0.240	0.303	117.3E-6	2.17	0.65	3192
383.3	375.0	34.144	0.210	0.333	110.2E-6	2.03	0.65	2988
425.0	416.7	29.641	0.183	0.361	103.1E-6	1.89	0.65	2784
466.7	458.3	25.436	0.157	0.387	96.01E-6	1.75	0.65	2579
508.3	500.0	21.533	0.133	0.411	88.93E-6	1.61	0.66	2373
550.0	541.7	17.946	0.111	0.433	81.85E-6	1.47	0.66	2166

Table O.10 12 mm triangular orifice results (2.81% CMC)

Time [s]	Diff.Time [s]	Mass in tank [kg]	Height [m]	Diff.Height [m]	Flow rate [m ³ /s]	Orifice Velocity		
						C _d	Re ₂	
2.492	0	87.031	0.536	0	0	0	0	0
17.49	15	81.419	0.502	0.035	362.5E-6	3.14	0.62	6904
32.49	30	75.968	0.468	0.068	350.2E-6	3.03	0.62	6669
47.49	45	70.708	0.436	0.101	337.9E-6	2.92	0.62	6434
62.49	60	65.628	0.405	0.132	325.7E-6	2.82	0.62	6198
77.49	75	60.745	0.374	0.162	313.4E-6	2.71	0.62	5963
92.49	90	56.031	0.345	0.191	301.1E-6	2.60	0.62	5727
107.5	105	51.506	0.317	0.219	288.8E-6	2.50	0.62	5491
122.5	120	47.180	0.291	0.246	276.6E-6	2.39	0.62	5255
137.5	135	43.025	0.265	0.271	264.3E-6	2.28	0.62	5019
152.5	150	39.067	0.241	0.296	252.0E-6	2.17	0.62	4782
167.5	165	35.295	0.218	0.319	239.8E-6	2.07	0.62	4545
182.5	180	31.709	0.195	0.341	227.5E-6	1.96	0.62	4308
197.5	195	28.318	0.175	0.362	215.2E-6	1.85	0.62	4071
212.5	210	25.108	0.155	0.382	202.9E-6	1.74	0.62	3834
227.5	225	22.091	0.136	0.400	190.7E-6	1.63	0.62	3596
242.5	240	19.258	0.119	0.418	178.4E-6	1.53	0.62	3358

Table O.11 16 mm triangular orifice results (2.81% CMC)

Time [s]	Diff.Time [s]	Mass in tank [kg]	Height [m]	Diff.Height [m]	Flow rate [m ³ /s]	Orifice Velocity		
						C _d	Re ₂	[m ³ /s]
1.658	0	87.415	0.539	0	0	0	0	0
11.66	10	81.026	0.499	0.039	619.4E-6	3.13	0.62	9006
21.66	20	74.883	0.462	0.077	595.4E-6	3.01	0.62	8658
31.66	30	68.915	0.425	0.114	571.4E-6	2.89	0.62	8306
41.66	40	63.235	0.390	0.149	547.4E-6	2.77	0.62	7956
51.66	50	57.810	0.356	0.182	523.4E-6	2.64	0.62	7607
61.66	60	52.680	0.325	0.214	499.5E-6	2.52	0.62	7262
71.66	70	47.715	0.294	0.245	475.5E-6	2.40	0.62	6911
81.66	80	43.019	0.265	0.274	451.5E-6	2.28	0.62	6562
91.66	90	38.555	0.238	0.301	427.5E-6	2.16	0.62	6213
101.7	100	34.365	0.212	0.327	403.5E-6	2.04	0.62	5865
111.7	110	30.362	0.187	0.352	379.5E-6	1.92	0.62	5513
121.7	120	26.633	0.164	0.375	355.6E-6	1.79	0.62	5163
131.7	130	23.148	0.143	0.396	331.6E-6	1.67	0.62	4814
141.7	140	19.924	0.123	0.416	307.6E-6	1.55	0.62	4466

Table O.12 20 mm triangular orifice results (2.81% CMC)

Time [s]	Diff.Time [s]	Mass in tank [kg]	Height [m]	Diff.Height [m]	Flow rate [m ³ /s]	Orifice Velocity		
						C _d	Re ₂	
0.825	0	82.847	0.511	0	0	0	0	0
5.825	5	77.818	0.480	0.031	974.8E-6	3.07	0.61	11227
10.83	10	72.961	0.450	0.061	943.9E-6	2.97	0.61	10871
15.83	15	68.251	0.421	0.090	913.1E-6	2.87	0.61	10515
20.83	20	63.711	0.393	0.118	882.2E-6	2.78	0.61	10159
25.83	25	59.311	0.366	0.145	851.4E-6	2.68	0.61	9802
30.83	30	55.063	0.339	0.171	820.5E-6	2.58	0.61	9444
35.83	35	51.015	0.314	0.196	789.7E-6	2.48	0.61	9090
40.83	40	47.068	0.290	0.221	758.8E-6	2.39	0.61	8732
45.83	45	43.283	0.267	0.244	728.0E-6	2.29	0.61	8373
50.83	50	39.685	0.245	0.266	697.1E-6	2.19	0.61	8018
55.83	55	36.203	0.223	0.288	666.3E-6	2.09	0.61	7658
60.83	60	32.930	0.203	0.308	635.4E-6	2.00	0.61	7303
65.83	65	29.792	0.184	0.327	604.6E-6	1.90	0.61	6947
70.83	70	26.812	0.165	0.345	573.7E-6	1.80	0.61	6590
75.83	75	23.971	0.148	0.363	542.9E-6	1.70	0.62	6231
80.83	80	21.274	0.131	0.380	512.0E-6	1.60	0.62	5870
85.83	85	18.791	0.116	0.395	481.2E-6	1.51	0.62	5517

APPENDIX P: 20.34% kaolin suspension

Rheological and physical parameters

n=	0.36
k=	3.975 Pa.s ⁿ
T _y =	39.373 Pa.s
Density=	1344 kg/m ³
g=	9.81 m/s ²

Circular orifices

Table P.1 8 mm circular orifice results (20.34% kaolin)

Time [s]	Diff.Time [s]	Mass in tank [kg]	Height [m]	Diff.Height [m]	Flow rate [m ³ /s]	Orifice Velocity		
						Orifice Velocity [m/s]	C _d	Re ₂
4.158	0	59.350	0.276	0.000	0	0	0	0
29.16	25	56.772	0.264	0.012	75.36E-6	2.28	0.65	538
54.16	50	54.283	0.252	0.024	73.27E-6	2.23	0.65	517
79.16	75	51.856	0.241	0.035	71.17E-6	2.18	0.64	496
104.2	100	49.499	0.230	0.046	69.08E-6	2.13	0.64	476
129.2	125	47.207	0.220	0.056	66.98E-6	2.08	0.64	457
154.2	150	44.985	0.209	0.067	64.89E-6	2.03	0.63	437
179.2	175	42.846	0.199	0.077	62.80E-6	1.98	0.63	419
204.2	200	40.771	0.190	0.086	60.70E-6	1.93	0.62	401
229.2	225	38.783	0.180	0.096	58.61E-6	1.88	0.61	383
254.2	250	36.843	0.171	0.105	56.51E-6	1.83	0.61	366
279.2	275	34.976	0.163	0.113	54.42E-6	1.79	0.60	350
304.2	300	33.171	0.154	0.122	52.32E-6	1.74	0.59	333
329.2	325	31.461	0.146	0.130	50.23E-6	1.69	0.58	318
354.2	350	29.823	0.139	0.137	48.13E-6	1.65	0.57	303
379.2	375	28.221	0.131	0.145	46.04E-6	1.60	0.57	289
404.2	400	26.722	0.124	0.152	43.95E-6	1.56	0.55	275
429.2	425	25.268	0.118	0.158	41.85E-6	1.52	0.54	261
454.2	450	23.896	0.111	0.165	39.76E-6	1.48	0.53	249
479.2	475	22.598	0.105	0.171	37.66E-6	1.44	0.52	237

Table P.2 12 mm circular orifice results (20.34% kaolin)

Time	Diff.Time	Mass in tank	Height	Diff.Height	Flow rate	Orifice Velocity	C _d	Re ₂
[s]	[s]	[kg]	[m]	[m]	[m ³ /s]	[m/s]		
2.075	0	58.803	0.273	0	0	0	0	0
14.58	13	55.996	0.260	0.013	166.2E-6	2.26	0.65	580
27.08	25	53.255	0.248	0.026	161.3E-6	2.20	0.64	555
39.58	38	50.610	0.235	0.038	156.4E-6	2.15	0.64	530
52.08	50	48.034	0.223	0.050	151.6E-6	2.09	0.64	506
64.58	63	45.544	0.212	0.062	146.7E-6	2.04	0.63	482
77.08	75	43.143	0.201	0.073	141.9E-6	1.98	0.63	459
89.58	88	40.810	0.190	0.084	137.0E-6	1.93	0.62	437
102.1	100	38.560	0.179	0.094	132.1E-6	1.88	0.62	415
114.6	113	36.391	0.169	0.104	127.3E-6	1.82	0.61	394
127.1	125	34.312	0.160	0.114	122.4E-6	1.77	0.61	374
139.6	138	32.291	0.150	0.123	117.5E-6	1.72	0.60	354
152.1	150	30.385	0.141	0.132	112.7E-6	1.67	0.59	335
164.6	163	28.531	0.133	0.141	107.8E-6	1.61	0.59	317
177.1	175	26.781	0.125	0.149	102.9E-6	1.56	0.58	299
189.6	188	25.095	0.117	0.157	98.08E-6	1.51	0.57	282
202.1	200	23.509	0.109	0.164	93.22E-6	1.46	0.56	266
214.6	213	21.997	0.102	0.171	88.35E-6	1.42	0.55	251

Table P.3 16 mm circular orifice results (20.34% kaolin)

Time	Diff.Time	Mass in tank	Height	Diff.Height	Flow rate	Orifice Velocity	C _d	Re ₂
[s]	[s]	[kg]	[m]	[m]	[m ³ /s]	[m/s]		
0.825	0.00	58.286	0.271	0	0.00E+00	0.00	0.00	0
7.492	6.667	55.650	0.259	0.012	288.9E-6	2.25	0.63	612
14.16	13.33	53.122	0.247	0.024	281.3E-6	2.20	0.63	587
20.83	20.00	50.642	0.236	0.036	273.7E-6	2.15	0.63	562
27.49	26.67	48.199	0.224	0.047	266.1E-6	2.10	0.63	538
34.16	33.33	45.868	0.213	0.058	258.5E-6	2.05	0.63	514
40.83	40.00	43.562	0.203	0.068	250.9E-6	1.99	0.62	491
47.49	46.67	41.360	0.192	0.079	243.3E-6	1.94	0.62	468
54.16	53.33	39.223	0.182	0.089	235.7E-6	1.89	0.62	447
60.83	60.00	37.150	0.173	0.098	228.1E-6	1.84	0.61	425
67.49	66.67	35.119	0.163	0.108	220.5E-6	1.79	0.61	404
74.16	73.33	33.205	0.154	0.117	212.9E-6	1.74	0.61	384
80.83	80.00	31.290	0.146	0.126	205.3E-6	1.69	0.60	364
87.49	86.67	29.490	0.137	0.134	197.7E-6	1.64	0.60	345
94.16	93.33	27.748	0.129	0.142	190.1E-6	1.59	0.59	327
100.8	100.0	26.108	0.121	0.150	182.5E-6	1.54	0.59	309
107.5	106.7	24.482	0.114	0.157	174.9E-6	1.49	0.58	292
114.2	113.3	22.988	0.107	0.164	167.3E-6	1.45	0.57	275

Table P.4 20 mm circular orifice results (20.34% kaolin)

Time	Diff.Time	Mass in tank	Height	Diff.Height	Flow rate	Orifice Velocity	C _d	Re ₂
[s]	[s]	[kg]	[m]	[m]	[m ³ /s]	[m/s]		
5.825	0	59.445	0.276	0	0	0	0	0
10.83	5	56.412	0.262	0.014	452.2E-6	2.27	0.63	647
15.83	10	53.434	0.248	0.028	438.7E-6	2.21	0.63	616
20.83	15	50.518	0.235	0.042	425.2E-6	2.15	0.63	586
25.83	20	47.720	0.222	0.055	411.6E-6	2.09	0.63	557
30.83	25	44.986	0.209	0.067	398.1E-6	2.03	0.62	528
35.83	30	42.361	0.197	0.079	384.5E-6	1.97	0.62	500
40.83	35	39.814	0.185	0.091	371.0E-6	1.91	0.62	472
45.83	40	37.349	0.174	0.103	357.5E-6	1.85	0.61	446
50.83	45	35.000	0.163	0.114	343.9E-6	1.79	0.61	420
55.83	50	32.736	0.152	0.124	330.4E-6	1.73	0.61	396
60.83	55	30.541	0.142	0.134	316.9E-6	1.67	0.60	371
65.83	60	28.469	0.132	0.144	303.3E-6	1.61	0.60	348
70.83	65	26.461	0.123	0.153	289.8E-6	1.55	0.59	326
75.83	70	24.577	0.114	0.162	276.3E-6	1.50	0.58	305
80.83	75	22.783	0.106	0.170	262.7E-6	1.44	0.58	285
85.83	80	21.080	0.098	0.178	249.2E-6	1.39	0.57	265

Square orifices

Table P.5 8 mm square orifice results (20.34% kaolin)

Time	Diff.Time	Mass in tank	Height	Diff.Height	Flow rate	orifice velocity	C _d	Re ₂
[s]	[s]	[kg]	[m]	[m]	[m ³ /s]	[m/s]		
4.158	0	57.422	0.267	0	0	0	0	0
29.16	25	54.191	0.252	0.015	94.09E-6	2.22	0.66	516
54.16	50	51.111	0.238	0.029	90.63E-6	2.16	0.65	490
79.16	75	48.110	0.224	0.043	87.16E-6	2.10	0.65	464
104.2	100	45.239	0.210	0.057	83.70E-6	2.03	0.64	439
129.2	125	42.487	0.198	0.069	80.24E-6	1.97	0.63	416
154.2	150	39.861	0.185	0.082	76.77E-6	1.91	0.63	393
179.2	175	37.326	0.174	0.093	73.31E-6	1.85	0.62	370
204.2	200	34.926	0.162	0.105	69.85E-6	1.79	0.61	349
229.2	225	32.627	0.152	0.115	66.38E-6	1.73	0.60	328
254.2	250	30.463	0.142	0.125	62.92E-6	1.67	0.59	309
279.2	275	28.409	0.132	0.135	59.46E-6	1.61	0.57	290
304.2	300	26.462	0.123	0.144	55.99E-6	1.55	0.56	272

Table P.6 12 mm square orifice results (20.34% kaolin)

Time	Diff.Height	Mass in tank	Height	Diff.Height	Flow rate	Orifice Velocity	C _d	Re ₂
[s]	[s]	[kg]	[m]	[m]	[m ³ /s]	[m/s]		
1.658	0	60.259	0.280	0	0	0	0	0
11.66	10	57.253	0.266	0.014	219.6E-6	2.29	0.66	591
21.66	20	54.329	0.253	0.028	212.9E-6	2.23	0.66	564
31.66	30	51.542	0.240	0.041	206.2E-6	2.17	0.66	538
41.66	40	48.803	0.227	0.053	199.5E-6	2.11	0.65	513
51.66	50	46.158	0.215	0.066	192.8E-6	2.05	0.65	488
61.66	60	43.622	0.203	0.077	186.2E-6	1.99	0.65	464
71.66	70	41.173	0.191	0.089	179.5E-6	1.94	0.64	440
81.66	80	38.796	0.180	0.100	172.8E-6	1.88	0.64	417
91.66	90	36.514	0.170	0.110	166.1E-6	1.83	0.63	395
101.7	100	34.336	0.160	0.121	159.4E-6	1.77	0.62	374
111.7	110	32.225	0.150	0.130	152.7E-6	1.71	0.62	353
121.7	120	30.230	0.141	0.140	146.1E-6	1.66	0.61	334
131.7	130	28.293	0.132	0.149	139.4E-6	1.61	0.60	314
141.7	140	26.465	0.123	0.157	132.7E-6	1.55	0.59	296
151.7	150	24.740	0.115	0.165	126.0E-6	1.50	0.58	278
161.7	160	23.090	0.107	0.173	119.3E-6	1.45	0.57	262

Table P.7 16 mm square orifice results (20.34% kaolin)

Time	Diff.Height	Mass in tank	Height	Diff.Height	Flow rate	Orifice Velocity	C _d	Re ₂
[s]	[s]	[kg]	[m]	[m]	[m ³ /s]	[m/s]		
1.242	0.0	60.935	0.283	0	0	0	0	0
8.742	7.5	57.163	0.266	0.018	372.8E-6	2.28	0.64	627
16.24	15.0	53.477	0.249	0.035	359.0E-6	2.21	0.63	590
23.74	22.5	49.943	0.232	0.051	345.1E-6	2.13	0.63	555
31.24	30.0	46.522	0.216	0.067	331.2E-6	2.06	0.63	521
38.74	37.5	43.269	0.201	0.082	317.3E-6	1.99	0.62	488
46.24	45.0	40.124	0.187	0.097	303.5E-6	1.91	0.62	456
53.74	52.5	37.130	0.173	0.111	289.6E-6	1.84	0.61	425
61.24	60.0	34.313	0.160	0.124	275.7E-6	1.77	0.61	396
68.74	67.5	31.604	0.147	0.136	261.9E-6	1.70	0.60	367
76.24	75.0	29.023	0.135	0.148	248.0E-6	1.63	0.59	340
83.74	82.5	26.602	0.124	0.160	234.1E-6	1.56	0.59	314
91.24	90.0	24.337	0.113	0.170	220.2E-6	1.49	0.58	290
98.74	97.5	22.206	0.103	0.180	206.4E-6	1.42	0.56	267

Table P.8 20 mm square orifice results (20.34% kaolin)

Time	Diff.Height	Mass in tank	Height	Diff.Height	Flow rate	Orifice Velocity	C _d	Re ₂
[s]	[s]	[kg]	[m]	[m]	[m ³ /s]	[m/s]		
0.825	0	57.871	0.269	0	0	0	0	0
5.825	5	54.038	0.251	0.018	559.4E-6	2.22	0.63	623
10.83	10	50.355	0.234	0.035	537.6E-6	2.14	0.63	584
15.83	15	46.819	0.218	0.051	515.8E-6	2.07	0.62	547
20.83	20	43.439	0.202	0.067	494.1E-6	1.99	0.62	511
25.83	25	40.168	0.187	0.082	472.3E-6	1.91	0.62	476
30.83	30	37.085	0.172	0.097	450.6E-6	1.84	0.61	443
35.83	35	34.116	0.159	0.110	428.8E-6	1.76	0.61	411
40.83	40	31.315	0.146	0.123	407.0E-6	1.69	0.60	380
45.83	45	28.623	0.133	0.136	385.3E-6	1.62	0.59	350
50.83	50	26.122	0.121	0.148	363.5E-6	1.54	0.59	322
55.83	55	23.769	0.111	0.159	341.8E-6	1.47	0.58	296
60.83	60	21.547	0.100	0.169	320.0E-6	1.40	0.57	270

Triangular orifices

Table P.9 8 mm triangular orifice results (20.34% kaolin)

Time	Diff.Time	Mass in tank	Height	Diff.Height	Flow rate	Orifice Velocity	C _d	Re ₂
[s]	[s]	[kg]	[m]	[m]	[m ³ /s]	[m/s]		
3.325	0	61.945	0.290	0	0	0	0	0
23.33	20	58.454	0.273	0.016	128.8E-6	2.32	0.66	552
43.33	40	55.059	0.258	0.032	124.1E-6	2.25	0.66	523
63.33	60	51.822	0.242	0.047	119.5E-6	2.18	0.65	496
83.33	80	48.682	0.228	0.062	114.8E-6	2.11	0.65	469
103.3	100	45.693	0.214	0.076	110.1E-6	2.05	0.64	443
123.3	120	42.796	0.200	0.090	105.5E-6	1.98	0.64	418
143.3	140	40.050	0.187	0.102	100.8E-6	1.92	0.63	394
163.3	160	37.417	0.175	0.115	96.13E-6	1.85	0.62	371
183.3	180	34.900	0.163	0.127	91.46E-6	1.79	0.61	349
203.3	200	32.515	0.152	0.138	86.79E-6	1.73	0.60	327
223.3	220	30.267	0.142	0.148	82.13E-6	1.67	0.59	307
243.3	240	28.143	0.132	0.158	77.46E-6	1.61	0.58	288
263.3	260	26.131	0.122	0.168	72.79E-6	1.55	0.56	269

Table P.10 12 mm triangular orifice results (20.34% kaolin)

Time	Diff.Time	Mass in tank	Height	Diff.Height	Flow rate	Orifice Velocity	C _d	Re ₂
[s]	[s]	[kg]	[m]	[m]	[m ³ /s]	[m/s]		
1.658	0	59.406	0.278	0	0	0	0	0
11.66	10	55.633	0.260	0.018	275.8E-6	2.26	0.65	576
21.66	20	52.045	0.243	0.034	265.0E-6	2.19	0.65	543
31.66	30	48.571	0.227	0.051	254.2E-6	2.11	0.64	510
41.66	40	45.236	0.212	0.066	243.4E-6	2.04	0.64	479
51.66	50	42.065	0.197	0.081	232.6E-6	1.96	0.63	448
61.66	60	39.025	0.183	0.095	221.9E-6	1.89	0.63	419
71.66	70	36.147	0.169	0.109	211.1E-6	1.82	0.62	391
81.66	80	33.399	0.156	0.122	200.3E-6	1.75	0.61	365
91.66	90	30.788	0.144	0.134	189.5E-6	1.68	0.60	339
101.7	100	28.319	0.132	0.145	178.7E-6	1.61	0.59	314
111.7	110	26.019	0.122	0.156	167.9E-6	1.55	0.58	291
121.7	120	23.847	0.112	0.166	157.2E-6	1.48	0.57	269

Table M.11 16 mm triangular orifice results (20.34% kaolin)

Time	Diff.Time	Mass in tank	Height	Diff.Height	Flow rate	Orifice Velocity	C _d	Re ₂
[s]	[s]	[kg]	[m]	[m]	[m ³ /s]	[m/s]		[m ³ /s]
0.825	0	57.601	0.269	0	0	0	0	0
5.825	5	54.512	0.255	0.014	463.6E-6	2.24	0.65	598
10.83	10	51.469	0.241	0.029	448.4E-6	2.17	0.64	568
15.83	15	48.511	0.227	0.043	433.2E-6	2.11	0.64	538
20.83	20	45.657	0.214	0.056	418.1E-6	2.05	0.64	510
25.83	25	42.915	0.201	0.069	402.9E-6	1.98	0.63	482
30.83	30	40.293	0.188	0.081	387.7E-6	1.92	0.63	455
35.83	35	37.732	0.177	0.093	372.6E-6	1.86	0.62	429
40.83	40	35.288	0.165	0.104	357.4E-6	1.80	0.62	404
45.83	45	32.942	0.154	0.115	342.3E-6	1.74	0.61	380
50.83	50	30.736	0.144	0.126	327.1E-6	1.68	0.61	357
55.83	55	28.602	0.134	0.136	311.9E-6	1.62	0.60	334
60.83	60	26.550	0.124	0.145	296.8E-6	1.56	0.59	312
65.83	65	24.627	0.115	0.154	281.6E-6	1.50	0.58	292
70.83	70	22.817	0.107	0.163	266.4E-6	1.45	0.57	272

Table P.12 20 mm triangular orifice results (20.34% kaolin)

Time	Diff.Time	Mass in tank	Height	Diff.Height	Flow rate	Orifice Velocity	C _d	Re ₂
[s]	[s]	[kg]	[m]	[m]	[m ³ /s]	[m/s]		
0.825	0.00	58.132	0.272	0	0	0	0	0
5.825	5	53.149	0.249	0.023	732.7E-6	2.21	0.64	613
10.83	10	48.399	0.226	0.046	694.9E-6	2.11	0.64	563
15.83	15	43.884	0.205	0.067	657.0E-6	2.01	0.63	515
20.83	20	39.592	0.185	0.087	619.2E-6	1.91	0.63	469
25.83	25	35.587	0.166	0.105	581.4E-6	1.81	0.62	426
30.83	30	31.817	0.149	0.123	543.5E-6	1.71	0.61	385
35.83	35	28.311	0.132	0.140	505.7E-6	1.61	0.61	346
40.83	40	25.045	0.117	0.155	467.8E-6	1.52	0.60	310
45.83	45	22.046	0.103	0.169	430.0E-6	1.42	0.58	276
50.83	50	19.364	0.091	0.181	392.2E-6	1.33	0.57	245

APPENDIX Q: 13.14% kaolin suspension

Rheological and physical parameters

n=	0.72
k=	0.067 Pa.s ⁿ
τ_y =	8.721 Pa.s
Density=	1224 kg/m ³
g=	9.81 m/s ²

Circular orifices

Table Q.1 8 mm circular orifice results (13.14% kaolin)

Time [s]	Diff.Time [s]	Mass in tank [kg]	Height [m]	Diff.Height [m]	Flow rate [m ³ /s]	Orifice Velocity		
						C _d	Re ₂	
4.158	0	58.482	0.299	0	0	0	0	0
29.16	25	56.014	0.286	0.013	80.29E-6	2.37	0.67	2060
54.16	50	53.588	0.274	0.025	78.59E-6	2.32	0.67	1992
79.16	75	51.218	0.262	0.037	76.89E-6	2.27	0.67	1925
104.2	100	48.887	0.250	0.049	75.20E-6	2.21	0.67	1858
129.2	125	46.626	0.238	0.061	73.50E-6	2.16	0.67	1792
154.2	150	44.398	0.227	0.072	71.80E-6	2.11	0.67	1726
179.2	175	42.228	0.216	0.083	70.11E-6	2.06	0.67	1661
204.2	200	40.096	0.205	0.094	68.41E-6	2.00	0.67	1596
229.2	225	38.031	0.194	0.104	66.71E-6	1.95	0.67	1533
254.2	250	36.006	0.184	0.115	65.02E-6	1.90	0.67	1470
279.2	275	34.033	0.174	0.125	63.32E-6	1.85	0.68	1407
304.2	300	32.119	0.164	0.135	61.62E-6	1.79	0.68	1345
329.2	325	30.253	0.154	0.144	59.93E-6	1.74	0.68	1284
354.2	350	28.451	0.145	0.153	58.23E-6	1.69	0.68	1225
379.2	375	26.700	0.136	0.162	56.53E-6	1.64	0.68	1166
404.2	400	25.008	0.128	0.171	54.84E-6	1.58	0.68	1107
429.2	425	23.364	0.119	0.179	53.14E-6	1.53	0.68	1050
454.2	450	21.772	0.111	0.187	51.44E-6	1.48	0.69	993

Table Q.2 12 mm circular orifice results (13.14% kaolin)

Time	Diff.Time	Mass in tank	Height	Diff.Height	Flow rate	Orifice Velocity	C _d	Re ₂
[s]	[s]	[kg]	[m]	[m]	[m ³ /s]	[m/s]		
2.492	0	58.541	0.299	0	0	0	0	0
17.49	15	55.380	0.283	0.016	170.0E-6	2.36	0.63	2459
32.49	30	52.313	0.267	0.032	165.4E-6	2.29	0.63	2352
47.49	45	49.329	0.252	0.047	160.8E-6	2.22	0.64	2246
62.49	60	46.408	0.237	0.062	156.3E-6	2.16	0.64	2141
77.49	75	43.590	0.223	0.076	151.7E-6	2.09	0.64	2037
92.49	90	40.855	0.209	0.090	147.1E-6	2.02	0.64	1936
107.5	105	38.182	0.195	0.104	142.6E-6	1.96	0.64	1835
122.5	120	35.602	0.182	0.117	138.0E-6	1.89	0.64	1735
137.5	135	33.118	0.169	0.130	133.4E-6	1.82	0.64	1638
152.5	150	30.711	0.157	0.142	128.9E-6	1.75	0.65	1542
167.5	165	28.368	0.145	0.154	124.3E-6	1.69	0.65	1447
182.5	180	26.144	0.133	0.165	119.7E-6	1.62	0.65	1355
197.5	195	23.972	0.122	0.177	115.1E-6	1.55	0.65	1264
212.5	210	21.906	0.112	0.187	110.6E-6	1.48	0.66	1175
227.5	225	19.920	0.102	0.197	106.0E-6	1.41	0.66	1087
242.5	240	18.035	0.092	0.207	101.4E-6	1.34	0.66	1002
257.5	255	16.230	0.083	0.216	96.87E-6	1.28	0.67	919

Table Q.3 16 mm circular orifice results (13.14% kaolin)

Time	Diff.Height	Mass in tank	Height	Diff.Height	Flow rate	Orifice Velocity	C _d	Re ₂
[s]	[s]	[kg]	[m]	[m]	[m ³ /s]	[m/s]		
1.242	0	57.110	0.292	0	0	0	0	0
8.742	8	54.366	0.278	0.014	293.8E-6	2.33	0.62	2732
16.24	15	51.703	0.264	0.028	286.8E-6	2.28	0.62	2624
23.74	23	49.108	0.251	0.041	279.8E-6	2.22	0.62	2517
31.24	30	46.578	0.238	0.054	272.8E-6	2.16	0.62	2413
38.74	38	44.091	0.225	0.066	265.8E-6	2.10	0.63	2308
46.24	45	41.699	0.213	0.079	258.8E-6	2.04	0.63	2206
53.74	53	39.352	0.201	0.091	251.8E-6	1.99	0.63	2105
61.24	60	37.099	0.189	0.102	244.8E-6	1.93	0.63	2007
68.74	68	34.842	0.178	0.114	237.8E-6	1.87	0.63	1907
76.24	75	32.697	0.167	0.125	230.8E-6	1.81	0.63	1810
83.74	83	30.618	0.156	0.135	223.8E-6	1.75	0.63	1716
91.24	90	28.597	0.146	0.146	216.8E-6	1.69	0.63	1622
98.74	98	26.617	0.136	0.156	209.8E-6	1.63	0.64	1529
106.2	105	24.726	0.126	0.165	202.8E-6	1.57	0.64	1439
113.7	113	22.907	0.117	0.175	195.8E-6	1.51	0.64	1351
121.2	120	21.142	0.108	0.184	188.8E-6	1.46	0.64	1264
128.7	128	19.450	0.099	0.192	181.8E-6	1.40	0.64	1179
136.2	135	17.813	0.091	0.201	174.8E-6	1.34	0.65	1096

Table Q.4 20 mm circular orifice results (13.14% kaolin)

Time [s]	Diff.Time [s]	Mass in tank [kg]	Height [m]	Diff.Height [m]	Flow rate [m ³ /s]	Orifice Velocity		
						C _d	Re ₂	
0.825	0	57.394	0.293	0	0	0	0	0
5.825	5	54.572	0.279	0.014	457.7E-6	2.34	0.62	2985
10.83	10	51.802	0.265	0.029	446.4E-6	2.28	0.62	2860
15.83	15	49.106	0.251	0.042	435.0E-6	2.22	0.62	2738
20.83	20	46.476	0.237	0.056	423.6E-6	2.16	0.62	2617
25.83	25	43.919	0.224	0.069	412.2E-6	2.10	0.62	2499
30.83	30	41.441	0.212	0.081	400.9E-6	2.04	0.62	2382
35.83	35	38.999	0.199	0.094	389.5E-6	1.98	0.62	2266
40.83	40	36.680	0.187	0.106	378.1E-6	1.92	0.63	2154
45.83	45	34.361	0.175	0.118	366.7E-6	1.86	0.63	2040
50.83	50	32.177	0.164	0.129	355.3E-6	1.80	0.63	1932
55.83	55	30.024	0.153	0.140	344.0E-6	1.73	0.63	1823
60.83	60	27.948	0.143	0.150	332.6E-6	1.67	0.63	1717
65.83	65	25.972	0.133	0.160	321.2E-6	1.61	0.63	1615
70.83	70	24.041	0.123	0.170	309.8E-6	1.55	0.63	1514
75.83	75	22.168	0.113	0.180	298.5E-6	1.49	0.63	1414
80.83	80	20.374	0.104	0.189	287.1E-6	1.43	0.64	1316

Square orifices

Table Q.5 8 mm square orifice results (13.14% kaolin)

Time [s]	Diff.Time [s]	Mass in tank [kg]	Height [m]	Diff.Height [m]	Flow rate [m ³ /s]	Orifice Velocity		
						C _d	Re ₂	
4.158	0	56.845	0.290	0	0	0	0	0
29.16	25	53.767	0.275	0.016	99.80E-6	2.32	0.67	1995
54.16	50	50.759	0.259	0.031	97.09E-6	2.26	0.67	1909
79.16	75	47.833	0.244	0.046	94.38E-6	2.19	0.67	1825
104.2	100	44.986	0.230	0.061	91.66E-6	2.12	0.67	1741
129.2	125	42.225	0.216	0.075	88.95E-6	2.06	0.67	1659
154.2	150	39.540	0.202	0.088	86.24E-6	1.99	0.67	1577
179.2	175	36.928	0.189	0.102	83.53E-6	1.92	0.68	1497
204.2	200	34.413	0.176	0.115	80.82E-6	1.86	0.68	1418
229.2	225	31.985	0.163	0.127	78.10E-6	1.79	0.68	1340
254.2	250	29.638	0.151	0.139	75.39E-6	1.72	0.68	1263
279.2	275	27.366	0.140	0.151	72.68E-6	1.66	0.68	1187
304.2	300	25.186	0.129	0.162	69.97E-6	1.59	0.68	1112
329.2	325	23.089	0.118	0.172	67.26E-6	1.52	0.69	1039
354.2	350	21.095	0.108	0.183	64.54E-6	1.45	0.69	968

Table Q.6 12 mm square orifice results (13.14% kaolin)

Time	Diff.Time	Mass in tank	Height	Diff.Height	Flow rate	Orifice Velocity	C _d	Re ₂
[s]	[s]	[kg]	[m]	[m]	[m ³ /s]	[m/s]		
1.658	0	57.291	0.293	0	0	0	0	0
11.66	10	54.540	0.278	0.014	223.2E-6	2.34	0.66	2428
21.66	20	51.845	0.265	0.028	217.8E-6	2.28	0.66	2334
31.66	30	49.221	0.251	0.041	212.5E-6	2.22	0.66	2241
41.66	40	46.660	0.238	0.054	207.2E-6	2.16	0.66	2148
51.66	50	44.151	0.225	0.067	201.9E-6	2.10	0.66	2057
61.66	60	41.712	0.213	0.080	196.6E-6	2.04	0.67	1966
71.66	70	39.326	0.201	0.092	191.3E-6	1.98	0.67	1877
81.66	80	37.011	0.189	0.104	186.0E-6	1.93	0.67	1789
91.66	90	34.771	0.178	0.115	180.6E-6	1.87	0.67	1702
101.7	100	32.608	0.167	0.126	175.3E-6	1.81	0.67	1617
111.7	110	30.491	0.156	0.137	170.0E-6	1.75	0.67	1532
121.7	120	28.420	0.145	0.147	164.7E-6	1.69	0.68	1448
131.7	130	26.424	0.135	0.158	159.4E-6	1.63	0.68	1366
141.7	140	24.515	0.125	0.167	154.1E-6	1.57	0.68	1286
151.7	150	22.680	0.116	0.177	148.8E-6	1.51	0.68	1207
161.7	160	20.881	0.107	0.186	143.4E-6	1.45	0.69	1129
171.7	170	19.201	0.098	0.194	138.1E-6	1.39	0.69	1054

Table Q.7 16 mm square orifice results (13.14% kaolin)

Time	Diff.Time	Mass in tank	Height	Diff.Height	Flow rate	Orifice Velocity	C _d	Re ₂
[s]	[s]	[kg]	[m]	[m]	[m ³ /s]	[m/s]		
1.242	0.0	55.495	0.283	0	0	0	0	0
8.742	7.5	52.073	0.266	0.017	367.8E-6	2.28	0.63	2638
16.24	15.0	48.769	0.249	0.034	356.4E-6	2.21	0.63	2502
23.74	22.5	45.563	0.233	0.051	344.9E-6	2.14	0.63	2369
31.24	30.0	42.402	0.217	0.067	333.5E-6	2.06	0.63	2235
38.74	37.5	39.418	0.201	0.082	322.1E-6	1.99	0.63	2107
46.24	45.0	36.504	0.186	0.097	310.7E-6	1.91	0.63	1980
53.74	52.5	33.704	0.172	0.111	299.2E-6	1.84	0.63	1855
61.24	60.0	31.005	0.158	0.125	287.8E-6	1.76	0.64	1733
68.74	67.5	28.406	0.145	0.138	276.4E-6	1.69	0.64	1613
76.24	75.0	25.939	0.132	0.151	265.0E-6	1.61	0.64	1496
83.74	82.5	23.547	0.120	0.163	253.6E-6	1.54	0.64	1381
91.24	90.0	21.293	0.109	0.175	242.1E-6	1.46	0.65	1271
98.74	97.5	19.106	0.098	0.186	230.7E-6	1.38	0.65	1161

Table Q.8 20 mm square orifice results (13.14% kaolin)

Time [s]	Diff.Time [s]	Mass in tank [kg]	Height [m]	Diff.Height [m]	Flow rate [m ³ /s]	Orifice Velocity		
						C _d	Re ₂	
0.825	0	57.657	0.294	0	0	0	0	0
5.825	5	53.994	0.276	0.019	584.0E-6	2.33	0.63	2958
10.83	10	50.482	0.258	0.037	565.2E-6	2.25	0.63	2800
15.83	15	47.120	0.241	0.054	546.4E-6	2.17	0.63	2646
20.83	20	43.836	0.224	0.071	527.6E-6	2.10	0.63	2494
25.83	25	40.648	0.208	0.087	508.7E-6	2.02	0.63	2343
30.83	30	37.557	0.192	0.103	489.9E-6	1.94	0.63	2195
35.83	35	34.646	0.177	0.118	471.1E-6	1.86	0.63	2053
40.83	40	31.826	0.163	0.132	452.2E-6	1.79	0.63	1914
45.83	45	29.101	0.149	0.146	433.4E-6	1.71	0.63	1776
50.83	50	26.529	0.135	0.159	414.6E-6	1.63	0.63	1644
55.83	55	24.029	0.123	0.172	395.7E-6	1.55	0.64	1512
60.83	60	21.686	0.111	0.184	376.9E-6	1.47	0.64	1387
65.83	65	19.425	0.099	0.195	358.1E-6	1.40	0.64	1264
70.83	70	17.296	0.088	0.206	339.2E-6	1.32	0.64	1145

Triangular orifices

Table Q.9 8 mm triangular orifice results (13.14% kaolin)

Time [s]	Diff.Time [s]	Mass in tank [kg]	Height [m]	Diff.Height [m]	Flow rate [m ³ /s]	Orifice Velocity		
						C _d	Re ₂	
3.33	0.00	55.719	0.286	0	0.00E+00	0.00	0.00	0
23.33	20.00	52.546	0.270	0.016	129.2E-6	2.30	0.67	1958
43.33	40.00	49.464	0.254	0.032	125.5E-6	2.23	0.67	1870
63.33	60.00	46.459	0.239	0.048	121.7E-6	2.16	0.67	1783
83.33	80.00	43.549	0.224	0.062	118.0E-6	2.09	0.67	1697
103.33	100.00	40.714	0.209	0.077	114.3E-6	2.03	0.67	1612
123.33	120.00	37.993	0.195	0.091	110.6E-6	1.96	0.68	1528
143.33	140.00	35.326	0.181	0.105	106.8E-6	1.89	0.68	1445
163.33	160.00	32.760	0.168	0.118	103.1E-6	1.82	0.68	1363
183.33	180.00	30.284	0.156	0.131	99.39E-6	1.75	0.68	1283
203.33	200.00	27.905	0.143	0.143	95.67E-6	1.68	0.68	1204
223.33	220.00	25.622	0.132	0.155	91.94E-6	1.61	0.68	1126
243.33	240.00	23.436	0.120	0.166	88.21E-6	1.54	0.69	1050
263.33	260.00	21.333	0.110	0.177	84.49E-6	1.47	0.69	976
283.33	280.00	19.345	0.099	0.187	80.76E-6	1.40	0.69	903
303.33	300.00	17.450	0.090	0.197	77.04E-6	1.33	0.69	833

Table Q.10 12 mm triangular orifice results (13.14% kaolin)

Time	Diff.Time	Mass in tank	Height	Diff.Height	Flow rate	Orifice Velocity	C _d	Re ₂
[s]	[s]	[kg]	[m]	[m]	[m ³ /s]	[m/s]		
1.658	0	59.170	0.304	0	0	0	0	0
11.66	10	55.656	0.286	0.018	287.1E-6	2.37	0.65	2463
21.66	20	52.214	0.268	0.036	278.5E-6	2.29	0.65	2343
31.66	30	48.875	0.251	0.053	269.9E-6	2.22	0.65	2224
41.66	40	45.629	0.234	0.070	261.3E-6	2.14	0.65	2107
51.66	50	42.520	0.218	0.086	252.7E-6	2.07	0.65	1993
61.66	60	39.481	0.203	0.101	244.1E-6	1.99	0.65	1880
71.66	70	36.573	0.188	0.116	235.5E-6	1.92	0.66	1769
81.66	80	33.745	0.173	0.131	226.9E-6	1.84	0.66	1659
91.66	90	31.049	0.159	0.144	218.3E-6	1.77	0.66	1552
101.7	100	28.439	0.146	0.158	209.7E-6	1.69	0.66	1447
111.7	110	25.941	0.133	0.171	201.1E-6	1.62	0.66	1344
121.7	120	23.546	0.121	0.183	192.5E-6	1.54	0.67	1243
131.7	130	21.272	0.109	0.195	183.9E-6	1.46	0.67	1145

Table Q.11 16 mm triangular orifice results (13.14% kaolin)

Time	Diff.Time	Mass in tank	Height	Diff.Height	Flow rate	Orifice Velocity	C _d	Re ₂
[s]	[s]	[kg]	[m]	[m]	[m ³ /s]	[m/s]		
1.242	0.00	55.396	0.284	0	0	0	0	0
8.742	7.5	51.033	0.262	0.022	465.9E-6	2.27	0.64	2572
16.24	15.0	46.889	0.241	0.044	447.2E-6	2.17	0.64	2403
23.74	22.5	42.890	0.220	0.064	428.5E-6	2.08	0.64	2236
31.24	30.0	39.057	0.201	0.084	409.8E-6	1.98	0.64	2073
38.74	37.5	35.402	0.182	0.103	391.1E-6	1.89	0.65	1915
46.24	45.0	31.932	0.164	0.121	372.4E-6	1.79	0.65	1760
53.74	52.5	28.631	0.147	0.137	353.7E-6	1.70	0.65	1610
61.24	60.0	25.452	0.131	0.154	335.0E-6	1.60	0.65	1461
68.74	67.5	22.479	0.115	0.169	316.2E-6	1.50	0.65	1319
76.24	75.0	19.687	0.101	0.183	297.5E-6	1.41	0.66	1181
83.74	82.5	17.078	0.088	0.197	278.8E-6	1.31	0.66	1049

Table Q.12 20 mm triangular orifice results (13.14% kaolin)

Time	Diff.Time	Mass in tank	Height	Diff.Height	Flow rate	Orifice Velocity	C _d	Re ₂
[s]	[s]	[kg]	[m]	[m]	[m ³ /s]	[m/s]		
0.408	0.00	56.257	0.289	0	0	0	0	0
4.575	4.167	52.405	0.269	0.020	754.7E-6	2.30	0.63	2881
8.742	8.333	48.637	0.250	0.039	728.2E-6	2.21	0.63	2711
12.91	12.50	45.036	0.231	0.058	701.8E-6	2.13	0.64	2545
17.08	16.67	41.513	0.213	0.076	675.4E-6	2.05	0.64	2380
21.24	20.83	38.145	0.196	0.093	648.9E-6	1.96	0.64	2220
25.41	25.00	34.924	0.179	0.110	622.5E-6	1.88	0.64	2063
29.58	29.17	31.819	0.163	0.126	596.0E-6	1.79	0.64	1910
33.74	33.33	28.887	0.148	0.141	569.6E-6	1.71	0.64	1762
37.91	37.50	26.064	0.134	0.155	543.2E-6	1.62	0.65	1617
42.08	41.67	23.377	0.120	0.169	516.7E-6	1.53	0.65	1475
46.24	45.83	20.833	0.107	0.182	490.3E-6	1.45	0.65	1339

APPENDIX R: 7.3% bentonite suspension

Rheological and physical parameters

n=	1.00
k=	0.021 Pa.s ⁿ
τ_y =	30.5 Pa.s
Density=	1046 kg/m ³
g=	9.81 m/s ²

Circular orifices

Table R.1 8 mm circular orifice results (7.3% bentonite)

Time	Diff.Time	Mass in tank	Height	Diff.Height	Flow rate	Orifice Velocity	C_d	Re_2
[s]	[s]	[kg]	[m]	[m]	[m ³ /s]	[m/s]		
8.325	0.00	96.715	0.578	0	0	0	0	0
66.66	58.33	89.999	0.538	0.040	108.4E-6	3.25	0.66	908
125.0	116.7	83.558	0.499	0.079	103.6E-6	3.13	0.65	865
183.3	175.0	77.387	0.462	0.115	98.88E-6	3.01	0.65	822
241.7	233.3	71.493	0.427	0.151	94.12E-6	2.89	0.64	780
300.0	291.7	65.898	0.394	0.184	89.36E-6	2.78	0.63	738
358.3	350.0	60.579	0.362	0.216	84.60E-6	2.66	0.63	697
416.7	408.3	55.539	0.332	0.246	79.85E-6	2.55	0.62	657
475.0	466.7	50.797	0.303	0.274	75.09E-6	2.44	0.61	618
533.3	525.0	46.350	0.277	0.301	70.33E-6	2.33	0.59	580
591.7	583.3	42.205	0.252	0.326	65.57E-6	2.22	0.58	544
650.0	641.7	38.345	0.229	0.349	60.81E-6	2.12	0.57	508
708.3	700.0	34.785	0.208	0.370	56.05E-6	2.02	0.55	474
766.7	758.3	31.533	0.188	0.389	51.30E-6	1.92	0.53	442
825.0	816.7	28.585	0.171	0.407	46.54E-6	1.83	0.50	412
883.3	875.0	25.899	0.155	0.423	41.78E-6	1.74	0.47	383
941.7	933.3	23.455	0.140	0.438	37.02E-6	1.66	0.44	356
1000	991.7	21.319	0.127	0.450	32.26E-6	1.58	0.402	332

Table R.2 12 mm circular orifice results (7.3% bentonite)

Time	Diff.Time	Mass in tank	Height	Diff.Height	Flow rate	Orifice Velocity	C_d	Re_2
[s]	[s]	[kg]	[m]	[m]	[m ³ /s]	[m/s]		
4.158	0	95.276	0.569	0	0	0	0	0
29.16	25	89.229	0.533	0.036	234.1E-6	3.23	0.64	1170
54.16	50	83.337	0.498	0.071	225.2E-6	3.13	0.63	1114
79.16	75	77.599	0.464	0.106	216.4E-6	3.02	0.63	1059
104.2	100	72.061	0.430	0.139	207.5E-6	2.91	0.63	1005
129.2	125	66.703	0.398	0.171	198.6E-6	2.80	0.62	951
154.2	150	61.580	0.368	0.201	189.7E-6	2.69	0.62	897
179.2	175	56.680	0.339	0.231	180.8E-6	2.58	0.62	844
204.2	200	52.019	0.311	0.258	171.9E-6	2.47	0.61	793
229.2	225	47.602	0.284	0.285	163.0E-6	2.36	0.61	743
254.2	250	43.428	0.259	0.310	154.1E-6	2.26	0.60	693
279.2	275	39.521	0.236	0.333	145.2E-6	2.15	0.59	646
304.2	300	35.854	0.214	0.355	136.3E-6	2.05	0.58	600
329.2	325	32.452	0.194	0.375	127.4E-6	1.95	0.57	556
354.2	350	29.321	0.175	0.394	118.5E-6	1.85	0.56	514

Table R.3 16 mm circular orifice results (7.3% bentonite)

Time [s]	Diff.Time [s]	Mass in tank [kg]	Height [m]	Diff.Height [m]	Flow rate [m ³ /s]	Orifice Velocity		
						C _d	Re ₂	
3.325	0	98.174	0.586	0	0	0	0	0
23.33	20	89.719	0.536	0.051	4.03E-04	3.24	0.61	1378
43.33	40	81.595	0.487	0.099	3.83E-04	3.09	0.61	1284
63.33	60	73.843	0.441	0.145	3.63E-04	2.94	0.61	1192
83.33	80	66.404	0.397	0.190	3.44E-04	2.79	0.61	1100
103.3	100	59.325	0.354	0.232	3.24E-04	2.64	0.61	1010
123.3	120	52.656	0.315	0.272	3.05E-04	2.48	0.61	921
143.3	140	46.420	0.277	0.309	2.85E-04	2.33	0.60	835
163.3	160	40.632	0.243	0.344	2.65E-04	2.18	0.60	753
183.3	180	35.324	0.211	0.375	2.46E-04	2.03	0.60	674
203.3	200	30.489	0.182	0.404	2.26E-04	1.89	0.59	599
223.3	220	26.147	0.156	0.430	2.06E-04	1.75	0.58	529

Table R.4 20 mm circular orifice results (7.3% bentonite)

Time [s]	Diff.Time [s]	Mass in tank [kg]	Height [m]	Diff.Height [m]	Flow rate [m ³ /s]	Orifice Velocity		
						C _d	Re ₂	
1.658	0	98.186	0.587	0	0	0	0	0
11.66	10	91.567	0.547	0.040	632.0E-6	3.28	0.61	1563
21.66	20	85.176	0.509	0.078	608.4E-6	3.16	0.61	1478
31.66	30	78.994	0.472	0.115	584.7E-6	3.04	0.61	1395
41.66	40	73.045	0.436	0.150	561.1E-6	2.93	0.61	1312
51.66	50	67.296	0.402	0.185	537.5E-6	2.81	0.61	1231
61.66	60	61.782	0.369	0.217	513.8E-6	2.69	0.61	1151
71.66	70	56.445	0.337	0.249	490.2E-6	2.57	0.60	1071
81.66	80	51.373	0.307	0.280	466.5E-6	2.45	0.60	994
91.66	90	46.555	0.278	0.308	442.9E-6	2.34	0.60	918
101.7	100	41.990	0.251	0.336	419.2E-6	2.22	0.60	845
111.7	110	37.700	0.225	0.361	395.6E-6	2.10	0.60	774
121.7	120	33.714	0.201	0.385	371.9E-6	1.99	0.59	706
131.7	130	30.017	0.179	0.407	348.3E-6	1.88	0.59	641
141.7	140	26.613	0.159	0.428	324.7E-6	1.77	0.58	580
151.7	150	23.507	0.140	0.446	301.0E-6	1.66	0.57	522

Square orifices

Table R.5 8 mm square orifice results (7.3% bentonite)

Time	Diff.Time	Mass in tank	Height	Diff.Height	Flow rate	Orifice Velocity	C _d	Re ₂
[s]	[s]	[Kg]	[m]	[m]	[m ³ /s]	[m/s]		
8.325	0	95.497	0.570	0	0	0	0	0
58.33	50	88.286	0.527	0.043	137.4E-6	3.22	0.66	895
108.3	100	81.326	0.486	0.085	130.7E-6	3.09	0.66	848
158.3	150	74.663	0.446	0.124	124.0E-6	2.96	0.65	801
208.3	200	68.338	0.408	0.162	117.2E-6	2.83	0.64	755
258.3	250	62.367	0.373	0.198	110.5E-6	2.70	0.64	710
308.3	300	56.741	0.339	0.232	103.8E-6	2.58	0.63	666
358.3	350	51.457	0.307	0.263	97.09E-6	2.46	0.61	623
408.3	400	46.541	0.278	0.292	90.38E-6	2.34	0.60	581
458.3	450	41.967	0.251	0.320	83.66E-6	2.22	0.59	541
508.3	500	37.766	0.226	0.345	76.94E-6	2.10	0.57	502
558.3	550	33.932	0.203	0.368	70.23E-6	1.99	0.55	465
608.3	600	30.446	0.182	0.389	63.51E-6	1.89	0.52	430
658.3	650	27.321	0.163	0.407	56.79E-6	1.79	0.49	398
708.3	700	24.545	0.147	0.424	50.08E-6	1.70	0.46	368
758.3	750	22.137	0.132	0.438	43.36E-6	1.61	0.42	341

Table R.6 12 mm square orifice results (7.3% bentonite)

Time	Diff.Time	Mass in tank	Height	Diff.Height	Flow rate	Orifice Velocity	C _d	Re ₂
[s]	[s]	[kg]	[m]	[m]	[m ³ /s]	[m/s]		
4.158	0	98.022	0.586	0	0	0	0	0
29.16	25	90.017	0.538	0.048	308.0E-6	3.25	0.66	1176
54.16	50	82.293	0.492	0.094	292.6E-6	3.11	0.65	1104
79.16	75	74.874	0.447	0.138	277.1E-6	2.96	0.65	1032
104.2	100	67.763	0.405	0.181	261.6E-6	2.82	0.64	961
129.2	125	61.040	0.365	0.221	246.1E-6	2.67	0.64	891
154.2	150	54.745	0.327	0.259	230.6E-6	2.53	0.63	823
179.2	175	48.860	0.292	0.294	215.2E-6	2.39	0.62	756
204.2	200	43.409	0.259	0.326	199.7E-6	2.26	0.61	693
229.2	225	38.399	0.229	0.356	184.2E-6	2.12	0.60	632
254.2	250	33.824	0.202	0.384	168.7E-6	1.99	0.59	574
279.2	275	29.711	0.177	0.408	153.2E-6	1.87	0.57	519
304.2	300	26.039	0.156	0.430	137.8E-6	1.75	0.55	469

Table R.7 16 mm square orifice results (7.3% bentonite)

Time [s]	Diff.Height [s]	Mass in tank [kg]	Height [m]	Diff.Height [m]	Flow rate [m ³ /s]	Orifice Velocity		
						C _d	Re ₂	
1.658	0.00	96.303	0.575	0	0	0	0	0
13.33	11.67	90.080	0.538	0.037	510.1E-6	3.25	0.61	1381
24.99	23.33	84.033	0.502	0.073	491.9E-6	3.14	0.61	1312
36.66	35.00	78.185	0.467	0.108	473.7E-6	3.03	0.61	1243
48.33	46.67	72.537	0.433	0.142	455.5E-6	2.92	0.61	1175
59.99	58.33	67.079	0.401	0.175	437.3E-6	2.80	0.61	1108
71.66	70.00	61.852	0.370	0.206	419.1E-6	2.69	0.61	1042
83.33	81.67	56.781	0.339	0.236	400.9E-6	2.58	0.61	976
94.99	93.33	51.931	0.310	0.265	382.7E-6	2.47	0.60	911
106.7	105.0	47.310	0.283	0.293	364.6E-6	2.35	0.60	847
118.3	116.7	42.949	0.257	0.319	346.4E-6	2.24	0.60	786
130.0	128.3	38.835	0.232	0.343	328.2E-6	2.13	0.60	726
141.7	140.0	34.986	0.209	0.366	310.0E-6	2.03	0.60	668
153.3	151.7	31.431	0.188	0.388	291.8E-6	1.92	0.59	613
165.0	163.3	28.129	0.168	0.407	273.6E-6	1.82	0.59	561

Table R.8 20 mm square orifice results (7.3% bentonite)

Time [s]	Diff.Time [s]	Mass in tank [kg]	Height [m]	Diff.Height [m]	Flow rate [m ³ /s]	Orifice Velocity		
						C _d	Re ₂	
1.658	0.00	95.372	0.570	0	0	0	0	0
11.66	10.00	87.075	0.520	0.050	785.2E-6	3.19	0.61	1503
21.66	20.00	79.142	0.473	0.097	746.1E-6	3.05	0.61	1396
31.66	30.00	71.567	0.428	0.142	707.1E-6	2.90	0.61	1291
41.66	40.00	64.357	0.384	0.185	668.1E-6	2.75	0.61	1188
51.66	50.00	57.532	0.344	0.226	629.1E-6	2.60	0.60	1087
61.66	60.00	51.100	0.305	0.264	590.1E-6	2.45	0.60	989
71.66	70.00	45.050	0.269	0.301	551.1E-6	2.30	0.60	894
81.66	80.00	39.451	0.236	0.334	512.1E-6	2.15	0.59	802
91.66	90.00	34.324	0.205	0.365	473.1E-6	2.01	0.59	716
101.7	100.00	29.650	0.177	0.393	434.1E-6	1.86	0.58	634
111.7	110.00	25.499	0.152	0.417	395.1E-6	1.73	0.57	559

Triangular orifice

Table R.9 8 mm triangular orifice results (7.3% bentonite)

Time	Diff.Time	Mass in tank	Height	Diff.Height	Flow rate	Orifice Velocity	C _d	Re ₂
[s]	[s]	[kg]	[m]	[m]	[m ³ /s]	[m/s]		
6.658	0	93.620	0.559	0	0	0	0	0
46.66	40	86.275	0.516	0.044	176.7E-6	3.18	0.66	882
86.66	80	79.161	0.473	0.086	167.8E-6	3.05	0.66	833
126.7	120	72.306	0.432	0.127	159.0E-6	2.91	0.65	785
166.7	160	65.805	0.393	0.166	150.1E-6	2.78	0.65	737
206.7	200	59.667	0.357	0.203	141.2E-6	2.64	0.64	689
246.7	240	53.911	0.322	0.237	132.3E-6	2.51	0.63	643
286.7	280	48.531	0.290	0.269	123.4E-6	2.39	0.62	598
326.7	320	43.540	0.260	0.299	114.6E-6	2.26	0.61	555
366.7	360	38.927	0.233	0.327	105.7E-6	2.14	0.59	513
406.7	400	34.716	0.207	0.352	96.79E-6	2.02	0.57	473
446.7	440	30.886	0.185	0.375	87.91E-6	1.90	0.55	435
486.7	480	27.448	0.164	0.395	79.03E-6	1.79	0.53	399
526.7	520	24.383	0.146	0.414	70.15E-6	1.69	0.50	366

Table R.10 12 mm triangular orifice results (7.3% bentonite)

Time	Diff.Time	Mass in tank	Height	Diff.Height	Flow rate	Orifice Velocity	C _d	Re ₂
[s]	[s]	[kg]	[m]	[m]	[m ³ /s]	[m/s]		
3.325	0	94.822	0.567	0	0	0	0	0
23.33	20	86.828	0.519	0.048	385.2E-6	3.19	0.64	1145
43.33	40	79.133	0.473	0.094	364.8E-6	3.05	0.64	1073
63.33	60	71.761	0.429	0.138	344.4E-6	2.90	0.63	1000
83.33	80	64.722	0.387	0.180	324.0E-6	2.75	0.63	929
103.3	100	58.081	0.347	0.220	303.6E-6	2.61	0.62	858
123.3	120	51.847	0.310	0.257	283.2E-6	2.47	0.61	790
143.3	140	46.071	0.275	0.291	262.8E-6	2.32	0.60	724
163.3	160	40.745	0.243	0.323	242.4E-6	2.19	0.59	660
183.3	180	35.865	0.214	0.352	222.0E-6	2.05	0.58	600
203.3	200	31.449	0.188	0.379	201.6E-6	1.92	0.56	542
223.3	220	27.502	0.164	0.402	181.2E-6	1.80	0.54	489
243.3	240	24.017	0.144	0.423	160.8E-6	1.68	0.51	440
263.3	260	21.019	0.126	0.441	140.4E-6	1.57	0.48	396

Table R.11 16 mm triangular orifice results (7.3% bentonite)

Time [s]	Diff.Time [s]	Mass in tank [kg]	Height [m]	Diff.Height [m]	Flow rate [m ³ /s]	Orifice Velocity		
						C _d	Re ₂	[m/s]
1.658	0	97.196	0.581	0	0	0	0	0
11.66	10	90.354	0.540	0.041	659.2E-6	3.25	0.63	1370
21.66	20	83.725	0.500	0.080	632.3E-6	3.13	0.63	1295
31.66	30	77.328	0.462	0.119	605.5E-6	3.01	0.63	1221
41.66	40	71.179	0.425	0.155	578.6E-6	2.89	0.62	1147
51.66	50	65.260	0.390	0.191	551.7E-6	2.77	0.62	1075
61.66	60	59.580	0.356	0.225	524.9E-6	2.64	0.62	1003
71.66	70	54.141	0.323	0.257	498.0E-6	2.52	0.62	932
81.66	80	48.990	0.293	0.288	471.1E-6	2.40	0.61	863
91.66	90	44.123	0.264	0.317	444.3E-6	2.27	0.61	796
101.7	100	39.572	0.236	0.344	417.4E-6	2.15	0.60	731
111.7	110	35.338	0.211	0.370	390.5E-6	2.04	0.60	668
121.7	120	31.421	0.188	0.393	363.7E-6	1.92	0.59	608
131.7	130	27.835	0.166	0.414	336.8E-6	1.81	0.58	552
141.7	140	24.586	0.147	0.434	309.9E-6	1.70	0.57	499
151.7	150	21.684	0.130	0.451	283.1E-6	1.59	0.55	450

Table R.12 20 mm triangular orifice results (7.3% bentonite)

Time [s]	Diff.Time [s]	Mass in tank [kg]	Height [m]	Diff.Height [m]	Flow rate [m ³ /s]	Orifice Velocity		
						C _d	Re ₂	[m/s]
1.242	0.0	94.795	0.566	0	0	0	0	0
8.742	7.5	86.641	0.518	0.049	1.021E-3	3.19	0.62	1495
16.24	15.0	78.833	0.471	0.095	967.8E-6	3.04	0.61	1390
23.74	22.5	71.395	0.427	0.140	914.8E-6	2.89	0.61	1287
31.24	30.0	64.299	0.384	0.182	861.8E-6	2.75	0.61	1186
38.74	37.5	57.584	0.344	0.222	808.8E-6	2.60	0.60	1087
46.24	45.0	51.207	0.306	0.260	755.8E-6	2.45	0.60	990
53.74	52.5	45.213	0.270	0.296	702.8E-6	2.30	0.59	896
61.24	60.0	39.601	0.237	0.330	649.8E-6	2.15	0.58	804
68.74	67.5	34.443	0.206	0.361	596.8E-6	2.01	0.57	717
76.24	75.0	29.699	0.177	0.389	543.8E-6	1.87	0.56	635
83.74	82.5	25.442	0.152	0.414	490.8E-6	1.73	0.55	558

APPENDIX S: 7.18% bentonite suspension

Rheological and physical parameters

n=	1.00
k=	0.014 Pa.s ⁿ
τ_y =	15.738 Pa.s
Density=	1044 kg/m ³
g=	9.81 m/s ²

Circular orifices

Table S.1 8 mm circular orifice results (7.18% bentonite)

Time [s]	Diff.Time [s]	Mass in tank [kg]	Height [m]	Diff.Height [m]	Flow rate [m ³ /s]	Orifice		
						Velocity [m/s]	C_d	Re_2
5.825	0	61.711	0.370	0	0	0	0	0
40.83	35	58.405	0.350	0.020	89.82E-6	2.62	0.68	1116
75.83	70	55.199	0.331	0.039	86.96E-6	2.55	0.67	1075
110.8	105	52.072	0.312	0.058	84.11E-6	2.47	0.67	1035
145.8	140	49.050	0.294	0.076	81.25E-6	2.40	0.67	995
180.8	175	46.149	0.276	0.093	78.40E-6	2.33	0.66	955
215.8	210	43.318	0.259	0.110	75.54E-6	2.26	0.66	916
250.8	245	40.596	0.243	0.126	72.69E-6	2.18	0.66	877
285.8	280	37.997	0.228	0.142	69.83E-6	2.11	0.65	838
320.8	315	35.482	0.212	0.157	66.98E-6	2.04	0.65	800
355.8	350	33.088	0.198	0.171	64.12E-6	1.97	0.64	763
390.8	385	30.794	0.184	0.185	61.27E-6	1.90	0.63	726
425.8	420	28.615	0.171	0.198	58.41E-6	1.83	0.63	690
460.8	455	26.536	0.159	0.211	55.56E-6	1.77	0.62	655
495.8	490	24.570	0.147	0.222	52.70E-6	1.70	0.61	621
530.8	525	22.697	0.136	0.234	49.85E-6	1.63	0.60	587
565.8	560	20.943	0.125	0.244	46.99E-6	1.57	0.59	554

Table S.2 12 mm circular orifice results (7.18% bentonite)

Time	Diff.Time	Mass in tank	Height	Diff.Height	Flow rate	Orifice Velocity	C _d	Re ₂
[s]	[s]	[kg]	[m]	[m]	[m ³ /s]	[m/s]		
2.492	0	61.428	0.368	0	0	0	0	0
17.49	15	58.420	0.350	0.018	192.3E-6	2.62	0.64	1450
32.49	30	55.474	0.332	0.036	187.2E-6	2.55	0.64	1398
47.49	45	52.613	0.315	0.053	182.1E-6	2.49	0.64	1347
62.49	60	49.798	0.298	0.070	177.0E-6	2.42	0.64	1296
77.49	75	47.075	0.282	0.086	171.9E-6	2.35	0.64	1245
92.49	90	44.408	0.266	0.102	166.8E-6	2.28	0.64	1194
107.5	105	41.817	0.250	0.117	161.7E-6	2.22	0.64	1144
122.5	120	39.322	0.235	0.132	156.6E-6	2.15	0.64	1094
137.5	135	36.894	0.221	0.147	151.5E-6	2.08	0.64	1045
152.5	150	34.557	0.207	0.161	146.4E-6	2.01	0.64	996
167.5	165	32.302	0.193	0.174	141.3E-6	1.95	0.64	948
182.5	180	30.123	0.180	0.187	136.2E-6	1.88	0.64	900
197.5	195	28.033	0.168	0.200	131.0E-6	1.81	0.63	854
212.5	210	26.017	0.156	0.212	125.9E-6	1.75	0.63	807
227.5	225	24.113	0.144	0.223	120.8E-6	1.68	0.63	763
242.5	240	22.283	0.133	0.234	115.7E-6	1.62	0.63	718
257.5	255	20.547	0.123	0.245	110.6E-6	1.55	0.63	675

Table S.3 16 mm circular orifice results (7.18% bentonite)

Time	Diff.Time	Mass in tank	Height	Diff.Height	Flow rate	Orifice Velocity	C _d	Re ₂
[s]	[s]	[kg]	[m]	[m]	[m ³ /s]	[m/s]		
1.658	0	58.202	0.348	0	0	0	0	0
11.66	10	54.875	0.329	0.020	316.6E-6	2.54	0.62	1629
21.66	20	51.629	0.309	0.039	307.2E-6	2.46	0.62	1557
31.66	30	48.504	0.290	0.058	297.8E-6	2.39	0.62	1487
41.66	40	45.461	0.272	0.076	288.5E-6	2.31	0.62	1416
51.66	50	42.494	0.254	0.094	279.1E-6	2.23	0.62	1346
61.66	60	39.636	0.237	0.111	269.8E-6	2.16	0.62	1277
71.66	70	36.851	0.221	0.128	260.4E-6	2.08	0.62	1208
81.66	80	34.151	0.204	0.144	251.1E-6	2.00	0.62	1140
91.66	90	31.567	0.189	0.159	241.7E-6	1.93	0.62	1073
101.7	100	29.067	0.174	0.174	232.4E-6	1.85	0.62	1006
111.7	110	26.679	0.160	0.189	223.0E-6	1.77	0.62	941
121.7	120	24.422	0.146	0.202	213.6E-6	1.69	0.62	878
131.7	130	22.263	0.133	0.215	204.3E-6	1.62	0.63	816
141.7	140	20.207	0.121	0.228	194.9E-6	1.54	0.63	756
151.7	150	18.275	0.109	0.239	185.6E-6	1.47	0.63	697

Table S.4 20 mm circular orifice results (7.18% bentonite)

Time	Diff.Time	Mass in tank	Height	Diff.Height	Flow rate	Orifice Velocity	C _d	Re ₂
[s]	[s]	[kg]	[m]	[m]	[m ³ /s]	[m/s]		
0.825	0.00	59.640	0.357	0	0	0	0	0
7.492	6.67	56.126	0.336	0.021	505.5E-6	2.57	0.62	1851
14.16	13.33	52.643	0.315	0.042	489.8E-6	2.49	0.62	1762
20.83	20.00	49.314	0.295	0.062	474.1E-6	2.41	0.62	1676
27.49	26.67	46.102	0.276	0.081	458.3E-6	2.33	0.62	1591
34.16	33.33	42.980	0.257	0.100	442.6E-6	2.25	0.62	1506
40.83	40.00	39.941	0.239	0.118	426.8E-6	2.17	0.62	1422
47.49	46.67	36.994	0.222	0.136	411.1E-6	2.08	0.63	1339
54.16	53.33	34.181	0.205	0.152	395.3E-6	2.00	0.63	1257
60.83	60.00	31.464	0.188	0.169	379.6E-6	1.92	0.63	1177
67.49	66.67	28.878	0.173	0.184	363.9E-6	1.84	0.63	1099
74.16	73.33	26.355	0.158	0.199	348.1E-6	1.76	0.63	1020
80.83	80.00	24.011	0.144	0.213	332.4E-6	1.68	0.63	946
87.49	86.67	21.769	0.130	0.227	316.6E-6	1.60	0.63	873
94.16	93.33	19.639	0.118	0.240	300.9E-6	1.52	0.63	802

Square orifices

Table S.5 8 mm square orifice results (7.18% bentonite)

Time	Diff.Time	Mass in tank	Height	Diff.Height	Flow rate	velocity	C _d	Re ₂
[s]	[s]	[kg]	[m]	[m]	[m ³ /s]	[m/s]		
4.158	0	62.021	0.371	0	0	0	0	
29.16	25	59.006	0.353	0.018	115.3E-6	2.63	0.68	1121
54.16	50	56.065	0.336	0.036	112.1E-6	2.57	0.68	1084
79.16	75	53.206	0.319	0.053	108.9E-6	2.50	0.68	1048
104.2	100	50.411	0.302	0.070	105.6E-6	2.43	0.67	1011
129.2	125	47.687	0.286	0.086	102.4E-6	2.37	0.67	975
154.2	150	45.064	0.270	0.102	99.12E-6	2.30	0.67	939
179.2	175	42.518	0.255	0.117	95.87E-6	2.23	0.67	903
204.2	200	40.031	0.240	0.132	92.63E-6	2.17	0.66	867
229.2	225	37.650	0.225	0.146	89.38E-6	2.10	0.66	832
254.2	250	35.354	0.212	0.160	86.14E-6	2.04	0.66	797
279.2	275	33.132	0.198	0.173	82.89E-6	1.97	0.65	762
304.2	300	31.008	0.186	0.186	79.64E-6	1.91	0.65	729
329.2	325	28.974	0.173	0.198	76.40E-6	1.84	0.64	695
354.2	350	27.037	0.162	0.209	73.15E-6	1.78	0.64	663
379.2	375	25.173	0.151	0.221	69.91E-6	1.72	0.63	630
404.2	400	23.407	0.140	0.231	66.66E-6	1.66	0.62	599
429.2	425	21.730	0.130	0.241	63.42E-6	1.60	0.62	568
454.2	450	20.132	0.121	0.251	60.17E-6	1.54	0.61	538

Table S.6 12 mm square orifice results (7.18% bentonite)

Time [s]	Diff.Time [s]	Mass in tank [kg]	Height [m]	Diff.Height [m]	Flow rate [m ³ /s]	Orifice Velocity		
						C _d	Re ₂	
1.658	0	61.032	0.365	0	0.00E+00	0.00	0.00	0
11.66	10	58.419	0.350	0.016	249.8E-6	2.62	0.66	1449
21.66	20	55.877	0.335	0.031	244.2E-6	2.56	0.66	1404
31.66	30	53.384	0.320	0.046	238.7E-6	2.50	0.66	1360
41.66	40	50.944	0.305	0.060	233.1E-6	2.45	0.66	1316
51.66	50	48.530	0.291	0.075	227.5E-6	2.39	0.66	1271
61.66	60	46.168	0.276	0.089	222.0E-6	2.33	0.66	1227
71.66	70	43.893	0.263	0.103	216.4E-6	2.27	0.66	1183
81.66	80	41.654	0.249	0.116	210.8E-6	2.21	0.66	1140
91.66	90	39.462	0.236	0.129	205.3E-6	2.15	0.66	1096
101.7	100	37.325	0.223	0.142	199.7E-6	2.09	0.66	1053
111.7	110	35.253	0.211	0.154	194.1E-6	2.04	0.66	1010
121.7	120	33.228	0.199	0.166	188.6E-6	1.98	0.66	967
131.7	130	31.304	0.187	0.178	183.0E-6	1.92	0.66	926
141.7	140	29.437	0.176	0.189	177.5E-6	1.86	0.66	884
151.7	150	27.610	0.165	0.200	171.9E-6	1.80	0.66	843
161.7	160	25.868	0.155	0.211	166.3E-6	1.74	0.66	803
171.7	170	24.216	0.145	0.220	160.8E-6	1.69	0.66	764
181.7	180	22.579	0.135	0.230	155.2E-6	1.63	0.66	725

Table S.7 16 mm square orifice results (7.18% bentonite)

Time [s]	Diff.Height [s]	Mass in tank [kg]	Height [m]	Diff.Height [m]	Flow rate [m ³ /s]	Orifice Velocity		
						C _d	Re ₂	
1.658	0	60.210	0.361	0	0.00E+00	0.00	0.00	0
11.66	10	55.836	0.334	0.026	414.4E-6	2.56	0.63	1649
21.66	20	51.634	0.309	0.051	398.2E-6	2.46	0.63	1556
31.66	30	47.584	0.285	0.076	382.0E-6	2.36	0.63	1465
41.66	40	43.678	0.262	0.099	365.8E-6	2.27	0.63	1374
51.66	50	39.947	0.239	0.121	349.6E-6	2.17	0.63	1284
61.66	60	36.355	0.218	0.143	333.4E-6	2.07	0.63	1195
71.66	70	32.939	0.197	0.163	317.1E-6	1.97	0.63	1108
81.66	80	29.694	0.178	0.183	300.9E-6	1.87	0.63	1023
91.66	90	26.617	0.159	0.201	284.7E-6	1.77	0.63	939
101.7	100	23.719	0.142	0.218	268.5E-6	1.67	0.63	858
111.7	110	21.045	0.126	0.235	252.3E-6	1.57	0.63	780
121.7	120	18.506	0.111	0.250	236.1E-6	1.47	0.62	704
131.7	130	16.196	0.097	0.264	219.9E-6	1.38	0.62	632

Table S.8 20 mm square orifice results (7.18% bentonite)

Time	Diff.Time	Mass in tank	Height	Diff.Height	Flow rate	Orifice		
						Velocity	C _d	Re ₂
[s]	[s]	[kg]	[m]	[m]	[m ³ /s]	[m/s]		
0.825	0	57.736	0.346	0	0	0	0	0
5.825	5	54.411	0.326	0.020	635.0E-6	2.53	0.63	1807
10.83	10	51.175	0.306	0.039	615.4E-6	2.45	0.63	1724
15.83	15	48.043	0.288	0.058	595.9E-6	2.38	0.63	1642
20.83	20	44.975	0.269	0.076	576.3E-6	2.30	0.63	1560
25.83	25	42.038	0.252	0.094	556.7E-6	2.22	0.63	1480
30.83	30	39.169	0.235	0.111	537.2E-6	2.15	0.62	1400
35.83	35	36.410	0.218	0.128	517.6E-6	2.07	0.62	1321
40.83	40	33.778	0.202	0.143	498.0E-6	1.99	0.62	1245
45.83	45	31.195	0.187	0.159	478.4E-6	1.91	0.62	1168
50.83	50	28.727	0.172	0.174	458.9E-6	1.84	0.62	1094
55.83	55	26.396	0.158	0.188	439.3E-6	1.76	0.62	1021
60.83	60	24.123	0.144	0.201	419.7E-6	1.68	0.62	949
65.83	65	21.983	0.132	0.214	400.2E-6	1.61	0.62	880
70.83	70	19.943	0.119	0.226	380.6E-6	1.53	0.62	812
75.83	75	18.012	0.108	0.238	361.0E-6	1.45	0.62	746
80.83	80	16.197	0.097	0.249	341.5E-6	1.38	0.62	683
85.83	85	14.497	0.087	0.259	321.9E-6	1.31	0.62	622
90.83	90	12.953	0.078	0.268	302.3E-6	1.23	0.61	565

Triangular orifices**Table S.9 8 mm triangular orifice results (7.18% bentonite)**

Time	Diff.Time	Mass in tank	Height	Diff.Height	Flow rate	Orifice		
						Velocity	C _d	Re ₂
[s]	[s]	[kg]	[m]	[m]	[m ³ /s]	[m/s]		
4.158	0	61.336	0.367	0	0	0	0	0
29.16	25	57.465	0.344	0.023	147.6E-6	2.60	0.68	1103
54.16	50	53.715	0.322	0.046	142.1E-6	2.51	0.68	1055
79.16	75	50.076	0.300	0.067	136.7E-6	2.43	0.67	1007
104.2	100	46.572	0.279	0.088	131.2E-6	2.34	0.67	960
129.2	125	43.384	0.260	0.107	125.8E-6	2.26	0.67	915
154.2	150	39.988	0.239	0.128	120.3E-6	2.17	0.66	867
179.2	175	36.898	0.221	0.146	114.8E-6	2.08	0.66	821
204.2	200	33.969	0.203	0.164	109.4E-6	2.00	0.65	776
229.2	225	31.173	0.187	0.181	103.9E-6	1.91	0.65	732
254.2	250	28.547	0.171	0.196	98.4E-6	1.83	0.64	688
279.2	275	26.048	0.156	0.211	93.0E-6	1.75	0.64	646
304.2	300	23.721	0.142	0.225	87.5E-6	1.67	0.63	605
329.2	325	21.545	0.129	0.238	82.0E-6	1.59	0.62	565
354.2	350	19.504	0.117	0.250	76.6E-6	1.51	0.60	526

Table S.10 12 mm triangular orifice results (7.18% bentonite)

Time	Diff.Time	Mass in tank	Height	Diff.Height	Flow rate	Orifice Velocity	C _d	Re ₂
[s]	[s]	[kg]	[m]	[m]	[m ³ /s]	[m/s]		
1.658	0	60.825	0.364	0	0	0	0	0
11.66	10	57.529	0.344	0.020	317.3E-6	2.60	0.65	1432
21.66	20	54.296	0.325	0.039	307.9E-6	2.53	0.65	1375
31.66	30	51.139	0.306	0.058	298.5E-6	2.45	0.65	1318
41.66	40	48.074	0.288	0.076	289.1E-6	2.38	0.65	1262
51.66	50	45.101	0.270	0.094	279.7E-6	2.30	0.65	1206
61.66	60	42.240	0.253	0.111	270.3E-6	2.23	0.65	1151
71.66	70	39.417	0.236	0.128	260.9E-6	2.15	0.65	1095
81.66	80	36.748	0.220	0.144	251.5E-6	2.08	0.65	1040
91.66	90	34.149	0.204	0.160	242.1E-6	2.00	0.65	986
101.7	100	31.672	0.190	0.175	232.7E-6	1.93	0.64	933
111.7	110	29.278	0.175	0.189	223.3E-6	1.85	0.64	881
121.7	120	26.987	0.162	0.203	213.9E-6	1.78	0.64	829
131.7	130	24.842	0.149	0.215	204.5E-6	1.71	0.64	779
141.7	140	22.786	0.136	0.228	195.1E-6	1.64	0.64	730
151.7	150	20.836	0.125	0.239	185.7E-6	1.56	0.63	682

Table S.11 16 mm triangular orifice results (7.18% bentonite)

Time	Diff.Time	Mass in tank	Height	Diff.Height	Flow rate	Orifice Velocity	C _d	Re ₂
[s]	[s]	[kg]	[m]	[m]	[m ³ /s]	[m/s]		
1.242	0.00	60.233	0.361	0	0	0	0	0
8.742	7.50	56.125	0.336	0.025	524.0E-6	2.57	0.64	1638
16.24	15.00	52.164	0.312	0.048	504.6E-6	2.48	0.64	1552
23.74	22.50	48.277	0.289	0.072	485.2E-6	2.38	0.63	1466
31.24	30.00	44.544	0.267	0.094	465.8E-6	2.29	0.63	1380
38.74	37.50	40.967	0.245	0.115	446.4E-6	2.19	0.63	1296
46.24	45.00	37.545	0.225	0.136	427.0E-6	2.10	0.63	1213
53.74	52.50	34.235	0.205	0.156	407.6E-6	2.01	0.63	1131
61.24	60.00	31.100	0.186	0.174	388.2E-6	1.91	0.63	1050
68.74	67.50	28.142	0.169	0.192	368.8E-6	1.82	0.63	972
76.24	75.00	25.310	0.152	0.209	349.4E-6	1.72	0.63	895
83.74	82.50	22.685	0.136	0.225	330.0E-6	1.63	0.63	821
91.24	90.00	20.221	0.121	0.240	310.7E-6	1.54	0.63	750
98.74	97.50	17.898	0.107	0.253	291.3E-6	1.45	0.63	680

Table S.12 20 mm triangular orifice results (7.18% bentonite)

Time [s]	Diff.Time [s]	Mass in tank [kg]	Height [m]	Diff.Height [m]	Flow rate [m ³ /s]	Orifice Velocity [m/s]	C _d	Re ₂
0.408	0.00	54.683	0.327	0	810.7E-6	2.49	0.63	1759
2.908	2.50	52.598	0.315	0.012	794.8E-6	2.44	0.63	1704
5.408	5.00	50.480	0.302	0.025	778.9E-6	2.38	0.63	1650
7.908	7.50	48.412	0.290	0.038	763.0E-6	2.34	0.63	1597
10.41	10.00	46.410	0.278	0.050	747.2E-6	2.29	0.63	1544
12.91	12.50	44.450	0.266	0.061	731.3E-6	2.23	0.63	1491
15.41	15.00	42.492	0.254	0.073	715.4E-6	2.18	0.63	1439
17.91	17.50	40.627	0.243	0.084	699.5E-6	2.13	0.63	1388
20.41	20.00	38.782	0.232	0.095	683.6E-6	2.08	0.63	1336
22.91	22.50	36.963	0.221	0.106	667.8E-6	2.03	0.63	1287
25.41	25.00	35.244	0.211	0.116	651.9E-6	1.98	0.63	1235
27.91	27.50	33.464	0.200	0.127	636.0E-6	1.93	0.63	1186
30.41	30.00	31.827	0.191	0.137	620.1E-6	1.88	0.64	1136
32.91	32.50	30.139	0.180	0.147	604.2E-6	1.83	0.64	1088
35.41	35.00	28.582	0.171	0.156	588.4E-6	1.78	0.64	1040
37.91	37.50	27.018	0.162	0.166	572.5E-6	1.73	0.64	992
40.41	40.00	25.492	0.153	0.175	556.6E-6	1.68	0.64	944
42.91	42.50	23.975	0.144	0.184	540.7E-6	1.63	0.64	901
45.41	45.00	22.639	0.136	0.192				

APPENDIX T: 3.77% bentonite suspension

Rheological and physical parameters

n=	1.00
k=	0.006 Pa.s ⁿ
τ_y =	1.129 Pa.s
Density=	1023 kg/m ³
g=	9.81 m/s ²

Circular orifices

Table T.1 8 mm circular orifice results (3.77% bentonite)

Time [s]	Diff.Time [s]	Mass in tank [kg]	Height [m]	Diff.Height [m]	Flow rate [m ³ /s]	Orifice Velocity		
						C _d	Re ₂	
5	0	58.434	0.357	0	0	0	0	0
35	30	55.766	0.341	0.016	86.76E-6	2.59	0.66	3259
65	60	53.146	0.325	0.032	84.78E-6	2.52	0.66	3176
95	90	50.586	0.309	0.048	82.80E-6	2.46	0.66	3093
125	120	48.077	0.294	0.063	80.82E-6	2.40	0.66	3010
155	150	45.634	0.279	0.078	78.84E-6	2.34	0.66	2927
185	180	43.242	0.264	0.093	76.86E-6	2.28	0.66	2844
215	210	40.901	0.250	0.107	74.88E-6	2.21	0.67	2760
245	240	38.641	0.236	0.121	72.90E-6	2.15	0.67	2676
275	270	36.428	0.223	0.134	70.92E-6	2.09	0.67	2592
305	300	34.277	0.209	0.148	68.94E-6	2.03	0.67	2508
335	330	32.177	0.197	0.160	66.96E-6	1.96	0.67	2424
365	360	30.144	0.184	0.173	64.98E-6	1.90	0.67	2339
395	390	28.188	0.172	0.185	63.00E-6	1.84	0.68	2255
425	420	26.270	0.160	0.197	61.02E-6	1.77	0.68	2170
455	450	24.427	0.149	0.208	59.04E-6	1.71	0.68	2085
485	480	22.665	0.138	0.219	57.06E-6	1.65	0.68	2001
515	510	20.945	0.128	0.229	55.08E-6	1.58	0.68	1916
545	540	19.309	0.118	0.239	53.10E-6	1.52	0.69	1831
575	570	17.725	0.108	0.249	51.13E-6	1.46	0.69	1746

Table T.2 12 mm circular orifice results (3.77% bentonite)

Time	Diff.Time	Mass in tank	Height	Diff.Height	Flow rate	Orifice Velocity	C _d	Re ₂
[s]	[s]	[kg]	[m]	[m]	[m ³ /s]	[m/s]		
2.492	0	57.436	0.351	0	0	0	0	0
17.49	15	54.603	0.334	0.017	183.0E-6	2.56	0.63	4668
32.49	30	51.826	0.317	0.034	178.6E-6	2.49	0.63	4536
47.49	45	49.117	0.300	0.051	174.2E-6	2.43	0.63	4403
62.49	60	46.484	0.284	0.067	169.7E-6	2.36	0.63	4271
77.49	75	43.912	0.268	0.083	165.3E-6	2.29	0.63	4139
92.49	90	41.408	0.253	0.098	160.9E-6	2.23	0.63	4006
107.5	105	38.967	0.238	0.113	156.5E-6	2.16	0.64	3873
122.5	120	36.611	0.224	0.127	152.1E-6	2.09	0.64	3741
137.5	135	34.309	0.210	0.141	147.7E-6	2.03	0.64	3607
152.5	150	32.075	0.196	0.155	143.3E-6	1.96	0.64	3473
167.5	165	29.916	0.183	0.168	138.9E-6	1.89	0.64	3340
182.5	180	27.816	0.170	0.181	134.5E-6	1.83	0.65	3205
197.5	195	25.737	0.157	0.194	130.1E-6	1.76	0.65	3067
212.5	210	23.776	0.145	0.206	125.7E-6	1.69	0.65	2931
227.5	225	21.902	0.134	0.217	121.3E-6	1.62	0.66	2797
242.5	240	20.102	0.123	0.228	116.9E-6	1.55	0.66	2662
257.5	255.00	18.345	0.112	0.239	112.5E-6	1.48	0.67	2525

Table T.3 16 mm circular orifice results (3.77% bentonite)

Time	Diff.Time	Mass in tank	Height	Diff.Height	Flow rate	Orifice Velocity	C _d	Re ₂
[s]	[s]	[kg]	[m]	[m]	[m ³ /s]	[m/s]		
1.658	0	58.694	0.359	0	0	0	0	0
11.66	10	55.378	0.338	0.020	320.4E-6	2.58	0.62	6069
21.66	20	52.154	0.319	0.040	311.2E-6	2.50	0.62	5868
31.66	30	49.017	0.299	0.059	302.0E-6	2.42	0.62	5665
41.66	40	45.970	0.281	0.078	292.8E-6	2.35	0.62	5463
51.66	50	43.023	0.263	0.096	283.6E-6	2.27	0.62	5260
61.66	60	40.177	0.245	0.113	274.5E-6	2.19	0.62	5059
71.66	70	37.398	0.228	0.130	265.3E-6	2.12	0.62	4855
81.66	80	34.749	0.212	0.146	256.1E-6	2.04	0.62	4654
91.66	90	32.171	0.197	0.162	246.9E-6	1.96	0.62	4451
101.7	100	29.672	0.181	0.177	237.7E-6	1.89	0.62	4247
111.7	110	27.286	0.167	0.192	228.5E-6	1.81	0.63	4044
121.7	120	24.998	0.153	0.206	219.3E-6	1.73	0.63	3841
131.7	130	22.809	0.139	0.219	210.1E-6	1.65	0.63	3639
141.7	140	20.694	0.126	0.232	200.9E-6	1.57	0.63	3435
151.7	150	18.713	0.114	0.244	191.7E-6	1.50	0.63	3234
161.7	160	16.796	0.103	0.256	182.6E-6	1.42	0.64	3031

Table T.4 20 mm circular orifice results (3.77% bentonite)

Time	Diff.Time	Mass in tank	Height	Diff.Height	Flow rate	Orifice Velocity	C _d	Re ₂
[s]	[s]	[kg]	[m]	[m]	[m ³ /s]	[m/s]		
0.825	0.00	58.488	0.357	0.000	0	0	0	0
7.492	6.667	55.056	0.336	0.021	497.0E-6	2.57	0.61	7327
14.16	13.33	51.736	0.316	0.041	482.2E-6	2.49	0.61	7068
20.83	20.00	48.520	0.296	0.061	467.3E-6	2.41	0.61	6810
27.49	26.67	45.372	0.277	0.080	452.5E-6	2.33	0.62	6549
34.16	33.33	42.314	0.259	0.099	437.6E-6	2.25	0.62	6288
40.83	40.00	39.396	0.241	0.117	422.8E-6	2.17	0.62	6030
47.49	46.67	36.552	0.223	0.134	407.9E-6	2.09	0.62	5769
54.16	53.33	33.835	0.207	0.151	393.1E-6	2.01	0.62	5511
60.83	60.00	31.185	0.191	0.167	378.2E-6	1.93	0.62	5250
67.49	66.67	28.670	0.175	0.182	363.4E-6	1.85	0.62	4992
74.16	73.33	26.236	0.160	0.197	348.6E-6	1.77	0.62	4733
80.83	80.00	23.878	0.146	0.211	333.7E-6	1.69	0.63	4470
87.49	86.67	21.679	0.132	0.225	318.9E-6	1.61	0.63	4214
94.16	93.33	19.555	0.119	0.238	304.0E-6	1.53	0.63	3956
100.8	100.00	17.539	0.107	0.250	289.2E-6	1.45	0.63	3698
107.5	106.67	15.646	0.096	0.262	274.3E-6	1.37	0.64	3444

Square orifices

Table T.5 8 mm square orifice results (3.77% bentonite)

Time	Diff.Time	Mass in tank	Height	Diff.Height	Flow rate	Orifice Velocity	C _d	Re ₂
[s]	[s]	[kg]	[m]	[m]	[m ³ /s]	[m/s]		
4.158	0	58.608	0.358	0	0	0	0	0
29.16	25	55.756	0.341	0.017	109.3E-6	2.59	0.66	3251
54.16	50	52.977	0.324	0.034	106.8E-6	2.52	0.66	3163
79.16	75	50.329	0.307	0.051	104.4E-6	2.46	0.66	3078
104.2	100	47.686	0.291	0.067	101.9E-6	2.39	0.66	2990
129.2	125	45.101	0.276	0.083	99.48E-6	2.33	0.67	2902
154.2	150	42.593	0.260	0.098	97.04E-6	2.26	0.67	2814
179.2	175	40.130	0.245	0.113	94.59E-6	2.19	0.67	2725
204.2	200	37.691	0.230	0.128	92.14E-6	2.13	0.67	2635
229.2	225	35.426	0.216	0.142	89.69E-6	2.06	0.68	2548
254.2	250	33.154	0.203	0.156	87.24E-6	1.99	0.68	2458
279.2	275	30.975	0.189	0.169	84.79E-6	1.93	0.68	2369
304.2	300	28.791	0.176	0.182	82.34E-6	1.86	0.69	2276
329.2	325	26.755	0.163	0.195	79.89E-6	1.79	0.69	2187

Table T.6 12 mm square orifice results (3.77% bentonite)

Time [s]	Diff.Time [s]	Mass in tank [kg]	Height [m]	Diff.Height [m]	Flow rate [m ³ /s]	Orifice Velocity		
						C _d	Re ₂	
2.492	0	59.503	0.364	0	0	0	0	0
17.49	15	55.758	0.341	0.023	241.9E-6	2.59	0.65	4714
32.49	30	52.094	0.318	0.045	234.1E-6	2.50	0.65	4542
47.49	45	48.575	0.297	0.067	226.4E-6	2.41	0.65	4370
62.49	60	45.159	0.276	0.088	218.7E-6	2.33	0.65	4197
77.49	75	41.862	0.256	0.108	211.0E-6	2.24	0.65	4025
92.49	90	38.659	0.236	0.127	203.2E-6	2.15	0.65	3850
107.5	105	35.620	0.218	0.146	195.5E-6	2.07	0.65	3678
122.5	120	32.663	0.200	0.164	187.8E-6	1.98	0.66	3504
137.5	135	29.837	0.182	0.181	180.0E-6	1.89	0.66	3330
152.5	150	27.139	0.166	0.198	172.3E-6	1.80	0.66	3156
167.5	165	24.557	0.150	0.214	164.6E-6	1.72	0.66	2982
182.5	180	22.084	0.135	0.229	156.9E-6	1.63	0.67	2806
197.5	195	19.742	0.121	0.243	149.1E-6	1.54	0.67	2631
212.5	210	17.524	0.107	0.256	141.4E-6	1.45	0.68	2456

Table T.7 16 mm square orifice results (3.77% bentonite)

Time [s]	Diff.Height [s]	Mass in tank [kg]	Height [m]	Diff.Height [m]	Flow rate [m ³ /s]	Orifice Velocity		
						C _d	Re ₂	
1.242	0	59.314	0.362	0	0	0	0	0
8.742	8	56.126	0.343	0.019	412.6E-6	2.59	0.62	6109
16.24	15	53.013	0.324	0.038	401.3E-6	2.52	0.62	5915
23.74	23	49.960	0.305	0.057	390.0E-6	2.45	0.62	5720
31.24	30	47.017	0.287	0.075	378.8E-6	2.37	0.62	5527
38.74	38	44.141	0.270	0.093	367.5E-6	2.30	0.62	5332
46.24	45	41.385	0.253	0.110	356.2E-6	2.23	0.62	5140
53.74	53	38.696	0.236	0.126	344.9E-6	2.15	0.62	4946
61.24	60	36.091	0.220	0.142	333.7E-6	2.08	0.63	4751
68.74	68	33.555	0.205	0.157	322.4E-6	2.01	0.63	4556
76.24	75	31.142	0.190	0.172	311.1E-6	1.93	0.63	4363
83.74	83	28.768	0.176	0.187	299.9E-6	1.86	0.63	4166
91.24	90	26.521	0.162	0.200	288.6E-6	1.78	0.63	3973
98.74	98	24.363	0.149	0.214	277.3E-6	1.71	0.63	3779
106.2	105	22.281	0.136	0.226	266.1E-6	1.63	0.63	3585
113.7	113	20.275	0.124	0.239	254.8E-6	1.56	0.64	3390
121.2	120	18.381	0.112	0.250	243.5E-6	1.48	0.64	3196
128.7	128	16.540	0.101	0.261	232.2E-6	1.41	0.64	3000

Table T.8 20 mm square orifice results (3.77% bentonite)

Time	Diff.Time	Mass in tank	Height	Diff.Height	Flow rate	Orifice Velocity	C _d	Re ₂
[s]	[s]	[kg]	[m]	[m]	[m ³ /s]	[m/s]		
0.825	0	57.695	0.352	0	0	0	0	0
5.825	5	54.398	0.332	0.020	634.3E-6	2.55	0.62	7270
10.83	10	51.228	0.313	0.040	615.8E-6	2.48	0.62	7022
15.83	15	48.102	0.294	0.059	597.3E-6	2.40	0.62	6770
20.83	20	45.121	0.276	0.077	578.8E-6	2.33	0.62	6523
25.83	25	42.215	0.258	0.095	560.3E-6	2.25	0.62	6274
30.83	30	39.398	0.241	0.112	541.8E-6	2.17	0.62	6025
35.83	35	36.623	0.224	0.129	523.3E-6	2.10	0.62	5771
40.83	40	34.027	0.208	0.145	504.8E-6	2.02	0.62	5525
45.83	45	31.472	0.192	0.160	486.3E-6	1.94	0.62	5274
50.83	50	29.063	0.178	0.175	467.8E-6	1.87	0.63	5029
55.83	55	26.688	0.163	0.189	449.3E-6	1.79	0.63	4778
60.83	60	24.438	0.149	0.203	430.8E-6	1.71	0.63	4530
65.83	65	22.272	0.136	0.216	412.4E-6	1.63	0.63	4281
70.83	70	20.233	0.124	0.229	393.9E-6	1.56	0.63	4037
75.83	75	18.266	0.112	0.241	375.4E-6	1.48	0.63	3790
80.83	80	16.410	0.100	0.252	356.9E-6	1.40	0.63	3545

Triangular orifices

Table T.9 8 mm triangular orifice results (3.77% bentonite)

Time	Diff.Time	Mass in tank	Height	Diff.Height	Flow rate	Orifice Velocity	C _d	Re ₂
[s]	[s]	[kg]	[m]	[m]	[m ³ /s]	[m/s]		
4.158	0.00	57.918	0.354	0	0	0	0	0
25.83	21.67	54.739	0.334	0.019	142.4E-6	2.56	0.66	3222
47.49	43.33	51.628	0.315	0.038	138.6E-6	2.49	0.67	3123
69.16	65.00	48.564	0.296	0.057	134.8E-6	2.41	0.67	3022
90.83	86.67	45.607	0.278	0.075	131.0E-6	2.34	0.67	2922
112.49	108.3	42.731	0.261	0.093	127.2E-6	2.26	0.67	2822
134.16	130.0	39.967	0.244	0.110	123.4E-6	2.19	0.67	2722
155.83	151.7	37.325	0.228	0.126	119.6E-6	2.11	0.68	2623
177.49	173.3	34.708	0.212	0.142	115.8E-6	2.04	0.68	2522
199.16	195.0	32.187	0.196	0.157	112.0E-6	1.96	0.68	2421
220.83	216.7	29.734	0.182	0.172	108.1E-6	1.89	0.68	2319
242.49	238.3	27.312	0.167	0.187	104.3E-6	1.81	0.69	2214
264.16	260.0	25.053	0.153	0.201	100.5E-6	1.73	0.69	2111

Table T.10 12 mm triangular orifice results (3.77% bentonite)

Time	Diff.Time	Mass in tank	Height	Diff.Height	Flow rate	Orifice Velocity	C _d	Re ₂
[s]	[s]	[kg]	[m]	[m]	[m ³ /s]	[m/s]		
1.658	0.00	58.055	0.354	0	0	0	0	0
13.33	11.67	54.332	0.332	0.023	307.0E-6	2.55	0.64	4646
24.99	23.33	50.739	0.310	0.045	297.2E-6	2.47	0.64	4474
36.66	35.00	47.242	0.288	0.066	287.4E-6	2.38	0.65	4301
48.33	46.67	43.864	0.268	0.087	277.6E-6	2.29	0.65	4128
59.99	58.33	40.620	0.248	0.106	267.8E-6	2.21	0.65	3956
71.66	70.00	37.476	0.229	0.126	258.0E-6	2.12	0.65	3782
83.33	81.67	34.438	0.210	0.144	248.1E-6	2.03	0.65	3608
94.99	93.33	31.536	0.193	0.162	238.3E-6	1.94	0.65	3434
106.7	105.0	28.731	0.175	0.179	228.5E-6	1.86	0.66	3258
118.3	116.7	26.061	0.159	0.195	218.7E-6	1.77	0.66	3083
130.0	128.3	23.500	0.143	0.211	208.9E-6	1.68	0.66	2906
141.7	140.0	21.077	0.129	0.226	199.1E-6	1.59	0.67	2731
153.3	151.7	18.760	0.115	0.240	189.3E-6	1.50	0.67	2553
165.0	163.3	16.570	0.101	0.253	179.4E-6	1.41	0.68	2376

Table T.11 16 mm triangular orifice results (3.77% bentonite)

Time	Diff.Time	Mass in tank	Height	Diff.Height	Flow rate	Orifice Velocity	C _d	Re ₂
[s]	[s]	[kg]	[m]	[m]	[m ³ /s]	[m/s]		
0.825	0.00	57.465	0.351	0	0	0	0	0
7.492	6.67	53.836	0.329	0.022	518.6E-6	2.54	0.64	5866
14.16	13.33	50.367	0.307	0.043	502.3E-6	2.46	0.64	5650
20.83	20.00	46.994	0.287	0.064	486.0E-6	2.37	0.64	5433
27.49	26.67	43.757	0.267	0.084	469.7E-6	2.29	0.64	5217
34.16	33.33	40.563	0.248	0.103	453.3E-6	2.20	0.64	4997
40.83	40.00	37.565	0.229	0.121	437.0E-6	2.12	0.64	4782
47.49	46.67	34.631	0.211	0.139	420.7E-6	2.04	0.64	4564
54.16	53.33	31.790	0.194	0.157	404.4E-6	1.95	0.65	4344
60.83	60.00	29.106	0.178	0.173	388.1E-6	1.87	0.65	4127
67.49	66.67	26.528	0.162	0.189	371.7E-6	1.78	0.65	3910
74.16	73.33	24.022	0.147	0.204	355.4E-6	1.70	0.65	3689
80.83	80.00	21.639	0.132	0.219	339.1E-6	1.61	0.66	3468
87.49	86.67	19.396	0.118	0.232	322.8E-6	1.52	0.66	3250
94.16	93.33	17.262	0.105	0.245	306.5E-6	1.44	0.66	3030

Table T.12 20 mm triangular orifice results (3.77% bentonite)

Time [s]	Diff.Time [s]	Mass in tank [kg]	Height [m]	Diff.Height [m]	Flow rate [m ³ /s]	Orifice Velocity [m/s]	C _d	Re ₂
0.408	0.00	55.193	0.337	0	0	0	0	0
3.742	3.333	52.395	0.320	0.017	811.6E-6	2.51	0.63	7104
7.075	6.667	49.662	0.303	0.034	790.6E-6	2.44	0.63	6887
10.41	10.00	46.991	0.287	0.050	769.6E-6	2.37	0.63	6669
13.74	13.33	44.392	0.271	0.066	748.6E-6	2.31	0.63	6452
17.08	16.67	41.885	0.256	0.081	727.6E-6	2.24	0.63	6236
20.41	20.00	39.390	0.240	0.096	706.5E-6	2.17	0.63	6015
23.74	23.33	37.028	0.226	0.111	685.5E-6	2.11	0.63	5800
27.08	26.67	34.733	0.212	0.125	664.5E-6	2.04	0.63	5585
30.41	30.00	32.460	0.198	0.139	643.5E-6	1.97	0.63	5365
33.74	33.33	30.264	0.185	0.152	622.5E-6	1.90	0.63	5145
37.08	36.67	28.191	0.172	0.165	601.5E-6	1.84	0.63	4931
40.41	40.00	26.164	0.160	0.177	580.5E-6	1.77	0.63	4714
43.74	43.33	24.220	0.148	0.189	559.5E-6	1.70	0.63	4499
47.08	46.67	22.338	0.136	0.201	538.4E-6	1.64	0.64	4283
50.41	50.00	20.529	0.125	0.212	517.4E-6	1.57	0.64	4067
53.74	53.33	18.779	0.115	0.222	496.4E-6	1.50	0.64	3850
57.08	56.67	17.147	0.105	0.232	475.4E-6	1.43	0.64	3639